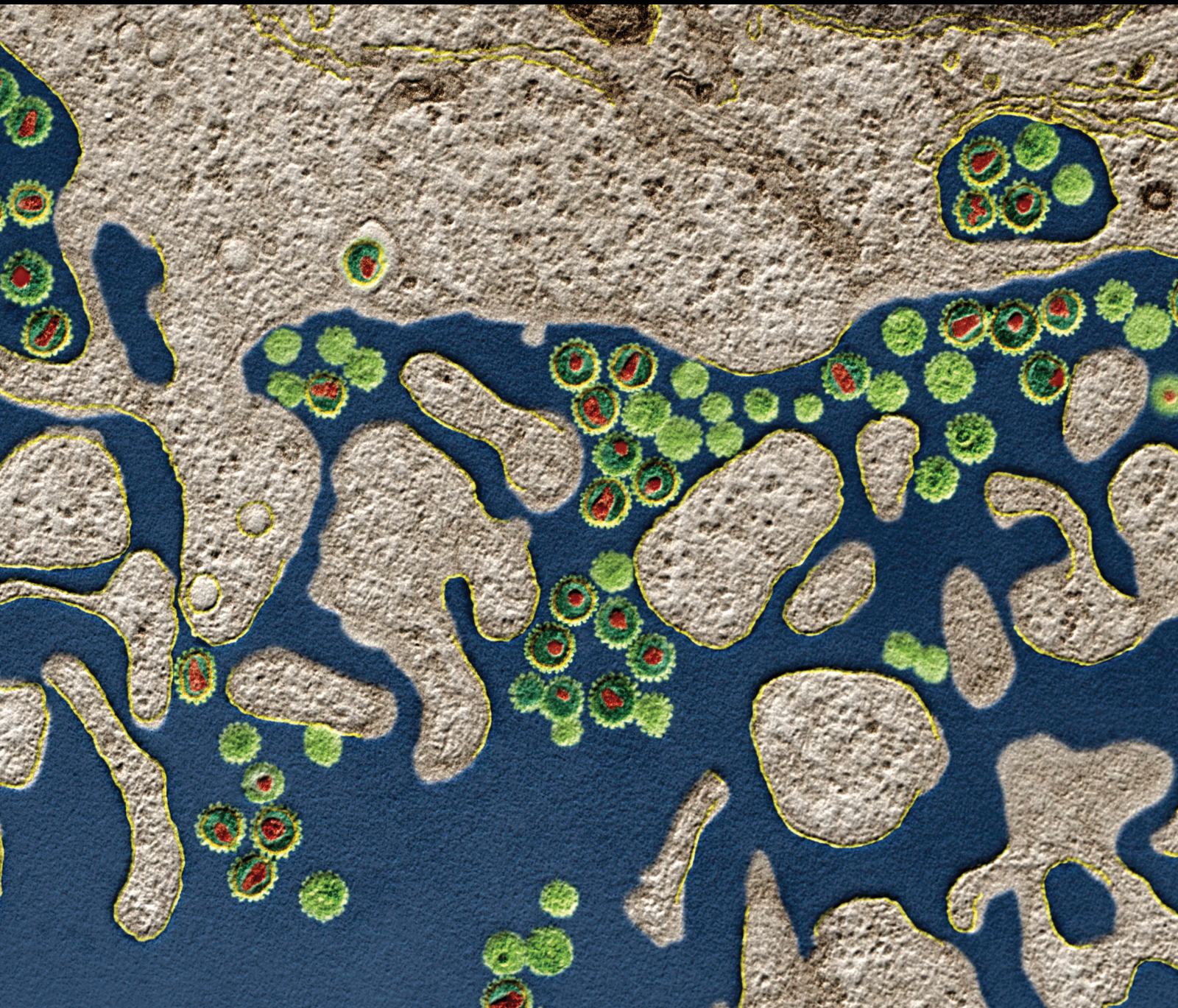# Recent advances in Innate Immunity at the Epithelial Barrier

Lead Guest Editor: Kong Chen
Guest Editors: Yanyan Qu and Xiang Zhang

Recent advances in Innate Immunity at the Epithelial Barrier

Recent advances in Innate Immunity at the Epithelial Barrier

Lead Guest Editor: Kong Chen
Guest Editors: Yanyan Qu and Xiang Zhang

Contents

Research Article

Enriched LPS Staining within the Germinal Center of a Lymph Node from an HIV-Infected Long-Term Nonprogressor but Not from Progressors

Lei Huang [iD],[1] Jianning Deng,[2] Ren Lang,[3] Guoyang Liao,[4] and Wei Jiang [iD][5,6]

[1]*Treatment and Research Center for Infectious Diseases, The Fifth Medical Center of Chinese PLA General Hospital, Beijing, China 100039*

[2]*Department of Tuberculosis, The Fourth People's Hospital of Nanning, Nanning, Guangxi, China 530023*

[3]*Department of Hepatobiliary Surgery, Beijing Chaoyang Hospital, Capital Medical University, Beijing, China 100020*

[4]*Chief of No. 5 Biologicals Department, Institute of Medical Biology, Chinese Academy of Medical Sciences & Peking Union Medical College, Kuming, China 650118*

[5]*Department of Microbiology and Immunology, Medical University of South Carolina, Charleston, USA 29425*

[6]*Division of Infectious Diseases, Department of Medicine, Medical University of South Carolina, Charleston, USA 29425*

Correspondence should be addressed to Lei Huang; huangleiwa@sina.com

An increased level of microbial translocation has been observed in HIV-infected individuals. The host response to microbial translocation is compromised in HIV-infected progressors but remains unknown in HIV-infected long-term nonprogressors (LTNPs). To evaluate microbial translocation in HIV, we assessed lipopolysaccharide (LPS) immunohistochemistry staining in lymph nodes. We found enriched bacterial LPS immunohistochemistry staining in the germinal center of a lymph node from an HIV-infected LTNP, evenly distributed from three progressors with impaired germinal center structures and rarely detected from two HIV-negative individuals. The impaired germinal center structures were consistent with collagen deposition in lymph nodes using immunohistochemistry staining. These results suggest greater immune responses against bacterial LPS translocation in LTNPs, which may reveal an important mechanism in controlling microbial translocation and disease progression in HIV LTNPs.

1. Introduction

HIV-infected long-term nonprogressors (LTNPs) comprise less than 1 percent of HIV-infected individuals who control HIV replication and do not progress to AIDS without medications [1]. The mechanisms of controlling disease progression in LTNPs include specific HLA types and greater HIV-specific CD8+ T cell cytotoxicity compared to progressors [2]. However, the mechanisms of host immunity to control viral replication and prevent CD4+ T cell depletion in LTNPs are not fully understood.

Chronic immune activation and inflammation are well-known hallmarks for CD4+ T cell depletion and HIV disease progression even in patients with antiretroviral therapy

(ART) treatment [3]. Different therapeutic strategies targeting immune activation and inflammation (e.g., statins) have been applied to HIV-infected patients in clinic, but the effects are not clear [4]. Inflammation and chronic immune activation can be driven by microbial product translocation and residual viral effects in patients with ART treatment [5]; thus, bacterial product translocation may contribute to HIV disease progression. It remains unclear whether there is an increased level of microbial translocation in LTNPs as shown in progressors compared to healthy individuals [6, 7]. Moreover, the host immune response to microbial translocation in LTNPs remains unknown. Here we report that enriched bacterial lipopolysaccharide (LPS) immunohistochemistry staining was observed mainly in the germinal center of a lymph

FIGURE 1: Identification of LPS staining in lymph nodes of two HIV-negative donors, three ART-naïve chronically HIV-infected progressors, and one chronically HIV-infected LTNP. Representative images of unselected lymph node (LN) sections stained for LPS-core antigen (red, 200x and 400x). The LTNP showed increased LPS infiltration within the germinal center; the progressors showed increased LPS infiltration in the LNs with impaired structures of the germinal center; LPS staining was rarely detected from the HIV-negative donors.

node from a LTNP; evenly distributed LPS was observed in lymph nodes from three progressors with impaired germinal center structures; and LPS staining was rarely observed in lymph nodes of two HIV-negative individuals.

2. Results and Discussion

In two HIV-negative donors, LPS staining was rarely detected in their lymph nodes (Figures 1(a) and 1(b) and Table 1). Consistent with HIV-associated "leaky" gut and microbial translocation [8], LPS staining was increased in three HIV+ progressors (Figures 1(c)–1(e)) and one HIV+ LTNP (Figure 1(f)) compared to the HIV-negative donors (Figures 1(a) and 1(b)). Intriguingly, LPS was enriched and

limited within the germinal center of a lymph node from the donor of LTNP, but not from the donor of progressors (Figures 1(c)–1(f)). Furthermore, the lymph nodes from HIV+ progressors exhibited impaired structures of germinal center (Figures 1(c)–1(e)), consistent with lymph node fibrosis observed in HIV+ progressors from previous studies [9]. Furthermore, to determine whether impaired germinal center structures are consistent with lymph node fibrosis, we also stained collagen I (Figure 2). Indeed, collagen deposition in the lymph node of LTNP was increased compared to those from HIV-negative control donors but decreased compared to those from HIV+ progressors (Figure 2 and Table 1). Collagen deposition was also increased in the lymphatic follicles from HIV+ progressors (e.g., progressor #1, Figure 2(c)).

TABLE 1

	Mean ± SD (LPS)	Mean ± SD (collagen I)
HIV-negative #1	586 ± 160	4817.56 ± 4190.63
HIV-negative #2	8.7 ± 9.1	2519.05 ± 1619.79
HIV+ progressor #1	3902 ± 2166	11665.71 ± 6021.23
HIV+ progressor #2	9518 ± 2568	17343.05 ± 7313.52
HIV+ progressor #3	2490 ± 983	16156.88 ± 5086.77
HIV+ LTNP #1	2273 ± 1659	8781.22 ± 6873.75

Therefore, the structure of lymph node from LTNP was relatively complete, and the structure of the lymph nodes of HIV + progressors was remarkably destroyed.

Microbial translocation may play a role in chronic immune activation and inflammation, which contribute to CD4+ T cell depletion and HIV disease progression [3, 8]. However, the fundamental mechanism of chronic immune activation and inflammation and potential therapeutic targets for preventing persistent immune activation in HIV are not fully understood.

HIV-infected LTNPs are patients who are not on ART but whose CD4+ T cells remain above 500 cells/mL and who exhibit low levels of viral replication for many years (~5-10 years) [2]. This group represents less than 1% of the HIV patient population and never progresses to AIDS, the last stage of HIV disease [2]. LTNPs have reduced chronic immune activation and inflammation, as well as increased HIV-specific CD8+ T cell cytotoxicity, compared to HIV+ progressors [2]. It is not clear whether the control of disease progression in LTNPs is due to viral defects, genomic factors, or host factors. Nonetheless, LTNPs provide an excellent model to study the mechanism of the control of HIV disease progression in the host without ART treatment.

In the current study, LPS was enriched and limited in the germinal center of the lymph node from the HIV+ LTNP donor but not from the HIV+ progressors. LPS is thought as nonprotein antigen and may directly induce immune responses through Toll-like receptor 4, which is not necessary through antigen presenting and processing by antigen-presenting cells [10]. However, immune cells from LTNPs efficiently deliver LPS to the germinal center of the lymph nodes, which may result in stronger T and B cell immune responses against LPS. In addition, differences in TLR4 expression and TLR4 signaling pathway may account for the difference in host immunity against LPS in LTNPs compared to HIV+ progressors. These potential mechanisms may contribute to reduced levels of inflammation and immune activation, as well as nonprogression to AIDS in LTNPs, and deserve further investigations.

3. Experimental Procedures

3.1. Study Subjects.
Six subjects were recruited for the current study: two HIV-negative subjects, three HIV+ progressors (ART-naïve and plasma HIV RNA >10,000 copies/mL), and one HIV+ LTNP. Their clinical characteristics are shown in Figure 1. The HIV+ LTNP was an HIV-infected patient who maintains low levels of plasma HIV RNA (<5000 copies/mL) and peripheral CD4+ T cell counts above 500 cells/μL without ART treatment for 7 years [11]. This study was approved by the institutional review board from the Fourth People's Hospital of Nanning (Nanning, China) and the Fifth Medical Center of Chinese PLA General Hospital (Beijing, China). All participants provided written informed consents.

3.2. Processing of Human Lymph Nodes.
Fresh human lymph nodes were obtained from an HIV-infected LTNP, three progressors, and two HIV-negative individuals who had lymph node pathological enlargements. These lymph node biopsies were fixed in formalin and embedded in paraffin for immunohistochemical staining.

3.3. Immunohistochemical Staining of LPS.
The tissues of lymph nodes were LPS stained by immunohistochemical techniques, as described in a previous study [12]. Briefly, paraffin was removed from paraffin sections by being roasted at 65°C for 20-30 min and immersed in three xylene jars for 10 min each. Xylene was removed as sections were immersed in dehydrated alcohol for 5 min three times. These sections were further immersed in 95% ethanol for 3 min twice, and in 90%, 85%, and 80% ethanol for 2 min each. Sections were then rinsed with tap water for 3 min twice and with distilled water for 3 min twice. Antigen was retrieved in the citrate buffer (pH 6.0) for 20 min in a microwave oven. Sections were cooled at room temperature and rinsed by tap water twice. Then sections were soaked in 2% H_2O_2-methanol for 30 min at room temperature and rinsed by tap water for 3 min twice, distilled water for 3 min three times, and PBS (pH 7.4) for 3 min twice. Subsequently, sections were incubated with fetal bovine serum (FBS, Fisher Scientific, Hampton, NH, USA) at room temperature for 25 min. FBS was washed out, and the mouse anti-human LPS-core antibody (Cat. no. HM6011, RRID: AB_2750644; Hycult Biotech, Inc., Wayne, PA, USA) was added (1 : 200-250) to each section and incubated overnight. PBS was used to rinse sections for 5 min three times, and the secondary antibody (Cat. no. ab205719, RRID: AB_2755049; 1 : 10,000; Abcam, Cambridge, UK) was added and incubated at 37°C for 30 min. Sections were rinsed in PBS for 5 min three times and incubated with AEC at room temperature without light for 15 min. Sections were rinsed in distilled water for 2 min twice. Sections were counterstained with hematoxylin, dehydrated, cleared, and mounted with neutral gums. The negative controls were carried out with the same steps as described above, but the antibody for LPS was replaced by PBS. All stained slides were observed at a magnification of 200x or 400x, using a light microscope (Olympus CX31; Olympus Corporation, Tokyo, Japan), and were blindly evaluated by a pathologist. Fluorescence intensity analysis was performed using the ImageJ software (ImageJ, Bethesda, USA) as described previously [13].

3.4. Immunohistochemical Staining of Collagen I.
Immunohistochemistry protocols of collagen I staining process were similar to LPS staining. The main differences in the experiment were as follows: antigen retrieval was performed using

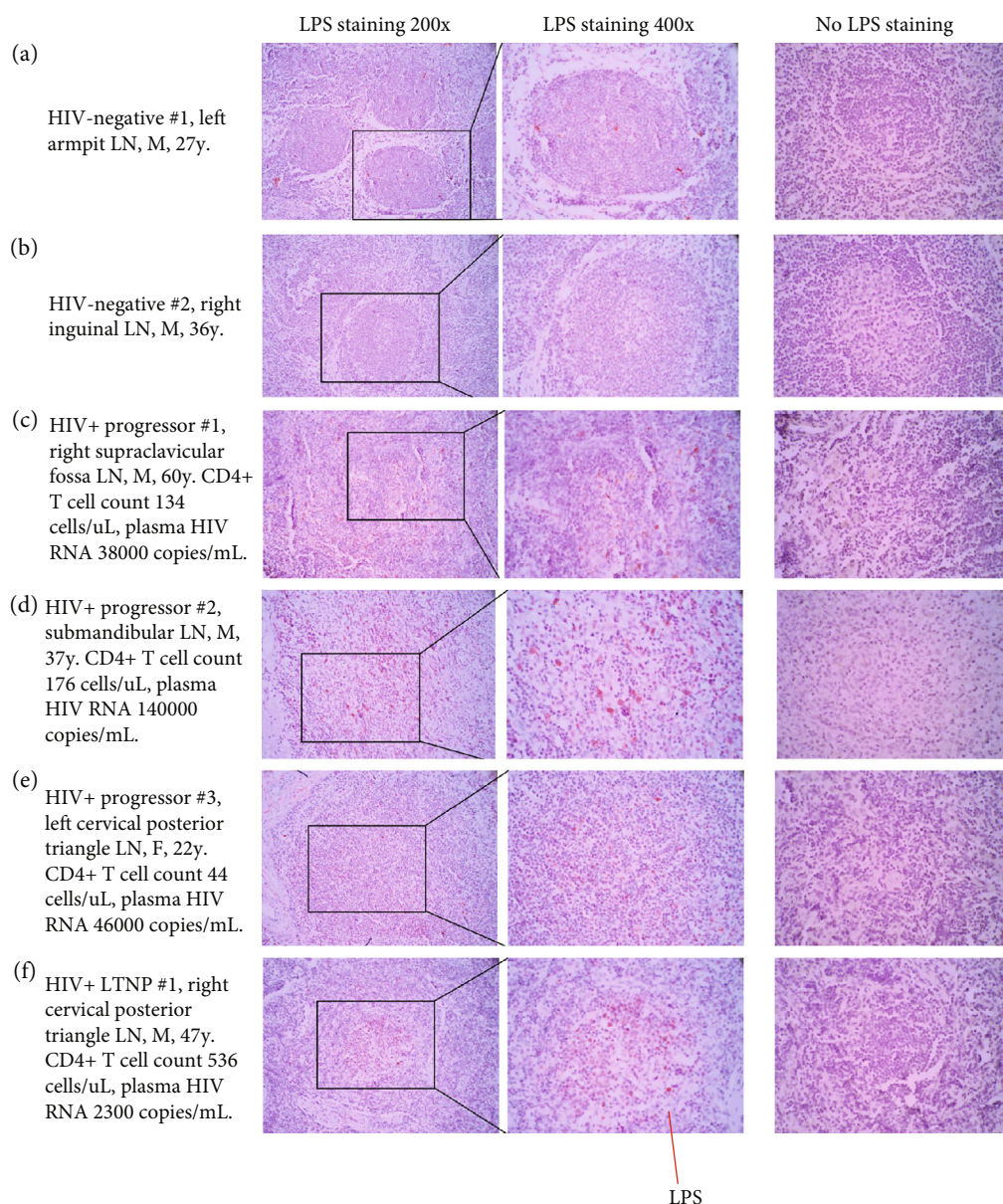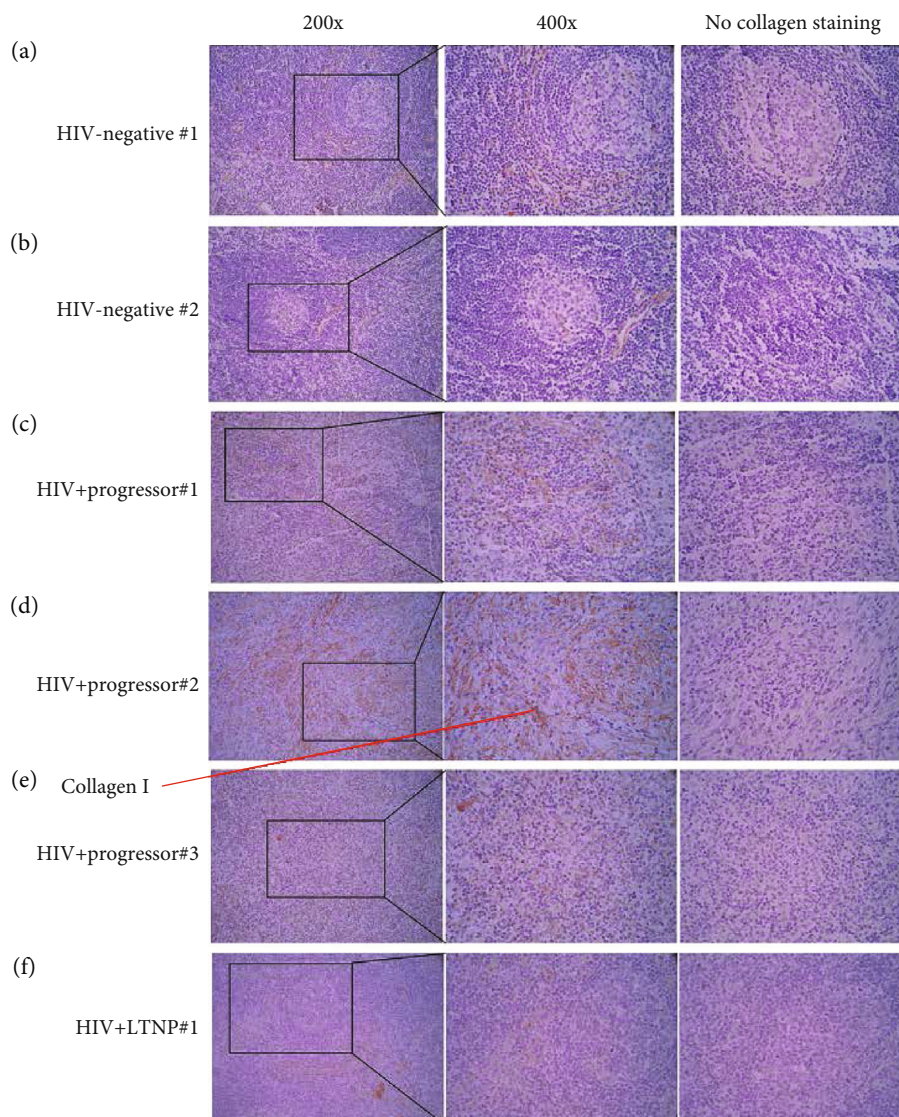FIGURE 2: Identification of collagen I staining in lymph nodes of two HIV-negative donors, three ART-naïve chronically HIV-infected progressors, and one chronically HIV-infected LTNP. Representative images of unselected LN sections stained for collagen I antigen (red, 200x and 400x). The HIV+ progressors showed increased collagen I staining in LNs; the LTNP and HIV-negative donors showed decreased collagen I staining in the LNs compared to HIV+ progressors.

EDTA buffer (pH 8.5); endogenous peroxidase was removed using 3% H_2O_2-methanol solution; DAB was used for staining; and the positive result was in red. The mouse anti-human collagen I antibody was purchased from the Abcam company (Cat. no. ab88147, RRID: AB_2081873; 1 : 100; Abcam, Cambridge, UK). Stained sections were randomly selected in each donor for analysis of 5 visual fields of a magnification of 400x to detect the optical density value with the Image-Pro Plus software 6.0 for collagen I, described from our previous study [13]. The integrated optical density (IOD) of each visual field was analyzed using the SPSS software 17.0. The summarized densities are shown in Table 1.

Abbreviations

LTNP: Long-term nonprogressor
LN: Lymph node

ART: Antiretroviral therapy
LPS: Lipopolysaccharide.

Data Availability

The data used to support the findings of this study are available from the corresponding author upon request.

Ethical Approval

This study was approved by the institutional review board from the Fourth People's Hospital of Nanning (Nanning, China) and the Fifth Medical Center of Chinese PLA General Hospital (Beijing, China). All participants provided written informed consents.

Consent

All authors have contributed to, seen, and approved the final submitted version of the manuscript. This manuscript has not been previously published and is not being submitted for publication elsewhere.

Conflicts of Interest

None of the authors have a financial conflict with the studies presented in this manuscript.

Authors' Contributions

LH and JD performed the experiments. RL and WJ wrote the manuscript. LH, JD, RL, LGY, and WJ contributed to the study design.

Acknowledgments

References

[1] S. A. Migueles and M. Connors, "Frequency and function of HIV-specific CD8+ T Cells," *Immunology Letters*, vol. 79, no. 1-2, article S0165247801002760, pp. 141–150, 2001.

[2] S. A. Migueles, A. C. Laborico, W. L. Shupert et al., "HIV-specific CD8$^+$ T cell proliferation is coupled to perforin expression and is maintained in nonprogressors," *Nature Immunology*, vol. 3, no. 11, article BFni845, pp. 1061–1068, 2002.

[3] J. M. McCune, "The dynamics of CD4+ T-cell depletion in HIV disease," *Nature*, vol. 410, no. 6831, pp. 974–979, 2001.

[4] S. Elahi, R. H. Weiss, and S. Merani, "Atorvastatin restricts HIV replication in CD4+ T cells by upregulation of p 21," *AIDS*, vol. 30, no. 2, pp. 171–183, 2016.

[5] P. . W. Hunt, J. Brenchley, E. Sinclair et al., "Relationship between T cell activation and CD4+ T cell count in HIV-seropositive individuals with undetectable plasma HIV RNA levels in the absence of therapy," *The Journal of Infectious Diseases*, vol. 197, no. 1, pp. 126–133, 2008.

[6] A. D. Redd, D. Dabitao, J. H. Bream et al., "Microbial translocation, the innate cytokine response, and HIV-1 disease progression in Africa," *Proceedings of the National Academy of Sciences of the United States of America*, vol. 106, no. 16, pp. 6718–6723, 2009.

[7] A. Leon, L. Leal, B. Torres et al., "Association of microbial translocation biomarkers with clinical outcome in controllers HIV-infected patients," *AIDS*, vol. 29, no. 6, pp. 675–681, 2015.

[8] J. M. Brenchley, D. A. Price, T. W. Schacker et al., "Microbial translocation is a cause of systemic immune activation in chronic HIV infection," *Nature Medicine*, vol. 12, no. 12, pp. 1365–1371, 2006.

[9] T. W. Schacker, J. M. Brenchley, G. J. Beilman et al., "Lymphatic tissue fibrosis is associated with reduced numbers of naive CD4+ T cells in human immunodeficiency virus type 1 infection," *Clinical and Vaccine Immunology*, vol. 13, no. 5, pp. 556–560, 2006.

[10] S. I. Miller, R. K. Ernst, and M. W. Bader, "LPS, TLR4 and infectious disease diversity," *Nature Reviews. Microbiology*, vol. 3, no. 1, article BFnrmicro1068, pp. 36–46, 2005.

[11] A. Propato, E. Schiaffella, E. Vicenzi et al., "Spreading of HIV-specific CD8+ T-cell repertoire in long-term nonprogressors and its role in the control of viral load and disease activity," *Human Immunology*, vol. 62, no. 6, article S0198885901002452, pp. 561–576, 2001.

[12] J. D. Estes, L. D. Harris, N. R. Klatt et al., "Damaged intestinal epithelial integrity linked to microbial translocation in pathogenic simian immunodeficiency virus infections," *PLoS Pathogens*, vol. 6, no. 8, article e1001052, 2010.

[13] Z. Zhou, C. Bian, Z. Luo et al., "Progesterone decreases gut permeability through upregulating occludin expression in primary human gut tissues and Caco-2 cells," *Scientific Reports*, vol. 9, no. 1, article 44448, p. 8367, 2019.

Review Article

Innate Lymphoid Cells: Regulators of Gut Barrier Function and Immune Homeostasis

Hui Fan,[1] **Aiyun Wang** ⓘ**,**[1] **Yuan Wang,**[1] **Ye Sun,**[1] **Jing Han,**[1] **Wenxing Chen,**[1] **Shijun Wang,**[2] **Yuanyuan Wu** ⓘ**,**[1] **and Yin Lu** ⓘ[1]

[1]*Jiangsu Key Laboratory for Efficacy and Safety Evaluation of Chinese Material Medica, School of Pharmacy, Nanjing University of Chinese Medicine, Nanjing 210023, China*
[2]*Shandong Co-Innovation Center of TCM Formula, College of Traditional Chinese Medicine, Shandong University of Traditional Chinese Medicine, Shandong 250035, China*

Correspondence should be addressed to Yuanyuan Wu; ywu@njucm.edu.cn and Yin Lu; luyingreen@njucm.edu.cn

Innate lymphoid cells (ILCs), identified in the early years of this century as a new class of leukocyte family unlike the B or T lymphocytes, play a unique role bridging the innate and adaptive immune responses in mucosal immunity. Their origin, differentiation, and activation process and functions have caught global interest. Recently, accumulating evidence supports that ILCs are vital regulators for gastrointestinal mucosal homeostasis through interactions with other structural and stromal cells in gut epithelial barriers. This review will explore the functions of ILCs and other cells in maintaining gut homeostasis and feature the crosstalk between ILCs with other cells and potential pharmacotherapy targeting ILCs applicable in intestinal innate immunity.

1. Introduction

The gut barrier is a heterogeneous unit composed as a multilayer system and can be simplified as two components: a physical barrier surface and a deep functional barrier. The physical barrier surface prevents bacterial infiltration and adhesion and regulates paracellular diffusion to the host tissues while the deep functional barrier discriminates between pathogens and commensal microorganisms, organizing the immune tolerance and the immune response to pathogens [1]. There are many types of cells, microorganisms, mediators, and molecules constituting the gut barrier. The physical barrier then contains three major elements which are the intestinal mucosa, intestinal epithelial layer, and microbiota. The central element is the intestinal epithelial layer, which provides physical separation between the lumen and the body. The secretion of various molecules into the lumen reinforces the barrier function on the extraepithelial side, while a variety of immune cells provide additional protection below the epithelial layer. Among all the immune cells,

a group of lymphocytes which are termed innate lymphoid cells (ILCs) have been studied heavily in recent years and have important roles and close communications with other cells in the epithelial barrier. In this review, we are going to focus on the interaction and crosstalk among ILCs and other cells in the gut barrier and describe how they influence the barrier function and immune homeostasis.

1.1. First Line of Defense: Gut Barrier Function in Intestinal Physiology. The intestine represents a major gateway for potential pathogens, which also contains antigens from diets and extensive and diverse commensals that need to be tolerated. The gut barrier therefore plays important roles in intestinal physiology such as physical barrier, immune tolerance, pathogen clearance, and chronic inflammation. Its functions rely heavily on a complex group of cells and mediators in the tissue context containing structural cells such as epithelial cells, goblet cells, Paneth cells, and immune cells such as mast cells, dendritic cells, macrophages, and lymphocytes (Figure 1). We will give a brief
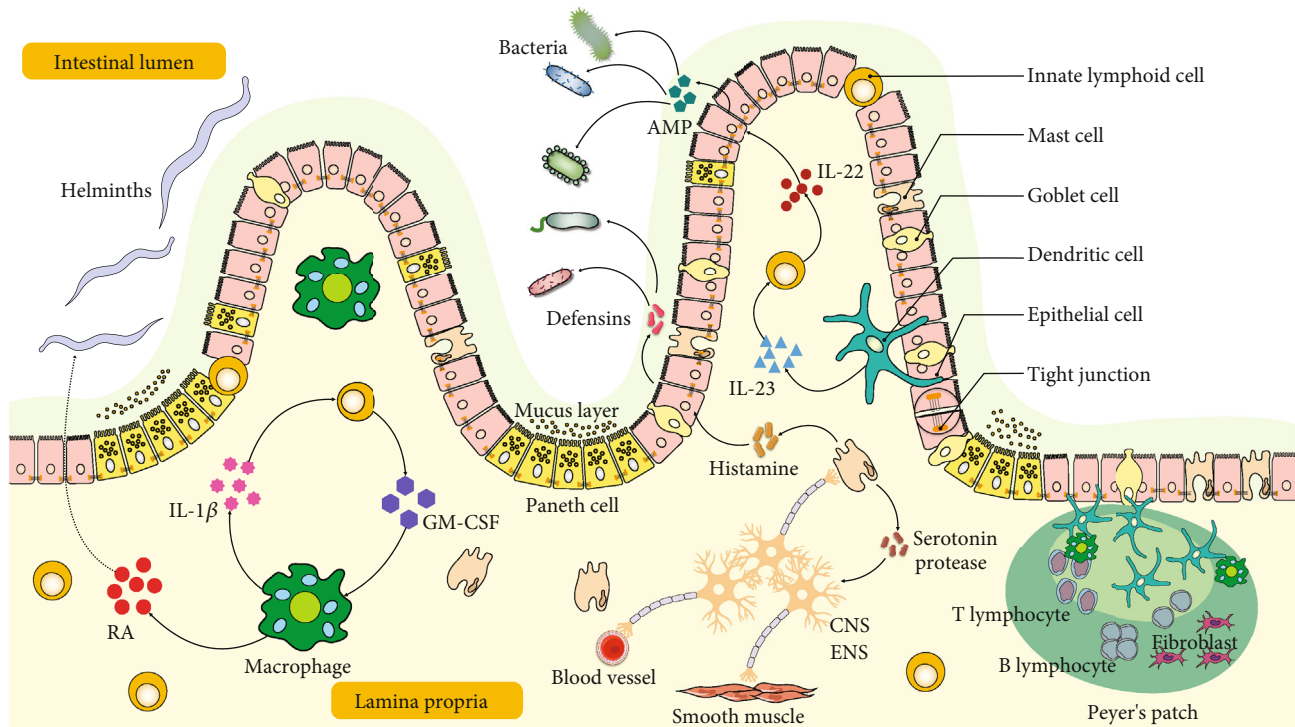
Figure 1: Illustration of intestinal barrier structure and functions. The intestine barrier contains the chemical barrier and the physical barrier. The chemical barrier is composed of antimicrobial peptides (AMPs) such as amphiregulin. It provides chemical agents attacking invading microorganisms including bacteria and helminths. The physical barrier includes the mucus layer and cell junctions between the epithelium. It serves as the wall spatially separating the invading microorganisms and host. There are many types of cells in the gut epithelium regulating the epithelium function. Disruption of the intestinal barrier allows the leak of gut bacteria from the lumen into the lamina propria, inducing excessive immune responses of the host immune cells. Retinoic acid (RA) released by macrophages or dendritic cells assists in host resist helminthic infection. IL-22 released by ILCs promotes epithelial cells secreting AMP in response to bacterial infection, which is regulated by IL-23 from dendritic cells. Moreover, macrophage-derived IL-1β promotes ILCs' production of GM-CSF, which further stimulates more macrophage differentiation from monocytes. The enteric nervous system including neuron and glial cells interacts closely with mast cells and regulates blood vessels. IL: interleukin; AMP: antimicrobial peptide; GM-CSF: granulocyte-macrophage colony stimulating factor; RA: retinoic acid; ENS: enteric nervous system; CNS: central nervous system.

description on the role of individual component cells in the gut barrier.

1.2. Intestinal Epithelial Cells. Intestinal epithelial cells constitute the majority of the cellular layer of the gut barrier. The weakening of intercellular junctions between intestinal epithelial cells will result in increased intestinal permeability and systemic exposure to bacterial antigens. The increased diffusion of bacterial components into the blood, lymph, and other extraintestinal tissues is closely related with critical illness, inflammatory bowel disease, celiac disease, food allergy, irritable bowel syndrome, and metabolic syndromes such as diabetes and obesity [2–4]. Therefore, intestinal epithelial permeability provides a novel target for disease prevention and therapy [5, 6].

In intact intestines, the intercellular junctions are primary determinants of normal barrier function. There are many kinds of intercellular junctions including the tight junction, adherens junction, gap junction, desmosome, and hemidesmosome. Tight junctions (TJs) are connected areas of the plasma membrane that stitch cells together therefore consisting a series of anastomosing strands. TJs play leading roles in paracellular permeability. Claudins, occludin, and ZO family proteins are critical components of TJs. Claudins are the most important tetratransmembrane TJs. Their extracellular domains form pores on adjacent cells and regulate TJ ion selectivity [6, 7]. Expression levels of the claudin protein are related with the intestinal barrier integrity in different ways depending on the type of claudin isoform [8]. For example, the downregulation of claudins 5 and 8 can drastically reduce the barrier integrity [9]; in contrast, claudin-2, required for the formation of paracellular water channels, is upregulated in IBDs and is highly expressed in leaky epithelial tissues and promotes inflammation [10]. Occludin is the first identified and an important protein for TJ stability. It has a dual role in the intestinal barrier. The expression of occluding was closely correlated with the barrier function both in vitro and in vivo [8, 11]. Interestingly, genetic manipulated mice which were deprived of occluding showed stability in several epithelial tissues including gastric and intestinal epithelia [12, 13]. Collectively, the functions of occludin and the mechanism by which occludin regulates the TJ are complex and still remain elusive. Unlike claudins and occludins which are integral membrane proteins and function as a gate, ZOs are peripheral membrane-associated proteins linking membrane protein to the cytoskeleton and ubiquitously

expressed in epithelial and endothelial cells [14]. The various isoforms, ZO-1, ZO-2, and ZO-3, are all characterized by their ability to interact with different cellular proteins such as claudins or occludins through a multitude of protein-binding domains, such as the SH3 domain, the PDZ domain, and the leucine-zipper domain. In DSS-induced colitis mouse models, complete loss of ZO-1 expression occurred during the preinflammatory stage [15]. Adherens junctions join the actin filaments of neighboring cells together. Gap junctions are clusters of channels that form tunnels of aqueous connectivity between cells. Desmosomes are even stronger connections that join the intermediate filaments of neighboring cells. Hemidesmosomes connect intermediate filaments of a cell to the basal lamina, a combination of extracellular molecules on other cell surfaces.

1.3. Goblet Cells. Goblet cells secrete mucins which constitute the hydrated gel coated on the luminal surface of the intestinal mucosa. The mucus layer is the front line of innate host defense and prevents large particles and bacteria from coming into direct contact with the underlying epithelium. In the small intestine, the goblet cell-secreted Muc2 mucin, which is the first human secretory mucin to be identified and characterized, constitutes the main component of the mucus layer [16]. The mucin structure is markedly altered in colitis mouse models, and transgenic mice lacking *Muc2* gene developed colitis spontaneously [17]. Besides the secretory mucin glycoproteins (MUC2), goblet cells synthesize many bioactive molecules such as epithelial membrane-bound mucins (MUC1, MUC3, and MUC17), trefoil factor peptides (TFF), resistin-like molecule β (RELMβ), and Fc-γ binding protein (Fcgbp) [18].

Mucin secretion is frequently coupled with increased synthesis of mucins. The biology of mucin compositions and syntheses have been summarized in details [19]. Activation of mucin synthesis can be induced Th1 cytokines (e.g., tumor necrosis factor- (TNF-) α) and Th2 cytokines (e.g., interleukin- (IL-) 4, IL-13), microbial products (e.g., lipopolysaccharide (LPS)), and neuropeptides. The regulation of mucin expression is controlled either by transcriptional regulation or by epigenetic regulation [18]. Due to the potent binding site in MUC2 promoters, cumulative evidences indicate that transcriptional regulation of *MUC2* is mediated by transcription factor nuclear factor- (NF-) κB, a common activated transcription factor during inflammation in the gastrointestinal tract [20, 21], intestine-specific transcription factors Cdx-1 and Cdx-2 [22], forkhead box transcription factors Foxa1 and Foxa2 [23], and CREB/ATF1 [24]. Epigenetic regulation includes DNA methylation, histone modifications, and microRNA silencing. *MUC2* gene expression is regulated closely by DNA methylation and histone modifications in the $5'$ flanking region of *MUC2* promoter [25]. In mucinous and nonmucinous colorectal cancer tissues, *MUC2* expression is downregulated by methylation of CpG islands in the specific regions of *MUC2* promoter [26].

1.4. Paneth Cells. Paneth cells reside mainly in small intestine epithelium and are located at the base of crypts of Lieberkühn (just below the intestinal stem cells in the intestinal glands) and contribute to intestinal innate immunity by secreting a diverse repertoire of antimicrobial peptides and proteins [27].

Paneth cells are vital in controlling intestinal barrier penetration by commensal and pathogenic bacteria. They sense enteric bacteria through cell-autonomous MyD88-dependent toll-like receptor (TLR) activation, triggering expression of multiple antimicrobial factors such as lysozyme and defensins (called cryptdins in mice) [28]. Defensins are the principal molecules secreted by Paneth cells. Defensins have a hydrophobic domain which can interact with phospholipids on bacterial cell membranes and thus lead to bacteria cell lysis. Paneth cells are daughter cells differentiated from intestinal stem cells [27]. Interestingly, a recent ex vivo study by Dr. Han Clevers group showed that Paneth cells lose their secretory expression signature, reenter the cell cycle, and acquire stem-like properties, contributing to the tissue regenerative response to inflammation [29].

1.5. Mast Cells. Mast cells in the gastrointestinal (GI) tract are located in close proximity to sensory nerve fibers, which by communicating bidirectionally play roles in the brain-gut axis [30, 31]. The interactions between mast cells and enteric neurons ensure the function of the enteric nervous system (ENS) regulation of the GI tract physiology such as motility, secretion, and microcirculation as well as immune responses [32, 33]. Moreover, the interactions are closely correlated with severity and frequency of GI tract disorders such as abdominal pain [34]. Mast cells in the GI tract comprise 1-5% of mononuclear cells in the lamina propria, submucosa, and epithelial layers [30]. Mast cells are derived from the myeloid stem cells and are similar to granulocytes. They exert their functions in two steps, which contain activation inducing degranulation and release of inflammatory mediators, including histamine, cytokines, proteoglycans, and proteases [35]. They contribute to innate and acquired immunities and are important effector cells in host defense in GI tracts overloaded every day with external stimuli such as food, pathogens, toxic substances, commensal flora, and moreover endogenous small molecules such as neurotransmitters, neuropeptides, growth factors, and hormones. Generally, mast cell activation is classically stimulated by interaction of antigens coming from allergens with its specific IgE antibody bound to the mast cell membrane through the high-affinity receptor FcεRI [36]. Besides, mast cells also express receptors for IgG (FcRI), immunoglobulin free-light chains (IgLCs), other Ig-associated receptors, complement fractions, and toll-like receptors. Activation via one of these receptors results in phosphorylation cascades and activation motifs that lead to intracellular calcium flux, activation of transcription factors such as activator protein 1 (AP-1), microphthalmia-associated transcription factor (MITF), and signal transducers and activators of transcription 5 (STAT-5) and downstream protease, cytokines, and mediator expression [30, 32]. Based on different protease contents, most mast cells can be divided into two categories: MC_T containing mainly tryptase and MC_{TC} containing

tryptase, chymase, and carboxypeptidases [33, 37]. In the GI tract, MC_T comprise ~98% of all mast cells in the mucosa and ~13% of all mast cells in the submucosa [33].

1.6. Dendritic Cells. Dendritic cells (DCs) are key modulators that shape the immune system. In mucosal tissues, DCs play surveillance roles to sense infection and also function as the major antigen-presenting cells that stimulate the differentiation of naive T cells. They function in bridging the innate signaling and adaptive immune systems to maintain the homeostasis of the intestinal immune environment [38]. Besides, DCs are able to open tight junctions and to sample antigens directly across the epithelium both in vivo and in vitro [39]. Intestinal DC can be divided into several subsets based on the surface expression of integrins CD11c and CD103. More recently, CD24 and Sirpα have been introduced for better discrimination of DCs from macrophages [40].

Although DCs are located primarily in lamina propria and mucosa-associated lymphoid tissues rather than in the epithelial barrier, DCs have intimate interactions with the epithelial layer. Goblet cells were shown to transfer small soluble antigens from the intestinal lumen to CD103+ DC [41]. Chemokines secreted by enterocytes in response to TLR ligand exposure can induce the above-mentioned relocation of lamina propria DC to the epithelium [42]. Epithelial and stromal cells secrete factors, which are thought to induce DC tolerance, such as RA, TGF-β, PGE-2, and TSLP [43]. Establishing intestinal tolerance is critical for the prevention of intestinal diseases such as IBD, and manipulating mucosal DCs provides potential therapeutic strategies to protect against infectious diseases.

1.7. Macrophages. The intestine contains the largest pool of macrophages in the body. Located in the subepithelial lamina propria, intestinal macrophages are the most abundant mononuclear phagocytes. They maintain mucosal homeostasis by capturing and eliminating bacteria that cross the epithelial barrier and meet the constant phagocytosis need for epithelial renewal [43, 44]. They are important components of protective immunity and are involved in the pathology of inflammatory bowel disease (IBD) [45]. Macrophage-restricted IL-10 receptor deficiency causes severe spontaneous colitis [46]. Mouse model genetically inactivation of stat3 in macrophages will develop inflammation in the colon spontaneously and tumor lesions including invasive carcinoma with a frequency similar to that observed in human IBD patients [47].

Defining the biological roles of intestinal macrophages, characterizing the phenotype, and defining the origins of different populations of myeloid cells in the mucosa have been studied quite extensively recently [45]. Intestinal macrophages originate from yolk sacs or fetal livers at the embryonic stage and are replaced in the gut by $Ly6C^+$ blood monocytes shortly after birth [48]. In adult guts, they undergo continuous renewal from monocyte-derived cells. In the process differentiation, monocytes lose Ly6C expression while other macrophage surface markers are upregulated such as MHCII, F4/80, CD11c, and CX3CR1 [43, 49].

While it has been known for many years that macrophages are present in deeper layers of the gut wall, only recently has work begun to interrogate their role in intestinal homeostasis [44]. Macrophages are also found in the submucosa, and recent depletion studies have revealed a role for these cells in maintaining the integrity of the submucosal vasculature [50].

1.8. Intraepithelial Lymphocytes. The intraepithelial lymphocytes (IELs) that reside between the intestinal epithelial cells (IECs) form one of the main branches of the immune system [51]. The small intestine contains approximately 1 IEL per 10 intestinal epithelial cells (IECs), and this ratio is lower in the colon [52]. IELs are resident in the intestinal epithelium and do not recirculate [53]. They express several characteristic surface receptors such as the chemokine receptor CCR9, which interacts with CCL25 produced by IECs and thus assists in recruiting IELs to the gut mucosa [52]. Intestinal IELs also express integrin αEβ7 ($α_E$ is also known as CD103), which interacts with E-cadherin on enterocytes to facilitate entry and retention in the intestinal epithelium. Approximately 90% of all IELs express T cell receptors (TCRs), and these cells have been the main focus of studies on IEL biology.

1.9. Neurons. Intestinal neurons can be classified as intrinsic and extrinsic. The former can also be termed as enteric neurons which have cell bodies within the gut, while the latter refers to neurons which have cell bodies located outside the intestine such as sympathetic and parasympathetic autonomic nervous systems [54]. The intestine is the largest immune cell compartment with millions of enteric neurons in the body. Therefore, it is also called the second brain [55]. Enteric neurons include myenteric and submucosal neurons. Submucosal neurons control gut secretions, nutrient absorption, and local blood flow whereas myenteric neurons orchestrate smooth muscle contractions [56, 57] (Figure 1).

Apart from enteric neurons, there are enteric glial cells found in enteric ganglia in lamina propria and smooth muscle [54]. They outnumber enteric neurons. Together, they constitute the enteric nervous system (ENS), which could continuously extend from the base of the crypts to the mucosa. Glial cells are vital to intestinal barrier integrity. Complete deletion of glial cells leads to fatal jejunoileitis in mice due to barrier integrity disruption [58, 59]. However, partial conditional depletion of enteric glial cells failed to induce inflammation and barrier disruption in intestines [60]. Enteric glial cells participate in sensing pathogens and produce neurotrophic factors and help maintain the epithelial barrier integrity. Finally, when neurons are damaged, enteric glial cells can transdifferentiate into enteric neurons to compensate [54].

1.10. Innate Lymphoid Cells in the Gut Barrier. Innate lymphoid cells (ILCs) are a relatively recently discovered

TABLE 1: List of some important studies in ILC research history.

Years	Events	Reference #
1975	Discovery of NK cells as the first subsets of ILCs	[63]
1997	Discovery of LTi cells (later defined as one subset of ILC3s) which are essential for the development of lymph nodes during embryogenesis	[64]
2006	Characterization of GATA3 and CD127 on ILC2s	[65]
2009	ILC3s are the source of endogenous IL-22 and constrain inflammation at the mucosal site	[66]
2010	Identification of ILC2s in mice that produce type 2 cytokines and contribute to antihelminth immunity and type 2 inflammation	[67]
2010	Identification of a role for ILC3-like cells in promoting intestinal inflammation	[68]
2011	First description of a tissue-protective role for ILC2s, describing how ILC2s produce amphiregulin, a ligand of EGFR, and contribute to lung-tissue repair following influenza A virus infection in mice	[69]
2013	First evidence of non-NK cell ILC1s in humans and the transcription factor T-bet responsible for ILC1s differentiation	[70, 71]
2013	First evidence that ILC3s directly regulate adaptive immune responses	[72]
2013	Experts described consensus nomenclature for ILC subsets	[73]

lymphocytes compared to its other counterpart lymphocytes such as Th cells or Th17 cells. ILCs do not express the type of diversified antigen receptors expressed on T cells and B cells, and they are largely tissue-resident cells and are deeply integrated into the residential tissues [61]. While adaptive lymphocytes are most numerous in lymphoid organs—hence the derivation of the term "lymphocyte"—ILCs are relatively rare in primary and secondary lymphoid tissues. Consequently, their existence has been overlooked for many years, as immunologists focused efforts on peripheral blood and lymphoid organs. However, it is now recognized that their positioning in peripheral tissues particularly abundant at barrier surfaces in the lung, skin, and intestinal tract affords a strategic advantage for ILCs as early responders to tissue perturbation. Indeed, as a result of their location and effector phenotype, ILCs are rapid-responding cells and they produce cytokines within hours of activation, in contrast to the days required for naive adaptive lymphocytes to be primed, expand, differentiate, and enter tissues [62]. Table 1 lists some of the remarkable findings in ILC research history about ILC discovery, identification, and functions.

ILCs have been identified with many subtypes mainly divided into three groups. Group 1 ILCs include noncytotoxic ILC1s and cytotoxic conventional NK cells. Conventional NK cells were first discovered in 1975 and have been studied well with a longer history compared to other types of ILCs. Many of their functions, interaction with microbiota, antitumor responses, and involvement in the gut barrier have been investigated and reviewed in details elsewhere [74, 75]. Hence, we are not going to review this part here. We will term group 1 ILCs as ILC1s thereafter. ILC1s are regulated by T-bet and can produce IFN-γ, GM-CSF, granzyme, and perforin in response to IL-12, IL-18, or other activators such as pathogens or tumors. They cooperate with Th1 cells against intracellular microbes such as viruses, bacteria, or parasites [71, 73, 76, 77]. Group 2 ILCs (ILC2s), similarly to Th2, express Gata3 and can produce IL-4, IL-5, IL-13, IL-9, and amphiregulin in response to IL-25, IL-33, and TSLP (thymic stromal lymphopoietin). ILC2s are essential in the immune response against large extracellular parasites and allergens. Their production of antimicrobial peptides promotes tissue damage repair [78, 79]. A recent discovery published by Huang et al. on *Science* by using mouse models and advanced imaging techniques to monitor ILC activation and movement showed that ILC2s originate in the gut, enter lymphatic vessels, circulate in the bloodstream, and can migrate to other organs to help fight infection against helminth [80]. The trafficking of ILC2s is in a partly sphingosine 1-phosphate- (S1P-) dependent manner [80]. Group 3 ILCs (ILC3s), mirroring Th17, express RORγt, the lymphotoxins α and β, IL-17 and IL-22, GM-CSF, and TNF-α. They can be activated by IL-23 and IL-1β or by NCR ligands, and they combat extracellular microbes, such as bacteria and fungi [77] (Table 2).

The classification of ILCs into ILC1, ILC2, and ILC3 subsets is a simplified theoretical approach for understanding ILC diversity. ILC function and differentiation programs are more complicated during immune responses. Heterogeneity and plasticity of ILCs have been identified in both human and mouse studies. Tissue-resident T-bet+ ILC1s may derive from four sources in humans: ILC precursors (ILCP); converted ILC2s exposed to IL-12 and IL-1β; converted ILC3s exposed to IL-2, IL-15, and IL-23; and NK cells exposed to TGF-β [81, 82]. Bernink and colleagues reported bidirectional plasticity between ILC1 and ILC3 in the intestinal lamina propria with different environment stimuli such as IL-23, IL-1β, retinoic acid, or dendritic cells [83].

2. Crosstalk between Innate Lymphoid Cells and Other Immune Cells

2.1. Crosstalk between Innate Lymphoid Cells and Dendritic Cell

TABLE 2: Innate lymphoid cells in the gut.

Types	Surface marker		Stimulus	Regulatory transcription factor	Signature released cytokines	Functions in the gut barrier
	Mouse	Human				
ILC1	CD160 NKp46 NK1.1	CD103 CD160 CD56 NKp46 NKp44	IL-12, IL-15	T-bet	IFN-γ, TNF-α, GM-CSF, granzyme, perforin	Defense against virus, pathogens
ILC2	IL17RB IL-33R CD25 CD127	IL17RB IL-33R CD25 CD127 CRTH2	IL-25, IL-33, TSLP	GATA3	IL-4, IL-5, IL-13, IL-9, amphiregulin	Helminth expulsion
ILC3	NKp46	NKp44	IL-1β, IL-23, NCR ligand	RORγT	IL-17, IL-22, GM-CSF, TNF-α	Defense against bacteria, fungi

2.1.1. ILC1s and DCs. ILCs are characterized by prompt response after infection or injury. Tissue-resident ILC1 confer early host protection at initial sites of viral infection [84]. In a mouse model infected with pathogenic DNA viruses, Wong et al. have found that migratory dendritic cells (mDCs) induce expression of NKG2D ligands after sensing the double-stranded DNA virus via TLR9/MyD88 and promote IFN-γ expression in classical NK cells and group 1 ILC (mainly NK cells) already in draining lymph nodes (dLNs) through NKG2D (Figure 2). Inflammatory monocytes are also recruited to dLNs by mDCs in a TLR9/MyD88-dependent manner responding to IFN-γ [85].

2.1.2. ILC2s and DCs. Crosstalk between ILC2s and DCs is believed to be necessary in the host to combat parasitic helminth infection executed by type 2 immune responses [78]. DCs are well-defined for antigen presentation and type 2 chemokine production during the memory Th2 cell recall-response, and it is also known that DCs can be stimulated by type 2 cytokines to produce chemokines CCL17 and CCL22, which attract its cognate-receptor CCR4-expressing memory TH2 cells. ILC2s act upstream of DCs and are essential for their production of memory TH2 cell chemoattractant CCL17. At the barrier sites, ILC2s respond to helminth infection and become activated by alarmins including IL-25, IL-33, and TSLP secreted by epithelium in the gut as an important early cellular event and produce high amounts of type 2 cytokines [86] (Figure 2). Halim et al. have reported that ILC2s-produced IL-13 has been linked to the migration of DCs in allergic asthma [87]. This interaction has been extended by Oliphant et al. that ILC2s and T cells cooperate through MHCII-dependent activation to promote DC migration to the draining lymph nodes to potentiate the Th2 generation from naïve T cells against helminth infection [78]. However, how IL-13 controls the migratory function of DCs still remains elusive.

2.1.3. ILC3 and DCs. The interactions between ILC3 and DCs are discussed below in ILC3 and Macrophages.

2.2. Crosstalk between Innate Lymphoid Cells and Macrophage

2.2.1. ILC1 and Macrophages. Studies on ILC1 and macrophages in intestinal tract have been scarce. Recent studies in inflammatory bowel disease animal models and intestinal infection with parasites such as *Toxoplasma gondii* have shown that ILC1s secrete IFN-γ and TNF-α and contribute to the inflammatory response and pathology in response to IL-12 and IL-15 together with macrophages [71, 88–90] (Figure 3(a)). However, studies of their interactions in obesity have shown promise. ILC1 displayed cytotoxic activity toward adipose tissue macrophages. During obesity, this killing ability was impaired and ILC1s were reported to be the major contributors for IFN-γ upregulation resulting in the expansion of proinflammatory M1 macrophages, and this could lead to the accumulation of pathogenic proinflammatory macrophages [91]. This interaction contributes to M1 macrophage polarization and systemic insulin resistance [92].

2.2.2. ILC2s and Macrophages. ILCs can promote plastic macrophages to differentiate into alternatively activated macrophages (or M2 macrophages) in some helminth infection models to provide protective functions and tissue repair responses against helminth infection [93]. IL-25- or IL-33-activated ILC2s were found to promote M2 polarization and Treg cell expansion contributing protective immunity [94]. IL-33-activated ILC2s induced M2 polarization through IL-4 receptor signaling and directly regulated beige fat biogenesis [95]. IL2Cs has also been described to promote M2 macrophage accumulation in visceral adipose tissue during helminth infection [96, 97] (Figure 3(b)). In an airway barrier, alveolar macrophages can secrete IL-33 which will elicit direct activation of ILC2cs to produce substantial amounts of IL-13 [97]. This crosstalk in gut barriers needs to be confirmed.

2.2.3. ILC3 and Macrophages. Intestinal mucosal tissue-resident macrophages together with DCs are the two main
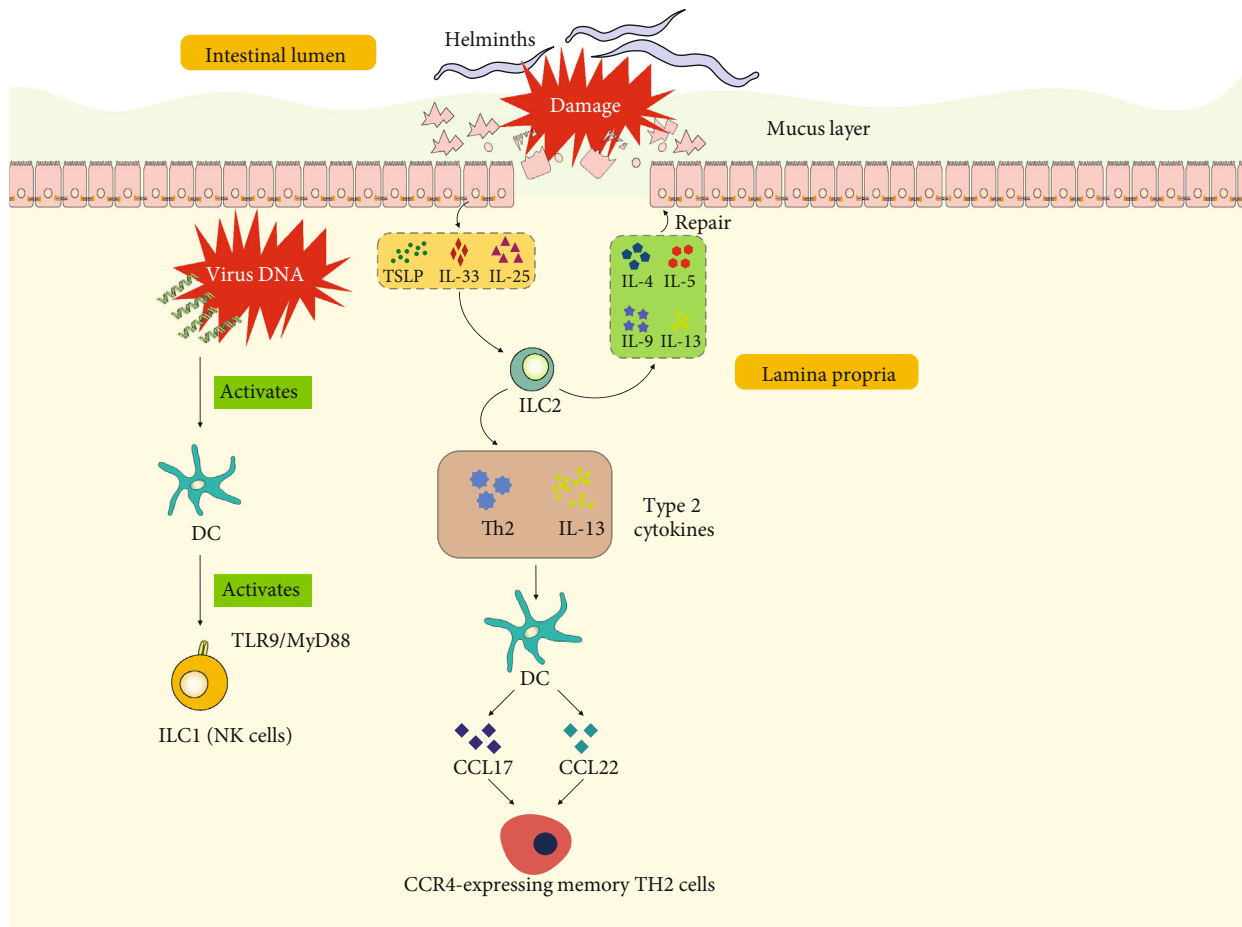
FIGURE 2: Illustration of interactions of ILCs and DCs in the intestinal tract. At the initial site of viral infection, virus DNA activates DCs, further activating ILC1 (mainly NK cells) by the TLR9/MyD88 pathway. After damage caused by helminths, epithelial cells produce TSLP, IL-33, and IL-25. These cytokines stimulate ILC2s producing type 2 cytokines including IL-4, IL-5, IL-9, and IL-13 which participate in repair of epithelial cells and mucus layer. In addition, ILC2-derived Th2 and IL-13 stimulate DCs, inducing the release of CCL17 and CCL22 and recruitment of CCR4-expressing memory TH2 cells. IL: interleukin; TSLP: thymic stromal lymphopoietin; DC: dendritic cell; ILC: innate lymphoid cell; CCL: chemokine (C-C motif) ligand; Th: helper T cell.

cell populations to detect microbial signals and to capture and process extracellular antigens. Meanwhile, macrophages and DCs contribute to the maintenance of immune tolerance by the induction or expansion of FoxP3$^+$ Treg cells in the intestine by producing retinoic acid (RA). GM-CSF (or Csf-2) is needed to maintain DCs and macrophage numbers in the colon as well as for the Treg cells. A seminal work by Mortha et al. demonstrated that RORγt$^+$ innate lymphoid cells (ILC3s) are the primary source of GM-CSF in the gut and that ILC-driven GM-CSF production was dependent on the ability of macrophages to sense microbial signals [98]. Macrophages detect microbial signals through a TLR-MyD88-dependent manner and produce interleukin-1β, which can act on ILC3s [98] (Figure 3(c)).

2.3. Crosstalk between Innate Lymphoid Cells and Epithelial Cells

2.3.1. *ILC1s and Epithelial Cells.* ILC1s are enriched in the upper GI tract [99]. In murine models, ILC1s protect epithe-

lial cells. *Helicobacter typhlonius* is commensal in the murine microbiota that closely resembles *Helicobacter pylori*, the frequent colonizer of the human stomach associated with gastritis, peptic ulcer, and gastric cancer. Mice lacking T-bet, the transcription factor controlling ILC1s differentiation, develop colitis triggered by *Helicobacter typhlonius* [100]. This result shows that ILC1 participate in the defense against bacterial infection. During pathological bacteria *Salmonella* infection at the intestinal tract, ILC1s are the main source of IFN-γ, which drives the secretion of mucus-forming glycoproteins required to protect the epithelial barrier [101].

2.3.2. *ILC2s and Epithelial Cells.* ILC2 activation is dependent on epithelial-derived cytokines, such as IL-25, IL-33, and TSLP [97], prostaglandin D2 (PGD2) [102], and leukotriene D4 [103]. After activation, ILC2 secrete type 2 cytokines such as IL-4, IL-5, IL-9, and IL-13, which have tissue repair functions and will eventually protect epithelial cells [97].

2.3.3. *ILC3 and Epithelial Cells.* ILC3s protect the intestinal epithelial cells and maintain the homeostasis against various
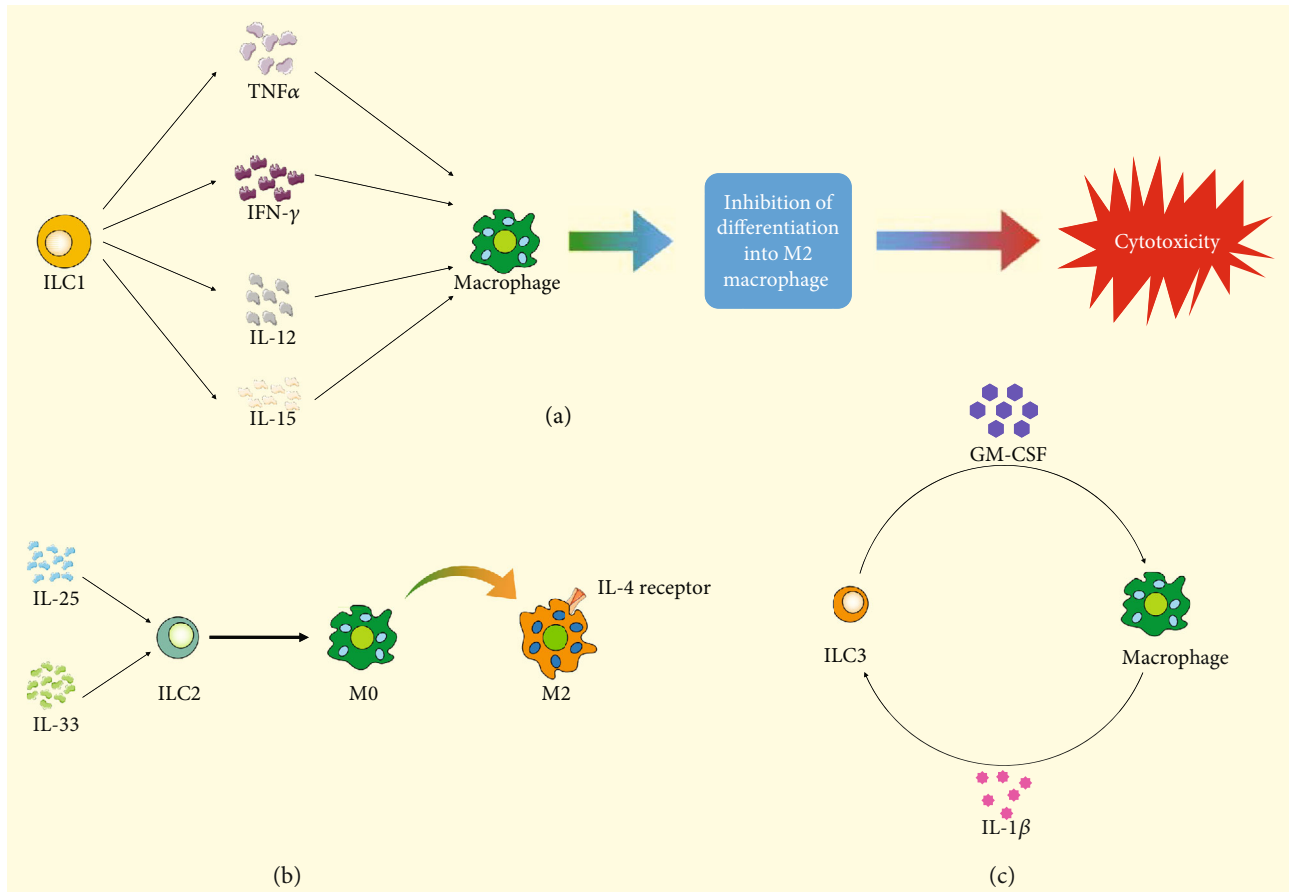
FIGURE 3: Illustration of interactions of macrophages and different ILCs. (a) TNF-α, IFN-γ, IL-12, and IL-15 released from ILC1 stimulate macrophage differentiating into cytotoxic macrophage and inhibit differentiation into M2 macrophage differentiation. (b) After being stimulated by IL-25 and IL-33, ILC2 promotes the transformation of M2 macrophage from M0 macrophage. (c) The crosstalk of ILC3 and macrophage is mainly induced by GM-CSF and IL-1β. ILC: innate lymphoid cell; TNF: tumor necrosis factor; IL: interleukin; M0: M0 macrophage; M2: M2 macrophage; GM-CSF: granulocyte-macrophage colony stimulating factor.

pathogens. The protective role of ILC3s on epithelial cells is fulfilled by signature cytokine IL-22 released by ILC3s. Upon activation, ILC3s secrete IL-22, IL-17, and GM-CSF. IL-22 is a member of the IL-10 family and displays a homologous secondary structure, binding to its heterodimeric receptors IL-22R1 and IL-10R2 on epithelial cells. IL-22 signaling orchestrates the production of mucin and mediates epithelial cell proliferation and survival upon infection [104]. Mechanistically, IL-22 promote the production of nucleotide oligomerization domain-containing protein 2 (NOD2), which functions as a mammalian cytosolic pathogen recognition molecule. NOD2 associates with the caspase activation and recruitment domain of RIP-like interacting caspase-like apoptosis regulatory protein kinase (RICK)/-RIP2 and activates nuclear factor- (NF-) κB in epithelial cells [105]. The activation of NF-κB induces epithelial cells to produce antimicrobial peptides and mucin. Moreover, ILC3-derived IL-22 can induce STAT3 phosphorylation and activate Lgr5$^+$ intestinal stem cells for epithelial regeneration to impede tissue damage [106, 107] (Figure 4(a)). In addition, ILC3s protect epithelial cells from gut bacteria by adjusting intestinal epithelial cell glycan metabolism. ILC3s have been reported to induce the expression of fucosyl-

transferase 2 (*Fut2*), which catalyze fucosylation in intestinal epithelial cells in mice [108]. This induction requires the cytokines IL-22 and lymphotoxin produced by ILC3s. Fucosylation is a major mechanism of commensal bacteria utilizing dietary carbohydrate in the host. Disruption of intestinal fucosylation results in increased susceptibility to infection by pathological bacteria such as *Salmonella typhimurium* [108] (Figure 4(b)).

2.4. Crosstalk between Innate Lymphoid Cells and Gut-Associated Lymphoid Tissue (GALT). GALT is a major component of the mucosa-associated lymphoid tissue (MALT) in the gut. It is the sensor for luminal content and is critical to lymphoid maturation, activation, and differentiation. It comprises isolated and aggregated lymphoid follicles, cryptopatches (CPs), and tertiary lymphoid tissue. ILCs play a central role within GALT. Prenatal GALT development is dependent on ILC lymphoid-inducer function. Postnatally, these cells rapidly respond to commensal and pathogenic intestinal bacteria, parasites, and food components by polarized cytokine production such as IL-22, IL-17, or IL-13 and further contribute to GALT formation and function [109].
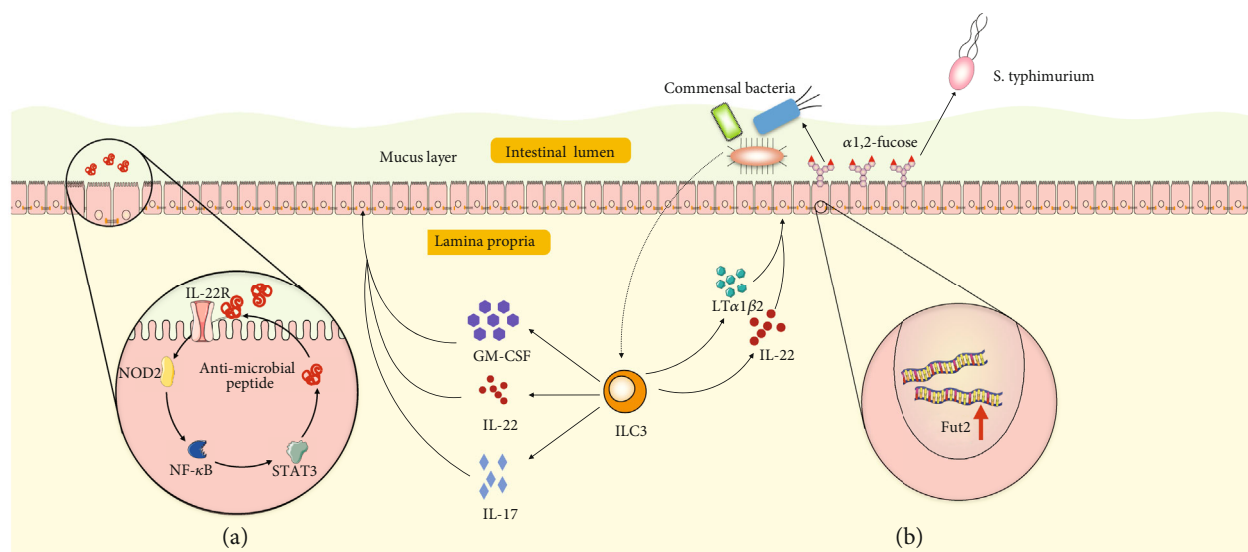
FIGURE 4: Illustration of epithelial cells and ILC3 interactions. (a) After bacterial infection, ILC3-derived GM-CSF, IL-22, and IL-17 stimulate epithelial cells by activating the IL-22R-NOD2-NF-κB signaling pathway and result in epithelial cells secreting antimicrobial peptides into the mucus layer. (b) ILC3-derived IL-22 and lymphotoxin (LT$\alpha1\beta2$) induce fucosyltransferase 2 (Fut2) gene expression in epithelial cells and result in fucose production in the intestinal tract. Fucose can be utilized by commensal bacteria but not by pathological bacteria such as *Salmonella typhimurium*. ILC: innate lymphoid cell; GM-CSF: granulocyte-macrophage colony stimulating factor; NOD2: nucleotide oligomerization domain-containing protein 2; NF-κB: nuclear factor- (NF-) κB; STAT3: signal transducers and activators of transcription 3.

2.5. Crosstalk between Innate Lymphoid Cells and Neurons in the Gut.

At mucosal barriers, ILCs reside in close proximity to neurons and glial cells, and the crosstalk composes the functional neuron-ILC units [54, 110].

In response to helminthic infection, intestinal cholinergic neurons regulate ILC2 function via production of neuromedin U (NMU) [111, 112]. NMU signals through NMU receptor 1 (NMUR1) expressed in ILC2s and leads to a rapid and potent production of type 2 inflammatory cytokines, IL-5 and IL-13, and of the tissue-protective cytokine amphiregulin (Figure 5) [111, 112]. In vivo activation of this signaling axis enhances ILC2 responses and confers immediate tissue protection against helminthic infection. Subsequently, neuron-ILC2 units were identified as part of a neuron-based regulatory circuit that dampens ILC2-mediated type 2 inflammation [113]. ILC2s express the β2-adrenergic receptor and colocalize with adrenergic neurons in the intestine. Abrogation of β2-adrenergic receptor-mediated signaling resulted in increased ILC2 responses, type 2 inflammation, and lower helminth infection burden, effects that were reversed by β2-adrenergic receptor agonist treatment [113]. Together, these studies demonstrate that ILC2s can integrate the cholinergic and sympathetic neuronal pathways to fulfill complex regulatory functions against helminth infection.

A cutting-edge study by Ibiza et al. revealed that enteric ILC3s are part of neuroglia-ILC3 units which are orchestrated by neurotrophic factors [114]. Enteric glial cells sense microbial and host alarmin cues, which leads to increased glia-derived production of neurotrophic factors that in turn induce IL-22 production by RET (a receptor for neurotrophic factors)-expressing ILC3s. Consequently, this glia-ILC3 axis is necessary for intestinal tissue repair upon inflammatory and infection insults [114].

3. Regulation of Innate Lymphoid Cells and Pharmacological Potentials in Intestinal Innate Immunity

Due to the close interactions with other cells and prompt response to enteric bacteria or injury in the intestinal tract, intestinal ILCs may be targeted to manipulate immune responses early during vaccination, immunotherapy, and inflammatory pathology. Therefore, it is imperative to study comprehensively the fundamental molecular signals that regulate ILC diversity and functions. Although ILC-specific targets have not yet been identified, the activation pathways and effector molecules that can modulate ILC may provide potential therapeutic benefits.

3.1. ILC Transcriptional Checkpoint Targeting Strategy.

Based on the transcription factors that govern the cell differentiation, function, and signature cytokine production, RORγt inhibitors have been identified primarily to block Th17-mediated inflammatory pathology [115–117]. These inhibitors can be used to block ILC3s as well, although there is a study showing that inhibition of RORγt selectively targets IL-17 producing iNKT and γt-T cells but not IL-22-expressing cells [118]. Similar strategies targeting the important transcriptional checkpoint may be followed such as modulation of the activity of NK cells and ILC1s by targeting T-bet [119]. However, selective loss of T-bet in ILC1s leads to the expansion and increased activity of ILC2s [120]. The controversy or unexpected results demonstrate that we still need to study comprehensively the functions and signaling pathways that regulate the pathogenic or protective immune responses.
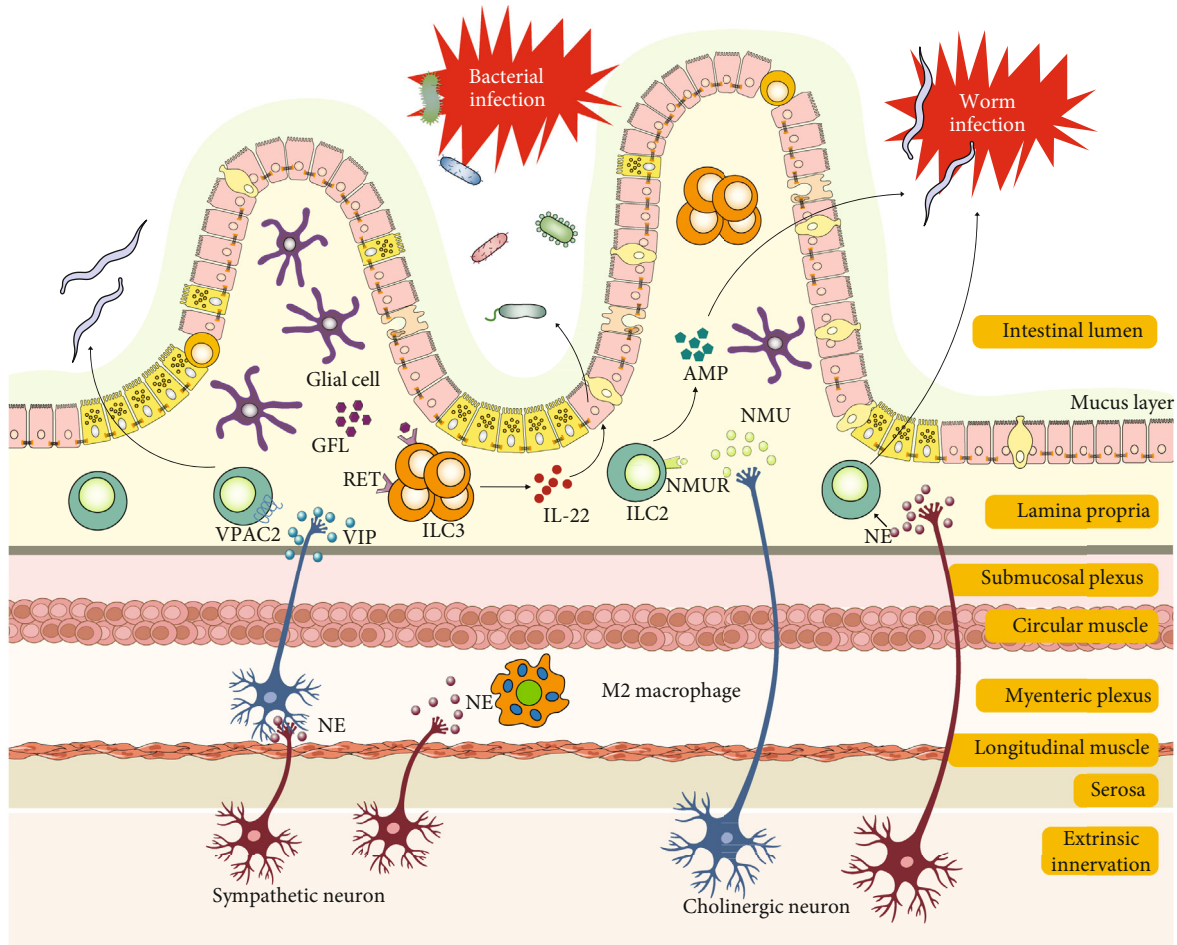
Figure 5: Illustration of crosstalk of ILC2 and ILC3 with neurons in helminth infection and gut inflammation, respectively. This image was modified from Reference [54]. Enteric cholinergic neuron-derived NMU activates ILC2 responses and protects against helminth infection. Lamina propria ILC2 function is also regulated by VIP and NE. Glial cell-derived neurotrophic factors stimulate IL-22 production by lamina propria ILC3s, promoting barrier integrity. SNS-derived NE induces a tissue-protective phenotype (M2) in muscularis macrophages. Abbreviations: AMP: antimicrobial peptide; NE: norepinephrine; NMU: neuromedin U; NMUR: neuromedin U receptor; SNS: sympathetic nervous system; GFL: glia cell-derived neurotrophic factor ligand; VIP: vasoactive intestinal peptide; VPAC2: vasoactive intestinal peptide receptor 2.

3.2. Lipid Mediators. Lipid mediators such as prostaglandin D2 (PGD2) that could regulate ILC2 responses were firstly reported in 2013 [121]. PGD_2 activates ILC2s from human peripheral blood and increased IL-13 production in the presence of IL-33 and IL-25 [121, 122]. Arachidonic acid metabolite leukotriene D4 (LTD4) was also shown to be able to promote ILC2 activation through the cysteinyl leukotriene receptor 1 (Cys-Lt1R) [123]. Montelukast, a leukotriene receptor antagonist, binds competitively and selectively to Cys-Lt1R. Thus, montelukast may be capable of modulating ILC2 activity. Besides, the arachidonic metabolites lipoxin A4 (LXA4) and macrophage mediator resolving inflammation-1 (maresin-1 or MaR1) can impair the activation of ILC2s [121, 124]. Therefore, a variety of lipid mediators or inhibitors of these mediators may be developed as ILC modulators [122].

3.3. Cytokines. The cytokines inducing the development and activity of specific subsets of ILCs may also be targeted—such as IL-12 and IL-15 for ILC1s; IL-25, IL-33, and TSLP for ILC2s; and IL-1β and IL-23 for ILC3s, respectively. Interestingly, IL-2, not a classical inducer of ILC activation, was shown to be a critical regulator of ILC2 during pulmonary inflammation [125]. Although the precise involvement of ILCs in specific diseases still remains elusive, treatment blocking these pathways showed some effects in different scenarios besides the intestinal tract. Treatment of multiple sclerosis patients with daclizumab, an antibody targeting IL-2Rα (CD25), resulted in an increase in the numbers of NK cells that correlated with drug efficacy [126]. Blockade of CD25 inhibits effector T cell activation, regulatory T cell expansion and survival, and activation-induced T-cell apoptosis. Because CD25 blockade reduces IL-2 consumption by effector T cells, it increases IL-2 bioavailability allowing for greater interaction with the intermediate-affinity IL-2R and therefore drives the expansion of CD56^{bright} NK cells. Unfortunately, daclizumab was withdrawn from the market in 2018 due to severe secondary autoimmune disease

directed against the central nervous system [127]. In addition, antibodies against IL-25 and IL-33 have shown efficacy in mouse models of allergic lung inflammation [128, 129], and antibody to TSLP intravenously given before allergen challenge in mild asthmatic patients improves asthma symptoms [130].

Apart from cytokines inducing ILC development, effector cytokines such as IFN-γ, IL-5, and IL-13, or IL-17, produced by ILCs may also be targeted. For example, mepolizumab (antibody to IL-5, NCT01000506) and lebrikizumab (antibody to IL-13, NCT02104674) have been shown effective in clinical trials against asthma [131, 132].

3.4. Microbial Compounds. The soluble excretory/secretory products of the helminth parasites impair the activity of ILC2s in response to airway challenges by suppression of IL-33 production [133]. Alternatively, microbial compounds may be used to boost one type of ILC in order to block the other types of ILCs.

4. Conclusion

In the past decade, accumulating studies have been carried out to delineate the biology of ILC differentiation, function, and regulation. Yet, still much remains to be investigated. Many discoveries are based on mouse models, and more needs to be described in human scenarios. The prompt response characteristics and antigen-independent activation place ILCs upstream of adaptive response. ILCs possess only few sensory elements for the recognition of nonself, and therefore, ILCs depend on extrinsic cellular sensory elements residing within the tissue [134]. Their crosstalk with T cells, DCs, and other cells need to be deciphered further. ILCs contribute significantly to human health and disease. They play protective roles in some mucosal infections while playing detrimental roles in IBD. Development of modulators to block the detrimental roles of ILCs is of great clinical benefit.

Abbreviations

ILCs:	Innate lymphoid cells
TJs:	Tight junctions
MUC2:	Mucin glycoproteins
TFF:	Trefoil factor peptides
RELMβ:	Resistin-like molecule β
Fcgbp:	Fc-γ binding protein
TNF-α:	Tumor necrosis factor-α
LPS:	Lipopolysaccharide
NF-κB:	Nuclear factor-κB
TLR:	Toll-like receptor
DCs:	Dendritic cells
IBD:	Inflammatory bowel disease
IELs:	Intraepithelial lymphocytes
IECs:	Intestinal epithelial cells
TCRs:	T cell receptors
TSLP:	Thymic stromal lymphopoietin
S1P:	Sphingosine 1-phosphate
mDCs:	Migratory dendritic cells
dLNs:	Draining lymph nodes
RA:	Retinoic acid
PGD2:	Prostaglandin D2
NOD2:	Nucleotide oligomerization domain-containing protein 2
RICK:	Regulatory protein kinase
Fut2:	Fucosyltransferase 2
LTD4:	Leukotriene D4
Cys-Lt1R:	Cysteinyl leukotriene receptor 1
LXA4:	Lipoxin A4
Maresin-1 or MaR1:	Macrophage mediator resolving inflammation-1.

Conflicts of Interest

The authors have declared that no competing interests exist.

Authors' Contributions

Yuanyuan Wu and Hui Fan wrote the manuscript. Yuanyuan Wu, Aiyun Wang, and Yin Lu constructed the idea. Shijun Wang made valuable comments to the manuscript. Hui Fan and Aiyun Wang contributed equally to this work and share co-first authorship.

Acknowledgments

References

[1] D. Viggiano, G. Ianiro, G. Vanella et al., "Gut barrier in health and disease: focus on childhood," *European Review for Medical and Pharmacological Sciences*, vol. 19, no. 6, pp. 1077–1085, 2015.

[2] A. Martin and S. Devkota, "Hold the door: role of the gut barrier in diabetes," *Cell Metabolism*, vol. 27, no. 5, pp. 949–951, 2018.

[3] D. A. Winer, H. Luck, S. Tsai, and S. Winer, "The intestinal immune system in obesity and insulin resistance," *Cell Metabolism*, vol. 23, no. 3, pp. 413–426, 2016.

[4] G. J. Randolph, S. Bala, J.-F. Rahier et al., "Lymphoid aggregates remodel lymphatic collecting vessels that serve mesenteric lymph nodes in Crohn disease," *The American Journal of Pathology*, vol. 186, no. 12, pp. 3066–3073, 2016.

[5] S. C. Bischoff, G. Barbara, W. Buurman et al., "Intestinal permeability – a new target for disease prevention and therapy," *BMC Gastroenterology*, vol. 14, no. 1, 2014.

[6] M. A. Odenwald and J. R. Turner, "The intestinal epithelial barrier: a therapeutic target?," *Nature Reviews Gastroenterology & Hepatology*, vol. 14, no. 1, pp. 9–21, 2017.

[7] C. M. Van Itallie and J. M. Anderson, "Claudins and epithelial paracellular transport," *Annual Review of Physiology*, vol. 68, no. 1, pp. 403–429, 2005.

[8] C. Chelakkot, J. Ghim, and S. H. Ryu, "Mechanisms regulating intestinal barrier integrity and its pathological implications," *Experimental and Molecular Medicine*, vol. 50, no. 8, 2018.

[9] S. Zeissig, N. Burgel, D. Gunzel et al., "Changes in expression and distribution of claudin 2, 5 and 8 lead to discontinuous

tight junctions and barrier dysfunction in active Crohn's disease," *Gut*, vol. 56, no. 1, pp. 61–72, 2007.

[10] R. Ahmad, R. Chaturvedi, D. Olivares-Villagómez et al., "Targeted colonic claudin-2 expression renders resistance to epithelial injury, induces immune suppression, and protects from colitis," *Mucosal Immunology*, vol. 7, no. 6, pp. 1340–1353, 2014.

[11] M. S. Balda, J. A. Whitney, C. Flores, S. González, M. Cereijido, and K. Matter, "Functional dissociation of paracellular permeability and transepithelial electrical resistance and disruption of the apical- basolateral intramembrane diffusion barrier by expression of a mutant tight junction membrane protein," *The Journal of Cell Biology*, vol. 134, no. 4, pp. 1031–1049, 1996.

[12] M. Saitou, M. Furuse, H. Sasaki et al., "Complex phenotype of mice lacking occludin, a component of tight junction strands," *Molecular Biology of the Cell*, vol. 11, no. 12, pp. 4131–4142, 2000.

[13] J. D. Schulzke, A. H. Gitter, J. Mankertz et al., "Epithelial transport and barrier function in occludin-deficient mice," *Biochimica et Biophysica Acta (BBA) - Biomembranes*, vol. 1669, no. 1, pp. 34–42, 2005.

[14] L. Pastorelli, C. SalvoDe, J. R. Mercado, M. Vecchi, and T. T. Pizarro, "Central role of the gut epithelial barrier in the pathogenesis of chronic intestinal inflammation: lessons learned from animal models and human genetics," *Frontiers in Immunology*, vol. 4, 2013.

[15] L. S. Poritz, K. I. Garver, C. Green, L. Fitzpatrick, F. Ruggiero, and W. A. Koltun, "Loss of the tight junction protein ZO-1 in dextran sulfate sodium induced colitis," *The Journal of Surgical Research*, vol. 140, no. 1, pp. 12–19, 2007.

[16] H. Schneider, T. Pelaseyed, F. Svensson, and M. E. V. Johansson, "Study of mucin turnover in the small intestine by in vivo labeling," *Scientific Reports*, vol. 8, no. 1, 2018.

[17] M. Van der Sluis, B. A. E. De Koning, A. C. J. M. De Bruijn et al., "Muc2-deficient mice spontaneously develop colitis, indicating that MUC2 is critical for colonic protection," *Gastroenterology*, vol. 131, no. 1, pp. 117–129, 2006.

[18] Y. S. Kim and S. B. Ho, "Intestinal goblet cells and mucins in health and disease: recent insights and progress," *Current Gastroenterology Reports*, vol. 12, no. 5, pp. 319–330, 2010.

[19] R. Bansil and B. S. Turner, "The biology of mucus: composition, synthesis and organization," *Advanced Drug Delivery Reviews*, vol. 124, pp. 3–15, 2018.

[20] J.-D. Li, W. Feng, M. Gallup et al., "Activation of NF- B via a Src-dependent Ras-MAPK-pp90rsk pathway is required for Pseudomonas aeruginosa-induced mucin overproduction in epithelial cells," *Proceedings of the National Academy of Sciences*, vol. 95, no. 10, pp. 5718–5723, 2002.

[21] M. Andrianifahanana, N. Moniaux, and S. K. Batra, "Regulation of mucin expression: mechanistic aspects and implications for cancer and inflammatory diseases," *Biochimica et Biophysica Acta (BBA) - Reviews on Cancer*, vol. 1765, no. 2, pp. 189–222, 2006.

[22] P. Mesquita, N. Jonckheere, R. Almeida et al., "Human MUC2 mucin gene is transcriptionally regulated by Cdx homeodomain proteins in gastrointestinal carcinoma cell lines," *The Journal of Biological Chemistry*, vol. 278, no. 51, pp. 51549–51556, 2003.

[23] M. van der Sluis, A. Vincent, J. Bouma et al., "Forkhead box transcription factors Foxa1 and Foxa2 are important regulators of Muc2 mucin expression in intestinal epithelial cells," *Biochemical and Biophysical Research Communications*, vol. 369, no. 4, pp. 1108–1113, 2008.

[24] R. Hokari, H. Lee, S. C. Crawley et al., "Vasoactive intestinal peptide upregulates MUC2 intestinal mucin via CRE-B/ATF1," *American Journal of Physiology-Gastrointestinal and Liver Physiology*, vol. 289, no. 5, pp. G949–G959, 2005.

[25] N. Yamada, T. Hamada, M. Goto et al., "MUC2 expression is regulated by histone H3 modification and DNA methylation in pancreatic cancer," *International Journal of Cancer*, vol. 119, no. 8, pp. 1850–1857, 2006.

[26] K. Okudaira, S. Kakar, L. Cun et al., "MUC2 gene promoter methylation in mucinous and non-mucinous colorectal cancer tissues," *International Journal of Oncology*, vol. 36, no. 4, pp. 765–775, 2010.

[27] T. Sato, J. H. van Es, H. J. Snippert et al., "Paneth cells constitute the niche for Lgr5 stem cells in intestinal crypts," *Nature*, vol. 469, no. 7330, pp. 415–418, 2011.

[28] S. Vaishnava, C. L. Behrendt, A. S. Ismail, L. Eckmann, and L. V. Hooper, "Paneth cells directly sense gut commensals and maintain homeostasis at the intestinal host-microbial interface," *Proceedings of the National Academy of Sciences*, vol. 105, no. 52, pp. 20858–20863, 2008.

[29] M. Schmitt, M. Schewe, A. Sacchetti et al., "Paneth cells respond to inflammation and contribute to tissue regeneration by acquiring stem-like features through SCF/c-Kit signaling," *Cell Reports*, vol. 24, no. 9, pp. 2312–2328.e7, 2018.

[30] M. M. Wouters, M. Vicario, and J. Santos, "The role of mast cells in functional GI disorders," *Gut*, vol. 65, no. 1, pp. 155–168, 2016.

[31] E. A. Mayer, K. Tillisch, and A. Gupta, "Gut/brain axis and the microbiota," *Journal of Clinical Investigation*, vol. 125, no. 3, pp. 926–938, 2015.

[32] S. Buhner and M. Schemann, "Mast cell–nerve axis with a focus on the human gut," *Biochimica et Biophysica Acta - Molecular Basis of Disease*, vol. 1822, no. 1, pp. 85–92, 2012.

[33] L. L. Reber, R. Sibilano, K. Mukai, and S. J. Galli, "Potential effector and immunoregulatory functions of mast cells in mucosal immunity," *Mucosal Immunology*, vol. 8, no. 3, pp. 444–463, 2015.

[34] G. Barbara, V. Stanghellini, R. De Giorgio et al., "Activated mast cells in proximity to colonic nerves correlate with abdominal pain in irritable bowel syndrome," *Gastroenterology*, vol. 126, no. 3, pp. 693–702, 2004.

[35] K. R. Groschwitz, R. Ahrens, H. Osterfeld et al., "Mast cells regulate homeostatic intestinal epithelial migration and barrier function by a chymase/Mcpt4-dependent mechanism," *Proceedings of the National Academy of Sciences*, vol. 106, no. 52, pp. 22381–22386, 2009.

[36] S. J. Galli, M. Grimbaldeston, and M. Tsai, "Immunomodulatory mast cells: negative, as well as positive, regulators of immunity," *Nature Reviews Immunology*, vol. 8, no. 6, pp. 478–486, 2008.

[37] E. Z. M. da Silva, M. C. Jamur, and C. Oliver, "Mast cell function: a new vision of an old cell," *Journal of Histochemistry and Cytochemistry*, vol. 62, no. 10, pp. 698–738, 2014.

[38] S. Y. Chang, H. J. Ko, and M. N. Kweon, "Mucosal dendritic cells shape mucosal immunity," *Experimental and Molecular Medicine*, vol. 46, no. 3, pp. e84–e84, 2014.

[39] M. Rimoldi, M. Chieppa, M. Vulcano, P. Allavena, and M. Rescigno, "Intestinal epithelial cells control dendritic cell

function," *Annals of the New York Academy of Sciences*, vol. 1029, no. 1, pp. 66–74, 2004.

[40] M. Becker, S. Güttler, A. Bachem et al., "Ontogenic, phenotypic, and functional characterization of XCR1+ dendritic cells leads to a consistent classification of intestinal dendritic cells based on the expression of XCR1 and SIRPα," *Frontiers in Immunology*, vol. 5, 2014.

[41] J. R. McDole, L. W. Wheeler, K. G. McDonald et al., "Goblet cells deliver luminal antigen to CD103+ dendritic cells in the small intestine," *Nature*, vol. 483, no. 7389, pp. 345–349, 2012.

[42] J. Farache, I. Koren, I. Milo et al., "Luminal bacteria recruit CD103+ dendritic cells into the intestinal epithelium to sample bacterial antigens for presentation," *Immunity*, vol. 38, no. 3, pp. 581–595, 2013.

[43] M. Gross, T. M. Salame, and S. Jung, "Guardians of the gut - murine intestinal macrophages and dendritic cells," *Frontiers in Immunology*, vol. 6, 2015.

[44] C. C. Bain and A. Schridde, "Origin, differentiation, and function of intestinal macrophages," *Frontiers in Immunology*, vol. 9, 2018.

[45] J. R. Grainger, J. E. Konkel, T. Zangerle-Murray, and T. N. Shaw, "Macrophages in gastrointestinal homeostasis and inflammation," *Pflügers Archiv - European Journal of Physiology*, vol. 469, no. 3-4, pp. 527–539, 2017.

[46] E. Zigmond, B. Bernshtein, G. Friedlander et al., "Macrophage-restricted interleukin-10 receptor deficiency, but not IL-10 deficiency, causes severe spontaneous colitis," *Immunity*, vol. 40, no. 5, pp. 720–733, 2014.

[47] L. Deng, J.-F. Zhou, R. S. Sellers et al., "A novel mouse model of inflammatory bowel disease links mammalian target of rapamycin-dependent hyperproliferation of colonic epithelium to inflammation-associated tumorigenesis," *The American Journal of Pathology*, vol. 176, no. 2, pp. 952–967, 2010.

[48] C. C. Bain, A. Bravo-Blas, C. L. Scott et al., "Constant replenishment from circulating monocytes maintains the macrophage pool in the intestine of adult mice," *Nature Immunology*, vol. 15, no. 10, pp. 929–937, 2014.

[49] C. C. Bain, C. L. Scott, H. Uronen-Hansson et al., "Resident and pro-inflammatory macrophages in the colon represent alternative context-dependent fates of the same Ly6C hi monocyte precursors," *Mucosal Immunology*, vol. 6, no. 3, pp. 498–510, 2013.

[50] S. De Schepper, S. Verheijden, J. Aguilera-Lizarraga et al., "Self-maintaining gut macrophages are essential for intestinal homeostasis," *Cell*, vol. 175, no. 2, pp. 400–415.e13, 2018.

[51] H. Cheroutre, F. Lambolez, and D. Mucida, "The light and dark sides of intestinal intraepithelial lymphocytes," *Nature Reviews Immunology*, vol. 11, no. 7, pp. 445–456, 2011.

[52] D. Olivares-Villagómez and L. Van Kaer, "Intestinal intraepithelial lymphocytes: sentinels of the mucosal barrier," *Trends in Immunology*, vol. 39, no. 4, pp. 264–275, 2018.

[53] D. Masopust, D. Choo, V. Vezys et al., "Dynamic T cell migration program provides resident memory within intestinal epithelium," *The Journal of Experimental Medicine*, vol. 207, no. 3, pp. 553–564, 2010.

[54] C. Godinho-Silva, F. Cardoso, and H. Veiga-Fernandes, "Neuro–immune cell units: a new paradigm in physiology," *Annual Review of Immunology*, vol. 37, no. 1, pp. 19–46, 2019.

[55] M. D. Gershon, "The enteric nervous system: a second brain," *Hospital Practice*, vol. 34, no. 7, pp. 31–52, 1999.

[56] J. B. Furness, "Types of neurons in the enteric nervous system," *Journal of the Autonomic Nervous System*, vol. 81, no. 1-3, pp. 87–96, 2000.

[57] G. Matteoli, P. J. Gomez-Pinilla, A. Nemethova et al., "A distinct vagal anti-inflammatory pathway modulates intestinal muscularis resident macrophages independent of the spleen," *Gut*, vol. 63, no. 6, pp. 938–948, 2014.

[58] T. G. Bush, T. C. Savidge, T. C. Freeman, H. J. Cox, and E. A. Campbell, "Fulminant jejuno-ileitis induced by ablation of enteric glia in adult transgenic mice," *Gastroenterology*, vol. 120, no. 5, pp. A186–A187, 2001.

[59] A. Cornet, T. C. Savidge, J. Cabarrocas et al., "Enterocolitis induced by autoimmune targeting of enteric glial cells: a possible mechanism in Crohn's disease?," *Proceedings of the National Academy of Sciences of the United States of America*, vol. 98, no. 23, pp. 13306–13311, 2001.

[60] M. Rao, D. Rastelli, L. Dong et al., "Enteric glia regulate gastrointestinal motility but are not required for maintenance of the epithelium in mice," *Gastroenterology*, vol. 153, no. 4, pp. 1068–1081.e7, 2017.

[61] E. Vivier, D. Artis, M. Colonna et al., "Innate lymphoid cells: 10 years on," *Cell*, vol. 174, pp. 1054–1066, 2018.

[62] M. E. Kotas and R. M. Locksley, "Why innate lymphoid cells?," *Immunity*, vol. 48, pp. 1081–1090, 2018.

[63] E. Klein and H. Wigzell, ""Natural" killer cells in the mouse. I. Cytotoxic cells with specificity for mouse Moloney leukemia cells. Specificity and distribution according to genotype," vol. 5, no. 2, pp. 112–117, 1975.

[64] Y.-J. Park, D.-S. Kuen, and Y. Chung, "Future prospects of immune checkpoint blockade in cancer: from response prediction to overcoming resistance," *Experimental & Molecular Medicine*, vol. 50, p. 109, 2018.

[65] C. A. J. Vosshenrich, M. E. García-Ojeda, S. I. Samson-Villéger et al., "A thymic pathway of mouse natural killer cell development characterized by expression of GATA-3 and CD127," *Nature Immunology*, vol. 7, no. 11, pp. 1217–1224, 2006.

[66] M. Cella, A. Fuchs, W. Vermi et al., "A human natural killer cell subset provides an innate source of IL-22 for mucosal immunity," *Nature*, vol. 457, no. 7230, pp. 722–725, 2009.

[67] A. E. Price, H.-E. Liang, B. M. Sullivan et al., "Systemically dispersed innate IL-13-expressing cells in type 2 immunity," *Proceedings of the National Academy of Sciences of the United States of America*, vol. 107, no. 25, pp. 11489–11494, 2010.

[68] S. Buonocore, P. P. Ahern, H. H. Uhlig et al., "Innate lymphoid cells drive interleukin-23-dependent innate intestinal pathology," *Nature*, vol. 464, no. 7293, pp. 1371–1375, 2010.

[69] L. A. Monticelli, G. F. Sonnenberg, M. C. Abt et al., "Innate lymphoid cells promote lung-tissue homeostasis after infection with influenza virus," *Nature Immunology*, vol. 12, no. 11, pp. 1045–1054, 2011.

[70] J. H. Bernink, C. P. Peters, M. Munneke et al., "Human type 1 innate lymphoid cells accumulate in inflamed mucosal tissues," *Nature Immunology*, vol. 14, no. 3, pp. 221–229, 2013.

[71] A. Fuchs, W. Vermi, J. S. Lee et al., "Intraepithelial type 1 innate lymphoid cells are a unique subset of IL-12- and IL-15-responsive IFN-γ-producing cells," *Immunity*, vol. 38, no. 4, pp. 769–781, 2013.

[72] M. R. Hepworth, L. A. Monticelli, T. C. Fung et al., "Innate lymphoid cells regulate CD4 + T-cell responses to intestinal commensal bacteria," *Nature*, vol. 498, no. 7452, pp. 113–117, 2013.

[73] D. Artis and H. Spits, "The biology of innate lymphoid cells," *Nature*, vol. 517, no. 7534, pp. 293–301, 2015.

[74] S. Middendorp and E. E. S. Nieuwenhuis, "NKT cells in mucosal immunity," *Mucosal Immunology*, vol. 2, no. 5, pp. 393–402, 2009.

[75] C. Ma, M. Han, B. Heinrich et al., "Gut microbiome–mediated bile acid metabolism regulates liver cancer via NKT cells," *Science*, vol. 360, 2018.

[76] L. Han, X.-m. Wang, S. Di et al., "Innate lymphoid cells: a link between the nervous system and microbiota in intestinal networks," *Mediators of Inflammation*, vol. 2019, Article ID 1978094, 11 pages, 2019.

[77] M. Bruchard and F. Ghiringhelli, "Deciphering the roles of innate lymphoid cells in cancer," *Frontiers in Immunology*, vol. 10, 2019.

[78] C. J. Oliphant, Y. Y. Hwang, J. A. Walker et al., "MHCII-mediated dialog between group 2 innate lymphoid cells and CD4 + T cells potentiates type 2 immunity and promotes parasitic helminth expulsion," *Immunity*, vol. 41, no. 2, pp. 283–295, 2014.

[79] M. Wagner, K. Moro, and S. Koyasu, "Plastic heterogeneity of innate lymphoid cells in cancer," *Trends in Cancer*, vol. 3, no. 5, pp. 326–335, 2017.

[80] Y. Huang, K. Mao, X. Chen et al., "S1P-dependent interorgan trafficking of group 2 innate lymphoid cells supports host defense," *Science*, vol. 359, no. 6371, pp. 114–119, 2018.

[81] M. Colonna, "Innate lymphoid cells: diversity, plasticity, and unique functions in immunity," *Immunity*, vol. 48, pp. 1104–1117, 2018.

[82] A. I. Lim, Y. Li, S. Lopez-Lastra et al., "Systemic human ILC precursors provide a substrate for tissue ILC differentiation," *Cell*, vol. 168, no. 6, pp. 1086–1100.e10, 2017.

[83] J. H. Bernink, L. Krabbendam, K. Germar et al., "Interleukin-12 and -23 control plasticity of Cd127+ group 1 and group 3 innate lymphoid cells in the intestinal lamina propria," *Immunity*, vol. 43, no. 1, pp. 146–160, 2015.

[84] O.-E. Weizman, N. M. Adams, I. S. Schuster et al., "ILC1 confer early host protection at initial sites of viral infection," *Cell*, vol. 171, no. 4, pp. 795–808.e12, 2017.

[85] E. Wong, R.-H. Xu, D. Rubio et al., "Migratory dendritic cells, group 1 innate lymphoid cells, and inflammatory monocytes collaborate to recruit NK cells to the virus-infected lymph node," *Cell Reports*, vol. 24, no. 1, pp. 142–154, 2018.

[86] T. Y. F. Halim, Y. Y. Hwang, S. T. Scanlon et al., "Group 2 innate lymphoid cells license dendritic cells to potentiate memory TH2 cell responses," *Nature Immunology*, vol. 17, no. 1, pp. 57–64, 2016.

[87] T. Y. F. Halim, C. A. Steer, L. Mathä et al., "Group 2 innate lymphoid cells are critical for the initiation of adaptive T helper 2 cell-mediated allergic lung inflammation," *Immunity*, vol. 40, no. 3, pp. 425–435, 2014.

[88] F. Flores-Borja, S. Irshad, P. Gordon et al., "Crosstalk between innate lymphoid cells and other immune cells in the tumor microenvironment," *Journal of Immunology Research*, vol. 2016, Article ID 7803091, 14 pages, 2016.

[89] A. Rivera, M. C. Siracusa, G. S. Yap, and W. C. Gause, "Innate cell communication kick-starts pathogen-specific immunity," *Nature Immunology*, vol. 17, no. 4, pp. 356–363, 2016.

[90] C. S. N. Klose, M. Flach, L. Möhle et al., "Differentiation of type 1 ILCs from a common progenitor to all helper-like innate lymphoid cell lineages," *Cell*, vol. 157, no. 2, pp. 340–356, 2014.

[91] S. Boulenouar, X. Michelet, D. Duquette et al., "Adipose type one innate lymphoid cells regulate macrophage homeostasis through targeted cytotoxicity," *Immunity*, vol. 46, no. 2, pp. 273–286, 2017.

[92] T. E. O'Sullivan, M. Rapp, X. Fan et al., "Adipose-resident group 1 innate lymphoid cells promote obesity-associated insulin resistance," *Immunity*, vol. 45, no. 2, pp. 428–441, 2016.

[93] S. J. Van Dyken and R. M. Locksley, "Interleukin-4- and interleukin-13-mediated alternatively activated macrophages: roles in homeostasis and disease," *Annual Review of Immunology*, vol. 31, no. 1, pp. 317–343, 2013.

[94] A.-G. Besnard, R. Guabiraba, W. Niedbala et al., "IL-33-mediated protection against experimental cerebral malaria is linked to induction of type 2 innate lymphoid cells, M2 macrophages and regulatory T cells," *PLoS Pathogens*, vol. 11, no. 2, 2015.

[95] M.-W. Lee, J. I. Odegaard, L. Mukundan et al., "Activated type 2 innate lymphoid cells regulate beige fat biogenesis," *Cell*, vol. 160, no. 1-2, pp. 74–87, 2015.

[96] A. B. Molofsky, J. C. Nussbaum, H.-E. Liang et al., "Innate lymphoid type 2 cells sustain visceral adipose tissue eosinophils and alternatively activated macrophages," *The Journal of Experimental Medicine*, vol. 210, no. 3, pp. 535–549, 2013.

[97] G. Gasteiger and A. Y. Rudensky, "Interactions between innate and adaptive lymphocytes," *Nature Reviews Immunology*, vol. 14, no. 9, pp. 631–639, 2014.

[98] A. Mortha, A. Chudnovskiy, D. Hashimoto et al., "Microbiota-dependent crosstalk between macrophages and ILC3 promotes intestinal homeostasis," *Science*, vol. 343, no. 6178, pp. 1249288–1249288, 2014.

[99] A. Geremia and C. V. Arancibia-Cárcamo, "Innate lymphoid cells in intestinal inflammation," *Frontiers in Immunology*, vol. 8, 2017.

[100] N. Powell, A. W. Walker, E. Stolarczyk et al., "The transcription factor T-bet regulates intestinal inflammation mediated by interleukin-7 receptor+ innate lymphoid cells," *Immunity*, vol. 37, no. 4, pp. 674–684, 2012.

[101] C. S. N. Klose, E. A. Kiss, V. Schwierzeck et al., "A T-bet gradient controls the fate and function of CCR6–RORγt+ innate lymphoid cells," *Nature*, vol. 494, no. 7436, pp. 261–265, 2013.

[102] E. D. T. Wojno, L. A. Monticelli, S. V. Tran et al., "The prostaglandin D2 receptor CRTH2 regulates accumulation of group 2 innate lymphoid cells in the inflamed lung," *Mucosal Immunology*, vol. 8, no. 6, pp. 1313–1323, 2015.

[103] T. A. Doherty, N. Khorram, S. Lund, A. K. Mehta, M. Croft, and D. H. Broide, "Lung type 2 innate lymphoid cells express cysteinyl leukotriene receptor 1, which regulates TH2 cytokine production," *The Journal of Allergy and Clinical Immunology*, vol. 132, no. 1, pp. 205–213, 2013.

[104] B. Zeng, S. Shi, G. Ashworth, C. Dong, J. Liu, and F. Xing, "ILC3 function as a double-edged sword in inflammatory bowel diseases," *Cell Death & Disease*, vol. 10, no. 4, 2019.

[105] N. Barnich, J. E. Aguirre, H. C. Reinecker, R. Xavier, and D. K. Podolsky, "Membrane recruitment of NOD2 in intestinal epithelial cells is essential for nuclear factor–κB activation in muramyl dipeptide recognition," *The Journal of Cell Biology*, vol. 170, no. 1, pp. 21–26, 2005.

[106] C. A. Lindemans, M. Calafiore, A. M. Mertelsmann et al., "Interleukin-22 promotes intestinal-stem-cell-mediated epithelial regeneration," *Nature*, vol. 528, no. 7583, pp. 560–564, 2015.

[107] J. A. Dudakov, A. M. Hanash, and M. R. M. van den Brink, "Interleukin-22: immunobiology and pathology," *Annual Review of Immunology*, vol. 33, no. 1, pp. 747–785, 2015.

[108] Y. Goto, T. Obata, J. Kunisawa et al., "Innate lymphoid cells regulate intestinal epithelial cell glycosylation," *Science*, vol. 345, no. 6202, pp. 1254009–1254009, 2014.

[109] C. Pearson, H. H. Uhlig, and F. Powrie, "Lymphoid microenvironments and innate lymphoid cells in the gut," *Trends in Immunology*, vol. 33, no. 6, pp. 289–296, 2012.

[110] H. Veiga-Fernandes and D. Artis, "Neuronal–immune system cross-talk in homeostasis," *Science*, vol. 359, no. 6383, pp. 1465-1466, 2018.

[111] C. S. N. Klose, T. Mahlakõiv, J. B. Moeller et al., "The neuropeptide neuromedin U stimulates innate lymphoid cells and type 2 inflammation," *Nature*, vol. 549, no. 7671, pp. 282–286, 2017.

[112] V. Cardoso, J. Chesné, H. Ribeiro et al., "Neuronal regulation of type 2 innate lymphoid cells via neuromedin U," *Nature*, vol. 549, no. 7671, pp. 277–281, 2017.

[113] S. Moriyama, J. R. Brestoff, A.-L. Flamar et al., "β2-Adrenergic receptor-mediated negative regulation of group 2 innate lymphoid cell responses," *Science*, vol. 359, no. 6379, pp. 1056–1061, 2018.

[114] S. Ibiza, B. García-Cassani, H. Ribeiro et al., "Glial-cell-derived neuroregulators control type 3 innate lymphoid cells and gut defence," *Nature*, vol. 535, pp. 440–443, 2016.

[115] J. R. Huh, M. W. L. Leung, P. Huang et al., "Digoxin and its derivatives suppress T H17 cell differentiation by antagonizing RORγ3t activity," *Nature*, vol. 472, no. 7344, pp. 486–490, 2011.

[116] U. Guendisch, J. Weiss, F. Ecoeur et al., "Pharmacological inhibition of RORγt suppresses the Th17 pathway and alleviates arthritis in vivo," *PLoS One*, vol. 12, no. 11, 2017.

[117] I. Dulubova, X. Jiang, I. Trevino et al., "RTA 1701 is an orally-bioavailable, potent, and selective RORγt inhibitor that suppresses Th17 differentiation in vitro and is efficacious in mouse models of autoimmune disease," *Journal of Immunology*, vol. 200, 2018.

[118] K. Venken, P. Jacques, C. Mortier et al., "RORγt inhibition selectively targets IL-17 producing iNKT and γδ-T cells enriched in spondyloarthritis patients," *Nature Communications*, vol. 10, no. 1, 2019.

[119] G. Eberl, M. Colonna, J. P. D. Santo, and A. N. J. McKenzie, "Innate lymphoid cells: a new paradigm in immunology," *Science*, vol. 348, no. 6237, pp. aaa6566–aaa6566, 2015.

[120] N. Garrido-Mesa, J.-H. Schroeder, E. Stolarczyk et al., "T-bet controls intestinal mucosa immune responses via repression of type 2 innate lymphoid cell function," *Mucosal Immunology*, vol. 12, no. 1, pp. 51–63, 2019.

[121] C. Barnig, M. Cernadas, S. Dutile et al., "Lipoxin A4 regulates natural killer cell and type 2 innate lymphoid cell activation in asthma," *Science Translational Medicine*, vol. 5, no. 174, pp. 174ra26–174ra26, 2013.

[122] T. A. Doherty and D. H. Broide, "Lipid regulation of group 2 innate lymphoid cell function: moving beyond epithelial cytokines," *The Journal of Allergy and Clinical Immunology*, vol. 141, no. 5, pp. 1587–1589, 2018.

[123] L. Xue, M. Salimi, I. Panse et al., "Prostaglandin D 2 activates group 2 innate lymphoid cells through chemoattractant receptor-homologous molecule expressed on T H2 cells," *The Journal of Allergy and Clinical Immunology*, vol. 133, no. 4, pp. 1184–1194.e7, 2014.

[124] N. Krishnamoorthy, P. R. Burkett, J. Dalli et al., "Cutting edge: maresin-1 engages regulatory T cells to limit type 2 innate lymphoid cell activation and promote resolution of lung inflammation," *Journal of Immunology*, vol. 194, no. 3, pp. 863–867, 2015.

[125] B. Roediger, R. Kyle, S. S. Tay et al., "IL-2 is a critical regulator of group 2 innate lymphoid cell function during pulmonary inflammation," *The Journal of Allergy and Clinical Immunology*, vol. 136, no. 6, pp. 1653–1663.e7, 2015.

[126] J. S. A. Perry, S. Han, Q. Xu et al., "Inhibition of LTi cell development by CD25 blockade is associated with decreased intrathecal inflammation in multiple sclerosis," *Science Translational Medicine*, vol. 4, no. 145, pp. 145-ra106–145ra106, 2012.

[127] S. L. Cohan, E. B. Lucassen, M. C. Romba, and S. N. Linch, "Daclizumab: mechanisms of action, therapeutic efficacy, adverse events and its uncovering the potential role of innate immune system recruitment as a treatment strategy for relapsing multiple sclerosis," *Biomedicine*, vol. 7, no. 1, 2019.

[128] S. J. Ballantyne, J. L. Barlow, H. E. Jolin et al., "Blocking IL-25 prevents airway hyperresponsiveness in allergic asthma," *The Journal of Allergy and Clinical Immunology*, vol. 120, no. 6, pp. 1324–1331, 2007.

[129] A. J. Coyle, C. Lloyd, J. Tian et al., "Crucial role of the interleukin 1 receptor family member T1/St2 in T helper cell type 2–mediated lung mucosal immune responses," *The Journal of Experimental Medicine*, vol. 190, no. 7, pp. 895–902, 2002.

[130] G. M. Gauvreau, P. M. O'Byrne, L.-P. Boulet et al., "Effects of an anti-TSLP antibody on allergen-induced asthmatic responses," *The New England Journal of Medicine*, vol. 370, no. 22, pp. 2102–2110, 2014.

[131] I. D. Pavord, S. Korn, P. Howarth et al., "Mepolizumab for severe eosinophilic asthma (DREAM): a multicentre, double-blind, placebo-controlled trial," *Lancet*, vol. 380, no. 9842, pp. 651–659, 2012.

[132] P. Korenblat, E. Kerwin, I. Leshchenko et al., "Efficacy and safety of lebrikizumab in adult patients with mild-to-moderate asthma not receiving inhaled corticosteroids," *Respiratory Medicine*, vol. 134, pp. 143–149, 2018.

[133] H. J. McSorley, N. F. Blair, K. A. Smith, A. N. J. McKenzie, and R. M. Maizels, "Blockade of IL-33 release and suppression of type 2 innate lymphoid cell responses by helminth secreted products in airway allergy," *Mucosal Immunology*, vol. 7, no. 5, pp. 1068–1078, 2014.

[134] A. Mortha and K. Burrows, "Cytokine networks between innate lymphoid cells and myeloid cells," *Frontiers in Immunology*, vol. 9, 2018.

Research Article

Preoperative Risk Assessment of Lymph Node Metastasis in cT1 Lung Cancer: A Retrospective Study from Eastern China

Chengyan Zhang ⓘD, **Guanchao Pang** ⓘD, **Chengxi Ma** ⓘD, **Jingni Wu** ⓘD, **Pingli Wang** ⓘD, **and Kai Wang** ⓘD

Department of Respiratory and Critical Care Medicine, Second Affiliated Hospital, Zhejiang University School of Medicine, 310009 Hangzhou, China

Correspondence should be addressed to Pingli Wang; pingliwang@zju.edu.cn and Kai Wang; kaiw@zju.edu.cn

Background. Lymph node status of clinical T1 (diameter ≤ 3 cm) lung cancer largely affects the treatment strategies in the clinic. In order to assess lymph node status before operation, we aim to develop a noninvasive predictive model using preoperative clinical information. *Methods*. We retrospectively reviewed 924 patients (development group) and 380 patients (validation group) of clinical T1 lung cancer. Univariate analysis followed by polytomous logistic regression was performed to estimate different risk factors of lymph node metastasis between N1 and N2 diseases. A predictive model of N2 metastasis was established with dichotomous logistic regression, externally validated and compared with previous models. *Results*. Consolidation size and clinical N stage based on CT were two common independent risk factors for both N1 and N2 metastases, with different odds ratios. For N2 metastasis, we identified five independent predictors by dichotomous logistic regression: peripheral location, larger consolidation size, lymph node enlargement on CT, no smoking history, and higher levels of serum CEA. The model showed good calibration and discrimination ability in the development data, with the reasonable Hosmer-Lemeshow test ($p = 0.839$) and the area under the ROC being 0.931 (95% CI: 0.906-0.955). When externally validated, the model showed a great negative predictive value of 97.6% and the AUC of our model was better than other models. *Conclusion*. In this study, we analyzed risk factors for both N1 and N2 metastases and built a predictive model to evaluate possibilities of N2 metastasis of clinical T1 lung cancers before the surgery. Our model will help to select patients with low probability of N2 metastasis and assist in clinical decision to further management.

1. Introduction

Preoperative staging of patients with malignant lung cancer suggests the prognosis and the life quality afterwards. An accurate clinical staging can guide physicians to choose a proper treatment according to the authorized guideline and therefore standardizes the management procedure. Especially for those with positive mediastinal lymph nodes (N2 disease), preoperative chemotherapy is reported to reduce tumor size by 25% [1], downstage nearly half of the N2-positive patients [2–6], and increase the 5-year survival rate of 5-20% compared with surgery alone [7–11]. In that case, the accuracy of TNM staging before surgery is of paramount important.

The European Society of Thoracic Surgeons (ESTS) guidelines compared the diagnostic accuracy of different preoperative examinations for lymph node evaluation. Computed tomography is common and available in most countries, despite its low sensitivity (55%) and specificity (81%) [12, 13]. PET-CT scan is reported to be superior to CT in mediastinal lymph node staging and exhibits a high negative predictive value (NPV) for peripheral tumors. The sensitivity of PET-CT is 80-90%, and the specificity is 85-95% [12, 13]. However, PET-CT requires more expensive facilities and is not as popularized as CT. Besides, the negative predictive value of PET-CT decreases in patients with central tumors, tumors > 3 cm, and suspected N1 metastasis [12].
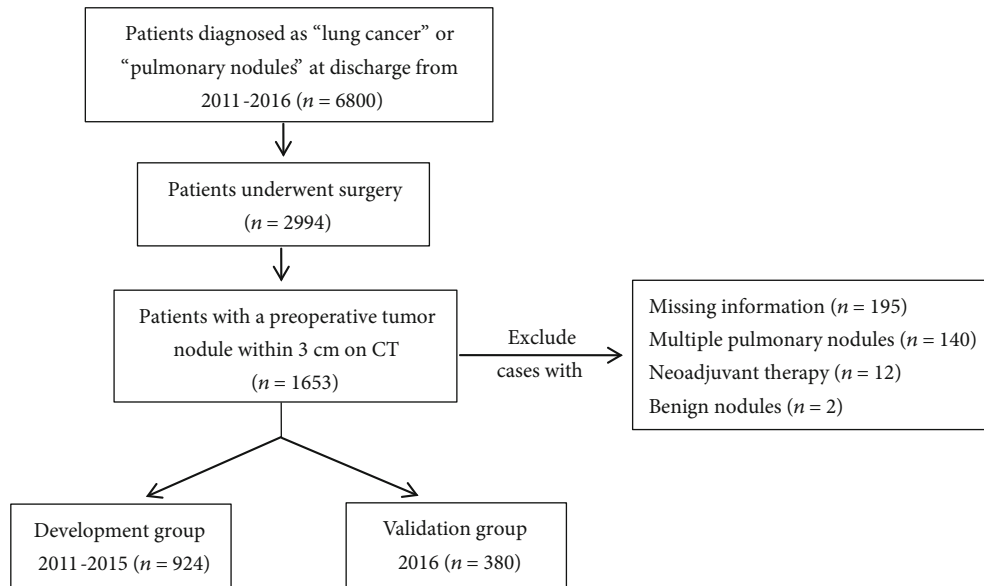
Figure 1: Flowchart of patient selection and exclusion.

Reported data shows the prevalence of occult N2 disease in patients with clinical stage I NSCLC is about 5.0-6.5% [14, 15]. In order not to omit this part of patients, a predictive model in combination of assisted examination is needed and previous efforts have been made by researchers. In this study, we aim to analyze the clinical features of patients with lymph node metastasis and create a predicted formula of N2 metastasis for clinical T1 lung cancers.

2. Methods

2.1. Patients. We retrospectively reviewed patients who were diagnosed with lung cancer and underwent radial surgical recession in Second Affiliated Hospital of Zhejiang University (SAHZU) during 2011-2016. Patients with a malignant nodule within 3 centimeters on CT (staged as cT1) were selected, all of which underwent lymph node evaluation via surgical operation. The exclusion criteria were as follows: (1) patients with multiple pulmonary cancers or metastatic pulmonary nodules, (2) patients with a history of preoperative therapy, and (3) patients without CT scan images before surgery. Patients from 2011 to 2015 were enrolled in the development group ($n = 924$), while patients from 2016 were included in the validation group ($n = 380$), as shown in Figure 1. This study was approved by the Institutional Ethics of Committee of SAHZU (2017-031).

2.2. Clinicopathological Variables. All the clinicopathological information was collected in the hospital information system (HIS). Information included gender, age, symptoms at presentation, smoking history, smoking index, chronic pulmonary diseases, cancer history, family history of cancer, levels of tumor markers within one month before surgery, histological type of lung cancer, pathological report of resected lymph nodes, tumor location (upper/middle/lower lobe, central/-peripheral location), tumor size, consolidation size, C/T ratio (consolidation size/tumor size), and clinical N stage based on

CT. Chronic pulmonary diseases included chronic bronchitis, emphysema, and chronic obstructive pulmonary disease (COPD). Tumor size was measured as the largest dimension on CT section in pulmonary window while consolidation size was measured in mediastinal window. Tumors were defined as peripherally located if the center of tumor mass was in the outer one-thirds of pulmonary parenchyma and otherwise as centrally located. A lymph node was considered an enlarged one when its short axis exceeded 1 cm. The seventh edition of TNM classification was referred to in this study.

2.3. Data Analysis. All the continuous variables were described with means and standard deviations, while categorical variables were described with frequencies. In univariate analysis, we performed one-way analysis of variance for continuous variables and Pearson's chi-square tests (adjusted p values using Bonferroni method) for categorical variables. Significant variables in the univariate analysis were further analyzed in multivariate analysis using polytomous logistic regression, in order to estimate different risk factors and odds ratios for each N stage (pN0, pN1, and pN2).

The dichotomous logistic regression was performed to build a predictive model for N2 metastasis, since N2 metastasis is worse in TNM staging and requires different preoperative treatment strategies. All variables collected from HIS were analyzed with forward stepwise selection, which was based on statistics of a conditional likelihood ratio test. A significant p value for entering variables was 0.05, and the p value for excluding variables was 0.10. The optimal cutoff point of the model was set according to the highest Youden's index. A nomogram was developed using the package of rms based on the logistic regression. In addition, calibration of the model was established with the Hosmer-Lemeshow goodness-of-fit test as well as the calibration curve, and the discrimination ability of the model was assessed by receiver operating characteristic (ROC)

analysis. The DeLong test was performed for the comparison of different ROC curves.

All statistical analysis was performed using SPSS Statistics 22.0 (IBM Armonk, NY, USA), EmpowerStats software (X&Y Solutions, Boston, USA, http://www.empowerstats .com/), and R 3.5.2 software (R Foundation for Statistical Computing, Vienna, Austria). We considered the differences as statistically significant when two-sided p values were less than 0.05.

3. Results

3.1. Clinicopathological Characteristics for Patients in the Development Group.
The clinicopathological characteristics of 924 patients in the development group are shown in Table 1. Patients were at a mean age of 59.1 ± 9.7, and tumor sizes were 1.70 ± 0.62 cm on average. The incidence for lymph node metastasis was 10.82% (100/924), with N1 metastasis being 3.24% (30/924) and N2 metastasis being 7.58% (70/924).

In univariate analysis (Table 1), lymph node metastasis was prone to be found in smoking males who suffered from chronic pulmonary diseases and were hospitalized with respiratory- or cancer-related symptoms (RCRS) and higher levels of carcinoembryonic antigen (CEA). Tumors with larger size (or consolidation size), central location, and lymph node enlargement on CT images were associated with higher likelihood of lymph node metastasis. Besides, patients with squamous carcinoma were more likely to have N1 metastasis, while N2 metastasis in patients with adenocarcinoma was three times more likely to occur than N1 metastasis.

3.2. Odds Ratios of N1 and N2 Metastases versus N0 Status.
In polytomous logistic regression (Table 2), significant variables in univariate analysis were further analyzed to estimate the risk factors and odds ratios of nodal metastasis stratified by the 7th TNM staging. Significantly elevated odds ratios were seen in tumors with larger consolidation size and lymph node enlargement on CT for N1 metastasis ($OR_{consolidation size} = 5.449$, 95% CI: 2.817-10.541; $OR_{lymph node enlargement on CT} = 11.424$, 95% CI: 3.316-39.360) and N2 metastasis ($OR_{consolidation size} = 8.640$, 95% CI: 5.002-14.923; $OR_{lymph node enlargement on CT} = 8.703$, 95% CI: 4.326-17.509) compared to N0 status. A significantly decreased odds ratio was seen in smokers for N2 metastasis ($OR_{smoking history} = 0.217$, 95% CI: 0.080-0.590) compared to N0 status in nonsmokers. Tumors with a central location seemed to have a negative correlation with N2 metastasis though there was no significant difference.

3.3. Logistic Regression Model and Predictors of N2 Metastasis.
Dichotomous logistic regression identified five independent predictors for N2 metastasis: peripheral location, consolidation size, lymph node enlargement on CT, no smoking history, and levels of serum CEA (Table 3). Gender, histological type, and C/T ratio were not involved as significant factors. The formula predicting N2 metastasis for small tumor nodules was established: $e^x/(1 + e^x)$, $x = -0.756^{\times}$central location $+ 1.921^{\times}$

consolidation size $+ 2.145^{\times}$lymph node enlargement on CT $- 1.065^{\times}$smoking history $+ 0.064^{\times}$CEA level $- 6.165$. The unit for "consolidation size" is cm and for "CEA level" is ng/ml. The value of "lymph node enlargement on CT," "central location," and "smoking history" should be 1 for yes and otherwise 0. A nomogram predicting the probability for N2 metastasis in cT1 patients was developed on the basis of multivariate logistic analysis (Figure 2).

The Hosmer-Lemeshow goodness-of-fit test, which was not statistically significant ($p = 0.839$), indicated that the predicted probability was of high concordance to the observed probability. A calibration curve is shown in Figure 3. The area under the receiver operating characteristic curve was 0.931, with 95% confidence interval between 0.906 and 0.955 (Figure 4(a)). We selected the numerical value with the highest Youden's index as our cutoff point for the predicted probability (cutoff for probability = 7.43%).

3.4. Validation of the Model and Comparison with Previous Models.
The characteristics of patients in the validation group were shown in Supplementary Table 1. In the external validation, the AUC of our model was 0.906 (95% CI: 0.857-0.956, Figure 4(b)). With the cutoff point set above (cutoff = 7.43%), we tested our model in the validation group. The sensitivity and specificity were 60.0% and 90.3%, respectively. The negative and positive predictive values (NPV and PPV) were 97.6% and 25.5%, respectively. In a subgroup analysis of adenocarcinoma (ADC) and squamous cell carcinoma (SCC), the validated AUC of ADC patients was 0.856 (95% CI: 0.790-0.922) and the validated AUC of SCC patients was 0.864 (95% CI: 0.777-0.952) ($p = 0.885$, DeLong test).

We also compared our model with the Fudan model [16] and Beijing model [17], as all three studies included clinical T1 NSCLC. Analyzed with all the data from our validation group, the validated AUC of the Beijing model was 0.879 (95% CI: 0.821-0.937) compared with 0.906 (95% CI: 0.857-0.956) of our model ($p = 0.405$, DeLong test). Based on the inclusion criteria of the Fudan model, patients with cT1N0M0 lung cancers were selected from the validation group of our study. And the validated AUC of the Fudan model was 0.712 (95% CI: 0.602-0.822) while the AUC of our model was 0.885 (95% CI: 0.820-0.949) ($p = 0.002$, DeLong test). Our model showed a larger area under the ROC curve compared to other models (Figure 5).

4. Discussion

Lymph node status, especially the assessment of N2 metastasis, largely affects the treatment strategies in the clinic. Therefore, it is of great significance to make an accurate and noninvasive assessment of lymph nodes before operation. In this study, we established a five-variable formula predicting N2 metastasis for malignant nodules within 3 cm. Our model showed a high negative predictive value of 97.6% and specificity of 90.3%, which can select patients with low risks of N2 metastasis and help with the clinical decision-making.

TABLE 1: Characteristics of patients in the development group.

	Patients with negative LNs (%)	Patients with positive N1 nodes (%)	Patients with positive N2 nodes (%)	p value*
Age (year)	59.1 ± 9.7	58.1 ± 10.0	58.9 ± 10.4	0.742
Gender				
Male	346 (85.4)	21 (5.2)	38 (9.4)	0.011
Female	478 (92.1)	9 (1.7)	32 (6.2)	
Symptoms				
RCE	456 (91.9)	8 (1.6)	32 (6.5)	0.010
RCRS	256 (85.6)	16 (5.4)	27 (9.0)	
ICD	112 (86.8)	6 (4.7)	11 (8.5)	
Asymptomatic	568 (90.9)	14 (2.2)	43 (6.9)	0.008
Symptomatic	256 (85.6)	16 (5.4)	27 (9.0)	
Cancer history				
Yes	58 (85.3)	4 (5.9)	6 (8.8)	0.454
No	766 (89.5)	26 (3.0)	64 (7.5)	
Family history of cancer				
Yes	122 (91.0)	1 (0.8)	11 (8.2)	0.169
No	702 (88.9)	29 (3.7)	59 (7.4)	
Pathology				
Adenocarcinoma	760 (91.2)	16 (1.9)	57 (6.9)	<0.001
Squamous	52 (75.4)	10 (14.5)	7 (10.1)	
Adenosquamous	3 (37.5)	1 (12.5)	4 (50.0)	
Neuroendocrine	8 (66.7)	3 (25.0)	1 (8.3)	
Other tumor type	1 (50.0)	0 (0.0)	1 (50.0)	
Smoking history				
Yes	220 (85.3)	17 (6.6)	21 (8.1)	0.001
No	604 (90.7)	13 (2.0)	49 (7.3)	
Location				
Upper lobe	445 (90.1)	14 (2.8)	35 (7.1)	0.670
Lower lobe	270 (88.8)	9 (3.0)	25 (8.2)	
Middle lobe	109 (86.5)	7 (5.6)	10 (7.9)	
Central	316 (86.6)	18 (4.9)	31 (8.5)	0.042
Peripheral	508 (90.9)	12 (2.1)	39 (7.0)	
Nodule size on CT				
Tumor size (cm)	1.63 ± 0.59	2.25 ± 0.57	2.33 ± 0.50	<0.001
Consolidation size (cm)	0.91 ± 0.83	2.19 ± 0.69	2.22 ± 0.59	<0.001
C/T ratio	0.51 ± 0.41	0.95 ± 0.19	0.95 ± 0.15	<0.001
Chronic pulmonary disease				
Yes	68 (78.2)	8 (9.2)	11 (12.6)	0.001
No	756 (90.3)	22 (2.6)	59 (7.1)	
Clinical nodal stage on CT				
Enlarged LNs in N2 station	72 (64.3)	7 (6.3)	33 (29.4)	<0.001
Enlarged LNs in N1 station	10 (38.5)	6 (23.0)	10 (38.5)	
Normal-sized LNs	742 (94.4)	17 (2.2)	27 (3.4)	
Levels of tumor markers				
CEA (ng/ml)	3.26 ± 4.84	3.55 ± 2.56	10.21 ± 17.58	<0.001
AFP (ng/ml)	3.03 ± 1.80	2.68 ± 0.89	3.25 ± 2.71	0.542
CA199 (U/ml)	10.48 ± 15.24	9.99 ± 9.26	15.67 ± 17.16	0.013
CA125 (U/ml)	11.31 ± 11.22	13.23 ± 10.04	26.53 ± 77.33	0.093

TABLE 1: Continued.

	Patients with negative LNs (%)	Patients with positive N1 nodes (%)	Patients with positive N2 nodes (%)	p value*
CA242 (U/ml)	5.42 ± 4.34	4.80 ± 3.22	5.54 ± 3.31	0.996
CA211 (ng/ml)	1.12 ± 0.84	1.49 ± 1.07	1.36 ± 1.01	0.006
NSE (ng/ml)	9.58 ± 4.55	8.48 ± 4.87	9.99 ± 5.32	0.793
SCC (ng/ml)	0.84 ± 0.83	1.15 ± 0.78	0.93 ± 0.59	0.143

RCE: routine chest examination; RCRS: respiratory- or cancer-related symptoms; ICD: incidental chest discovery; C/T ratio: consolidation size/tumor size ratio. *p value acquired from one-way analysis of variance and Pearson's chi-square tests.

TABLE 2: Odds ratios of likelihood of lymph node metastasis stratified by seventh TNM staging using polytomous logistic regression.

Variable	N1 metastasis ($n = 30$) Odds ratio (95% CI)	p value[#]	N2 metastasis ($n = 70$) Odds ratio (95% CI)	p value[#]
Male gender	2.366 (0.726-7.707)	0.153	2.019 (0.868-4.697)	0.103
Chronic pulmonary disease	1.827 (0.665-5.021)	0.242	1.231 (0.489-3.102)	0.659
Smoking history	0.479 (0.138-1.663)	0.246	0.217 (0.080-0.590)	0.003
Respiratory- or cancer-related symptoms	1.558 (0.692-3.508)	0.284	0.741 (0.374-1.467)	0.389
Adenocarcinoma histology	1.742 (0.619-4.901)	0.293	0.849 (0.330-2.181)	0.733
Consolidation size (cm)	5.449 (2.817-10.541)	<0.001	8.640 (5.002-14.923)	<0.001
Central location	1.069 (0.448-2.547)	0.881	0.508 (0.255-1.014)	0.055
Clinical nodal stage on CT				
Enlarged LNs in N1 station	11.424 (3.316-39.360)	<0.001	14.046 (4.226-46.682)	<0.001
Enlarged LNs in N2 station	1.615 (0.582-4.480)	0.357	8.703 (4.326-17.509)	<0.001
Levels of serum CEA (ng/ml)	0.932 (0.806-1.077)	0.340	1.063 (1.027-1.099)	0.001

[#]p value represented the comparison with N0 patients.

TABLE 3: Multivariate dichotomous logistic regression of the development group for predicting N2 metastasis.

Variable	Regression coefficient	p value	Odds ratio	95% confidence interval Lower	Upper
Central location	-0.756	0.029	0.469	0.239	0.924
Consolidation size (cm)	1.921	<0.001	6.824	4.095	11.373
Enlarged lymph node on CT	2.145	<0.001	8.546	4.491	16.262
Smoking history	-1.065	0.003	0.345	0.169	0.704
Level of serum CEA (ng/ml)	0.064	<0.001	1.066	1.031	1.102

As a truly multidisciplinary process, preoperative evaluation of lymph node evaluation has confused clinical physicians for many years. An algorithm that integrates imaging, endoscopic, and surgical techniques recommended by ESTS guidelines has been widely practiced and prospectively validated, with the negative predictive value as high as 0.94 [18]. However, some researchers are more interested in creating a predictive model ahead of biopsy strategy [16, 17, 19–21], because the accuracy of preoperative invasive staging such as TBNA may largely depend on the experience of operators.

Shafazand and Gould reported the first quantitative model to pretest the probability for N2 metastasis in NSCLC of all stages [20]. The formula consisted of six independent predictors, which were age, tumor size, central location,

adenocarcinoma histology, onset of primary symptoms, and abnormal mediastinum on chest X-ray. However, their data was directly collected from a previous randomized controlled trial and no CT images were included at that time. After that, Zhang and colleagues reported a four-predictor model for N2 metastasis in CT-defined T1N0M0 NSCLC in 2012 [16]. Younger patients with a central-located and larger-sized lung adenocarcinoma had higher risks of N2 disease. However, patients with a histology of AIS (adenocarcinoma in situ) and MIA (microinvasive adenocarcinoma) were excluded from their study, despite the fact that the pathology of AIS or MIA could only be confirmed from a resected specimen. In that case, the percentage of adenocarcinoma might be underestimated in their model because there will be AIS
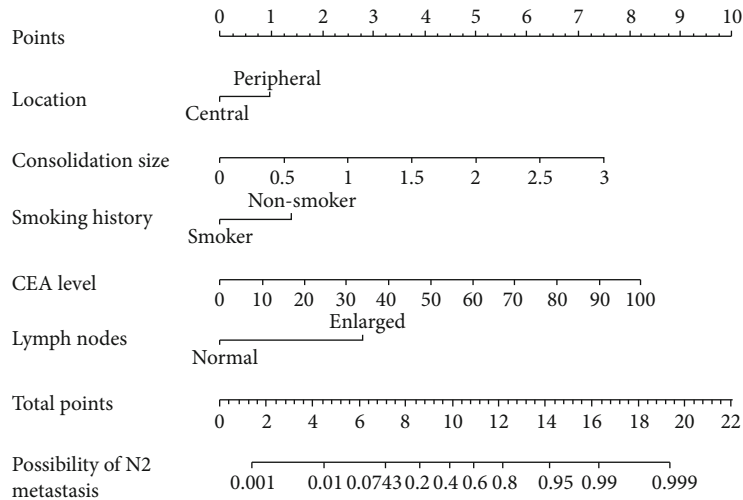
FIGURE 2: Nomogram predicting the likelihood of N2 metastasis in early lung cancers (tumor ≤ 3 cm). According to the location of value from the 2nd to the 6th axis, we can get the vertically corresponding points on the first axis. By summing up each points, we get a total point, and the vertically corresponding predicted value on the last axis shows the predicted possibility of N2 metastasis.
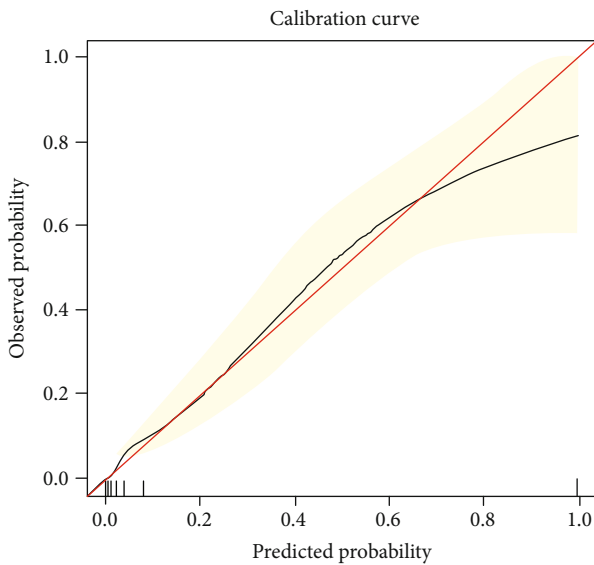
FIGURE 3: Calibration curve of the logistic regression model. The red line indicated a perfect prediction of observed possibilities. The black line represented the entire development group ($n = 924$).

and MIA patients in reality. More recently, there were predictive models evaluating N2 metastasis for NSCLC of all stages [21] and models estimating nodal metastasis in clinical T1a stages [17].

No models above have referred to the different risk factors of N1 and N2 metastases. Analyzed by polytomous logistic regression, we found that consolidation tumor size and lymph node enlargement on CT scan were the most related factors to both N1 and N2 metastases in patients with early malignant nodules (diameter ≤ 3 cm, stage T1). Though it is difficult to differentiate benign lymphadenectasis from lymph node metastasis on CT, our results showed that lymphadenectasis in N1 station was of higher correlation to N2 metastasis. This could be explained by the lymphatic drainage, and the rate for skip N2 metastasis was only 29% [22]. This result was partly in accordance with the previous literature and the ESTS recommendation [13, 23].

In both polytomous and dichotomous logistic analyses, consolidation tumor size and lymph node enlargement on CT and CEA levels were correlated to N2 metastasis, which is consistent with previous studies [16, 17, 24, 25]. Smoking history seemed to be negatively associated with N2 disease, as the odds ratio was less than 1 in both analyses. Despite the lack of molecular mechanisms, nonsmokers are more prone to a delayed or incidental detection of lung cancer than smokers and thus are more likely to progress into nodal metastasis, as supported by data from Lee et al. [26]. Apart from that, tumors with peripheral location were found with a higher likelihood of N2 metastasis in this study. The inconsistency between different research studies [27, 28] could result from the different criteria of the definition as "central location" and the different target population. Takeda et al. also found that peripheral tumors are more likely to have N2 metastasis by subpleural lymph drainage pathways [29].

Compared with previous logistic analysis, this study exhibited a larger sample size and reduced selective bias by enrolling patients with all pathological type including AIS and MIA, which constituted 8.2% and 16.7% of groundglass nodules in the development group. Our data suggested that consolidation size was a stronger predictive factor of nodal metastasis compared with tumor size and C/T ratio in the multivariate analysis. Squamous cell carcinoma also fit in with this model though it was a minority type of histology. Besides, pathological type was not an independent factor in this multivariate model, suggesting that preoperative histology might not be a necessity for predicting N2 metastasis.

Nevertheless, this study also had several limitations. Firstly, it was a retrospective study and there was no standard on the number of resected lymph nodes. In 2014, American
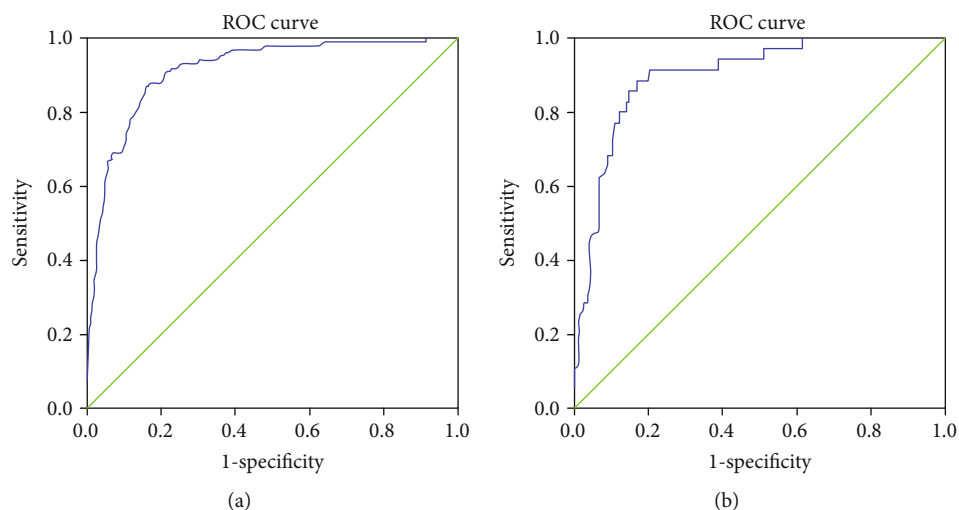
FIGURE 4: The receiver operating characteristic curve for the development and validation groups. (a) The ROC curve for the development group. The AUC was 0.931 (95% CI: 0.906-0.955). (b) The ROC curve for the validation group. The AUC was 0.906 (95% CI: 0.857-0.956).
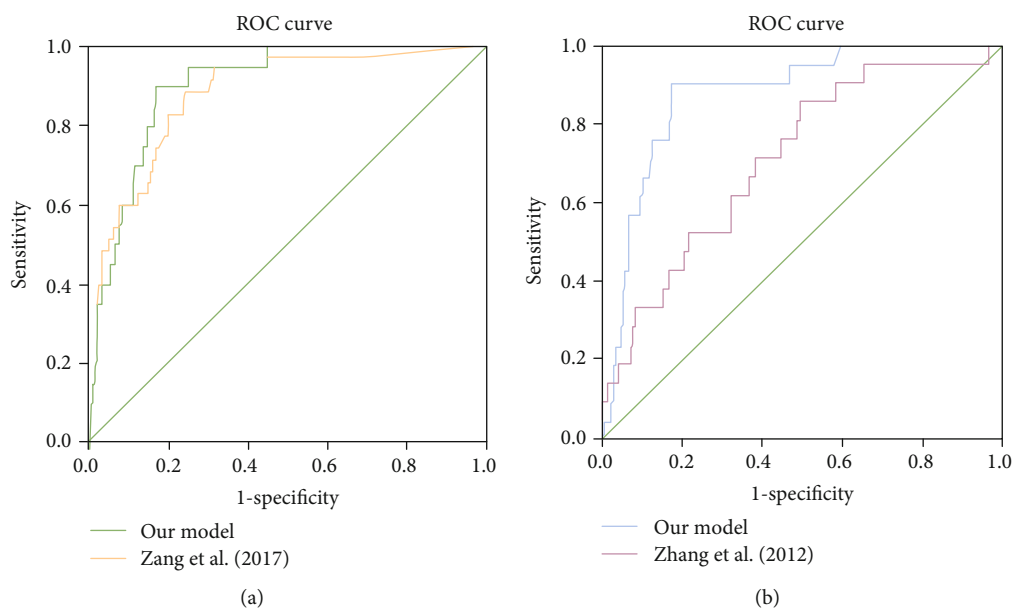
FIGURE 5: Comparison of our model and other published models using data from the same validation group. (a) Comparison with Zang et al. (2017) in cT1NxM0 patients. The AUC was 0.879 validated by our data (95% CI: 0.821-0.937). DeLong test for comparing two ROC curves: $p = 0.405$. (b) Comparison of our model with Zhang et al. (2012) in cT1N0M0 patients. The AUC was 0.712 validated by our data (95% CI: 0.602-0.822). DeLong test for comparing two ROC curves: $p = 0.002$.

College of Surgeons Commission on Cancer recommended at least 10 regional lymph nodes to be removed and pathologically examined for resectable NSCLC [30]. Thus, a diagnostic bias might occur in our study. Secondly, we only collected data from a single-center institution and reflected patient characteristics in local areas. Finally, in order to ensure the general use of the model, the proportion of lymph node metastasis in this study was coherent with the prevalence in reality, which was insufficient and influenced the positive predictive value of the model. Therefore, a larger-sized study

with more positive data from multiple medical centers will be needed to carry out a more practical model for clinical use.

5. Conclusions

In this study, we analyzed the clinical features of patients with lymph node metastasis and produced a model predicting the possibility of N2 nodal metastasis for early lung cancers (tumor ≤ 3 cm). Stratified by the cutoff point, a low predicted probability may suggest an operation directly

without neoadjuvant therapies, while a relatively high predicted probability needs support from further invasive and expensive examinations. Our model will provide some clues for clinical decision-making.

Data Availability

All relevant data are within the article and the supplementary materials.

Ethical Approval

This study was approved by the Institutional Ethics of Committee of SAHZU (2017-031).

Conflicts of Interest

The authors have no conflicts of interest to declare.

Authors' Contributions

Chengyan Zhang and Guanchao Pang contributed equally to this work.

Acknowledgments

Supplementary Materials

Supplementary Table 1: characteristics of patients in the validation group. (Supplementary Materials)

References

[1] T. Bilfinger, R. Keresztes, D. Albano, and B. Nemesure, "Five-year survival among stage IIIA lung cancer patients receiving two different treatment modalities," *Medical Science Monitor*, vol. 22, pp. 2589–2594, 2016.

[2] J. van Meerkbeeck, P. Van Schil, G. Kramer et al., "Pr5 A randomized trial of radical surgery (S) versus thoracicradiotherapy (TRT) in patients (pts) with stage IIIA-N2 non-small cell lung cancer (NSCLC) after response to induction chemotherapy (ICT) (EORTC 08941)," *Lung Cancer*, vol. 49, article S4, Supplement 2, 2005.

[3] K. S. Albain, R. S. Swann, V. R. Rusch et al., "Phase III study of concurrent chemotherapy and radiotherapy (CT/RT) vs CT/RT followed by surgical resection for stage IIIA(pN2) non-small cell lung cancer (NSCLC): outcomes update of North American Intergroup 0139 (RTOG 9309)," *Journal of Clinical Oncology*, vol. 23, no. 16, pp. 7014–7014, 2005.

[4] R. Bueno, W. G. Richards, S. J. Swanson et al., "Nodal stage after induction therapy for stage IIIA lung cancer determines patient survival," *The Annals of Thoracic Surgery*, vol. 70, no. 6, pp. 1826–1831, 2000.

[5] D. C. Betticher, S. F. Hsu Schmitz, M. Tötsch et al., "Mediastinal lymph node clearance after docetaxel-cisplatin neoadjuvant chemotherapy is prognostic of survival in patients with stage IIIA pN2 non-small-cell lung cancer: a multicenter phase II trial," *Journal of Clinical Oncology*, vol. 21, no. 9, pp. 1752–1759, 2003.

[6] N. Lorent, P. de Leyn, Y. Lievens et al., "Long-term survival of surgically staged IIIA-N2 non-small-cell lung cancer treated with surgical combined modality approach: analysis of a 7-year prospective experience," *Annals of Oncology*, vol. 15, no. 11, pp. 1645–1653, 2004.

[7] J. A. Roth, E. N. Atkinson, F. Fossella et al., "Long-term follow-up of patients enrolled in a randomized trial comparing perioperative chemotherapy and surgery with surgery alone in resectable stage IIIA non-small-cell lung cancer," *Lung Cancer*, vol. 21, no. 1, pp. 1–6, 1998.

[8] R. Rosell, J. Gomez-Codina, C. Camps et al., "Preresectional chemotherapy in stage IIIA non-small-cell lung cancer: a 7-year assessment of a randomized controlled trial," *Lung Cancer*, vol. 26, no. 1, pp. 7–14, 1999.

[9] A. Depierre, V. Westeel, B. Milleron et al., "O-211 5-year results of the French randomized study comparing preoperative chemotherapy followed by surgery and primary surgery in resectable stage I (except T1N0), II and IIIA non-small cell lung cancer," *Lung Cancer*, vol. 41, pp. S62–S62, 2003.

[10] D. Gilligan, M. Nicolson, I. Smith et al., "Preoperative chemotherapy in patients with resectable non-small cell lung cancer: results of the MRC LU22/NVALT 2/EORTC 08012 multicentre randomised trial and update of systematic review," *The Lancet*, vol. 369, no. 9577, pp. 1929–1937, 2007.

[11] NSCLC Meta-analysis Collaborative Group, "Preoperative chemotherapy for non-small-cell lung cancer: a systematic review and meta-analysis of individual participant data," *The Lancet*, vol. 383, no. 9928, pp. 1561–1571, 2014.

[12] P. De Leyn, C. Dooms, J. Kuzdzal et al., "Revised ESTS guidelines for preoperative mediastinal lymph node staging for non-small-cell lung cancer," *European Journal of Cardio-Thoracic Surgery*, vol. 45, no. 5, pp. 787–798, 2014.

[13] P. De Leyn, D. Lardinois, P. E. Van Schil et al., "ESTS guidelines for preoperative lymph node staging for non-small cell lung cancer," *European Journal of Cardio-Thoracic Surgery*, vol. 32, no. 1, pp. 1–8, 2007.

[14] B. F. Meyers, F. Haddad, B. A. Siegel et al., "Cost-effectiveness of routine mediastinoscopy in computed tomography- and positron emission tomography-screened patients with stage I lung cancer," *The Journal of Thoracic and Cardiovascular Surgery*, vol. 131, no. 4, pp. 822–829.e2, 2006.

[15] P. C. Lee, J. L. Port, R. J. Korst, Y. Liss, D. N. Meherally, and N. K. Altorki, "Risk factors for occult mediastinal metastases in clinical stage I non-small cell lung cancer," *The Annals of Thoracic Surgery*, vol. 84, no. 1, pp. 177–181, 2007.

[16] Y. Zhang, Y. Sun, J. Xiang, Y. Zhang, H. Hu, and H. Chen, "A prediction model for N2 disease in T1 non-small cell lung cancer," *The Journal of Thoracic and Cardiovascular Surgery*, vol. 144, no. 6, pp. 1360–1364, 2012.

[17] R. C. Zang, B. Qiu, S. G. Gao, and J. He, "A model predicting lymph node status for patients with clinical stage T1aN0-2M0 nonsmall cell lung cancer," *Chinese Medical Journal*, vol. 130, no. 4, pp. 398–403, 2017.

[18] P. De Leyn, C. Dooms, J. Kuzdzal et al., "Preoperative mediastinal lymph node staging for non-small cell lung cancer: 2014 update of the 2007 ESTS guidelines," *Translational Lung Cancer Research*, vol. 3, no. 4, pp. 225–233, 2014.

[19] O. J. O'Connell, F. A. Almeida, M. J. Simoff et al., "A prediction model to help with the assessment of adenopathy in lung cancer: HAL," *American Journal of Respiratory and Critical Care Medicine*, vol. 195, no. 12, pp. 1651–1660, 2017.

[20] S. Shafazand and M. K. Gould, "A clinical prediction rule to estimate the probability of mediastinal metastasis in patients with non-small cell lung cancer," *Journal of Thoracic Oncology*, vol. 1, no. 9, pp. 953–959, 2006.

[21] K. Chen, F. Yang, G. Jiang, J. Li, and J. Wang, "Development and validation of a clinical prediction model for N2 lymph node metastasis in non-small cell lung cancer," *The Annals of Thoracic Surgery*, vol. 96, no. 5, pp. 1761–1768, 2013.

[22] P. Misthos, E. Sepsas, K. Athanassiadi, S. Kakaris, and I. Skottis, "Skip metastases: analysis of their clinical significance and prognosis in the IIIA stage of non-small cell lung cancer," *European Journal of Cardio-Thoracic Surgery*, vol. 25, no. 4, pp. 502–508, 2004.

[23] A. F. H. Martínez, M. D. G. Jiménez, A. G. Vicente et al., "Ratio between maximum standardized uptake value of N1 lymph nodes and tumor predicts N2 disease in patients with non-small cell lung cancer in ^{18}F-FDG PET-CT scan," *Revista Española de Medicina Nuclear e Imagen Molecular*, vol. 35, no. 3, pp. 159–164, 2016.

[24] T. Koike, T. Koike, Y. Yamato, K. Yoshiya, and S. Toyabe, "Predictive risk factors for mediastinal lymph node metastasis in clinical stage IA non-small-cell lung cancer patients," *Journal of Thoracic Oncology*, vol. 7, no. 8, pp. 1246–1251, 2012.

[25] J. Xiong, R. Wang, Y. Sun, and H. Chen, "Clinical analysis of sixty-four patients with T1aN2M0 stage non-small cell lung cancer who had undergone resection," *Thorac Cancer*, vol. 7, no. 2, pp. 215–221, 2016.

[26] J. Y. Lee, I. I. Na, S. H. Jang et al., "Differences in clinical presentation of non-small cell lung cancer in never-smokers versus smokers," *Journal of Thoracic Disease*, vol. 5, no. 6, pp. 758–763, 2013.

[27] S. J. Gao, A. W. Kim, J. T. Puchalski et al., "Indications for invasive mediastinal staging in patients with early non-small cell lung cancer staged with PET-CT," *Lung Cancer*, vol. 109, pp. 36–41, 2017.

[28] A. Gómez-Caro, S. Garcia, N. Reguart et al., "Incidence of occult mediastinal node involvement in cN0 non-small-cell lung cancer patients after negative uptake of positron emission tomography/computer tomography scan," *European Journal of Cardio-Thoracic Surgery*, vol. 37, no. 5, pp. 1168–1174, 2010.

[29] A. H. Takeda, Y. Watanabe, T. Nagata et al., "Detection of alternative subpleural lymph flow pathways using indocyanine green fluorescence," *Surgery Today*, vol. 48, no. 6, pp. 640–648, 2018.

[30] American College of Surgeons Commission on Cancer, *CoC quality of care measures, non-small cell lung cancer, 2015*, American College of Surgeons, 2018, March 2019, https://www.facs.org/quality%20programs/cancer/ncdb/qualitymeasures.

Research Article

Efficacy of Shenqi Pollen Capsules for High-Altitude Deacclimatization Syndrome via Suppression of the Reoxygenation Injury and Inflammatory Response

Binfeng He,[1] Mingdong Hu,[1] Zhihui Liang,[2] Qianli Ma ⓘ,[1] Yunhai Zi,[1] Zhiwei Dong,[3] Qi Li,[1] Yongjun Luo,[4] Guisheng Qian,[1] Liang Guo,[1] Kexiong Lin,[5] Zhenyu Liu ⓘ,[6] and Guansong Wang ⓘ[1]

[1]*Institute of Respiratory Diseases, Xinqiao Hospital of the Third Military Medical University, Chongqing 400037, China*
[2]*Bethune International Peace Hospital of PLA, Shijiazhuang, Hebei 050000, China*
[3]*Center for Disease Control and Prevention of Zhengzhou City and First Affiliated Hospital of Zhengzhou University, Zhengzhou, Henan 450000, China*
[4]*College of High Altitude Military Medicine, Third Military Medical University, Chongqing 400038, China*
[5]*Department of Respiration, Tongren City People's Hospital, Guizhou 554300, China*
[6]*Department of Emergency, The First Affiliated Hospital of Nanchang University, Nanchang 330006, China*

Correspondence should be addressed to Zhenyu Liu; 3123891447@qq.com and Guansong Wang; wanggs2003@163.com

High-altitude deacclimatization syndrome (HADAS) is involved in hypoxia-reoxygenation injury and inflammatory response, induced a series of symptoms, and has emerged as a severe public health issue. Here, we investigated the mechanism as well as potential means to prevent HADAS using Shenqi pollen capsules (SPCs) in subjects with HADAS in a multicenter, double-blinded, randomized, placebo-controlled study. All subjects were at the same high altitude (3650 m) for 4-8 months before returning to lower altitudes. Subjects ($n = 288$) in 20 clusters were diagnosed with mild or moderate HADAS on the third day of the study. We randomly allocated 20 clusters of subjects ($1:1$) to receive SPCs or a placebo for 7 weeks, and they were then followed up to the 14th week. The primary endpoints were subjects' HADAS scores recorded during the 14 weeks of follow-up. Compared with the placebo, SPC treatment significantly decreased the subjects' HADAS scores and reduced the incidence of symptom persistence. SPC therapy also reduced the serum levels of CK, CK-MB, LDH, IL-17A, TNF-α, and miR-155 and elevated IL-10 and miR-21 levels. We thus demonstrate that SPCs effectively ameliorated HADAS symptoms in these subjects via suppression of the hypoxia-reoxygenation injury and inflammatory response.

1. Introduction

High-altitude deacclimatization syndrome (HADAS) is a serious form of high-altitude deacclimatization (HADA), in which the loss of high-altitude acclimatization provokes complex and multifaceted physiological and functional changes in individuals who have acclimated to a high altitude and then returned to a lower altitude or sea level [1–7]. In general, HADA occurs under typical environmental reacclimatization in which individuals return to lower altitudes from high altitudes. Similar to the process of high-altitude

acclimatization (HAC), the physiological processes associated with the progression of HADA in a time-dependent manner: acclimatory changes and acquired hypoxia tolerance are not lost immediately upon returning to lower altitudes but instead disappear gradually over time. HADA also involves several physiological adjustments, including decreased erythrocyte, hemoglobin, and hormone levels [8]. Interestingly, HADA symptoms are similar to those of individuals who suffer from high-altitude stress. A previous study showed that migrants from high plateaus suffered from excessive somnolence, diminished reflexes, and inadequate

fine motor coordination while living at sea level [9]. Cui and colleagues showed that 70.76% of individuals who live at high altitudes for 10–30 years suffered from a series of clinical symptoms, including fatigue, headaches, and sleepiness while undergoing HADA [10]. Individuals undergoing HADA can suffer from multiple symptoms, including sleepiness, insomnia, unresponsiveness, memory loss, fidgetiness, headache, throat pain or discomfort, coughing, expectoration, chest tightness, flustering, increased appetite or decreased appetite, diarrhea, abdominal distention, abdominal pain, lumbago, and arthralgia [1, 11]. In addition, cardiovascular, hematological, and respiratory system abnormalities were observed in subjects when they returned to lower altitudes [7, 11]. Other studies have shown that several of these symptoms can last many years in some severe cases, and 1‰ of subjects experienced such severe symptoms that they had to return to high altitudes [12]. We refer to all of the above pathological conditions as features of HADAS [1, 13, 14].

HADAS is an important public health issue. First, there are a large number of individuals with HADAS owing to the increasing number of individuals who have worked and traveled to high altitudes worldwide. In China, more than one million people live and work at high altitudes. They return to lower altitudes when they have finished their work, for trade contacts or other reasons. Some of them will develop HADAS [8, 15]. Cui demonstrated that 71% of individuals who lived at high altitudes for 10 to 30 years suffered from HADAS upon returning to lower altitudes [10]. Our previous study showed that 84% of individuals who lived in Tibet for 10 to 20 years had suffered from HADAS [11]. Additionally, the incidence of HADAS was very high, reaching 100%, in individuals who worked in earthquake relief at Yushu in Qinghai Province [15]. Second, HADAS severely impairs the quality of life of affected individuals. Previous studies showed that subjects with HADAS suffer a series of clinical symptoms, including sleepiness, insomnia, unresponsiveness, memory loss, and fidgetiness [1, 10, 11]. Another study showed that some subjects who had worked at high altitudes for 20 years (Tibet and Qinghai Province, >3000 m) suffered from severe HADAS, with symptoms lasting many years [12]. Although HADAS has received increasing attention in recent years from the medical community, treatment options are limited and are often ignored by public health advocates.

Treating HADAS remains a major challenge. Recently, several studies showed some traditional Chinese drugs and hyperbaric oxygen (HBO) treatments could relieve symptoms of subjects with HADAS. Shenqi pollen capsules (SPCs) consist of a compound prepared with the following raw materials [16]: *Codonopsis pilosula*, the root of *Astragalus propinquus*, cattail pollen, zasiokaurin, and sunflower pollen. SPCs have been processed and analyzed by colorimetric methods and high-performance liquid chromatography. The active ingredients of SPCs include flavonoids, quercetin, kaempferol, isorhamnetin, astragaloside, atractylenolide III, and lobetyolin. Our previous study showed that SPCs, Herba Rhodiolae capsules, and Sankang capsules were effective in improving the symptoms of HADAS compared with the effects of a placebo, and SPCs were better at decreasing HADAS scores compared to the effects of Rhodiolae capsules and Sankang capsules in a single-blinded, randomized, controlled trial [17]. Another study examined 380 subjects (280 males and 100 females) who had worked building a factory at high altitude (4300 m) for 5 days and then returned to camp (2800 m) for 2 days. Over the 3 years of the study, 82.37% of the subjects felt uncomfortable or suffered from HADAS symptoms, including sleepiness, insomnia, and unresponsiveness. The symptoms were partly alleviated in 117 subjects who took SPCs orally for 2 weeks [18]. In addition, Cui et al. showed that *Ginkgo biloba* leaf extract tablets, compound *Codonopsis pilosula extract* capsules, and Herba Rhodiolae capsules decreased plasma viscosity and improved tissue microcirculation in subjects with HADAS compared to the effects of a placebo [19]. Jin and colleagues demonstrated that dizziness, chest tightness, and memory loss was significantly relieved after subjects with HADAS underwent 5 rounds of HBO therapy [20].

Although previous study showed SPCs can be effective in treating HADAS in short-term, single center trials, these trials did not fully clarify the long-term effectiveness and safety of SPCs in treating HADAS. Therefore, we aimed to evaluate the efficacy of SPCs for treating HADAS and explore its novel mechanism.

2. Methods

2.1. Study Design. A multicenter, double-blinded, placebo-controlled, randomized trial was performed. All subjects presented at four centers in four hospitals: Xinqiao Hospital (in Chongqing), the 478th Hospital of PLA (in Kunming), First Hospital of Zhengzhou University (in Zhengzhou), and Wuwei City People's Hospital (in Wuwei). The trial methods were carried out in accordance with the approved guidelines. All subjects provided written informed consent before enrollment. The researchers conducting this trial were respiratory and ultrasonography physicians at the four hospitals. The screening, enrollment, and study visits occurred at the four trial sites, and the safety of the study, as well as the data, was monitored by an independent data and safety monitoring board.

All researchers were trained in the assessment of HADAS symptoms, including the classification decisions and scoring criteria, in group sessions at four meetings throughout the trial and in individual training sessions with the trial manager. All researchers recruited between meetings were trained by the trial manager, and local supplementary training was provided whenever necessary. This study was approved by the medical ethics committee of Xinqiao Hospital and the Third Military Medical University, and all subjects provided written informed consent. The report of the study adheres to the Consolidated Standards of Reporting Trials (CONSORT) statement (Supplementary File S1), and the trial was registered at Chinese Clinical Trial Register (ChiCTR) with the identifier number ChiCTR-TRC-12002653 (URL: http://www.chictr.org.cn/showproj.aspx?proj=6899).

2.2. Subjects. Enrollment occurred from February 2011 through October 2012. Individuals aged 18–60 years were eligible for inclusion if they were diagnosed with HADAS and presented scores of 6 to 25 upon returning to a lower altitude from Lhasa (3650 m), where they had worked for 4–7 months [1]. The subjects were followed up with active surveillance. The principal exclusion criteria comprised symptoms directly attributable to primary diseases affecting the cardiovascular, respiratory, nervous, urinary, and hematological systems; cancer or leukemia; and a recent history of influenza, upper respiratory tract infection, infectious diarrhea, or similar symptoms.

The subjects from the cities of Chongqing (180 m), Kunming (1800 m), Zhengzhou (110 m), and Wuwei (1500 m) worked at four spring water or beer factories at the same altitude (3650 m). The working conditions and intensity and the dietary patterns of the subjects were similar to those of individuals at the lower altitude factories where the subjects originally worked.

2.3. Randomization and Masking. In our study, 10 to 17 subjects always lived and worked together as a cluster, for a total of 20 units ($n = 288$) across the research centers. Because the subjects who lived in a given unit might exchange drugs under the masked conditions, we considered each unit as one cluster when applying random assignments, i.e., all subjects in a unit took the same drug. The 20 clusters were randomly assigned (1 : 1) to receive SPCs or a placebo. The randomization sequence was computer generated using permuted block randomization with a block size of four by an individual who was independent of the study team. The allocation was concealed using vials coded for each subject. At every drug-refill visit, a constructor assigned the container numbers to be dispensed to the subjects. Henan Fenghuang Drugs Manufacture Stock Co. Ltd. (Xinxiang City, Henan Province) prepared the trial drugs and containers, which were labeled with numbers according to the randomized treatments to ensure that the stocks matched the assignments at each site.

All subjects, physicians, outcome assessors, inspectors, and researchers (persons conducting the study) were blinded to the treatment allocations until the study was unblinded and completed, and the database was frozen. The vials for SPCs and placebo capsules and their contents were indistinguishable in external appearance, texture, taste, and smell.

2.4. SPC Production. SPCs were manufactured with raw material according to a previous patent [16] in Henan Fenghuang Drugs Manufacture Stock Co. Ltd. (Xinxiang City, Henan Province). Briefly, 4 kg *Codonopsis pilosula* and 4 kg Mongolian milkvetch root were mixed, and their active ingredients were extracted by water extraction. These active ingredients were concentrated, dried, and made into powdered extracts, which then underwent size reduction. Additionally, 1 kg each of corn pollen, sunflower pollen, rape bee pollen, cattail pollen and honey was mixed and fermented at 37°C for 72 h. The fermentation products were dried, made into a powder, and mixed with the powdered *Codonopsis*

pilosula and Mongolian milkvetch extract. The mixed products were then made into Shenqi pollen capsules (SPCs).

2.5. Procedures. The subjects ingested three SPCs or placebo capsules orally three times a day (t.i.d.) for 7 weeks. The subjects also underwent follow-up visits at 7 and 14 weeks.

The study procedures included checking vital signs upon returning to a lower altitude from a high altitude; the subjects' level of discomfort and symptoms were evaluated and recorded on days 1 through 7. The symptom scores, routine blood analyses, myocardial enzyme levels, and heart function assessments were evaluated on the third day after the subjects returned to a lower altitude from a high altitude, similar to our previous study. The subjects were evaluated at the four sites at 7 and 14 weeks after the administration of the drug or a placebo. Subjects were enrolled in our study upon being diagnosed with mild or moderate HADAS [1, 3], and they began to take SPCs or placebo capsules on the fourth day after returning to a lower altitude from a high altitude. All subjects were followed up by telephone or oral interview each month until the end of the trial. If any other medication or therapy was required to treat concomitant diseases, the name of the drug or therapy, actual dosage, dosing frequency, and start/stop time were well-documented. Adverse events (AEs) reported by the subjects or observed by the investigator were recorded regardless of whether they were considered to be drug related and were reported according to the State Food and Drug Administration Criteria.

2.6. Diagnostic and Scoring Criteria for HADAS. Establishing diagnostic and scoring criteria is crucial to further explore the pathophysiology of HADAS, as well as its prevention and treatment. The diagnostic criteria for HADAS were first reported in Zhang et al.'s book *People and High Altitudes* [13] in 1996. Based on a large-scale epidemiological investigation, we modified these diagnostic criteria and established a scoring criterion to more accurately evaluate HADAS and explore its pathophysiology [1, 11]. This system contains essential diagnostic criteria, auxiliary diagnostic criteria, and exclusion criteria for HADAS, as well as a classification and scoring criteria of the symptoms of HADAS. Symptom scores were evaluated according to the scoring criteria for fixed-duration high-altitude deacclimatization syndrome (the details in Supplementary File S1).

2.7. Outcome Measures. The primary outcome was the subjects' HADAS scores in the records taken over the 14 weeks. The HADAS scoring criteria had been previously validated in adults living at high altitudes and who were acclimatized to high-altitude environments before returning to a lower altitude. The scores ranged from 0 to 63 (0 to 5 points representing no HADAS symptoms and 26 or more points representing very severe symptoms). The scores were evaluated by a physician who had received specialized training.

The secondary endpoints included the levels of routine blood measures (RBC, Hb, and Hct levels), myocardial enzyme (creatine kinase (CK), CK-MB, and LDH), and measures of heart function (e.g., LVEF) in the subjects with HADAS. Routine blood and myocardial enzyme analyses

were performed as previously described at the 7- and 14-week follow-up visit as previously described [1]. Serum was isolated and stored at -80°C until the assays were conducted. A color Doppler ultrasonography system (GE LOGIQ-3) was used to measure the LVEF and LVFS and other parameters. The heart function of all subjects was evaluated by the ultrasonography specialist from Xinqiao Hospital (the details in Supplementary File S1).

2.8. Evaluation of the Level of Serums IL-17A, IL-10, and TNF-α. The ELISA kit for human serum IL-17A, TNF-?, and IL-10 ELISA kits was ordered from R&D Systems (Abingdon, UK). The level of IL-17A, TNF-?, and IL-10 levels was detected according to the manufacturer's instructions [21].

2.9. Detection of the Levels of Serums SOD and MDA. The analysis kit of serums SOD and MDA was ordered from the Nanjing Jiancheng Bioengineering Institute (Nanjing, China). All samples had been evaluated according to the previous study [21].

2.10. Isolation of Serum Small RNA and Analysis of the Level of miR-155 and miR-21. Total RNA was isolated from subject's serum samples according to a previous study [22]. Briefly, these serum samples were pretreated with proteinase K in 37°C for 30 min, and synthetic C. elegans microRNA 39 (cel-miR-39), as an external reference, was added into these samples. Small RNA was isolated using TRIzol reagent (Sigma, Lot: #T9242) according to the manufacturer's instructions. Small RNAs were reverse-transcribed using miRNA First Strand cDNA Synthesis (Tailing Reaction) (Sangon Biotech, Lot: # B532451), and qPCR were carried out with the following conditions: 95°C for 10 min, 95°C for 25 s, and 60°C for 30 s at the annealing temperature through 40 cycles. The data was analyzed as previous description [23].

2.11. Statistical Analysis. We calculated that a sample size of 288 individuals was needed to provide 80% power to detect a two-point difference in HADAS scores between the SPC and the placebo groups at 7 and 14 weeks, with a type I error rate of 0.05 and allowing for a 20% loss during follow-up. An interim analysis using the O'Brien-Fleming stopping boundaries was performed after 173 subjects were recruited. All analyses were based on intention-to-treat (ITT) analyses, defined as an analysis of all randomized individuals who received at least one dose of the study drug. Missing data were handled using the last observation carried forward (LOCF) imputation technique. All subjects in the random assignment of the 20 clusters were included in the final analyses. Missing values were assumed to be missing at random. Two-sided tests with p values less than 0.05 were considered statistically significant.

We summarized continuous variables as the means (SE, 95% CIs) and categorical variables as n (%). Statistical differences between groups were analyzed using a t test for quantitative data and Fisher's exact test for categorical data at baseline. The analysis of the primary endpoint, the treatment-related difference in the mean difference from baseline to measurements taken at follow-up, used a linear

mixed-effects model for repeated measures and represents the average treatment effect at weeks 7 and 14. The model included main effects for time, treatment group, height differences, work intensity, smoking status, alcohol consumption status, and occurrence of acute mountain sickness (AMS) at high altitude and age, as well as the interaction between the time and the treatment group as fixed effects, whereas subject differences were included as random effects with an unstructured within-subject variance-covariance structure, and results were estimated using a restricted maximum likelihood model. Continuous variables for the secondary outcomes were evaluated using the same linear mixed-effects model for repeated measures used in the analysis of the primary endpoint. In cases of interactions, the effects of a group at each time point were compared, and the Bonferroni corrections were used to adjust for multiple comparisons.

The incidence of symptoms and HADAS severity were compared between the SPC and the placebo groups using Fisher's exact test. The overall incidence of adverse events and symptoms of drug-related events in both groups were analyzed by Fisher's exact test. SPSS 15.0 for Windows (SPSS Inc., Chicago) was used for all statistical analyses.

3. Results

The flow diagram for subject selection and follow-up in the trial is shown in Figure 1. We recruited subjects between January 2011 and March 2012, and follow-up interviews were completed by June 2012. A total of 475 subjects were assessed for eligibility, of whom 288 were enrolled. Subjects were randomly assigned to two groups: 146 (50.69%) received SPC treatment and 142 (49.31%) received placebo treatment.

Of the 146 individuals in the SPC group, 23 (15.75%) had withdrawn by week 14, as had 21 (14.78%) of the 142 subjects in the placebo group. By week 7, 15 of the 146 individuals in the SPC group had withdrawn (10.27%, 11 withdrew from treatment and 4 refused further participation), as had 12 of 142 from the placebo group (8.45%, 11 withdrew from treatment and 4 refused further participation). Between weeks 7 and 14, 8 of the 131 subjects from the SPC group had withdrawn (6.10%, 5 withdrew from treatment and 3 refused further participation), as had 9 of 130 subjects from the placebo group (5 withdrew from treatment and 4 refused further participation). The dropout rate was not different between the SPC and the placebo groups ($p > 0.05$).

Descriptive, baseline characteristics of the study population are shown in Table 1. No significant differences were found between the SPC and the placebo groups in demographic characteristics, working intensity, smoking status, alcohol consumption status, or incidence of acute mountain sickness ($p > 0.05$).

Primary outcomes at baseline, week 7, and week 14 can be found in Table 2. During the 14 weeks of the study, the subjects' HADAS scores were evaluated by interview or telephone follow-up. The scores decreased from 13.08 to 1.36 in the SPC group and from 12.80 to 2.80 in the placebo group. No significant difference is found between the SPC and the
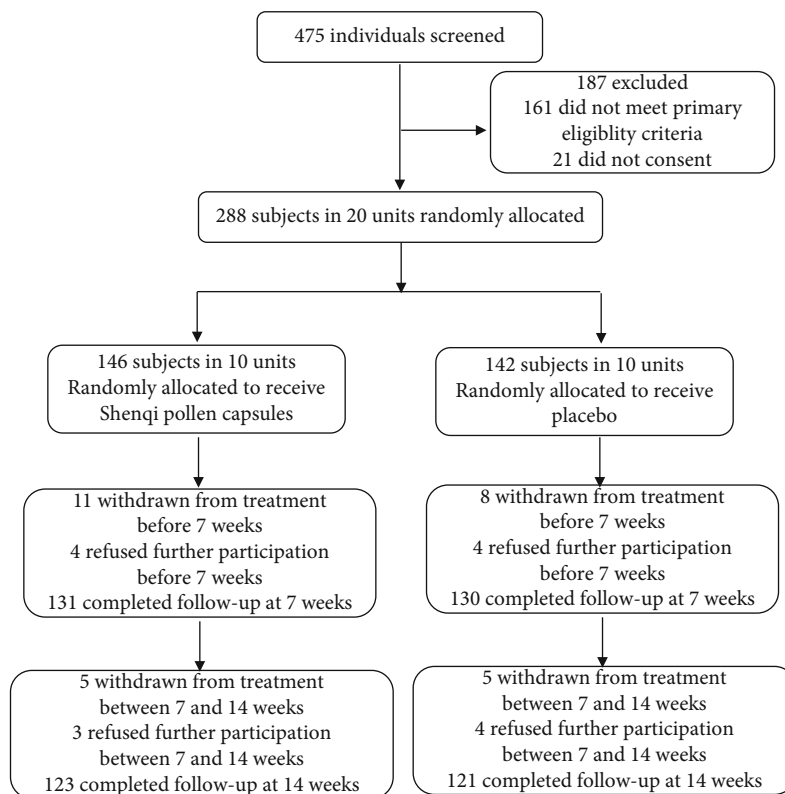
```
                    475 individuals screened

                                    187 excluded
                                    161 did not meet primary
                                        eligiblity criteria
                                    21 did not consent

              288 subjects in 20 units randomly allocated


   146 subjects in 10 units              142 subjects in 10 units
   Randomly allocated to receive         Randomly allocated to receive
   Shenqi pollen capsules                placebo


   11 withdrawn from treatment           8 withdrawn from treatment
        before 7 weeks                        before 7 weeks
   4 refused further participation       4 refused further participation
        before 7 weeks                        before 7 weeks
   131 completed follow-up at 7 weeks    130 completed follow-up at 7 weeks


   5 withdrawn from treatment            5 withdrawn from treatment
        between 7 and 14 weeks                between 7 and 14 weeks
   3 refused further participation       4 refused further participation
        between 7 and 14 weeks                between 7 and 14 weeks
   123 completed follow-up at 14 weeks   121 completed follow-up at 14 weeks
```

FIGURE 1: The flow diagram of the trial.

placebo groups for HADAS scores at baseline ($p > 0.05$). There were significant main effects for time, group, and time-group interaction for HADAS scores ($p < 0.001$ for all effects). Mean differences between the groups were -1.34 (95% CI, -1.74 to -0.95; $p < 0.001$) at week 7 and -1.47 (95% CI, -1.87 to -1.07; $p < 0.001$) at week 14. These data indicated that the primary outcomes were dependent on the treatment received, time, and time-group interaction.

The incidence of HADAS symptoms is shown in Table 3. No significant difference was found between the SPC and the placebo groups for symptom incidence at baseline ($p > 0.05$). After 7 weeks of treatment with SPCs or placebo capsules, the incidences of all symptoms decreased over time in both groups. The incidences of symptoms such as sleepiness, insomnia, unresponsiveness, memory loss, agitation, headache, dizziness, coughing, chest tightness, and flustering among subjects in the SPC group were significantly lower at week 7 than they were in the placebo group ($p < 0.05$). The incidences of symptoms such as sleepiness, insomnia, unresponsiveness, headache, dizziness, coughing, expectoration, chest tightness, flustering, and diarrhea were also significantly lower in the SPC group than in the placebo group at week 14 ($p < 0.05$) (Table 3). Additionally, at week 14, the overall proportion of mild reactions was 0.68% in the SPC group, which was significantly lower than the proportion observed in the placebo group (9.15%, $p < 0.01$) (Table 4). Other symptoms did not appear in either group, and no subjects suffered from moderate HADAS at week 14. These data suggest that SPC therapy may ameliorate HADAS symptoms.

Similar to the primary outcome findings, there were significant main effects for time, group, and time-group interaction for creatine kinase (CK), CK-MB, and lactate dehydrogenase (LDH) ($p < 0.001$ for all effects) (Table 5). Additionally, there were significant main effects for time and time-group interaction for pulmonary artery systolic pressure (PASP) ($p_t < 0.001$ and $p_{t+g} < 0.001$). The mean differences between the groups in PASP were not significant at week 7 ($p > 0.05$) but were significant at week 14 ($p < 0.05$). Additionally, there were no significant time-group interactions or main effects of group for the secondary outcomes of heart rate (HR), left ventricular ejection fraction (LVEF), left ventricular fractional shortening (LVFS), pulmonary artery inner diameter, or pulmonary artery opening velocity (PAOV) ($p_g > 0.05$ and $p_{g+t} > 0.05$) (Table 5). There were significant main effects for time for these parameters ($p_t < 0.05$), indicating that they are not dependent on the treatment received, as both groups showed similar improvements at each follow-up.

In our previous study, the levels of inflammatory mediators, such as IL-17A and TNF-?, were elevated and the IL-10 level descended upon the subjects returned to sea level from a high-altitude region and were diagnosed as HADAS. Herein, the level of serums IL-17A, IL-10, and TNF-? was evaluated and compared between the SPC and the placebo groups (Figure 2). After subjects received SPC treatment, the serum concentration of IL-17A and TNF-? was significantly decreased and the IL-10 level increased at 7th week, compared to the placebo group ($p < 0.05$). At the 14th week, the

TABLE 1: Baseline characteristics of subjects at randomization according to the study group.

	SPC group ($n = 146$)	Placebo group ($n = 142$)	p value
Demographic characteristics			
Chongqing (180 m) (%)	44 (30.13%)	42 (29.58%)	0.92
Kunming (1800 m) (%)	34 (23.29%)	33 (23.24%)	0.99
Zhengzhou (110 m) (%)	38 (26.03%)	37 (26.06%)	0.95
Wuwei (1500 m) (%)	30 (20.55%)	30 (21.12%)	0.90
Age, years (SD, range)	25.09 (5.08, 18-35)	24.60 (4.66, 18-34)	0.40
Race, Han (%)	146 (100%)	142 (100%)	1.00
Sex, male (%)	146 (100%)	142 (100%)	1.00
Work intensity			
Mild	42 (28.77%)	44 (30.98%)	0.42
Moderate	86 (58.90%)	88 (61.97%)	0.63
Severe	14 (9.58)	14 (9.85)	0.94
Smoking	114 (78.08%)	106 (74.64%)	0.49
Alcohol consumption	113 (77.39%)	109 (76.76%)	0.90
AMS occurrence	19 (13.01%)	17 (11.97%)	0.79

The data are presented as n (%) or the mean ((SD; range) or (SE, 95% CI)). AMS occurrence: subjects suffered from acute mountain sickness (AMS) at high altitude. Statistical differences between groups were tested for using a t test for quantitative data and a chi-square test for categorical data.

TABLE 2: Primary outcomes for research worker-rated HADAS scores.

	Placebo group ($n = 146$)	SPC group ($n = 142$)	Mean difference from placebo[†]	p_m value[*]	p_t value[‡]	p_g value[§]	p_{g+t} value[‖]
Baseline	12.80 (0.28, 12.25-13.34)	13.08 (0.28, 12.52-13.63)					
Week 7	5.26 (0.16, 4.96 - 5.59)	3.95 (0.16, 3.64 - 4.26)	-1.34 (0.20, -1.74- -0.95)	<0.001			
Week 14	2.80 (0.12, 2.57 - 3.04)	1.36 (0.12, 1.13 - 1.58)	1.47 (0.20, -1.87- -1.07)	<0.001			
Collapsed across time, baseline to week 14					<0.001	<0.001	<0.001

[†]Values are the adjusted mean change (SE, 95% CI). [*]Comparisons of the mean differences were made at weeks 7 and 14 from the final adjusted linear mixed model, p_m. [‡]The overall change over time, p_t. [§]The average group difference, p_g. [‖]The interaction between time and group, p_{t+g}.

serum concentration of TNF-? was lower in the SPC group than in the placebo group ($p < 0.05$). Moreover, the level of IL-17A and IL-10 was no difference between the SPC and the placebo groups ($p > 0.05$).

miRNAs are small endogenous RNA molecules and relatively stable at serum/plasma. Several reports showed that miRNAs were considered as a biomarker for several diseases [24]. In our study, we found that the serum miR-155 levels of all subjects were notably decreased as time goes on in sea level. After subjects received SPC treatment, the levels of miR-155 were decreased compared to placebo treatment at 50th day and 100th day ($p < 0.05$) (Figure 3(a)). On the contrary, the levels of serum miR-21 of all subjects were elevated at 7th and 14th week, compared to baseline ($p < 0.05$) (Figure 3(b)). Moreover, serum miR-21 levels were higher in the SPC group than the placebo group at 7th week ($p < 0.05$), and no difference between the SPC and the placebo groups ($p > 0.05$). Furthermore, we also analyzed the SOD and MDA level in all subjects' serum. These data showed that there was no difference between the SPC and the placebo groups at 7th week and 14th week ($p > 0.05$).

4. Discussion

Exploring the pathological mechanism and recovery process of HADAS is very important. In recent decades, an increasing number of people (more than 1,000,000) who work in commerce, the construction of manufacturing facilities, research and wildlife protection, or for relief agencies have traveled to Tibet and other high-altitude regions (average altitude > 3000 m) in Qinghai or Xinjiang Province in China. Each year, many of these individuals, who are also called temporary migrants, work for 7–10 months at high altitude and then rest for 2 to 3 months at a lower altitude [25]. Our previous study showed that the HADAS symptoms of subjects who were exposed to high altitude for a fixed duration (6 to 8 months) could persist for more than 100 days [1]. HADAS clearly threatens the quality of life of temporary migrants and has become a public health issue. Therefore, it is necessary for physicians and researchers to explore new treatment approaches for HADAS.

To our knowledge, this is the first double-blinded, randomized, controlled study to investigate the potential benefits of traditional Chinese medicine (SPCs) to treat HADAS.

TABLE 3: Analysis of symptom incidences of HADAS.

Symptoms	Baseline			Week 7				Week 14			
	Placebo group ($n = 142$)	SPC group ($n = 146$)	p value	Placebo group ($n = 142$)	SPC group ($n = 146$)	RR	p value	Placebo group ($n = 142$)	SPC group ($n = 146$)	RR	p value
Sleepiness	97 (68.30%)	87 (59.58%)	0.13	50 (35.21%)	35 (23.97%)	0.58	0.04	23 (16.20%)	9 (6.16%)	0.34	0.009
Insomnia	60 (42.25%)	62 (42.46%)	0.94	44 (30.99%)	26 (17.81%)	0.51	0.02	26 (18.31%)	10 (10.96%)	0.44	0.03
Unresponsiveness	93 (65.49%)	100 (68.49%)	0.63	60 (42.25%)	44 (30.13%)	0.58	0.03	29 (20.42%)	14 (9.59%)	0.47	0.04
Memory loss	86 (60.56%)	88 (60.27%)	0.99	59 (41.54%)	41 (28.08%)	0.55	0.02	28 (19.72%)	17 (11.64%)	0.70	0.28
Agitation	52 (36.61%)	45 (30.82%)	0.27	27 (19.01%)	15 (10.27%)	0.49	0.04	15 (10.56%)	10 (6.85%)	0.58	0.23
Headache	66 (46.47%)	67 (45.89%)	0.97	44 (33.10%)	32 (21.91%)	0.58	0.04	23 (16.20%)	12 (8.22%)	0.46	0.04
Dizziness	100 (70.42%)	111 (79.02%)	0.28	67 (47.18%)	47 (32.19%)	0.53	0.01	44 (30.99%)	18 (12.33%)	0.42	0.004
Throat pain or discomfort	50 (35.21%)	43 (29.45%)	0.26	24 (16.90%)	25 (17.12%)	1.06	0.87	12 (8.45%)	13 (8.90%)	1.40	0.41
Coughing	97 (68.30%)	114 (78.08%)	0.06	57 (40.14%)	40 (27.39%)	0.54	0.02	31 (21.83%)	11 (7.53%)	0.42	0.01
Expectoration	68 (47.88%)	68 (46.57%)	0.75	28 (19.72%)	27 (18.49%)	0.90	0.74	19 (13.38%)	6 (4.11%)	0.38	0.03
Chest tightness	64 (45.07%)	55 (37.67%)	0.18	41 (28.87%)	24 (16.43%)	0.47	0.01	17 (11.97%)	7 (4.79%)	0.37	0.03
Flustering	82 (57.74%)	74 (50.68%)	0.25	52 (36.61%)	36 (24.66%)	0.57	0.03	28 (19.72%)	13 (8.90%)	0.47	0.02
Increased appetite	68 (47.88%)	67 (45.89%)	0.77	49 (34.51%)	35 (21.91%)	0.60	0.05	22 (15.49%)	9 (6.16%)	0.51	0.08
Decreased appetite	58 (40.84%)	56 (38.35%)	0.64	44 (30.99%)	32 (21.92%)	0.60	0.06	21 (14.79%)	8 (5.48%)	0.32	0.009
Diarrhea	66 (46.47%)	50 (36.98%)	0.10	22 (15.49%)	25 (17.12%)	1.12	0.73	8 (5.63%)	0 (0.00%)	0.10	0.03
Abdominal distention	48 (33.80%)	50 (34.24%)	0.97	37 (26.06%)	23 (15.75%)	0.97	0.99	12 (8.45%)	8 (5.48%)	0.71	0.46
Abdominal pain	37 (26.05%)	35 (23.97%)	0.71	19 (13.38%)	14 (9.59%)	1.11	0.71	5 (3.52%)	1 (0.07%)	0.17	0.12
Lumbago	50 (35.21%)	42 (28.76%)	0.23	23 (16.19%)	24 (16.43%)	1.37	0.23	17 (11.97%)	14 (11.64%)	0.77	0.51
Arthralgia	68 (47.88%)	61 (41.78%)	0.35	25 (17.61%)	24 (16.44%)	1.25	0.35	19 (13.38%)	11 (7.53%)	0.56	0.14

The data are presented as the number (%) of subjects. RR represents the relative risk for the SPC versus the placebo group. The symptom incidences were compared using Fisher's exact tests.

TABLE 4: Analysis of the overall proportions of HADAS severity in subjects.

HADAS severity	Week 7				Week 14			
	Placebo group ($n = 142$)	SPC group ($n = 146$)	RR	p value	Placebo group ($n = 142$)	SPC group ($n = 146$)	RR	p value
Moderate reaction (n, %)	0 (0.00%)	0 (0.00%)			0 (0.00%)	0 (0.00%)		
Mild reaction (n, %)	62 (43.66%)	34 (23.29%)	0.17	<0.001	13 (9.15%)	1 (0.68%)	0.04	0.004
Almost no reaction (n, %)	80 (56.34%)	112 (76.71%)			129 (90.85%)	145 (99.32%)		

The data are presented as the number (%) of subjects. RR represents the relative risk for the SPC versus the placebo group. Symptom severities were compared using Fisher's exact tests.

Our findings revealed that oral administration of SPCs to subjects with mild or moderate HADAS significantly decreased HADAS scores and symptom incidence in the SPC group compared with the placebo group. Serum CK, CK-MB, and LDH concentrations were significantly reduced after subjects received SPC treatment compared with the effects of placebo treatment. The time span of serums IL-17A, IL-10, and TNF-? restored to a normal level was shorter in the SPC group than the placebo group. Moreover, SPC could decrease the level of serum miR-155 and upregulated miR-21 expression. However, heart function and serum SOD and MDA levels did not significantly differ between the SPC and the placebo groups. Taken together, these data demonstrate that SPCs may effectively expedite the process of recovering from HADAS.

The mechanism underlying the accelerated recuperation of HADAS subjects in the SPC group remains unclear. Although HADAS occurs at lower altitudes after subjects return from high altitudes, the occurrence and progression of HADAS involve damage from hypoxia and reoxygenation [21]. The subjects suffered from hypoxia while living at high altitude, but upon returning to a lower altitude, they were suddenly exposed to the oxygen content of the lowlands, approximately 21%. As reoxygenation proceeded, the O_2 percentage increased by 6–8% [1]. Hypoxia and reoxygenation injury can induce oxidative stress-related homeostatic dysregulation [26, 27] and other related physiological and pathological changes, which in turn can activate many signaling pathways in neurons, myocardial cells, and endothelial cells. Several studies have reported that hypoxia and reoxygenation cause injury and inflammatory response to the nervous system, myocardium, and small intestine, as well as arthrosis [28–35], the appearance of painful symptoms, and increasing levels of myocardial enzymes.

SPCs are a patented Chinese medicine made of raw materials that include flavonoids, quercetin, kaempferol, isorhamnetin, astragaloside, and atractylenolide III [16]. SPC ingredients can play important roles as antioxidants, which prevent oxidative stress-induced damage, inflammation, and apoptosis [36–41]. Our previous study found that serums IL-17A and TNF-α were elevated and the IL-10 level was descended upon the individuals return to sea level from a high-altitude region, and the level of serums IL-10 and TNF-α returns to normal at 50th day or even earlier, as well as the IL-17 level restored to normal almost needs 100 days [21]. Herein, we demonstrated that SPC played an important role to accelerate inflammatory mediator return to a normal level, suggesting SPC might have an anti-inflammation effect due

to its contained variety of anti-inflammatory ingredients. Additionally, serum MDA and SOD levels have no difference between the SPC and the placebo groups. Our pervious study showed that the serum of MDA and SOD in HADAS subjects had already return to normal levels at 50th day from high altitude to sea level [21]. Therefore, we speculated that these data could not mean the antioxidant effect of SPC was not working and the antioxidant effect of SPC needs to clarify in further study.

It is well known that the abnormal expression and location of miRNA are involved in several pathophysiology and disease, including inflammatory response, ischemia reperfusion injury, and cancer, through regulated target gene post-transcription [42]. Several documents showed that miR-155 promoted inflammatory response involved in atherosclerosis [43], obesity-induced renal inflammation [44, 45], and ischemia-reperfusion injury [46–48]. In this study, we found that the serum miR-155 level was higher at baseline than at 50th day and 100th day. Given the above results about inflammatory mediator, we speculated that miR-155 was involved in inflammatory response in HADAS. Moreover, SPC decreased the level of serum miR-155, suggesting that SPC suppresses inflammatory response in HADAS through downregulation of miR-155 expression. miR-21 plays an import role to attenuate hypoxia-reoxygenation injury [49–52]. Our previous study proved that hypoxia-reoxygenation injury is involved in HADAS [21]. In this study, the level of serum miR-21 was lower at baseline than at 50th day and 100th day for both groups. After subjects received SPC treatment, the serum miR-21 level increased rapidly compared to the placebo group, hinting that miR-21 is involved in HADAS, and SPC might elevate miR-21 to attenuate hypoxia-reoxygenation injury.

Our trial has some limitations. First, all of the subjects were young men, and the majority was between 18 and 35 years old. Second, the spans between evaluation time points were too long to evaluate certain parameters, such as CK and IL-17A, which had already recovered to similar, normal levels in both groups before measurements were made. Most subjects were particularly reluctant to have blood drawn and only agreed to have their symptoms evaluated and biological measurements taken at day 3 and weeks 7 and 14. All of these factors may have introduced bias into the results.

5. Conclusions

In this trial, the oral administration of SPCs to subjects with mild or moderate HADAS significantly decreased HADAS

TABLE 5: Analysis of secondary outcomes.

Secondary outcome	Baseline		Week 7		Week 14		p_t value[‡]	p_g value[§]	p_{g+t} value[‖]
	Placebo group	SPC group	Placebo group	SPC group	Placebo group	SPC group			
Myocardial enzymes									
CK (IU/L)	122.14 (2.94, 116.42- 128.06)	124.14 (3.34, 117.52- 130.75)	116.53 (2.12, 112.33 - 120.73)	92.30 (1.92, 88.51- 96.10)*	104.90 (2.64, 99.67 - 110.13)	99.60 (2.25, 95.13 - 104.08)	<0.001	<0.001	<0.001
CK-MB (IU/L)	21.70 (0.61, 20.49- 22.91)	21.37 (0.49, 20.38-22.35)	19.42 (0.24, 18.95- 19.90)	15.47 (0.23, 14.99- 15.95)*	17.48 (0.32, 16.84 - 18.13)	15.89 (0.16, 15.56 - 16.21)*	<0.001	<0.001	<0.001
LDH (IU/L)	198.89 (2.29, 194.37- 203.41)	195.87 (2.80, 189.43- 199.48)	170.53 (3.15, 169.37 - 183.31)	156.95 (2.70, 143.89 - 155.19)*	151.03 (2.65, 145.78 - 156.27)	133.47 (2.01, 129.49 - 137.46)*	<0.001	<0.001	<0.001
Heart function									
HR (beats/min)	75.07 (0.45, 74.17- 75.96)	74.36 (0.95, 72.47- 76.25)	71.14 (0.45, 70.24 - 72.03)	70.89 (0.67, 69.56 - 72.22)	70.03 (0.67, 68.69 - 71.37)	70.56 (0.49, 69.56 - 71.50)	<0.001	0.84	0.59
LVEF (%)	64.22 (0.46, 63.30- 65.14)	64.07 (0.40, 63.27- 64.87)	63.51 (0.39, 62.72 - 64.30)	63.45 (0.47, 62.62 - 64.38)	58.87 (0.35, 58.16 - 59.58)	57.90 (0.34, 57.22 to 58.58)	<0.001	0.26	0.405
LVFS (%)	34.12 (0.38, 33.36- 34.88)	34.63 (0.30, 34.03- 35.24)	34.82 (0.27, 34.27 - 35.37)	34.87 (0.31, 34.26 - 35.49)	31.45 (0.29, 30.88 - 32.03)	30.92 (0.22, 30.48 to 31.36)	<0.001	0.94	0.18
Pulmonary artery inner diameter (mm)	27.34 (0.12, 24.38- 30.30)	26.84 (0.09, 24.62- 29.05)	24.14 (0.07, 24.00 - 24.28)	24.27 (0.05, 24.16 - 24.37)	20.83 (0.12, 20.58 - 21.08)	20.93 (0.05, 20.83 to 21.03)	<0.001	0.11	0.367
PAOV (m/s)	81.78 (0.54, 80.7- 82.86)	80.67 (0.47, 79.73- 81.60)	95.14 (0.52, 94.11 - 96.17)	93.26 (0.54, 92.19 - 94.34)	81.78 (0.54, 80.70 - 82.86)	81.01 (0.51, 79.99 to 82.02)	<0.001	0.01	0.60
PASP (mmHg)	2.79 (0.31, 2.7 - 2.85)	2.73 (0.30, 2.67- 2.79)	3.64 (0.07, 3.51 - 3.77)*	3.45 (0.35, 3.38 - 3.52)	2.73 (0.03, 2.67 - 2.79)	2.71 (0.03, 2.64 to 2.78)	<0.001	0.18	0.01

The data are presented as the means (SE, 95% CI). RBC = red blood cells, Hb = hemoglobin, Hct = hematocrit, MCV = mean corpuscular volume. CK = creatine kinase, CK-MB = creatine kinase-MB, LDH = lactate dehydrogenase. HR = heart rate, LVEF = left ventricular ejection fraction, LVFS = left ventricular fractional shortening, PAOV = pulmonary artery opening velocity, PASP = pulmonary artery systolic pressure. *Comparisons of the mean differences were made at weeks 7 and 14 from the final adjusted linear mixed model, $p < 0.05$. [‡]The overall change over time, p_t. [§]The average group difference, p_g. [‖]The interaction between time and group, p_{t+g}.
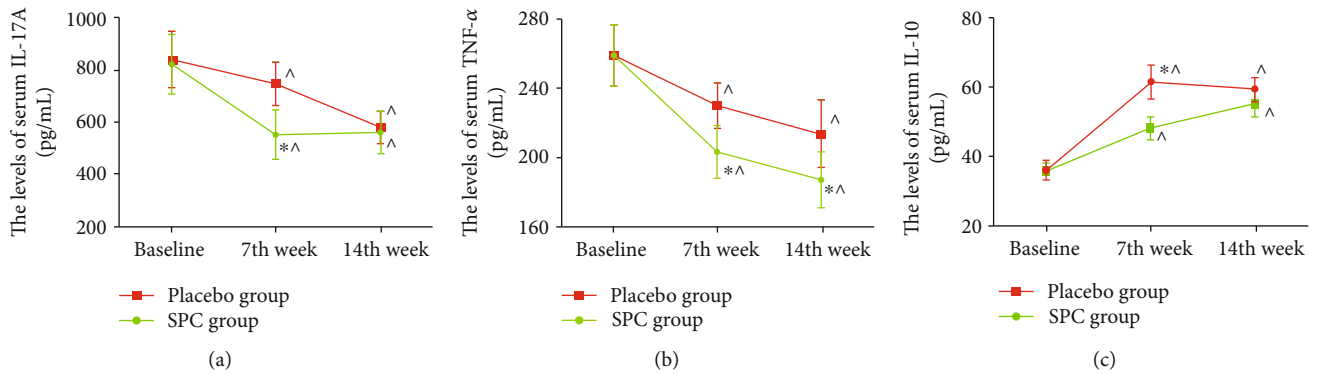
(a)

(b)

(c)

FIGURE 2: The serum IL-17A, IL-10, and TNF-α level of subjects between the SPC and the placebo groups. Data are presented as mean ± SD. The serums IL-17A (a), TNF-α (b), and IL-10 (c) of subjects in both groups were assayed at baseline, 7th week, and 14th week. $^*p < 0.05$, relative to the placebo group, $^\wedge p < 0.05$, relative to baseline.
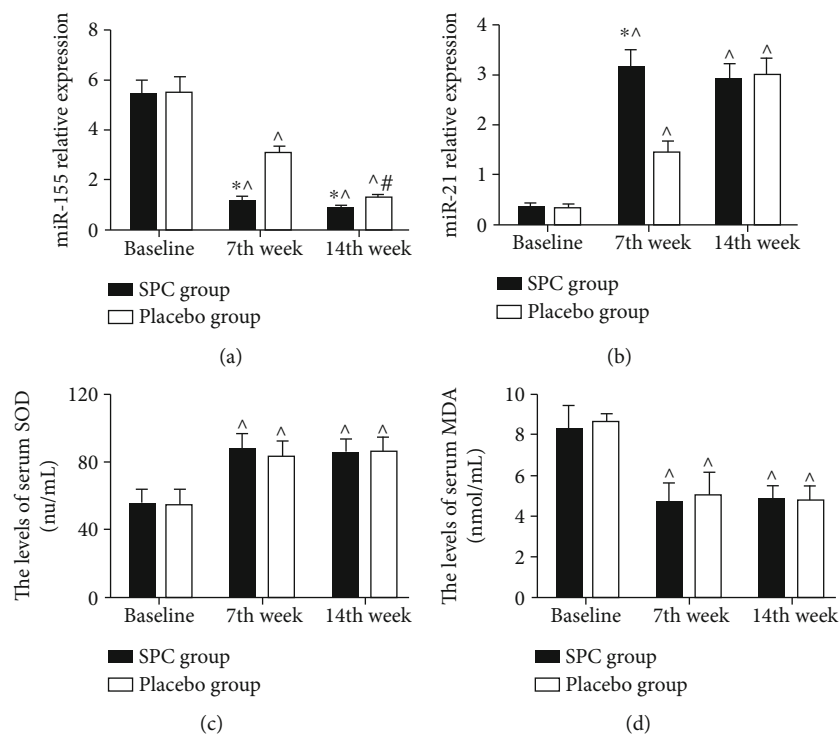

(a)

(b)

(c)

(d)

FIGURE 3: The serum miR-155 and miR-21 level of subjects between the SPC and the placebo groups. Data are presented as mean ± SD. The serums miR-155 (a), miR-21 (b), SOD (c), and MDA (d) of subjects in both groups were assayed at baseline, 50th day, and 100th day. $^*p < 0.05$, relative to the placebo group, $^\wedge p < 0.05$, relative to baseline, and $^\# p < 0.05$, relative to the 7th week.

scores in the trial group compared with effects in the placebo group at week 14. SPC treatment improves hypoxia-reoxygenation cause injury and inflammatory response and promotes subjects' body return to normal state. These findings from this multicenter trial suggest that oral SPCs may improve HADAS symptoms and expedite recovery via improve hypoxia-reoxygenation cause injury and inflammatory response.

Data Availability

The data used to support the findings of this study are available from the corresponding author upon request.

Conflicts of Interest

The authors declare that they have no competing interests.

Authors' Contributions

Wang G. and He B. designed the study and the experiments. Hu M., Liang Z., Ma Q., Zi Y., Dong Z., Li Q., Luo Y., Huang Q., Lin K., and Liu Z. were responsible for the data collection. Hu M., He B., and Guo L. analyzed the data. Wang G., He B., Liu Z., Hu M., and Qian G. drafted the manuscript. Wang G., He B., Liu Z., and Hu M. revised the manuscript, and all

authors approved the final manuscript. Binfeng He and Mingdong Hu contributed equally to this work.

Supplementary Materials

This supplement file included the CONSORT 2010 table, diagnostic and scoring criteria for fixed period high-altitude deacclimatization syndrome, method of biological measurements and cardiac function, and sample size calculation. *(Supplementary Materials)*

References

[1] B. He, J. Wang, G. Qian et al., "Analysis of high-altitude de-acclimatization syndrome after exposure to high altitudes: a cluster-randomized controlled trial," *PLoS One*, vol. 8, no. 5, article e62072, 2013.

[2] G. Cavaletti and G. Tredici, "Long-lasting neuropsychological changes after a single high altitude climb," *Acta Neurologica Scandinavica*, vol. 87, no. 2, pp. 103–105, 1993.

[3] B. J. Ryan, N. B. Wachsmuth, W. F. Schmidt et al., "AltitudeOmics: rapid hemoglobin mass alterations with early acclimatization to and de-acclimatization from 5260 m in healthy humans," *PLoS One*, vol. 9, no. 10, article e108788, 2014.

[4] G. Savourey, N. Garcia, Y. Besnard, A. Guinet, A. M. Hanniquet, and J. Bittel, "Pre-adaptation, adaptation and de-adaptation to high altitude in humans: cardio-ventilatory and haematological changes," *European Journal of Applied Physiology and Occupational Physiology*, vol. 73, no. 6, pp. 529–535, 1996.

[5] G. Savourey, N. Garcia, J. P. Caravel et al., "Pre-adaptation, adaptation and de-adaptation to high altitude in humans: hormonal and biochemical changes at sea level," *European Journal of Applied Physiology and Occupational Physiology*, vol. 77, no. 1-2, pp. 37–43, 1998.

[6] J. A. Dempsey, F. L. Powell, G. E. Bisgard, G. M. Blain, M. J. Poulin, and C. A. Smith, "Role of chemoreception in cardiorespiratory acclimatization to, and deacclimatization from, hypoxia," *Journal of Applied Physiology*, vol. 116, no. 7, pp. 858–866, 2014.

[7] Q. Zhou, S. Yang, Y. Luo et al., "A randomly-controlled study on the cardiac function at the early stage of return to the plains after short-term exposure to high altitude," *PLoS One*, vol. 7, no. 2, article e31097, 2012.

[8] J. A. Deere and S. L. Chown, "Testing the beneficial acclimation hypothesis and its alternatives for locomotor perfor-

mance," *The American Naturalist*, vol. 168, no. 5, pp. 630–644, 2006.

[9] C. G. Zubieta, *Human Adaptation to High Altitude and to Sea Level: Acid-Base Equilibrium, Ventilation and Circulation in Chronic Hypoxia*, VDM Verlag Dr. Müller, Düsseldorf, German, 1st edition, 2010.

[10] S. Cui, S. Tang, Y. Wu, and W. Niu, "The high altitude de-acclimatization symptom investigation of 626 cases Tibetan settlers after return to sea level," *Xinan Guofang Yixue Zazhi*, vol. 8, pp. 63-64, 1998.

[11] Q. Zhou, S. Yang, Z. Yuan et al., "A research in diagnostic criteria of high altitude de-adaptation for plateau migrants returning to the plains: a multicenter randomized controlled trial," *Jifangjun Yixue Zazhi*, vol. 37, pp. 146–155, 2012.

[12] H. Zhang, Y. Zhang, Z. Yang, H. Peng, F. Wang, and F. Kong, "High altitude acclimatization and de-acclimatization," *Zhongguo Yingyong Shengli xue Zazhi*, vol. 28, pp. 94–96, 2012.

[13] Y. B. Zhang, Y. Wang, and X. L. Liu, *People and High Altitude-Qinghai Plateau Medical Research*, Qinghai People's Publishing House, Xining City, China, 1st ed edition, 1996.

[14] Y. Gao, *High Altitude Military Medicine*, Chongqing Publishing House, Chongqing City, China, 1st edition, 2005.

[15] Z. Shi, Q. Zhou, S. Ma, J. Cheng, and L. Xiang, "Investigation of high altitude de-accliamziton in the earthquest relief unit," *Jifangjun Yufan Yixue Zazhi*, vol. 29, pp. 114-115, 2011.

[16] X. Huang, "Preparation method of Shenqi pollen capsule. China," Patent ZL 200810006905.

[17] Z. F. Shi, Q. Q. Zhou, L. Xiang, S. D. Ma, C. J. Yan, and H. Luo, "Three preparations of compound Chinese herbal medicines for de-adaptation to high altitude: a randomized, placebo-controlled trial," *Zhong Xi Yi Jie He Xue Bao*, vol. 9, pp. 395–401, 2011.

[18] X. Lou, X. Zhang, Q. Zhou, and S. Wang, "Curative effect observation of Shenqipollen tablet on deacclimatization during exposure period of the chronic intermittent hypoxia in high altitude regions," *Xiandai Yufang Yixue*, vol. 40, pp. 1227–1229, 2013.

[19] J. Cui, Y. Wang, B. Li et al., "Effects on hemorheology of several different medicines to de-adaptation to high altitude," *Zhongguo Xueyeliubianxue Zazhi*, vol. 16, pp. 52–54, 2006.

[20] X. Jin, Y. Liu, X. Chen et al., "Effect of hyperbaric oxygen in high-altitude de-acclimatization syndrome," *Zhonghua Hanghai Yixue Zazhi*, vol. 7, pp. 88–90, 2000.

[21] B. He, H. Li, M. Hu et al., "Association between serum interleukin-17A level and high-altitude deacclimatization syndrome," *Mediators of Inflammation*, vol. 2016, Article ID 1732352, 8 pages, 2016.

[22] S. Khoury, P. Ajuyah, and N. Tran, "Isolation of small noncoding RNAs from human serum," *Journal of Visualized Experiments*, no. 88, article e51443, 2014.

[23] J. S. Yuan, A. Reed, F. Chen, and C. N. Stewart Jr., "Statistical analysis of real-time PCR data," *BMC Bioinformatics*, vol. 7, no. 1, p. 85, 2006.

[24] C. Backes, E. Meese, and A. Keller, "Specific miRNA disease biomarkers in blood, serum and plasma: challenges and prospects," *Molecular Diagnosis & Therapy*, vol. 20, no. 6, pp. 509–518, 2016.

[25] L. Tanzen and R. Ma, *Temporary labor migration in three cities, in the Tibet autonomous region*, China Tibetology, 2011, http://

qikan.cqvip.com/Qikan/Article/Detail?id=44702445&from=Qikan_Search_Index.

[26] S. Nistri, G. Boccalini, A. Bencini et al., "A new low molecular weight, MnII-containing scavenger of superoxide anion protects cardiac muscle cells from hypoxia/reoxygenation injury," *Free Radical Research*, vol. 49, no. 1, pp. 67–77, 2015.

[27] C. Li and R. M. Jackson, "Reactive species mechanisms of cellular hypoxia-reoxygenation injury," *American Journal of Physiology. Cell Physiology*, vol. 282, no. 2, pp. C227–C241, 2002.

[28] M. Tagami, K. Yamagata, K. Ikeda et al., "Vitamin E prevents apoptosis in cortical neurons during hypoxia and oxygen reperfusion," *Laboratory Investigation*, vol. 78, no. 11, pp. 1415–1429, 1998.

[29] L. D. Terada, "Hypoxia-reoxygenation increases O_2-. efflux which injures endothelial cells by an extracellular mechanism," *American Journal of Physiology-Heart and Circulatory Physiology*, vol. 270, pp. H945–H950, 1996.

[30] G. A. Ngoh, H. T. Facundo, T. Hamid, W. Dillmann, N. E. Zachara, and S. P. Jones, "Unique hexosaminidase reduces metabolic survival signal and sensitizes cardiac myocytes to hypoxia/reoxygenation injury," *Circulation Research*, vol. 104, no. 1, pp. 41–49, 2009.

[31] K. Ban and R. A. Kozar, "Protective role of p70S6K in intestinal ischemia/reperfusion injury in mice," *PLoS One*, vol. 7, no. 7, article e41584, 2012.

[32] K. Katayama, K. Sato, H. Matsuo, K. Ishida, K. Iwasaki, and M. Miyamura, "Effect of intermittent hypoxia on oxygen uptake during submaximal exercise in endurance athletes," *European Journal of Applied Physiology*, vol. 92, no. 1-2, pp. 75–83, 2004.

[33] T. Kambara, K. Ohashi, R. Shibata et al., "CTRP9 protein protects against myocardial injury following ischemia-reperfusion through AMP-activated protein kinase (AMPK)-dependent mechanism," *The Journal of Biological Chemistry*, vol. 287, no. 23, pp. 18965–18973, 2012.

[34] X. Ma, H. Liu, S. R. Foyil et al., "Impaired autophagosome clearance contributes to cardiomyocyte death in ischemia/reperfusion injury," *Circulation*, vol. 125, no. 25, pp. 3170–3181, 2012.

[35] M. H. Zhao, Z. T. Jiang, T. Liu, and R. Li, "Flavonoids in *Juglans regia* L. leaves and evaluation of *in vitro* antioxidant activity via intracellular and chemical methods," *The Scientific World Journal*, vol. 2014, Article ID 303878, 6 pages, 2014.

[36] J. H. Yang, B. Y. Shin, J. Y. Han et al., "Isorhamnetin protects against oxidative stress by activating Nrf2 and inducing the expression of its target genes," *Toxicology and Applied Pharmacology*, vol. 274, no. 2, pp. 293–301, 2014.

[37] P. Rajendran, T. Rengarajan, N. Nandakumar, R. Palaniswami, Y. Nishigaki, and I. Nishigaki, "Kaempferol, a potential cytostatic and cure for inflammatory disorders," *European Journal of Medicinal Chemistry*, vol. 86, pp. 103–112, 2014.

[38] Y.-Y. Qiu, J.-X. Zhu, T. Bian et al., "Protective effects of astragaloside IV against ovalbumin-induced lung inflammation are regulated/mediated by T-bet/GATA-3," *Pharmacology*, vol. 94, pp. 51–59, 2014.

[39] L. Sun, W. Li, W. Li, L. Xiong, G. Li, and R. Ma, "Astragaloside IV prevents damage to human mesangial cells through the inhibition of the NADPH oxidase/ROS/Akt/NF-κB pathway under high glucose conditions," *International Journal of Molecular Medicine*, vol. 34, no. 1, pp. 167–176, 2014.

[40] Q. Sun, N. Jia, W. Wang, H. Jin, J. Xu, and H. Hu, "Protective effects of astragaloside IV against amyloid beta1-42 neurotoxicity by inhibiting the mitochondrial permeability transition pore opening," *PLoS One*, vol. 9, no. 6, article e98866, 2014.

[41] B. R. Yun, J. B. Weon, J. Lee, M. R. Eom, and C. J. Ma, "Neuroprotective effect of the fermented Gumiganghwal-tang," *Journal of Bioscience and Bioengineering*, vol. 118, no. 2, pp. 235–238, 2014.

[42] A. M. Ardekani and M. M. Naeini, "The role of microRNAs in human diseases," *Avicenna Journal of Medical Biotechnology*, vol. 2, no. 4, pp. 161–179, 2010.

[43] J. Ye, R. Guo, Y. Shi, F. Qi, C. Guo, and L. Yang, "miR-155 regulated inflammation response by the SOCS1-STAT3-PDCD4 axis in atherogenesis," *Mediators of Inflammation*, vol. 2016, Article ID 8060182, 14 pages, 2016.

[44] C. Zheng, J. Zhang, X. Chen et al., "MicroRNA-155 mediates obesity-induced renal inflammation and dysfunction," *Inflammation*, vol. 42, no. 3, pp. 994–1003, 2019.

[45] K. Barker, "miR-155 modifies inflammation, endothelial activation and blood-brain barrier dysfunction in cerebral malaria," *Molecular Medicine*, vol. 23, no. 1, pp. 24–33, 2017.

[46] H. Wu, T. Huang, L. Ying et al., "MiR-155 is involved in renal ischemia-reperfusion injury via direct targeting of FoxO3a and regulating renal tubular cell pyroptosis," *Cellular Physiology and Biochemistry*, vol. 40, no. 6, pp. 1692–1705, 2016.

[47] Y. Li, D. Ma, Z. Wang, and J. Yang, "MicroRNA-155 deficiency in Kupffer cells ameliorates liver ischemia-reperfusion injury in mice," *Transplantation*, vol. 101, no. 7, pp. 1600–1608, 2017.

[48] S. U. Eisenhardt, J. B. Weiss, C. Smolka et al., "MicroRNA-155 aggravates ischemia-reperfusion injury by modulation of inflammatory cell recruitment and the respiratory oxidative burst," *Basic Research in Cardiology*, vol. 110, no. 3, p. 32, 2015.

[49] Y. Jiang, H. Xie, W. Tu et al., "Exosomes secreted by HUVECs attenuate hypoxia/reoxygenation-induced apoptosis in neural cells by suppressing miR-21-3p," *American Journal of Translational Research*, vol. 10, no. 11, pp. 3529–3541, 2018.

[50] H. Shen, Z. Yao, W. Zhao, Y. Zhang, C. Yao, and C. Tong, "miR-21 enhances the protective effect of loperamide on rat cardiomyocytes against hypoxia/reoxygenation, reactive oxygen species production and apoptosis via regulating Akap8 and Bard1 expression," *Experimental and Therapeutic Medicine*, vol. 17, no. 2, pp. 1312–1320, 2019.

[51] T. Pan, P. Jia, N. Chen et al., "Delayed remote ischemic preconditioning ConfersRenoprotection against septic acute kidney injury via exosomal miR-21," *Theranostics*, vol. 9, no. 2, pp. 405–423, 2019.

[52] R. Jiang, Y. Guo, N. Chen, C. Gao, Z. Ding, and B. Jin, "Total Flavonoids from _Carya cathayensis_ Sarg. Leaves Alleviate H9c2 Cells Hypoxia/Reoxygenation Injury via Effects on miR-21 Expression, PTEN/Akt, and the Bcl-2/Bax Pathway," *Evidence-Based Complementary and Alternative Medicine*, vol. 2018, Article ID 8617314, 13 pages, 2018.

Review Article

Critical Roles of Balanced Innate Lymphoid Cell Subsets in Intestinal Homeostasis, Chronic Inflammation, and Cancer

Jing Wu [1], **Xinping Lv** [1], **Shan Zhu,**[1] **Tete Li** [1], **Hang Cheng,**[2] **and Jingtao Chen** [1]

[1]*Institute of Translational Medicine, The First Hospital, Jilin University, Changchun 130061, China*
[2]*Department of Pediatrics, The First Hospital, Jilin University, Changchun 130021, China*

Correspondence should be addressed to Jingtao Chen; jtchen@jlu.edu.cn

Innate lymphoid cells (ILCs) comprise a recently identified subset of innate immune cells that are mainly localized to mucosa-associated tissues. Although they have not yet been fully characterized, they can generally be divided into ILC1s, ILC2s, and ILC3s. ILCs and their corresponding cytokines act as important mediators of the early stages of the immune response during inflammation, tissue repair, and the maintenance of epithelial integrity. Consequently, the dysregulation of ILC subsets might promote inflammation and cancer. Numerous studies have demonstrated that these cells play an important role in maintaining the microecological balance of the small intestine; however, their specific roles in mediating inflammation in this tissue and tumorigenesis remain unclear and controversial. In this review, we focus on recent progress that has helped to gain a better understanding of the role of ILCs in intestinal homeostasis, chronic inflammation, and cancer. Further focused research on the regulation and role of ILCs in intestinal homeostasis and pathology will help to reveal valuable diagnostic and therapeutic targets for the treatment of intestinal diseases.

1. Introduction

Intestinal epithelial cells (IECs) cover the luminal surface of both the small and large intestines of the gastrointestinal tract. As part of the intestinal mucosa layer, IECs are single-layer, columnar cells organized with tight junctions that form a contiguous and relative impermeable membrane [1]. The primary functions of these cells are to absorb water, electrolytes, and dietary nutrients into the body, while restricting the entry of harmful pathogens. IECs not only provide an important physical barrier to microorganisms but also express cytokines and chemokines that interact with mucosal immune cells to maintain immune homeostasis [2, 3].

Innate lymphoid cells (ILCs) are recently identified mucosal immune cells considered the gatekeeper of mucosa-associated tissues such as the gut. Their function is regulated by IEC-secreted cytokines in response to physiological and pathological processes including immune defense, tissue remodeling, inflammation, and cancer [2, 4, 5]. ILCs develop from precursors that express integrin $\alpha_4\beta_7$ in the bone

marrow, which interacts with the chemokine receptor CXCR6 and adhesion molecule MadCAM-1 when cells migrate to the intestine [6, 7]. ILCs are specifically localized to the lamina propria of the small and large intestines and are rarely replenished from the bone marrow; under both steady-state and homeostasis-disruptive conditions, these tissue-resident cells remain in the intestine and exhibit local self-renewal via the proliferation of tissue-resident progenitor cells [8]. Unlike classical lymphocytes such as T and B cells, ILCs lack antigen-specific receptors. They rapidly respond to environmental challenges and provide immunity to fight against the invasion of a variety of infectious pathogens, all while playing an important role in organ homeostasis by producing factors that act on epithelial cells [9].

Based on their phenotypic and functional characteristics, ILCs can be generally divided into cytolytic and noncytolytic ILCs [4, 10]. Cytolytic ILCs, also referred to as conventional natural killer (NK) cells, release cytolytic effector molecules including perforin and granzyme B, which can kill tumors or virus-infected tissue. In contrast to NK cells, noncytolytic or "helper" ILC populations can be classified into three

Table 1: Characteristics of intestinal innate lymphoid cells (ILCs).

	NKs	ILC1s	ILC2s	ILC3s	ILCregs
Transcription factors	T-bet	T-bet	GATA3, RORα	RORγt	Id3
Active factors	TGF-β, GM-CSF	IL-15	IL-25, IL-33, TSLP	IL-23	TGF-β
Effective factors	IFN-γ, IL-22, VEGF, CXCL8	IFN-γ, TNF-α	IL-5, IL-13	IL-22, IL-17, GM-CSF, IFN-γ	IL-10

groups (groups 1–3) [11–13] (Table 1). Group 1 ILCs (ILC1s) are characterized by the production of interferon- (IFN-) γ and lack the production of T helper 2- (Th2-) and Th17-associated cytokines. ILC1s express high levels of the transcription factor T-bet and low levels of the transcription factor retinoid-related orphan receptor γt (RORγt) but lack expression of CD117 [14]. Group 2 ILCs (ILC2s) are characterized by the production of the Th2-associated cytokines interleukin- (IL-) 5 and IL-13 after stimulation by thymic stromal lymphopoietin (TSLP) [15], IL-33, and IL-25 [16]. The development of ILC2s requires the presence of IL-7 [17] and the transcription factors GATA-3 in humans, and the transcription factors GATA-3 and RORα in mice [12, 18, 19]. Group 3 ILCs (ILC3s) are similar to ILC2s with regard to their dependence on IL-7, but they also require the transcription factor RORγt for their development and function and produce IL-17A and/or IL-22 [12, 20]. This group includes lymphoid tissue inducer cells, which are natural cytotoxicity receptor (NCR)$^{+/-}$ ILC3s.

In addition, recent studies have revealed a regulatory subpopulation of ILCs (called ILCregs) and memory ILCs, which include circulating memory NK cells and tissue-resident memory ILCs [21–23]. ILCregs exist in the gut and control intestinal inflammation via the secretion of IL-10 [21] (Table 1). Tissue-resident memory ILCs exist in the liver or lung and have adaptive features, including virus and hapten-induced memory NK cells, hapten-induced memory ILC1s, and cytokine-induced memory ILC2s [22, 23]. Accumulating evidence also suggests that tissue-resident memory ILCs might represent the innate counterparts of resident memory T (T_{RM}) cells owing to some common features [22].

ILCs display certain levels of functional diversity and plasticity. Under the influence of IL-12, IL-18, and IL-1β, ILC2s and ILC3s can transdifferentiate into ILC1s, which can in turn transdifferentiate back into ILC2s and ILC3s in the presence of IL-4 and IL-23, respectively [24–27]. Thus, ILCs are important regulators of epithelial barriers, are involved in immune defense, and participate in various diseases of the intestine including inflammation and cancer. Accordingly, gaining a better understanding of the complex biological mechanisms underlying these roles will facilitate the development and recognition of the diagnostic and therapeutic potential of ILCs for the treatment of various diseases. To promote this goal, here, we review the research progress on the physiological and pathological roles of ILCs in immune defense and the maintenance of the intestinal microecological balance to highlight targets for the treatment of intestinal diseases including chronic inflammation and cancer.

2. ILCs in Normal Intestinal Tissue

The intestinal epithelium is the largest barrier that isolates an organ system from the immediate environment. ILC subsets have been found to play a role in gut homeostasis in both humans and mice [8, 28]. In healthy conditions, very few ILCs are detected, with NCR$^+$ ILCs accounting for 5% and 2% of total lymphocytes in the human and mouse small intestine, respectively [29], and ILC2s comprising approximately 5% of all small intestinal lymphoid cells [30]. Given their localization, ILCs are among the first immune cells to react to invading pathogens and are also involved in maintaining the integrity of the epithelial barrier. Thus, these cells play vital roles in the reciprocal interactions between the gut microbiota and immune system.

Cytolytic ILCs (NK cells) and noncytolytic ILC1s are known as T-bet$^+$ and IFN-γ-producing subsets, respectively. However, although they share many characteristics, based on recent studies, NK cells and ILC1s develop from different bone marrow progenitors, and therefore, they are substantially different in their tissue tropism, migratory capacity, and effector functions [31, 32]. ILC2s can mediate protection against helminth infection in murine models [33]. In the steady state, most intestinal ILC3s express RORγt and NKp44 in humans and NKp46 in mice [34]. NCR$^+$ ILC3s produce IL-22 upon interaction with the transcription factor aryl hydrocarbon receptor ligand, which can be derived from the diet and microflora [35]. Although ILCs are rarely present in healthy conditions, understanding their characteristics in the steady state will help to further elucidate their possible roles in disease and their potential as targets to prevent or treat these diseases.

3. Roles of ILCs in Intestinal Tissue Immune Defense and Maintenance of the Intestinal Microecological Balance

The functional activity of ILCs requires exposure to the gut microbiota, as shown by a mouse model study in which germ-free or antibiotic-treated mice displayed impaired NK cell activity [36]. Intestinal NK cells interact with many strains of probiotics to maintain the integrity of the epithelial cell barrier, such as interactions with *Lactobacillus plantarum* to attenuate enterotoxigenic *Escherichia coli*- (ETEC-) induced epithelial damage. Moreover, defense against ETEC is considered to involve the stimulation of NK cells to enhance IL-22 production [37] (Figure 1).

The absence of ILC1s in T-bet$^{-/-}$ mice is linked to their increased susceptibility to enteric infections [38]. ILC1s
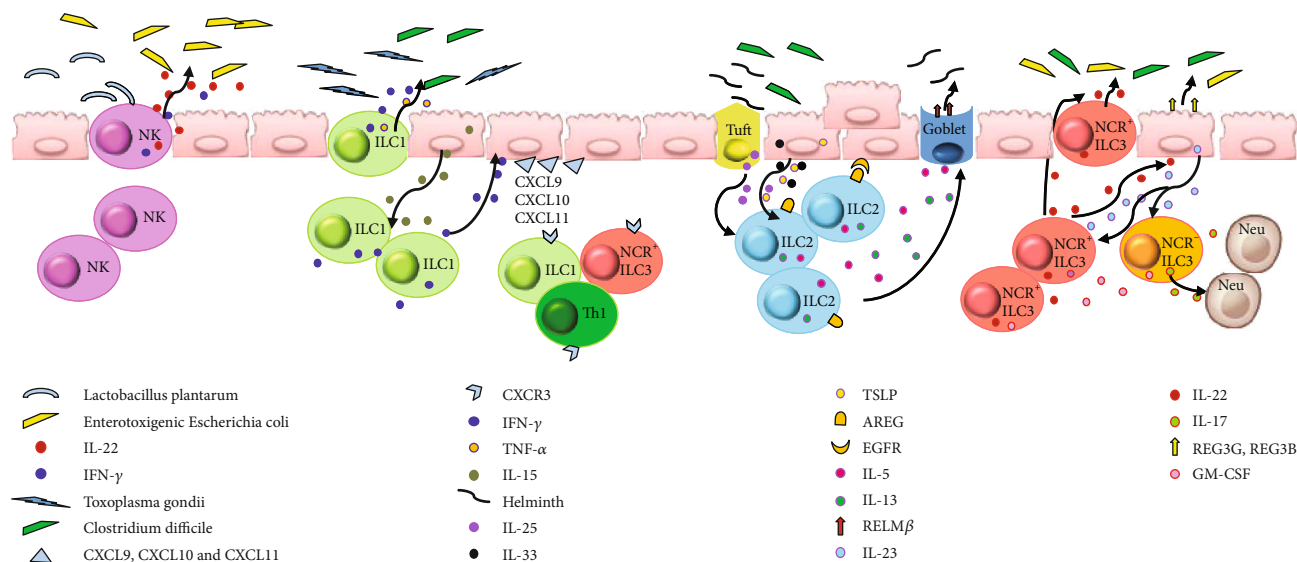
FIGURE 1: The multiple roles of innate lymphoid cells (ILCs) in intestinal tissue immune defense and tissue remodeling. NK cells can attenuate intestinal damage by producing IL-22 and IFN-γ after infection. ILC1s mediate protection via IFN-γ and TNF-α production after infection and attract CXCR3$^+$ leukocyte accumulation. ILC2s produce multiple important effector molecules after activation, promote intestinal repair, and limit parasitic infections. In response to IL-23 stimulation, NCR$^+$ ILC3s and NCR$^-$ ILC3s mainly produce IL-22 and IL-17, respectively, and GM-CSF from both kinds of cells, and participate in homeostasis of the intestine.

mediate protective responses during *Toxoplasma gondii* and intestinal *Clostridium difficile* infections via T-bet, with the consequent production of IFN-γ and tumor necrosis factor-(TNF-) α [6, 39]. Similarly, tissue-resident ILC1s play an essential role in viral infections, enabling the rapid production of IFN-γ to limit the early viral burden [40]. IL-15 produced from IECs induces the release of IFN-γ by ILC1s, which enhances the expression of chemokines CXCL9, CXCL10, and CXCL11 in IECs, which recruit CXCR3$^+$ leukocytes including Th1, ILC1s, and NKp46$^+$ ILC3 cells [5] (Figure 1). Furthermore, the transfer of ILC precursors into a lymphoid mouse model promotes the recruitment of monocytes, which helps to limit extensive inflammation [6].

ILC2s express the signature transcription factor GATA-3, as well as CD90, CD127, CD25, IL-25R, and IL-33R, and are distributed throughout the intestinal lamina propria [41, 42]. ILC2s are activated by epithelial cell-derived alarmins such as IL-25, IL-33, and TSLP [43, 44] and produce multiple important effector molecules including amphiregulin (AREG) [45], IL-5, IL-9, and IL-13 [46]. AREG is a ligand of a widely expressed transmembrane tyrosine kinase epidermal growth factor receptor (EGFR) [47], and binding between AREG and EGFR stimulates the proliferation of epithelial cells [48]. An analogous IL-33–ILC2–AREG pathway also plays an important role in intestinal epithelial cell renewal and intestinal repair [45].

During *C. difficile* infection, ILC1s provide immune protection, whereas ILC2s are activated by IL-33 as an essential pathway for in recovery from *C. difficile* infection-associated colitis [49]. Importantly, ILC2s coordinate the inflammatory response to helminth infection in the gut. Stimulation with TSLP, IL-25, and IL-33 induces ILC2s to release cytokines IL-5 and IL-13, which promote mucus and antimicrobial peptide (RELMβ) production by intestinal

goblet cells, which help to limit parasitic infections [33, 41, 50, 51]. Recently, tuft cells were identified as the major source of intestinal IL-25 production, which in turn promotes the production of IL-13 by ILC2s [52, 53] (Figure 1).

ILC3s are involved in defense against bacterial and fungal infection, the regulation of commensal bacteria, and the development and repair of lymphoid tissues. In response to IL-23 stimulation, NCR$^+$ ILC3s and NCR$^-$ ILC3s mainly produce the Th17- and Th22-associated cytokines IL-17 and IL-22, respectively. IL-22 plays a critical role in intestinal epithelial injury repair after bacterial pathogen invasion [54]. As primary producers of mucosal IL-22, intestinal ILC3s play a crucial role in protecting against gut bacterial infections [28, 55, 56]. In response to IL-22, epithelial cells secrete antimicrobial peptides (REG3G, REG3B), lipocalin, and mucus to reinforce barrier protection in response to microbial damage. Furthermore, ILC3-derived IL-22 helps to contain gut-associated lymphoid tissue-resident commensal bacteria and to protect intestinal stem cells in graft-versus-host disease models [57, 58]. Epithelial cells can also indirectly regulate ILC3s during interactions with commensal bacteria. For example, IECs can produce IL-25 to suppress the production of IL-22 by ILC3s, whereas IL-7 production by IECs stabilizes the transcription factor RORγt to boost IL-22 production [59, 60]. Expression of the IL-22 receptor subunit IL-22Rα1 in intestinal stem cells [61, 62] mediates epithelial regeneration, and constant IL-22 production is essential to maintain barrier integrity and commensal bacteria in a steady state. IL-17A participates in the recruitment of neutrophils, as important effector cells for extracellular pathogen immunity, and induces IECs to express high levels of CXCL1 and CXCL2 [5]. Granulocyte-macrophage colony-stimulating factor (GM-CSF) is another important cytokine produced by both NCR$^+$ ILC3s and NCR$^-$ ILC3s, which helps to maintain the
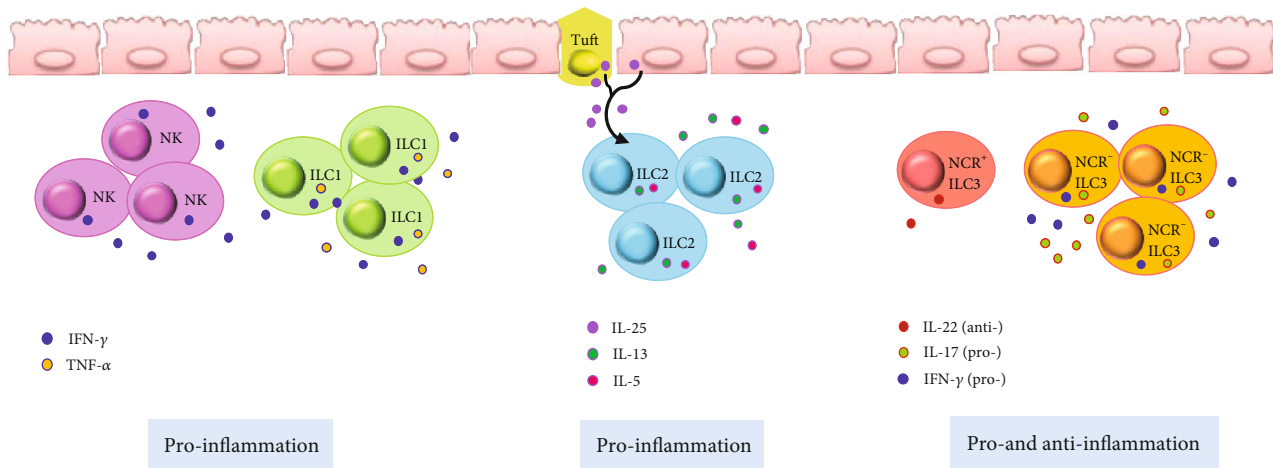
FIGURE 2: Potential pro- and anti-inflammatory roles of ILCs in intestinal chronic inflammation. NK cells and ILC1s are increased in the colonic lamina propria tissue of inflammatory bowel disease (IBD) patients. NK cells produce IFN-γ, whereas ILC1s produce IFN-γ and TNF-α. ILC2s play a pathogenic role by promoting IL-13- and IL-5-driven inflammation in a mouse model of colitis, which is ameliorated by blocking IL-25. IL22$^+$ NCR$^+$ ILC3s are decreased dramatically and NCR$^-$ ILC3s are increased under chronic inflammation conditions. The NCR$^-$ ILC3 subset can contribute to intestinal chronic inflammation through the production of IL-17A and IFN-γ.

homeostasis of mononuclear phagocytes in the intestine [5] (Figure 1). Collectively, these studies demonstrate the importance of the microflora in shaping the development and function of ILCs via direct or indirect interactions with IECs during intestinal tissue immune defense, while maintaining the intestinal micro-ecological balance.

4. ILCs in Intestinal Chronic Inflammation

NK cells are involved in the pathogenesis of inflammatory bowel disease (IBD) including ulcerative colitis (UC) and Crohn's disease (CD) [63–65]. Steel's group reported that the number of CD16$^+$ NK cells is increased in the colonic lamina propria tissue of patients with IBD [63] and Takayama's group showed that NKp46$^+$ NK cells might mediate the pathogenesis of CD via IFN-γ production [64] (Figure 2). Ng's group further identified that a subset of CD56$^+$ HLA-DR$^+$ NK cells in the colonic lamina propria is associated with intestinal inflammation in UC patients [66]. Further, Yusung's group showed that the number of NK cells in the colon decreases after therapy with the immunosuppressive drug 6-mercaptopurine in CD patients [67]. Together, these findings support the contention that NK cells are a very attractive immunotherapy target for IBD patients.

As described previously herein, ILC1s play a critical role in host defense against intracellular pathogens by secreting TNF-α and IFN-γ in the gut during steady-state conditions. However, under inflamed conditions, the frequency of ILC1s increases resulting in excessive cytokine production. Several groups reported that the frequency of ILC1s is increased in the intestines of patients with CD [14, 68, 69] (Figure 2). Li's group reported that an increase in IFN-γ-producing-CD127$^+$ ILC1s in the inflamed intestine is associated with disease severity [70, 71], and Bernink's group further reported that under the control of the cytokines IL-12 and IL-23, NKp44$^+$ ILC1s can convert into IFN-γ-producing ILC1s [14].

ILC2s play a pathogenic role by promoting IL-13-driven inflammation in an oxazolone-induced mouse model of colitis, which could be ameliorated by blocking IL-25 [72] (Figure 2). Monticelli's group revealed that ILC2s mediate tissue protection during intestinal injury by limiting inflammation and promoting epithelial repair through AREG secretion in a mouse model [45]. Bailey's group suggested a potential role for ILC2-derived IL-13 in collagen accumulation via the downregulation of fibroblast matrix metalloproteinase synthesis in CD patients [73]. However, there are still very limited data available about the role of human ILC2s in gut inflammation.

In the steady state, NCR$^+$ ILC3s are the dominant form of ILC3s, comprising 60–75% of total noncytotoxic ILCs, and IL-22 produced by this subset is the major source of this cytokine, which is required for mucosal immunity [14, 74, 75]. Moreover, an initial increase in the production of IL-22 by ILC3s correlates with mucosal healing in human IBD [76]. IL-22, mainly produced by NCR$^+$ ILC3s, can be triggered in the steady state by epithelial-adherent commensal microbiota such as adherent-invasive *E. coli* and segmented filamentous bacteria [77, 78]. This homeostatic IL-22 induction has been correlated with mucosal healing in IBD and helps to limit inflammatory colitis [55, 76, 79]. IBD-associated TNF-like ligand 1A (TL1A) production from intestinal mononuclear phagocytes can also induce the release of IL-22 from ILC3s and mediates protection during acute colitis [80].

However, NCR$^+$ ILC3s decrease dramatically in chronic inflammation conditions, whereas NCR$^-$ ILC3s are increased in IBD patients [68, 81, 82]. NCR$^-$ ILC3s can contribute to intestinal chronic inflammation [68, 81] through the production of IL-17A and IFN-γ [81]. We propose that imbalances in NCR$^+$ ILC3s and NCR$^-$ ILC3s lead to disparity in IL-22 and IL-17 production, as a main contributor to the pathology of the IBD (Figure 2). Moreover, chronic colitis might reflect a state of transition from tissue-repairing ILC3s to inflammatory RORγt$^+$ ILC1s [14, 68]. The action of ILC3s
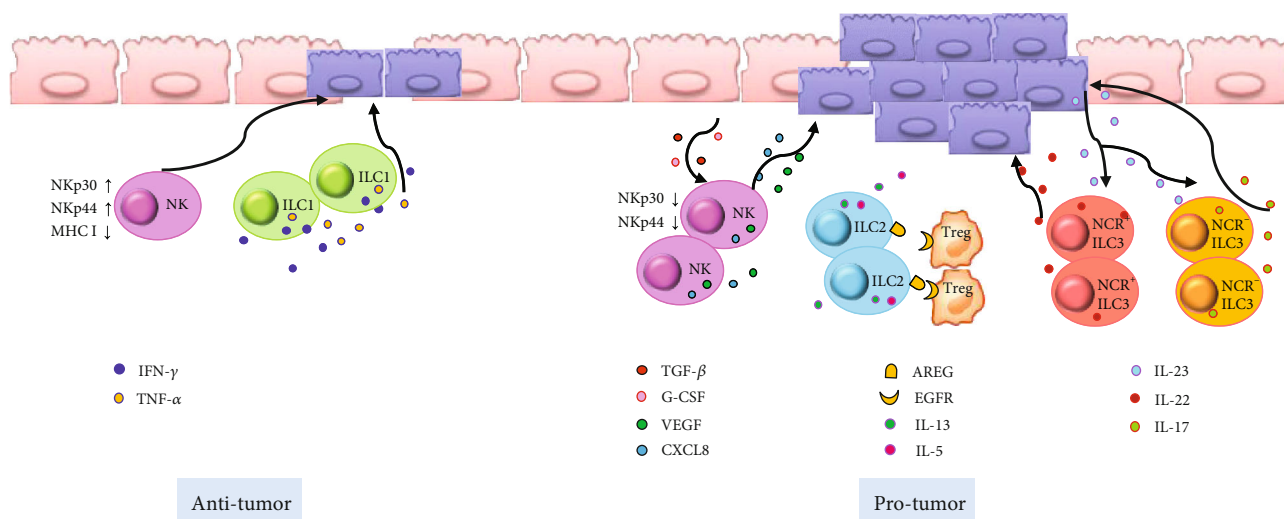
FIGURE 3: Potential pro- and antitumorigenic roles of ILCs in intestinal cancer. NK cells express high levels of the activating receptors NKp30 and NKp44 and contribute to the fight against tumor cells. Under the influence of transforming growth factor beta 1 (TGF-β) and granulocyte colony-stimulating factor (G-CSF), NK cells also have a tumor-promoting effect. ILC1s might be involved in antitumor immunity through the release of IFN-γ and TNF-α. ILC2-derived cytokines, IL-5 and IL-13, are associated with a high risk of developing inflammation-driven colorectal cancer. ILC2-derived AREG stimulates regulatory T cells and establishes an immune-suppressive tumor microenvironment. In response to IL-23 stimulation, NCR$^+$ ILC3s and NCR$^-$ ILC3s mainly produce IL-22 and IL-17, respectively. The IL-23–ILC3–IL-22/IL-17 axis is a critical pathway that promotes tumor growth.

in IBD confers is protective in controlling the microbiota, which could inform the development of future therapies that target chronic inflammation via ILC3s.

ILCregs are a regulatory subpopulation of ILCs that can be induced in the intestine and suppress the activation of ILC1s and ILC3s through the release of IL-10, thus playing an inhibitory role in intestinal inflammation [21]. Since the functions of ILCregs have thus far only been studied in mice, their detailed effects are still unclear, necessitating further exploration in humans.

To date, tissue-resident memory ILCs have been investigated in the liver and lungs, but not in the small intestine. Owing to common features such as migration patterns and memory potential, tissue-resident memory ILCs could be regarded as the innate counterparts of T_{RM} cells. T_{RM} cells are a group of self-renewing cells that persist at the site of infection in multiple organs including the intestine and control the development and progression of chronic intestinal inflammation [56]. Therefore, tissue-resident memory ILCs might play a certain role in mediating inflammation of the small intestine, and further research and verification of this are warranted.

5. ILCs in Intestinal Cancer

The antitumor function of NK cells in both human and mouse models has been well established [83, 84]. In contrast to tumor-specific cytotoxic T lymphocytes, NK cells, as an important member of the innate immune system, mediate cellular cytotoxicity without priming bispecific antigens [85]. As efficient cytolytic effectors, NK cells can fight against cancer-initiating cells (CICs), which play an important role in malignant tumor recurrence or metastasis [31]. In particular, colorectal cancer-derived CICs are sensitive

to NK cell-mediated killing, which is considered related to their high expression levels of ligands that activate NKp30 and NKp44 receptors and low expression levels of major histocompatibility class I molecules that typically inhibit NK cell activity [86] (Figure 3). In different mouse tumor models, the absence of NK cell activation was found to be associated with tumor aggression. Moreover, the absence of a cytotoxic effect of NK cells in colorectal cancer patients before surgery can predict recurrence after local tumor resection [87–89].

However, NK cells might not always act as potent antitumor effectors, as the cytotoxic function of these cells in the tumor microenvironment can be dampened, and NK cells can even have a tumor-promoting effect under certain conditions [85]. The expression of NK cell activation receptors was shown to be decreased in the blood and tumor tissue of colorectal cancer patients [90]. *In vitro*, NK cells cocultured with colorectal cancer cells can release cytotoxic molecules with the impaired production of IFN-γ [90]. A possible explanation for the dampened cytotoxicity of NK cells in the tumor microenvironment is the influence of granulocyte colony-stimulating factor (G-CSF) and transforming growth factor beta 1 (TGF-β1) [91–94]. In addition, in colorectal cancer patients, tumor-infiltrating NK cells also release high levels of vascular endothelial growth factor and CXCL8 to promote angiogenesis and tumor growth [95] (Figure 3).

Owing to the limited quantity of cytotoxic tumor-infiltrating NK cells and their markedly impaired cytotoxic function in colorectal cancer, the adoptive transfer of activated NK cells has emerged as a potential strategy for clinical therapy. A phase I clinical trial with colorectal cancer patients showed that patients who had previously undergone IgG1-based chemotherapy could tolerate the autologous

transfer of NK cells well and could successfully induce type-1 immune responses *in vivo* [96].

Nevertheless, the detailed role of ILC1s in colorectal tumors remains unclear. However, their well-established function in intestinal chronic inflammation could provide a clue based on their potential to create a suitable environment for subsequent malignant transformation [87]. Upon the activation of ILC1, key effector cytokines IFN-γ and TNF-α are released, and these cytokines promote chronic gut inflammation. IFN-γ and TNF-α are involved in antitumor immunity [97] (Figure 3). IFN-γ plays a role in cell-mediated tumor cell lysis, which inhibits tumor cell proliferation, reduces neoangiogenesis, and suppresses tumor progression [97]. In turn, TNF-α can facilitate tumor cell apoptosis and macrophage and dendritic cell infiltration into the local tumor, suggesting direct and indirect antitumor immune responses [98, 99]. However, further research is warranted to illustrate the role of ILC1s in intestinal tumors.

Further, the function of ILC2s during intestinal carcinogenesis has been well researched in both mouse models and humans. Bie's group reported increased numbers of ILC2s, as well as the transcription of ILC2-related genes including *CRTH2*, *GATA3*, and *RORα*, in the peripheral blood of gastric cancer patients [100]. The frequency of ILC2s and the ILC2-related cytokines IL-5, IL-9, and IL-13 were also shown to be increased in patients with UC, which is a condition associated with high colorectal cancer risk due to chronic inflammation [101–103]. ILC2-derived AREG might also stimulate regulatory T cells to establish an immune-suppressive tumor microenvironment [104] (Figure 3). In addition, the ILC2-activated cytokine IL-33 mediates host antitumor immunity, angiogenesis, and stromal remodeling in colorectal cancer pathogenesis [105, 106] and supports the effector functions of cytotoxic NK and CD8$^+$ T cells [107]. Thus, further studies should consider the contribution of IL-33 and IL-33-activated ILC2s to the pathogenesis of colorectal cancer.

An increased frequency of ILC3s has also been found in colorectal cancer tissues in a mouse model, and this might play a role in tumor progression [82, 108]. As an ILC3-active factor, the cytokine IL-23 regulates homeostasis and intestinal inflammation. Increased IL-23 expression levels in human colon tumors have been observed, which were associated with tumor progression and worse prognosis [109, 110]. Moreover, IL-23-deficient mice are resistant to tumor formation [109–111], and the depletion of ILCs and IL-22 can reverse established tumors in a Rag1$^{-/-}$ mouse tumor model induced by *Helicobacter hepaticus* oral infection, indicating that ILCs and IL-22 are essential for the formation of colonic tumors. ILC3s are the main producers of IL-22, which generally has a tumor-promoting effect, but its condition-dependent nature has been proposed with different roles observed in different cancer microenvironments [112–114]. As another important cytokine produced by ILC3s, IL-17A has been implicated in human colorectal cancer, and increased IL-17-producing cells could independently predict worse clinical outcomes [115, 116] (Figure 3). A recent study showed that IL-23 can induce the conversion of ILC1s to ILC3s, demonstrating that the IL-23–ILC3–IL-17 axis is a critical pathway that promotes tumor growth [117]. Collectively, these results showed that imbalances in ILC3s could contribute to the progression of colorectal cancer and that IL-17 and IL-22 could be potential treatment targets.

Finally, monobenzone-induced memory CD49b$^+$ cNK cells were found to effectively control B16 tumor development in a mouse model [118]. Although there has been no study of the function of tissue-resident memory ILCs in intestinal cancer, as the apparent innate counterparts of T$_{RM}$ cells, they are considered to have potential benefits in long-term tumor control and vaccination, with promising clinical value for tumor immunotherapies and vaccine-development strategies [23].

6. Concluding Remarks

Mounting evidence has now demonstrated that ILCs are critical regulators of intestinal homeostasis, inflammation, and cancer. Although tremendous progress has been made in understanding the detailed roles of ILCs in the restoration of epithelial barrier integrity and protection against infiltrating pathogens, and intestinal inflammation and cancer, this research has also revealed that ILCs represent a highly heterogeneous group of cells. The different groups and subsets of ILCs and their corresponding cytokines have now emerged as important mediators of various pathological conditions, and even the same subtype might have diverse roles in different contexts or at different stages of disease. Moreover, ILCs also play roles in metabolic homeostasis and contribute to the pathogenesis of graft-versus-host disease. Thus, further studies focused on exploring the regulation and pathophysiology of ILCs might reveal potential targets for future therapeutic interventions.

Conflicts of Interest

The authors declare that there is no conflict of interest regarding the publication of this paper.

Acknowledgments

References

[1] N. Khan and A. R. Asif, "Transcriptional regulators of claudins in epithelial tight junctions," *Mediators of Inflammation*, vol. 2015, Article ID 219843, 6 pages, 2015.

[2] P. R. Giacomin, R. H. Moy, M. Noti et al., "Epithelial-intrinsic IKKα expression regulates group 3 innate lymphoid cell responses and antibacterial immunity," *The Journal of Experimental Medicine*, vol. 212, no. 10, pp. 1513–1528, 2015.

[3] K. Ke, T. (. H. P.). Chen, M. Arra, G. Mbalaviele, G. Swarnkar, and Y. Abu-Amer, "Attenuation of NF-κB in intestinal epithelial cells is sufficient to mitigate the bone loss comorbidity of experimental mouse colitis," *Journal of Bone and Mineral Research*, vol. 34, no. 10, pp. 1880–1893, 2019.

[4] A. N. J. McKenzie, H. Spits, and G. Eberl, "Innate lymphoid cells in inflammation and immunity," *Immunity*, vol. 41, no. 3, pp. 366–374, 2014.

[5] J. W. Bostick and L. Zhou, "Innate lymphoid cells in intestinal immunity and inflammation," *Cellular and Molecular Life Sciences*, vol. 73, no. 2, pp. 237–252, 2016.

[6] C. S. N. Klose, M. Flach, L. Möhle et al., "Differentiation of type 1 ILCs from a common progenitor to all helper-like innate lymphoid cell lineages," *Cell*, vol. 157, no. 2, pp. 340–356, 2014.

[7] N. Satoh-Takayama, N. Serafini, T. Verrier et al., "The chemokine receptor CXCR6 controls the functional topography of interleukin-22 producing intestinal innate lymphoid cells," *Immunity*, vol. 41, no. 5, pp. 776–788, 2014.

[8] J. K. Bando, H. E. Liang, and R. M. Locksley, "Identification and distribution of developing innate lymphoid cells in the fetal mouse intestine," *Nature Immunology*, vol. 16, no. 2, pp. 153–160, 2015.

[9] K. Gronke, M. Kofoed-Nielsen, and A. Diefenbach, "Isolation and flow cytometry analysis of innate lymphoid cells from the intestinal lamina propria," in *Inflammation*, B. Clausen and J. Laman, Eds., vol. 1559 of Methods in Molecular Biology, pp. 255–265, Humana Press, New York, NY, 2017.

[10] J. G. Castellanos and R. S. Longman, "The balance of power: innate lymphoid cells in tissue inflammation and repair," *Journal of Clinical Investigation*, vol. 129, no. 7, pp. 2640–2650, 2019.

[11] H. Spits, D. Artis, M. Colonna et al., "Innate lymphoid cells — a proposal for uniform nomenclature," *Nature Reviews Immunology*, vol. 13, no. 2, pp. 145–149, 2013.

[12] E. Vivier, D. Artis, M. Colonna et al., "Innate lymphoid cells: 10 years on," *Cell*, vol. 174, no. 5, pp. 1054–1066, 2018.

[13] D. E. Cherrier, N. Serafini, and J. P. Di Santo, "Innate lymphoid cell development: a T cell perspective," *Immunity*, vol. 48, no. 6, pp. 1091–1103, 2018.

[14] J. H. Bernink, C. P. Peters, M. Munneke et al., "Human type 1 innate lymphoid cells accumulate in inflamed mucosal tissues," *Nature Immunology*, vol. 14, no. 3, pp. 221–229, 2013.

[15] T. Y. Halim, R. H. Krauss, A. C. Sun, and F. Takei, "Lung natural helper cells are a critical source of Th2 cell-type cytokines in protease allergen-induced airway inflammation," *Immunity*, vol. 36, no. 3, pp. 451–463, 2012.

[16] S. D. Hurst, T. Muchamuel, D. M. Gorman et al., "New IL-17 family members promote Th1 or Th2 responses in the lung: in vivo function of the novel cytokine IL-25," *Journal of Immunology*, vol. 169, no. 1, pp. 443–453, 2002.

[17] C. S. Klose and D. Artis, "Innate lymphoid cells as regulators of immunity, inflammation and tissue homeostasis," *Nature Immunology*, vol. 17, no. 7, pp. 765–774, 2016.

[18] T. Hoyler, C. S. N. Klose, A. Souabni et al., "The transcription factor GATA-3 controls cell fate and maintenance of type 2 innate lymphoid cells," *Immunity*, vol. 37, no. 4, pp. 634–648, 2012.

[19] J. Mjösberg, J. Bernink, K. Golebski et al., "The transcription factor GATA3 is essential for the function of human type 2 innate lymphoid cells," *Immunity*, vol. 37, no. 4, pp. 649–659, 2012.

[20] F. Melo-Gonzalez and M. R. Hepworth, "Functional and phenotypic heterogeneity of group 3 innate lymphoid cells," *Immunology*, vol. 150, no. 3, pp. 265–275, 2017.

[21] S. Wang, P. Xia, Y. Chen et al., "Regulatory Innate Lymphoid Cells Control Innate Intestinal Inflammation," *Cell*, vol. 171, no. 1, pp. 201–16.e18, 2017.

[22] X. Wang, Z. Tian, and H. Peng, "Tissue-resident memory-like ILCs: innate counterparts of T_{RM} cells," *Protein & Cell*, pp. 1–12, 2019.

[23] X. Wang, H. Peng, and Z. Tian, "Innate lymphoid cell memory," *Cellular & Molecular Immunology*, vol. 16, no. 5, pp. 423–429, 2019.

[24] N. K. Crellin, S. Trifari, C. D. Kaplan, N. Satoh-Takayama, J. P. di Santo, and H. Spits, "Regulation of Cytokine Secretion in Human CD127+ LTi- like Innate Lymphoid Cells by Toll-like Receptor 2," *Immunity*, vol. 33, no. 5, pp. 752–764, 2010.

[25] H. Kabata, K. Moro, and S. Koyasu, "The group 2 innate lymphoid cell (ILC2) regulatory network and its underlying mechanisms," *Immunological Reviews*, vol. 286, no. 1, pp. 37–52, 2018.

[26] J. H. Bernink, L. Krabbendam, K. Germar et al., "Interleukin-12 and -23 Control Plasticity of CD127+ Group 1 and Group 3 Innate Lymphoid Cells in the Intestinal Lamina Propria," *Immunity*, vol. 43, no. 1, pp. 146–160, 2015.

[27] H. Cheng, C. Jin, J. Wu, S. Zhu, Y. J. Liu, and J. Chen, "Guards at the gate: physiological and pathological roles of tissue-resident innate lymphoid cells in the lung," *Protein & Cell*, vol. 8, no. 12, article 379, pp. 878–895, 2017.

[28] F. Ciccia, G. Guggino, A. Rizzo et al., "Type 3 innate lymphoid cells producing IL-17 and IL-22 are expanded in the gut, in the peripheral blood, synovial fluid and bone marrow of patients with ankylosing spondylitis," *Annals of the Rheumatic Diseases*, vol. 74, no. 9, pp. 1739–1747, 2015.

[29] K. A. Buela, S. Omenetti, and T. T. Pizarro, "Cross-talk between type 3 innate lymphoid cells and the gut microbiota in inflammatory bowel disease," *Current Opinion in Gastroenterology*, vol. 31, no. 6, pp. 449–455, 2015.

[30] J. C. Nussbaum, S. J. van Dyken, J. von Moltke et al., "Type 2 innate lymphoid cells control eosinophil homeostasis," *Nature*, vol. 502, no. 7470, pp. 245–248, 2013.

[31] I. Atreya, M. Kindermann, and S. Wirtz, "Innate lymphoid cells in intestinal cancer development," *Seminars in Immunology*, vol. 41, article 101267, 2019.

[32] A. I. Lim and J. P. Di Santo, "ILC-poiesis: ensuring tissue ILC differentiation at the right place and time," *European Journal of Immunology*, vol. 49, no. 1, pp. 11–18, 2019.

[33] D. R. Neill, S. H. Wong, A. Bellosi et al., "Nuocytes represent a new innate effector leukocyte that mediates type-2 immunity," *Nature*, vol. 464, no. 7293, pp. 1367–1370, 2010.

[34] C. P. Peters, J. M. Mjosberg, J. H. Bernink, and H. Spits, "Innate lymphoid cells in inflammatory bowel diseases," *Immunology Letters*, vol. 172, pp. 124–131, 2016.

[35] J. Qiu, X. Guo, Z. M. Chen et al., "Group 3 innate lymphoid cells inhibit T-cell-mediated intestinal inflammation through aryl hydrocarbon receptor signaling and regulation of microflora," *Immunity*, vol. 39, no. 2, pp. 386–399, 2013.

[36] S. C. Ganal, S. L. Sanos, C. Kallfass et al., "Priming of natural killer cells by nonmucosal mononuclear phagocytes requires

instructive signals from commensal microbiota," *Immunity*, vol. 37, no. 1, pp. 171–186, 2012.

[37] Y. Qiu, Z. Jiang, S. Hu, L. Wang, X. Ma, and X. Yang, "*Lactobacillus plantarum* enhanced IL-22 production in natural killer (NK) cells that protect the integrity of intestinal epithelial cell barrier damaged by enterotoxigenic *Escherichia coli*," *International Journal of Molecular Sciences*, vol. 18, no. 11, article 2409, 2017.

[38] C. S. Klose, E. A. Kiss, V. Schwierzeck et al., "A T-bet gradient controls the fate and function of CCR6$^-$RORγt$^+$ innate lymphoid cells," *Nature*, vol. 494, no. 7436, pp. 261–265, 2013.

[39] M. C. Abt, B. B. Lewis, S. Caballero et al., "Innate immune defenses mediated by two ILC subsets are critical for protection against acute *Clostridium difficile* infection," *Cell Host & Microbe*, vol. 18, no. 1, pp. 27–37, 2015.

[40] O. E. Weizman, N. M. Adams, I. S. Schuster et al., "ILC1 confer early host protection at initial sites of viral infection," *Cell*, vol. 171, no. 4, pp. 795–808.e12, 2017.

[41] A. E. Price, H. E. Liang, B. M. Sullivan et al., "Systemically dispersed innate IL-13-expressing cells in type 2 immunity," *Proceedings of the National Academy of Sciences of the United States of America*, vol. 107, no. 25, pp. 11489–11494, 2010.

[42] J. A. Walker and A. N. McKenzie, "Development and function of group 2 innate lymphoid cells," *Current Opinion in Immunology*, vol. 25, no. 2, pp. 148–155, 2013.

[43] Y. Motomura, H. Morita, K. Moro et al., "Basophil-derived interleukin-4 controls the function of natural helper cells, a member of ILC2s, in lung inflammation," *Immunity*, vol. 40, no. 5, pp. 758–771, 2014.

[44] C. J. Oliphant, Y. Y. Hwang, J. A. Walker et al., "MHCII-mediated dialog between group 2 innate lymphoid cells and CD4$^+$ T cells potentiates type 2 immunity and promotes parasitic helminth expulsion," *Immunity*, vol. 41, no. 2, pp. 283–295, 2014.

[45] L. A. Monticelli, L. C. Osborne, M. Noti, S. V. Tran, D. M. Zaiss, and D. Artis, "IL-33 promotes an innate immune pathway of intestinal tissue protection dependent on amphiregulin-EGFR interactions," *Proceedings of the National Academy of Sciences of the United States of America*, vol. 112, no. 34, pp. 10762–10767, 2015.

[46] L. A. Monticelli, G. F. Sonnenberg, M. C. Abt et al., "Innate lymphoid cells promote lung-tissue homeostasis after infection with influenza virus," *Nature Immunology*, vol. 12, no. 11, pp. 1045–1054, 2011.

[47] C. Berasain and M. A. Avila, "Amphiregulin," *Seminars in Cell & Developmental Biology*, vol. 28, pp. 31–41, 2014.

[48] R. Avraham and Y. Yarden, "Feedback regulation of EGFR signalling: decision making by early and delayed loops," *Nature Reviews Molecular Cell Biology*, vol. 12, no. 2, pp. 104–117, 2011.

[49] A. L. Frisbee, M. M. Saleh, M. K. Young et al., "IL-33 drives group 2 innate lymphoid cell-mediated protection during *Clostridium difficile* infection," *Nature Communications*, vol. 10, no. 1, article 2712, 2019.

[50] K. Moro, T. Yamada, M. Tanabe et al., "Innate production of T$_H$2 cytokines by adipose tissue- associated c-Kit$^+$Sca-1$^+$ lymphoid cells," *Nature*, vol. 463, no. 7280, pp. 540–544, 2010.

[51] S. A. Saenz, M. C. Siracusa, J. G. Perrigoue et al., "IL25 elicits a multipotent progenitor cell population that promotes T$_H$2 cytokine responses," *Nature*, vol. 464, no. 7293, pp. 1362–1366, 2010.

[52] F. Gerbe, E. Sidot, D. J. Smyth et al., "Intestinal epithelial tuft cells initiate type 2 mucosal immunity to helminth parasites," *Nature*, vol. 529, no. 7585, pp. 226–230, 2016.

[53] M. R. Howitt, S. Lavoie, M. Michaud et al., "Tuft cells, taste-chemosensory cells, orchestrate parasite type 2 immunity in the gut," *Science*, vol. 351, no. 6279, pp. 1329–1333, 2016.

[54] G. F. Sonnenberg, L. A. Monticelli, M. M. Elloso, L. A. Fouser, and D. Artis, "CD4$^+$ lymphoid tissue-inducer cells promote innate immunity in the gut," *Immunity*, vol. 34, no. 1, pp. 122–134, 2011.

[55] J. H. Cox, N. M. Kljavin, N. Ota et al., "Opposing consequences of IL-23 signaling mediated by innate and adaptive cells in chemically induced colitis in mice," *Mucosal Immunology*, vol. 5, no. 1, pp. 99–109, 2012.

[56] S. Zundler, E. Becker, M. Spocinska et al., "Hobit- and Blimp-1-driven CD4$^+$ tissue-resident memory T cells control chronic intestinal inflammation," *Nature Immunology*, vol. 20, no. 3, pp. 288–300, 2019.

[57] G. F. Sonnenberg, L. A. Monticelli, T. Alenghat et al., "Innate lymphoid cells promote anatomical containment of lymphoid-resident commensal bacteria," *Science*, vol. 336, no. 6086, pp. 1321–1325, 2012.

[58] A. M. Hanash, J. A. Dudakov, G. Hua et al., "Interleukin-22 protects intestinal stem cells from immune-mediated tissue damage and regulates sensitivity to graft versus host disease," *Immunity*, vol. 37, no. 2, pp. 339–350, 2012.

[59] C. Vonarbourg, A. Mortha, V. L. Bui et al., "Regulated expression of nuclear receptor RORγt confers distinct functional fates to NK cell receptor-expressing RORγt$^+$ innate lymphocytes," *Immunity*, vol. 33, no. 5, pp. 736–751, 2010.

[60] N. Satoh-Takayama, C. A. Vosshenrich, S. Lesjean-Pottier et al., "Microbial flora drives interleukin 22 production in intestinal NKp46$^+$ cells that provide innate mucosal immune defense," *Immunity*, vol. 29, no. 6, pp. 958–970, 2008.

[61] S. Ibiza, B. García-Cassani, H. Ribeiro et al., "Glial-cell-derived neuroregulators control type 3 innate lymphoid cells and gut defence," *Nature*, vol. 535, no. 7612, pp. 440–443, 2016.

[62] M. Martínez-López, S. Iborra, R. Conde-Garrosa et al., "Microbiota sensing by Mincle-Syk axis in dendritic cells regulates interleukin-17 and -22 production and promotes intestinal barrier integrity," *Immunity*, vol. 50, no. 2, pp. 446–61.e9, 2019.

[63] A. W. Steel, C. M. Mela, J. O. Lindsay, B. G. Gazzard, and M. R. Goodier, "Increased proportion of CD16$^+$ NK cells in the colonic lamina propria of inflammatory bowel disease patients, but not after azathioprine treatment," *Alimentary Pharmacology & Therapeutics*, vol. 33, no. 1, pp. 115–126, 2011.

[64] T. Takayama, N. Kamada, H. Chinen et al., "Imbalance of NKp44$^+$NKp46$^-$ and NKp44$^-$NKp46$^+$ Natural Killer Cells in the Intestinal Mucosa of Patients With Crohn's Disease," *Gastroenterology*, vol. 139, no. 3, pp. 882–892.e3, 2010.

[65] J. Li and S. C. Glover, "Innate lymphoid cells in inflammatory bowel disease," *Archivum Immunologiae et Therapiae Experimentalis*, vol. 66, no. 6, pp. 415–421, 2018.

[66] S. C. Ng, S. Plamondon, H. O. al-Hassi et al., "A novel population of human CD56$^+$ human leucocyte antigen D-related (HLA-DR$^+$) colonic lamina propria cells is associated with inflammation in ulcerative colitis," *Clinical and Experimental Immunology*, vol. 158, no. 2, pp. 205–218, 2009.

[67] S. Yusung, D. McGovern, L. Lin, D. Hommes, V. Lagishetty, and J. Braun, "NK cells are biologic and biochemical targets of 6-mercaptopurine in Crohn's disease patients," *Clinical Immunology*, vol. 175, pp. 82–90, 2017.

[68] A. Geremia, C. V. Arancibia-Cárcamo, M. P. P. Fleming et al., "IL-23-responsive innate lymphoid cells are increased in inflammatory bowel disease," *The Journal of Experimental Medicine*, vol. 208, no. 6, pp. 1127–1133, 2011.

[69] A. Fuchs, W. Vermi, J. S. Lee et al., "Intraepithelial type 1 innate lymphoid cells are a unique subset of IL-12- and IL-15-responsive IFN-γ-producing cells," *Immunity*, vol. 38, no. 4, pp. 769–781, 2013.

[70] J. Li, A. L. Doty, A. Iqbal, and S. C. Glover, "The differential frequency of Lineage⁻CRTH2⁻CD45⁺NKp44⁻CD117⁻CD127⁺⁻ ILC subset in the inflamed terminal ileum of patients with Crohn's disease," *Cellular Immunology*, vol. 304-305, pp. 63–68, 2016.

[71] J. Li, A. L. Doty, Y. Tang et al., "Enrichment of IL-17A +IFN-γ⁺ and IL-22+IFN-γ⁺ T cell subsets is associated with reduction of NKp44+ILC3s in the terminal ileum of Crohn's disease patients," *Clinical and Experimental Immunology*, vol. 190, no. 1, pp. 143–153, 2017.

[72] A. Camelo, J. L. Barlow, L. F. Drynan et al., "Blocking IL-25 signalling protects against gut inflammation in a type-2 model of colitis by suppressing nuocyte and NKT derived IL-13," *Journal of Gastroenterology*, vol. 47, no. 11, pp. 1198–1211, 2012.

[73] J. R. Bailey, P. W. Bland, J. F. Tarlton et al., "IL-13 promotes collagen accumulation in Crohn's disease fibrosis by down-regulation of fibroblast MMP synthesis: a role for innate lymphoid cells?," *PLoS One*, vol. 7, no. 12, article e52332, 2012.

[74] M. Cella, A. Fuchs, W. Vermi et al., "A human natural killer cell subset provides an innate source of IL-22 for mucosal immunity," *Nature*, vol. 457, no. 7230, pp. 722–725, 2009.

[75] S. Sawa, M. Lochner, N. Satoh-Takayama et al., "RORγt⁺ innate lymphoid cells regulate intestinal homeostasis by integrating negative signals from the symbiotic microbiota," *Nature Immunology*, vol. 12, no. 4, pp. 320–326, 2011.

[76] R. S. Longman, G. E. Diehl, D. A. Victorio et al., "CX₃CR1 mononuclear phagocytes support colitis-associated innate lymphoid cell production of IL-22," *The Journal of Experimental Medicine*, vol. 211, no. 8, pp. 1571–1583, 2014.

[77] T. Sano, W. Huang, J. A. Hall et al., "An IL-23R/IL-22 circuit regulates epithelial serum amyloid a to promote local effector Th17 responses," *Cell*, vol. 164, no. 1-2, p. 324, 2016.

[78] M. Viladomiu, C. Kivolowitz, A. Abdulhamid et al., "IgA-coated *E. coli* enriched in Crohn's disease spondyloarthritis promote T_H17-dependent inflammation," *Science Translational Medicine*, vol. 9, no. 376, article eaaf9655, 2017.

[79] X. Guo, Y. Liang, Y. Zhang, A. Lasorella, B. L. Kee, and Y. X. Fu, "Innate lymphoid cells control early colonization resistance against intestinal pathogens through ID2-dependent regulation of the microbiota," *Immunity*, vol. 42, no. 4, pp. 731–743, 2015.

[80] J. G. Castellanos, V. Woo, M. Viladomiu et al., "Microbiota-Induced TNF-like Ligand 1A Drives Group 3 Innate Lymphoid Cell- Mediated Barrier Protection and Intestinal T Cell Activation during Colitis," *Immunity*, vol. 49, no. 6, pp. 1077–1089.e5, 2018.

[81] S. Buonocore, P. P. Ahern, H. H. Uhlig et al., "Innate lymphoid cells drive interleukin-23-dependent innate intestinal pathology," *Nature*, vol. 464, no. 7293, pp. 1371–1375, 2010.

[82] H. A. Penny, S. H. Hodge, and M. R. Hepworth, "Orchestration of intestinal homeostasis and tolerance by group 3 innate lymphoid cells," *Seminars in Immunopathology*, vol. 40, no. 4, pp. 357–370, 2018.

[83] E. Vivier, S. Ugolini, D. Blaise, C. Chabannon, and L. Brossay, "Targeting natural killer cells and natural killer T cells in cancer," *Nature Reviews Immunology*, vol. 12, no. 4, pp. 239–252, 2012.

[84] M. G. Morvan and L. L. Lanier, "NK cells and cancer: you can teach innate cells new tricks," *Nature Reviews Cancer*, vol. 16, no. 1, pp. 7–19, 2016.

[85] P. Vacca, E. Munari, N. Tumino et al., "Human natural killer cells and other innate lymphoid cells in cancer: friends or foes?," *Immunology Letters*, vol. 201, pp. 14–19, 2018.

[86] R. Tallerico, M. Todaro, S. di Franco et al., "Human NK cells selective targeting of colon cancer-initiating cells: a role for natural cytotoxicity receptors and MHC class I molecules," *Journal Of Immunology*, vol. 190, no. 5, pp. 2381–2390, 2013.

[87] L. Chiossone, P. Y. Dumas, M. Vienne, and E. Vivier, "Natural killer cells and other innate lymphoid cells in cancer," *Nature Reviews Immunology*, vol. 18, no. 11, pp. 671–688, 2018.

[88] J. J. P. van Beek, A. W. J. Martens, G. Bakdash, and I. J. M. de Vries, "Innate lymphoid cells in tumor immunity," *Biomedicines*, vol. 4, no. 1, p. 7, 2016.

[89] P. I. Tartter, B. Steinberg, D. M. Barron, and G. Martinelli, "The prognostic significance of natural killer cytotoxicity in patients with colorectal cancer," *Archives of Surgery*, vol. 122, no. 11, pp. 1264–1268, 1987.

[90] Y. S. Rocca, M. P. Roberti, J. M. Arriaga et al., "Altered phenotype in peripheral blood and tumor-associated NK cells from colorectal cancer patients," *Innate Immunity*, vol. 19, no. 1, pp. 76–85, 2013.

[91] S. Narai, M. Watanabe, H. Hasegawa et al., "Significance of transforming growth factor β1 as a new tumor marker for colorectal cancer," *International Journal of Cancer*, vol. 97, no. 4, pp. 508–511, 2002.

[92] F. Otegbeye, E. Ojo, S. Moreton et al., "Correction: inhibiting TGF-beta signaling preserves the function of highly activated, in vitro expanded natural killer cells in AML and colon cancer models," *PLoS One*, vol. 13, no. 5, article e0197008, 2018.

[93] K. T. Morris, E. F. Castillo, A. L. Ray et al., "Anti-G-CSF treatment induces protective tumor immunity in mouse colon cancer by promoting protective NK cell, macrophage and T cell responses," *Oncotarget*, vol. 6, no. 26, pp. 22338–22347, 2015.

[94] L. Schlahsa, Y. Jaimes, R. Blasczyk, and C. Figueiredo, "Granulocyte–colony-stimulatory factor: a strong inhibitor of natural killer cell function," *Transfusion*, vol. 51, no. 2, pp. 293–305, 2011.

[95] A. Bruno, B. Bassani, D. G. D'Urso et al., "Angiogenin and the MMP9-TIMP2 axis are up-regulated in proangiogenic, decidual NK-like cells from patients with colorectal cancer," *FASEB Journal*, vol. 32, no. 10, pp. 5365–5377, 2018.

[96] T. Ishikawa, T. Okayama, N. Sakamoto et al., "Phase I clinical trial of adoptive transfer of expanded natural killer cells in combination with IgG1 antibody in patients with gastric or colorectal cancer," *International Journal of Cancer*, vol. 142, no. 12, pp. 2599–2609, 2018.

[97] J. Mattner and S. Wirtz, "Friend or foe? The ambiguous role of innate lymphoid cells in cancer development," *Trends in Immunology*, vol. 38, no. 1, pp. 29–38, 2017.

[98] L. Bertazza and S. Mocellin, "The dual role of tumor necrosis factor (TNF) in cancer biology," *Current Medicinal Chemistry*, vol. 17, no. 29, pp. 3337–3352, 2010.

[99] A. Rizzo, V. de Mare, C. Rocchi et al., "Smad7 induces plasticity in tumor-infiltrating Th17 cells and enables TNF-alpha-mediated killing of colorectal cancer cells," *Carcinogenesis*, vol. 35, no. 7, pp. 1536–1546, 2014.

[100] Q. Bie, P. Zhang, Z. Su et al., "Polarization of ILC2s in peripheral blood might contribute to immunosuppressive microenvironment in patients with gastric cancer," *Journal of Immunology Research*, vol. 2014, Article ID 923135, 10 pages, 2014.

[101] M. Forkel, S. van Tol, C. Hoog, J. Michaelsson, S. Almer, and J. Mjosberg, "Distinct alterations in the composition of mucosal innate lymphoid cells in newly diagnosed and established Crohn's disease and ulcerative colitis," *Journal of Crohn's & Colitis*, vol. 13, no. 1, pp. 67–78, 2019.

[102] F. Heller, P. Florian, C. Bojarski et al., "Interleukin-13 is the key effector Th2 cytokine in ulcerative colitis that affects epithelial tight junctions, apoptosis, and cell restitution," *Gastroenterology*, vol. 129, no. 2, pp. 550–564, 2005.

[103] K. Gerlach, Y. Y. Hwang, A. Nikolaev et al., "T_H9 cells that express the transcription factor PU.1 drive T cell–mediated colitis via IL-9 receptor signaling in intestinal epithelial cells," *Nature Immunology*, vol. 15, no. 7, pp. 676–686, 2014.

[104] D. M. W. Zaiss, J. van Loosdregt, A. Gorlani et al., "Amphiregulin enhances regulatory T cell-suppressive function via the epidermal growth factor receptor," *Immunity*, vol. 38, no. 2, pp. 275–284, 2013.

[105] K. D. Mertz, L. F. Mager, M. H. Wasmer et al., "The IL-33/ST2 pathway contributes to intestinal tumorigenesis in humans and mice," *Oncoimmunology*, vol. 5, no. 1, article e1062966, 2016.

[106] R. L. Maywald, S. K. Doerner, L. Pastorelli et al., "IL-33 activates tumor stroma to promote intestinal polyposis," *Proceedings of the National Academy of Sciences of the United States of America*, vol. 112, no. 19, pp. E2487–E2496, 2015.

[107] W. V. Bonilla, A. Frohlich, K. Senn et al., "The alarmin interleukin-33 drives protective antiviral CD8$^+$ T cell responses," *Science*, vol. 335, no. 6071, pp. 984–989, 2012.

[108] A. Geremia and C. V. Arancibia-Carcamo, "Innate lymphoid cells in intestinal inflammation," *Frontiers in Immunology*, vol. 8, article 1296, 2017.

[109] J. L. Langowski, X. Zhang, L. Wu et al., "IL-23 promotes tumour incidence and growth," *Nature*, vol. 442, no. 7101, pp. 461–465, 2006.

[110] S. I. Grivennikov, K. Wang, D. Mucida et al., "Adenoma-linked barrier defects and microbial products drive IL-23/IL-17-mediated tumour growth," *Nature*, vol. 491, no. 7423, pp. 254–258, 2012.

[111] K. Wang, M. K. Kim, G. di Caro et al., "Interleukin-17 receptor a signaling in transformed enterocytes promotes early colorectal tumorigenesis," *Immunity*, vol. 41, no. 6, pp. 1052–1063, 2014.

[112] S. Kirchberger, D. J. Royston, O. Boulard et al., "Innate lymphoid cells sustain colon cancer through production of interleukin-22 in a mouse model," *The Journal of Experimental Medicine*, vol. 210, no. 5, pp. 917–931, 2013.

[113] P. Carrega, F. Loiacono, E. di Carlo et al., "NCR$^+$ILC3 concentrate in human lung cancer and associate with intratumoral lymphoid structures," *Nature Communications*, vol. 6, no. 1, article 8280, 2015.

[114] S. Irshad, F. Flores-Borja, K. Lawler et al., "RORγt$^+$ innate lymphoid cells promote lymph node metastasis of breast cancers," *Cancer Research*, vol. 77, no. 5, pp. 1083–1096, 2017.

[115] I. H. Chan, R. Jain, M. S. Tessmer et al., "Interleukin-23 is sufficient to induce rapid de novo gut tumorigenesis, independent of carcinogens, through activation of innate lymphoid cells," *Mucosal Immunology*, vol. 7, no. 4, pp. 842–856, 2014.

[116] J. Liu, Y. Duan, X. Cheng et al., "IL-17 is associated with poor prognosis and promotes angiogenesis via stimulating VEGF production of cancer cells in colorectal carcinoma," *Biochemical and Biophysical Research Communications*, vol. 407, no. 2, pp. 348–354, 2011.

[117] J. Koh, H. Y. Kim, Y. Lee et al., "IL23-producing human lung cancer cells promote tumor growth via conversion of innate lymphoid cell 1 (ILC1) into ILC3," *Clinical Cancer Research*, vol. 25, no. 13, pp. 4026–4037, 2019.

[118] J. G. van den Boorn, C. Jakobs, C. Hagen et al., "Inflammasome-dependent induction of adaptive NK cell memory," *Immunity*, vol. 44, no. 6, pp. 1406–1421, 2016.

Research Article

Mutated p53 Promotes the Symmetric Self-Renewal of Cisplatin-Resistant Lung Cancer Stem-Like Cells and Inhibits the Recruitment of Macrophages

Yu Xu,[1] Zhi Xu,[1] Qi Li,[1] Liang Guo,[1] Yao Wang,[1] Jianchun Zhou,[2] Guansong Wang[ID],[1] and Yuliang Liu[ID][2]

[1]*Department of Respiratory and Critical Care Medicine, Xinqiao Hospital, The Army Medical University, Chongqing, China*
[2]*Department of Respiratory and Critical Care Medicine, The First Affiliated Hospital of Chongqing Medical University, Chongqing, China*

Correspondence should be addressed to Guansong Wang; wanggs2003@163.com and Yuliang Liu; lbb861@qq.com

It has been proposed that mutant p53 is correlated with the recurrence of lung cancer. Recently, a small population of cells with asymmetric or symmetric self-renewal potential has been identified in lung cancer, which was termed as cancer stem-like cells (CSCs) and was speculated to be the reason for cancer recurrence after chemotherapy. In this study, we used lung cancer cell lines with different TP53 backgrounds to elucidate the potential role of mutant p53 in regulating lung CSC self-renewal and on lung cancer recurrence. Cisplatin-resistant lung cancer cells with different TP53 backgrounds were generated *in vitro* by exposing A549, H460, and H661 lung cancer cell lines repeatedly to cisplatin. CD44$^+$/CD90$^+$ stem-like cells were identified in above cisplatin-resistant lung cancers (termed as cisplatin-resistant lung cancer stem-like cells, (Cr-LCSCs)) and stained with PKH26 dye which was used to define the self-renewal pattern. The proportion of symmetric divisions was significantly higher in Cr-LCSCs with mutant (mt) p53 compared with Cr-LCSCs with wild-type (wt) p53, and forced expression of mt p53 promoted the symmetric division of Cr-LCSCs. Furthermore, fewer macrophages accumulated in subcutaneously implanted xenografts consisting of mt p53 Cr-LCSCs compared with wt p53 Cr-LCSCs. These results indicated that mt p53 might accelerate the recurrence of lung cancer by regulating the self-renewal kinetics of Cr-LCSCs as well as the recruitment of macrophages.

1. Introduction

The lung is a barrier organ that is the first line of defense against various threats ranging from pathogens to carcinogens and is susceptible to cancer. Lung cancer is becoming the leading cause of cancer-related death in men and women [1]. Targeted drugs have been developed to treat lung cancer patients harboring EGFR mutations [2] or EML4-ALK amplification [3]. Immune checkpoint inhibitors (ICIs), namely, programmed death-1 (PD-1) antibodies [4], have been approved by the FDA as the first-line treatments. However, traditional cisplatin-based chemotherapy remains the first-line treatment for nonresectable lung cancer without actionable mutations or with PD-l tumor proportion scores (TPSs) that are less than 50%. A cisplatin-based chemother-

apeutic strategy has been applied in patients with advanced IIIB or IV tumors and as an adjuvant therapy in earlier stages following surgery. However, the overall 5-year survival of NSCLC is under 40% [5], which is mainly attributed to the recurrence of lung cancer after chemotherapy.

It has been proposed that a small proportion of stem-like cells, termed as cancer-initiating cells (CIS) or cancer stem-like cells (CSCs), in tumors are responsible for the initiation, progression and, most importantly, the recurrence of cancer [6]. CSCs have been implicated in the recurrence of cancers by the ability to efflux chemotherapeutic drugs through the expression of several drug efflux and DNA repair proteins that are not eliminated after chemotherapy [7]. Besides, CSCs were divided symmetrically and asymmetrically similar to their normal counterparts, and the mode of propagation

depends on the requirements of the stem cell pool reserve, tissue repair, and genetic background. Symmetrical division produces identical daughter cells that supply the stem cell pool that is required for rapid tissue repair, and asymmetric division produces one undifferentiated and one differentiated designated for reserving stem cell pool [8]. The regeneration of a tumor mass after chemotherapy may be influenced by the balance between symmetric and asymmetric cell divisions, and factors that determine this balance could result in the aberrant expansion of CSCs and recurrence of cancer.

Wild-type p53, which is translated by the tumor suppressor gene TP53, functions to prevent DNA damage. Mutant p53 leads to the dysfunction of wild-type p53. TP53 mutations have been identified in various cancer types, including lung cancer. It has been observed that mt p53 is related to a poor prognosis and the recurrence of lung cancer in resected and cisplatin-treated lung cancer [9, 10]. To understand the role of mt p53 in the recurrence of lung cancer, we investigated the involvement of mt p53 in regulating Cr-LCSC self-renewal and its interaction with the host immune system, especially macrophages of innate immunity. Thus, we aimed to accomplish the following goals: (1) isolate Cr-LCSCs from 3 lung cancer cell lines with different p53 backgrounds; (2) investigate the involvement of mt p53 in regulating the Cr-LCSC self-renewal pattern; (3) investigate the effect of mt p53 on the tumorigenicity of Cr-LCSCs; and (4) compare the density of macrophage infiltration in subcutaneously implanted wt and mt p53 Cr-LCSC xenografts. The results provided new insights and targets for the prevention of lung cancer recurrence after chemotherapy.

2. Materials and Methods

2.1. Cell Lines and Reagents. A549, H460, H661, and H1299 lung cancer cell lines were obtained from the American Type Culture Collection (ATCC) (Manassas, VA, USA) and cultured with RPMI-1640 medium (Gibco, Grand Island, NY, USA) supplemented with 10% fetal bovine serum (Hyclone, South Logan, UT, USA). Cisplatin, $4'$,6-diamidino-2-phenylindole (DAPI), and a PKH-26 Red Fluorescent Cell Linker Kit were purchased from Sigma-Aldrich Chemical Company (St. Louis, MO, USA). FITC-conjugated CD44 antibody, APC-conjugated CD90 antibody, and corresponding isotype controls were purchased from BD Biosciences (San Jose, CA, USA). Anti-human CD44, CD90, and p53 primary antibodies were purchased from Abcam (Cambridge, MA, USA). CCR2 antibody was obtained from R&D (Minneapolis, MN, USA); CD68 antibody and Lipofectamine 2000 reagent were purchased from Invitrogen (Carlsbad, CA, USA). Secondary antibodies FITC-conjugated goat anti-rabbit IgG and Cy3-conjugated goat anti-mouse IgG were purchased from Jackson ImmunoResearch (West Grove, PA, USA). pCMV-Neo-Bam p53 R249S was a gift from Bert Vogelstein (Addgene plasmid # 16438), and pCMV-Neo-Bam p53 wt (wt p53) was a gift from Bert Vogelstein (Addgene plasmid # 16434).

2.2. Generation of Cisplatin-Resistant Lung Cancer Cell Lines. A549, H460, H661, and H1299 lung cancer cells were exposed to cisplatin according to the IC50 value for 72 h. The medium was removed, and the cells were cultured in normal medium until the cells fully recovered. Every 2-3 rounds of treatment, the IC50 concentrations were reassessed for each cell line. Cisplatin-resistant lung cancer cell lines were established when stable IC50 value was reached.

2.3. Isolation of Cr-LCSCs. CD44$^+$/CD90$^+$ cells were isolated from A549/Cr, H460/Cr, H661/Cr, and H1299/Cr cells using a MoFlo XDP flow cytometer stained with FITC-conjugated CD44 antibody and APC-conjugated CD90 antibody. Cell debris and dead cells doublets were gated based on cell size and complexity.

2.4. Immunofluorescence Staining. A549/Cr, H460/Cr, and H661/Cr cells were cultured on coverslip, fixed in 4% paraformaldehyde, and then labeled with anti-human CD44 and CD90 at 4°C overnight. The samples were incubated with FITC-conjugated goat anti-rabbit IgG and Cy3-conjugated goat anti-mouse IgG (1 : 200 dilution) for 1 h at 37°C. To stain macrophages in the tumors, frozen tissues were cut into 10 μm thick sections, fixed in cold acetone for 10 min, and blocked with 10% normal goat serum. The tumor sections were incubated with a primary anti-CD68 antibody (1 : 200 dilution) overnight in a humid chamber at 4°C, then incubated with a FITC-conjugated goat anti-rabbit IgG secondary antibody for 1 h at 37°. Nuclei were counter-stained with DAPI. Images were acquired by confocal microscopy.

2.5. Immunohistochemical (IHC) Analysis. The formalin-fixed, paraffin-embedded xenograft tissues were cut into 8 μm thick sections. Slides were dewaxed, put in microwave for antigen retrieval at 95 for 30 min, and then incubated with a CCR2 antibody (1 : 200 dilution), and color was developed by the DAB method. Microscopic images were acquired by phase contrast microscopy (BX41TF, OLYMPUS, Tokyo, Japan). CellSens Standard 1.13 (OLYMPUS) software was used to capture the images.

2.6. Transfection of wt p53 and mt p53 in H1299/Cr Cells. 4 μg of DNA of the control pCMV-Neo-Bam vector, pCMV-Neo-Bam p53 R249S vectors, and pCMV-Neo-Bam p53 wt vectors was mixed with Lipofectamine 2000 reagent in Opti-MEM Medium, incubated for 5 min at room temperature, and then added to H1299/Cr cells at 70% confluent and incubated for 48 h. 300 μg/mL of G418 was used to select stably transfected clones.

2.7. PKH-26 Staining. PKH-26 is a cell membrane fluorescent dye and is divided to daughter cells. The distribution of PKH-26 in the daughter cells was tracked, and a mathematic model provided by Cicalese et al. was used to define the division patterns [11]. PKH-26 dye was diluted as indicated and incubated with PBS-washed cells for 5 min at room temperature. The staining reaction was ceased by adding 2 ml serum. The cells were washed and centrifuged to remove unbound excess dye, resuspended in serum-free DMEM medium supplemented with 20 ng/ml EGF, 20 ng/ml bFGF, and 4 μg/ml insulin. Single cells were obtained by serial dilutions in a

96-well plate, labeled, and observed under fluorescence microscopy. The images were acquired by confocal microscopy.

2.8. Sphere Formation Assay.

To assess the spheroid formation ability, Cr-LCSCs were cultured in serum-free DMEM medium supplemented with 20 ng/ml EGF, 20 ng/ml bFGF, and 4 μg/ml insulin for 3 weeks. The sphere formation ability was assessed by the time of appearance and the number and size of sphere bodies and plotted as histograms.

2.9. Tumor Xenografts in Nude Mice.

BALB/c nude mice were used to establish tumor xenografts by injection of a 200 μl cell suspension of 1×10^5 H1299/Cr-mt-p53 and H1299/Cr-wt-p53 cells subcutaneously. Tumor volumes (mm^3) were calculated every week by the following formula: (major axis) $*$ (minor axis)^2/2. At 4 weeks, the mice were sacrificed, and the tumors were removed and measured at necropsy.

2.10. Statistical Analysis.

The results were presented as the mean ± standard deviation (SD). Differences were analyzed with two-tailed unpaired Student's t-test between 2 groups or one-way ANOVA between 3 groups. $p < 0.05$ was defined statistically significant. The data were analyzed using SPSS v16.0 software (SPSS Inc., Chicago, IL, USA), and graphs were performed using GraphPad Prism software (La Jolla, CA, USA).

3. Results

3.1. Isolation of Cr-LCSCs from Cisplatin-Resistant Nonsmall Cell Lung Cancer Cell Lines.

To recapitulate the recurrence of LCSCs following chemotherapy, A549 (wt P53), H460 (wt P53), and H661 (mt P53) human lung cancer cell lines were treated with cisplatin at concentrations ranging from 0.1 μM to 100 μM to determine the IC50 for the initial treatment, as previously reported [12]. The cells were then treated with cisplatin according to the IC50 for 72 h, and the remaining cells were cultured in RPMI-1640 complete medium until full recovery (Fig. S1). After approximately 20 cell passages with the treatment, the cells began to show stable IC50 values, and cells after 20 passages were defined as cisplatin-resistant (Cr) cells and used for subsequent investigations (Fig. S2) [12].

CD44 [13] and CD90 [14] are LCSC surface markers. We analyzed the expression of CD44 and CD90 in A549/Cr, H460/Cr, and H661/Cr cells using an immunofluorescence assay. CD44 and CD90 were detected in A549/Cr, H460/Cr, and H661/Cr cells (Figure 1(a)). Since CD44$^+$/CD90$^+$ were defined as LCSCs previously [90], we detected the proportion of CD44$^+$/CD90$^+$ cells in A549/Cr, H460/Cr, and H661/Cr cells. CD44$^+$/CD90$^+$ cells were identified in A549/Cr, H460/Cr, and H661/Cr cells, indicating LCSCs were enriched with cisplatin treatment in vitro (Figure 1(b)). The above double-positive cell population was designated as cisplatin-enriched LCSCs (Cr-LCSCs). Interestingly, we found the proportion of Cr-LCSCs in mt p53 H661/Cr was significantly higher compared with those in wt p53 A549/Cr and H460/Cr (Figure 1(b) and Fig. S3).

3.2. A549/Cr-LCSCs, H460/Cr-LCSCs, and H661/Cr-LCSCs Exhibited Discrepant Self-Renewal Properties and Propagated Differently.

To further study the intrinsic difference between Cr-LCSCs from A549/Cr, H460/Cr, and H661/Cr cells, which might be regulated by p53 status, we first isolated CD44$^+$/CD90$^+$ subpopulations using flow cytometry (Figure 2(a) and Fig. S4). A total of 1×10^4 sorted A549/Cr-LCSCs, H460/Cr-LCSCs, and H661/Cr-LCSCs were cultured in 24-well nonadherent plates in serum-free medium supplemented with EGF, bFGF, and insulin. Mutant P53 H661/Cr-LCSCs formed spheres in 3 days, and wild-type P53 A549/Cr-LCSC and H460/Cr-LCSC spheres appeared after 10 days of culture (Figure 2(b)), indicating that Cr-LCSCs exhibited self-renewal characteristics in vitro. After 3 weeks, we found that the number of H661/Cr-LCSC spheres was significantly greater than that of A549/Cr-LCSC and H460/Cr-LCSC spheres that were counted under microscopy (Figure 2(c)), and the measured size of the H661/Cr-LCSC spheres was larger than that of A549/Cr-LCSC and H460/Cr-LCSC spheres (Figure 2(d)). After staining the spheres with BrdU, no significant differences were observed in the proliferation of the wt p53 H460/Cr-LCSC and mt p53 H661/Cr-LCSC spheres (Figure 2(e)). The results showed that mt p53 influences Cr-LCSC propagation through mechanisms rather than manipulating proliferation.

The number of stem cells can be regulated by the balance between symmetric and asymmetric mitotic cell divisions. To further investigate the role of mt p53 on the division pattern of Cr-LCSCs, the above-mentioned cells were investigated using PKH-26 cell staining, as described previously [11, 12]. In this study, we found that the pattern of the cell division of the A549/Cr-LCSCs was 56.3% symmetric, 27.4% asymmetric, and 16.3% undefined (could not be classified by the PKH-26 dye using a mathematical model provided by Cicalese et al.). The cell division of the H460/Cr-LCSCs was 48.2% symmetric, 31.6% asymmetric, and 20.2% undefined. The pattern of the cell division of the H661/Cr-LCSCs was 91.2% symmetric, 3.5% asymmetric, and 5.3% undefined (Figure 3). These results were consistent with a previous study showing that drug-resistant NSCLCs are mainly divided symmetrically [12]. Furthermore, this study indicated that mt p53 H661/Cr-LCSCs nearly exclusively preferred symmetric division compared with wt p53 A549/Cr-LCSCs and H460/Cr-LCSCs, providing a reasonable explanation for the slower self-renewal rate of A549/Cr-LCSCs and H460/Cr-LCSCs.

3.3. mt p53 Promoted the Symmetric Self-Renewal of Cr-LCSCs.

To further investigate the role of mt p53 on the self-renewal of Cr-LCSCs, a p53 null H1299 lung cancer cell line was treated with cisplatin to generate H1299/Cr. We transfected H1299/Cr with wt p53 and mt p53 plasmids to obtain stably transfected cell lines, named H1299/Cr-wt-p53 and H1299/Cr-mt-p53, respectively. The degree of wt p53 and mt p53 overexpression in the stable clones was verified by western blot (Figure 4(a)). Furthermore, we isolated CD44$^+$/CD90$^+$ cells from H1299/Cr-wt-p53 and H1299/Cr-mt-p53 cells and cultured in serum-free medium. We stained Cr-LCSC spheres with BrdU to exclude the difference in
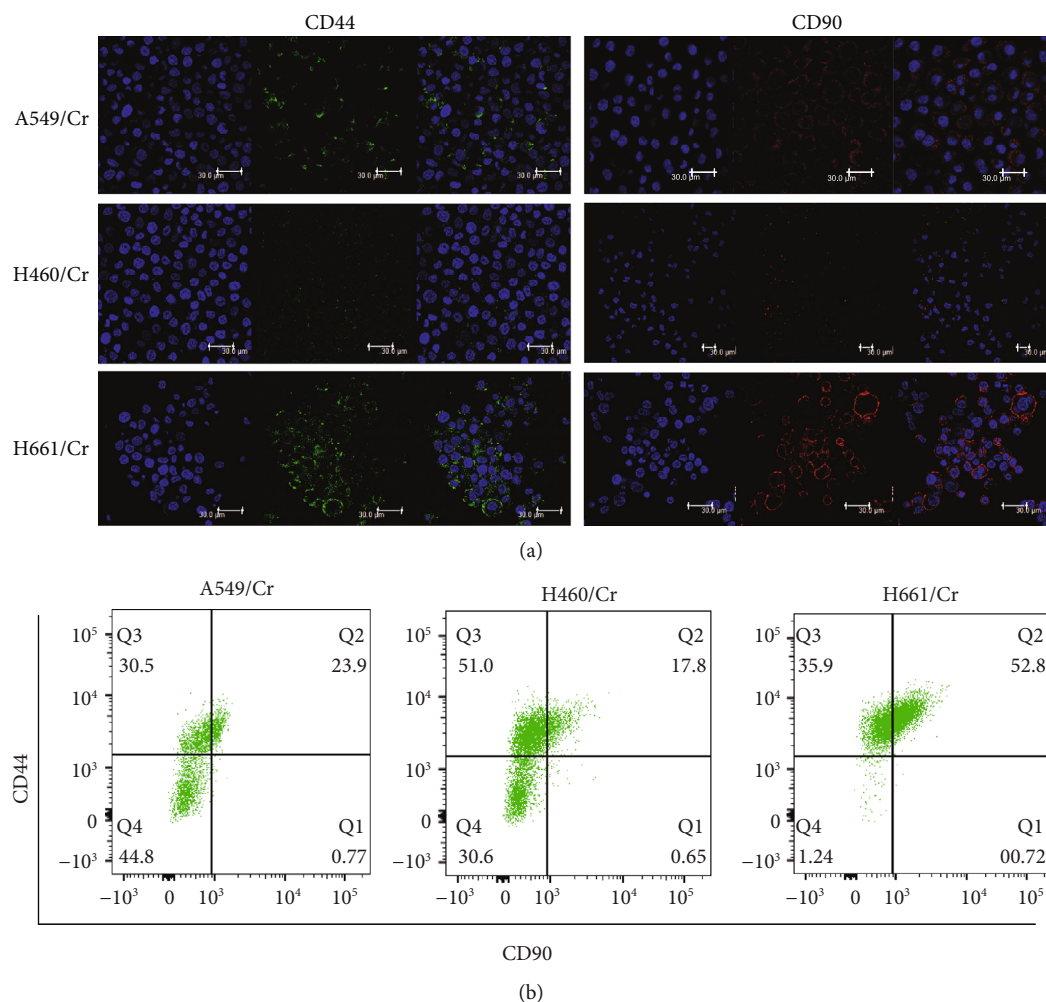
(a)

(b)

Figure 1: Increased LCSC markers in cisplatin-resistant lung cancer cell lines. (a) Immunostaining of the LCSC markers CD44 and CD90 in A549/Cr, H460/Cr, and H661/Cr cells. Scale bar = 30 μm. (b). FACS analysis of CD44$^+$/CD90$^+$ LCSCs in A549/Cr, H460/Cr, and H661/Cr cells.

proliferation; as expected, overexpression of wt p53 or mt p53 had no effect on the proliferation of Cr-LCSC spheres (Figure 4(b)). Then we studied the effect of overexpression of wt p53 or mt p53 on Cr-LCSC division with the PKH-26 staining. The division of LCSCs from H1299/Cr-wt-p53 cells was 32.4% symmetric, 56.9% asymmetric, and 10.7% undefined, and the division of LCSCs from H1299/Cr-mt-p53 cells was 86.8% symmetric, 6.3% asymmetric, and 6.9% undefined (Figure 4(c)). These results further demonstrated that mt p53 is capable of manipulating Cr-LCSC division towards a symmetric pattern.

3.4. mt p53 Cr-LCSCs Showed Increased Tumorigenicity in a Subcutaneous Xenograft Model and Suppressed the Accumulation of Macrophages. We examined the in vivo tumorigenicity of mt p53 Cr-LCSCs and wt p53 Cr-LCSCs using subcutaneous injections of CD44$^+$/CD90$^+$ cells isolated from H1299/Cr-wt-p53 and H1299/Cr-mt-p53 cells. The growth of subcutaneous tumors was monitored and measured every week until the fourth week. The growth rate of

tumors derived from H1299/Cr-mt-p53 LCSCs was markedly accelerated compared with H1299/Cr-wt-p53 LCSCs (Figure 5(a)). At the end of four weeks, 2 out of 6 mice injected with H1299/Cr-wt-p53 cells fail to develop tumors while all mice injected with H1299/Cr-mt-p53 cells developed. The volume of tumors derived from H1299/Cr-mt-p53 LCSCs was markedly larger compared with that from H1299/Cr-wt-p53 LCSCs (Figure 5(b)).

To further explore the increased tumorigenicity of mt p53 Cr-LCSCs in terms of the host immune defense, we focused on the macrophages of the host immune system because athymic nude mice are not suitable for the investigation of acquired immunity. Xenografts from H1299/Cr-wt-p53 and H1299/Cr-mt-p53 LCSCs were stained with a CD68 macrophage marker, and a decrease in CD68$^+$ macrophages was observed in H1299/Cr-mt-p53 xenografts compared with H1299/Cr-wt-p53 xenografts (Figure 5(c)). CCR2 has been proposed to accumulate macrophages at the tumor site, and we investigated the expression of CCR2 in H1299/Cr-wt-p53 and H1299/Cr-mt-p53 LCSC xenografts.
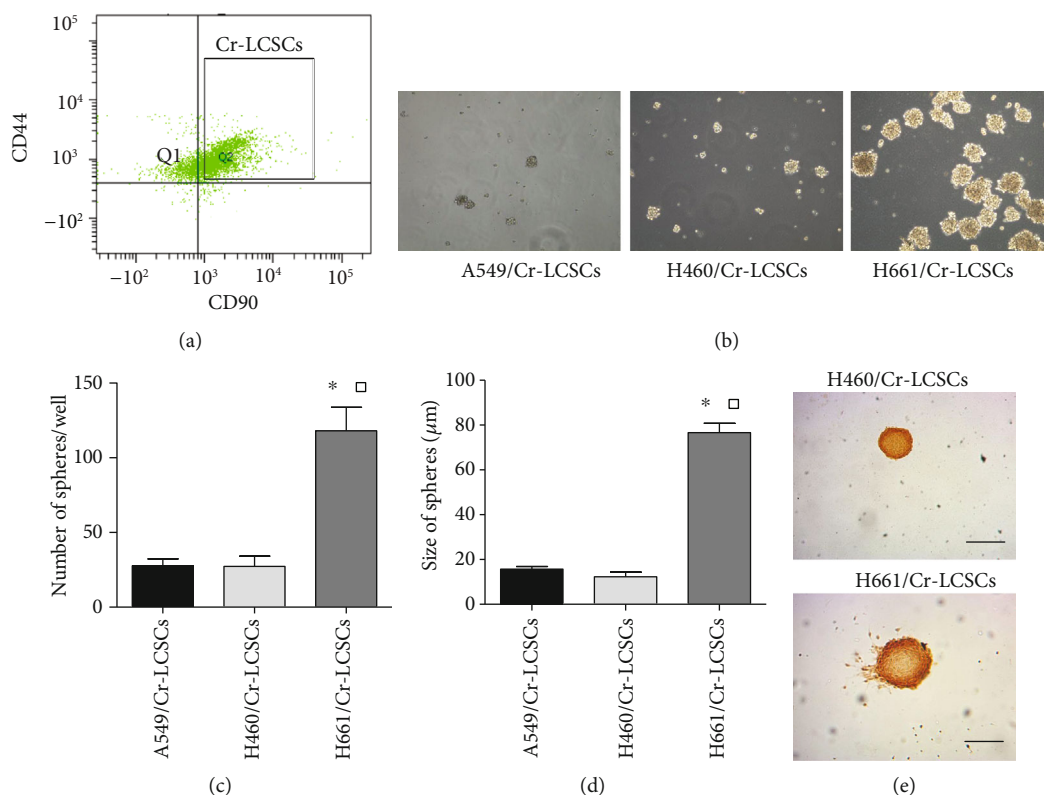
(a)

(b)

(c)

(d)

(e)

Figure 2: The isolation and continuous culture of Cr-LCSCs obtained from A549/Cr, H460/Cr, and H661/Cr cells. (a) Representative FACS plots demonstrating the isolation of CD44$^+$/CD90$^+$ LCSCs from A549/Cr, H460/Cr, and H661/Cr cells. (b) Bright field images of spheres generated from clonal density cultures of A549/Cr-LCSCs, H460/Cr-LCSCs, and H661/Cr-LCSCs collected 21 days after the start of the suspension cultures (100x magnification). (c) The number of A549/Cr-LCSC, H460/Cr-LCSC, and H661/Cr-LCSC spheres in 100 μl samples. The data are presented as the mean ± SD for triplicate counts. $^*p < 0.05$ compared with A549/Cr-LCSCs and $^\square p < 0.05$ compared with H460/Cr-LCSCs. (d) The sizes (μm) of the A549/Cr-LCSC, H460/Cr-LCSC, and H661/Cr-LCSC spheres. $^*p < 0.05$ compared with A549/Cr-LCSCs and $^\square p < 0.05$ compared with H460/Cr-LCSCs. (e) H460/Cr-LCSCs and H661/Cr-LCSCs were labeled with BrdU and identified with an anti-BrdU antibody. Scale bar = 50 μm.

We found that CCR2 expression was downregulated in H1299/Cr-mt-p53 LCSC xenografts compared with that in H1299/Cr-wt-p53 LCSC xenografts (Figure 5(d)).

4. Discussion

Platinum-based doublet chemotherapy is the standard first-line therapy for patients with NSCLC without actionable "driver genes" or a PD-L1 TPS < 50%. 20-40% of patents tend to relapse within 6 months, although with initial response to platinum-based doublet chemotherapy in lung cancer [15]. Many previous studies have proposed that this may be due to the existence of a chemotherapy-resistant phenotype with stem cell-like traits during chemotherapy treatment. Evidence has indicated that LCSCs are responsible for lung cancer recurrence because cytotoxic reagents eliminate the bulk of differentiated tumor cells, while LCSCs survive and continue to proliferate [12]. Theoretically, similar to its normal adult stem cell counterpart, LCSCs are predicted to remain quiescent and should have a slower growth rate than differentiated tumor cells. However, evidence has shown that the environment, signaling pathways, and epigenetic changes maintain the balance between the differentiation and quiescence of LCSCs. We proposed that LCSCs

might be activated during chemotherapeutic treatment and must quickly respond to expand and regenerate a damaged tumor mass. Using the method reported by Barr [16], we enriched drug-resistant lung cancer cells with stem cell properties after ~20 passages using cisplatin in three lung cancer cell lines that were designated as A549/Cr, H460/Cr, and H661/Cr cells. CD44 and CD90 have been reported to be markers of LCSCs, and CD44$^+$/CD90$^+$ LCSCs were isolated from A549/Cr, H460/Cr, and H661/Cr cells. In this study, we investigated the self-renewal, tumorigenicity, and immunogenicity of Cr-LCSCs and the regulatory factors.

During tissue repair, symmetric division is adopted by stem cells to generate more progeny for a quick response to expand and replace damaged cells. The tumor mass can be considered an abnormal organ in which CSCs might respond to damage, such as damage from chemotherapy and radiotherapy, that disrupts the normal balance between asymmetric division and symmetric division. Whether Cr-LCSCs adopt symmetric division or symmetric division under chemotherapy is unknown. In this study, to determine the self-renewal mode of isolated Cr-LCSCs, we used PKH-26 to label progeny of Cr-LCSCs. For symmetric division, PKH-26 is distributed equally to two daughter cells that are destined to have the same fate of either differentiation or maintained
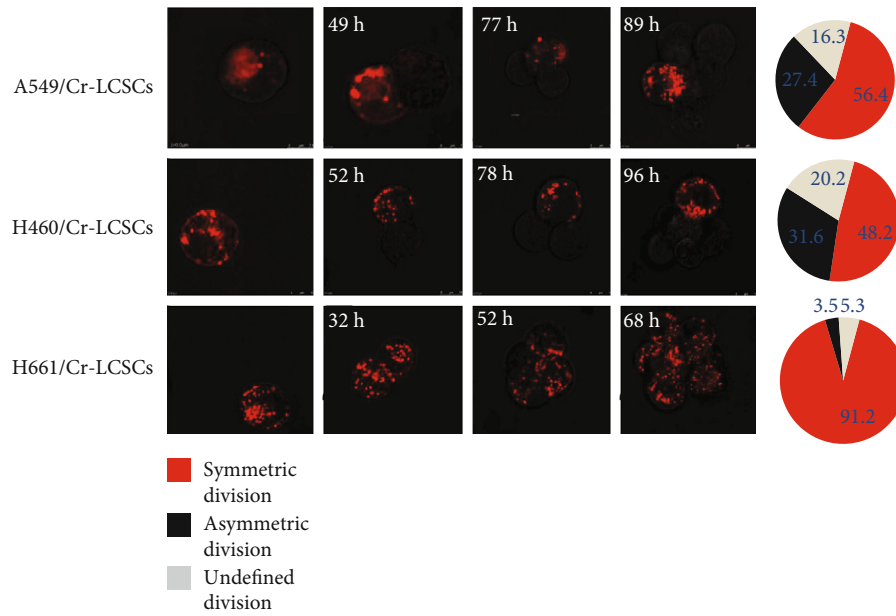
FIGURE 3: Fluorescence microscopy for the analysis of A549/Cr-LCSC, H460/Cr-LCSC, and H661/Cr-LCSC divisions following cell seeding. The accompanying pie charts indicate the relative frequencies of asymmetric and symmetric cell divisions. Undefined divisions are division patterns that could not be determined due to the loss of images during culture or an indistinct cell number following division.
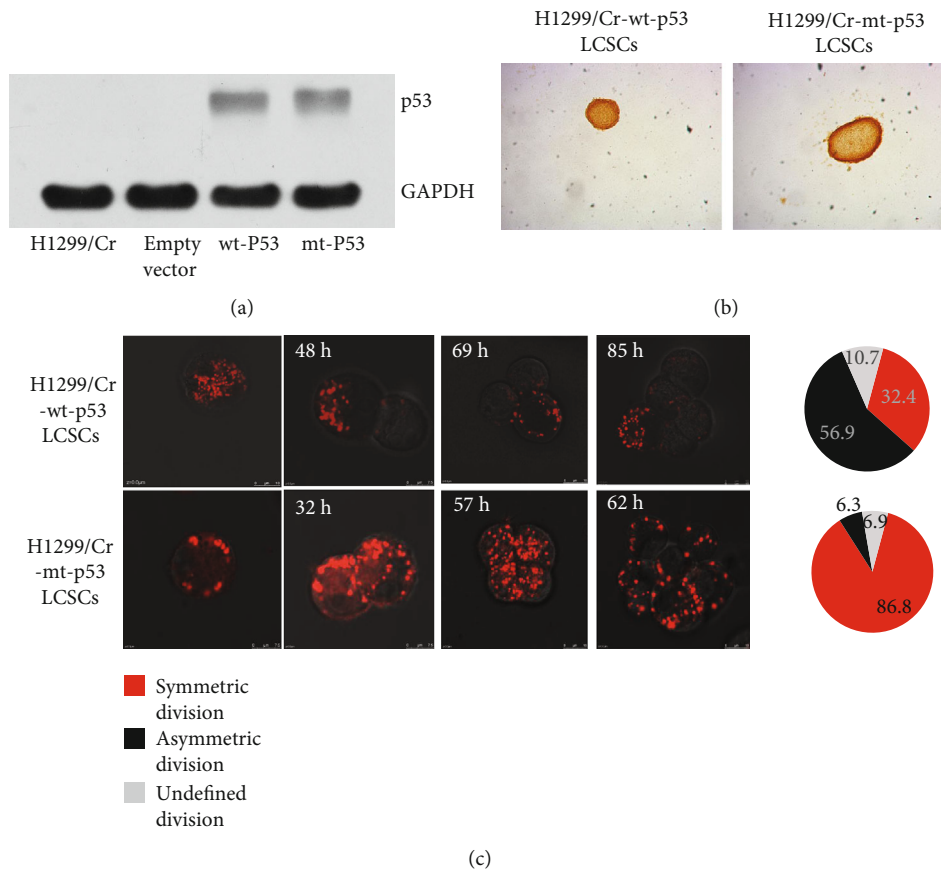
FIGURE 4: mt p53 promotes the symmetric cell division of cisplatin-resistant stem cell-like NSCLC cells. (a) Forced expression of wt p53 and mt p53 in p53 null H1299/CisR cells. Western blot analysis of lysates from H1299/Cr, H1299/Cr-wt-p53, and H1299/Cr-mt-p53 cells using an anti-p53 antibody. GAPDH was used as an internal control. (b, c) Fluorescence microscopy for the analysis of the division of CD44^{+}/CD90^{+} LCSCs isolated from H1299/Cr-wt-p53 and H1299/Cr-mt-p53 cells following cell seeding.

(a)

(b)

(c)

(d)
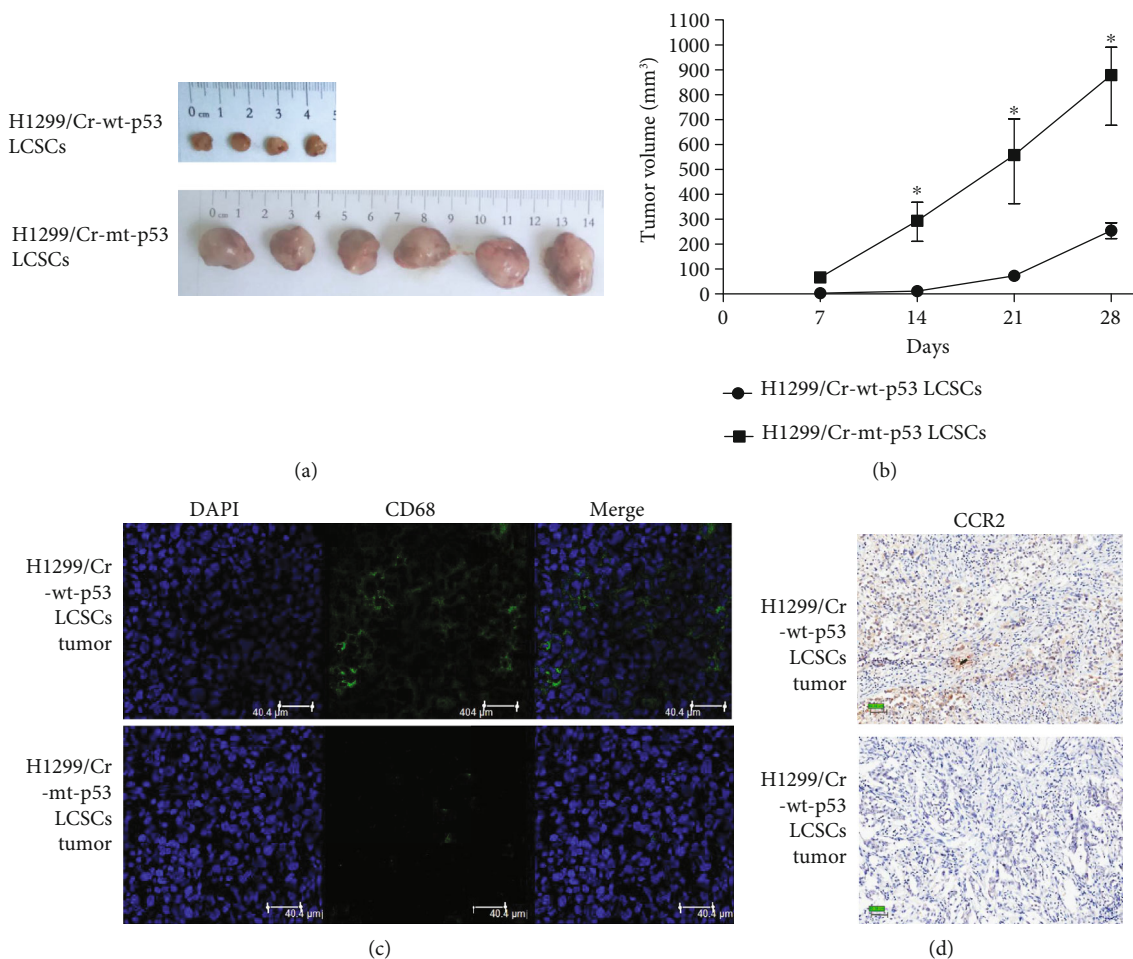
FIGURE 5: mt P53 promoted Cr-LCSC xenograft progression in nude mice and prevented the accumulation of macrophages at the tumor site. (a) The appearance of subcutaneous tumors in H1299/Cr-mt-p53 LCSC and H1299/Cr-wt-p53 LCSC xenografts. Four out of 6 mice formed subcutaneous tumors after the injection of H1299/Cr-wt-p53 LCSCs, while 6 out of 6 mice formed subcutaneous tumors after the injection of H1299/Cr-mt-p53 LCSCs. (b) Tumor volume growth curves of tumors developed in the xenograft models injected with H1299/Cr-mt-p53 and H1299/Cr-wt-p53 LCSCs. (c) Immunofluorescence staining showing the accumulation of CD68^{+} macrophages in H1299/Cr-wt-p53 LCSC xenografts and the scant accumulation of macrophages in H1299/Cr-mt-p53 LCSC xenografts. Scale bar = 40 μm. (d) IHC staining showed decreased CCR2 expression levels in H1299/Cr-mt-p53 LCSC xenografts. Scale bar = 50 μm.

stemness. Asymmetric division results in the retention of the PKH-26 dye in daughter stem cells, which are relatively more quiescent compared with differentiated progeny. The results showed that the majority of Cr-LCSCs isolated from lung cancer cell lines underwent symmetric division, indicating that exposure to chemotherapy in vitro promotes the symmetric self-renewal of LCSCs. The in vivo impact of chemotherapy on CSC self-renewal has also been reported in patients with breast cancer who received neoadjuvant chemotherapy because the self-renewal potential to form mammospheres was enhanced after neoadjuvant chemotherapy [17].

TP53 is a tumor suppressor gene that determines the cell fate of stressed or damaged cells by inducing reversible cell cycle arrest, DNA repair, or apoptosis [18]. TP53 gene mutations are frequent in NSCLC, and the mutations result in incorrect protein synthesis or alterations in the DNA-binding domain that impairs the tumor suppressor function of p53 [19]. Clinical data describing mutant p53 determining the prognosis of patients with NSCLC have been widely

reported [20, 21]. In stage I NSCLC, the risk of death increased in patients with tumor p53 mutations compared with tumor p53 wt [22]. p53 null mutation also leads to a poor outcome in patients with early-stage NSCLCs [23]. The tendency of a better prognosis in NSCLCs patients with wt p53 was presumed to be associated with the tumor suppressor activities of wt p53, while tumors with mt p53 escaped DNA damage-dependent cell senescence and apoptosis induced by chemotherapy or radiotherapy. Recently, p53 was reported to regulate the self-renewal mode of stem cells [11]. The effect of mt p53 on the self-renewal of Cr-LCSCs has not been investigated. In this study, we reported that mt p53 promotes the symmetric cell division of Cr-LCSCs, leading to the possibility of the accumulation of a stem cell pool in mt p53 NSCLC tumor masses following cisplatin treatment.

To further elucidate the possible role of mt p53 on the recurrence of lung cancer, we compared the tumorigenicity of mt p53 Cr-LCSCs and that of wt p53 Cr-LCSCs in vivo.

The mt p53 Cr-LCSCs are more tumorigenic compared with wt P53 Cr-LCSCs and have an increased tumor growth rate and end-point tumor mass. Mononuclear phagocytes are present in the lung from the earliest stages of lung development until death and are the most important innate immune system components in the lung that defend against cancer. The infiltration of leukocyte (including macrophages) in tumor was thought to be the result of an immune reaction to the tumor itself, specifically, the first innate immunity and later specific immunity to recognize tumor-associated antigens [24]. CD68^{+} macrophage infiltration in esophageal cancer is associated with better prognosis [25]. However, tumor-associated macrophages are recently thought to promote tumor initiation, growth, and development [26]. The role of tumor-associated macrophage in cancer is still controversial [27]. In this study, we explored the accumulation of macrophages in mt p53 Cr-LCSC and wt p53 Cr-LCSC xenografts. We found that mt p53 inhibited the accumulation of macrophages in xenografts with decreased CCR2 expression levels. It has been reported that p53 is a suppressor of inflammatory response in mice by repressed expression of inflammatory chemokine receptor CCR2 [28]. Whether mt p53 has a stronger repression effect on CCR2 needs further investigation. CCR2 is the most important chemokine receptor in the recruitment of macrophages in cancer; genetic deletion of CCR2 results in less infiltration of macrophages in mouse xenografts [29]. Our results showed that mt p53 inhibited CCR2 and resulted in decreased macrophages in xenografts and revealed a potential cross-talk between cancer cells and macrophage recruitment modulated by p53 somatic mutation in cancer.

Overall, this study suggested the possibility that current anticancer chemotherapy fail to eradicate resistant LCSC clones with symmetric cell division pattern may be associated with poor responses and lung cancer recurrence. mt p53 activation further increased Cr-LCSC expansion by promoting symmetric self-renewal division and inhibiting the accumulation of macrophages, resulting in increased tumorigenicity.

Data Availability

Supplementary data was available.

Conflicts of Interest

The authors declare that there is no conflict of interest.

Acknowledgments

Supplementary Materials

Fig. S1: the morphology of A549/CisR, H460/CisR, and H661/CisR cells. Fig. S2: the IC50 for cisplatin treatment in vitro. Fig. S3: the proportion of CD44^{+}/CD90^{+} cells in A549/CisR, H460/CisR, and H661/CisR cells. Fig. S4: FACS gating strategy of Cr-LCSCs. Fig. S5: flow cytometry analysis of CD44^{+}/CD90^{+} cells in 3rd-generation SB (sphere body) of A549/CisR (CD44^{+}/CD90^{+}), H460/CisR (CD44^{+}/CD90^{+}), H661/CisR (CD44^{+}/CD90^{+}), and H1299/CisR (CD44^{+}/CD90^{+}) cells. Data are presented as the mean $\pm$ SD for triplicate counts. *$p < 0.05$, compared with A549/CisR (CD44^{+}/CD90^{+}); □$p < 0.05$, compared with H460/CisR (CD44^{+}/CD90^{+}); △compared with H661/CisR (CD44^{+}/CD90^{+}); ◇compared with H1299/CisR (CD44^{+}/CD90^{+}). (Supplementary Materials)

References

[1] P. M. de Groot, C. C. Wu, B. W. Carter, and R. F. Munden, "The epidemiology of lung cancer," *Translational Lung Cancer Research*, vol. 7, no. 3, pp. 220–233, 2018.

[2] T. S. Mok, Y. L. Wu, S. Thongprasert et al., "Gefitinib or carboplatin–paclitaxel in pulmonary adenocarcinoma," *The New England Journal of Medicine*, vol. 361, no. 10, pp. 947–957, 2009.

[3] T. Uemura and T. Hida, "Alectinib can replace crizotinib as standard first-line therapy for *ALK*-positive lung cancer," *Annals of Translational Medicine*, vol. 5, no. 21, p. 433, 2017.

[4] R. Kumar, D. Collins, S. Dolly, F. McDonald, M. E. R. O'Brien, and T. A. Yap, "Targeting the PD-1/PD-L1 axis in non–small cell lung cancer," *Current Problems in Cancer*, vol. 41, no. 2, pp. 111–124, 2017.

[5] R. L. Siegel, K. D. Miller, and A. Jemal, "Cancer statistics, 2018," *CA: A Cancer Journal for Clinicians*, vol. 68, no. 1, pp. 7–30, 2018.

[6] J. C. Chang, "Cancer stem cells: role in tumor growth, recurrence, metastasis, and treatment resistance," *Medicine*, vol. 95, Supplement 1, pp. S20–S25, 2016.

[7] M. Dean, T. Fojo, and S. Bates, "Tumour stem cells and drug resistance," *Nature Reviews Cancer*, vol. 5, no. 4, pp. 275–284, 2005.

[8] S. J. Morrison and J. Kimble, "Asymmetric and symmetric stem-cell divisions in development and cancer," *Nature*, vol. 441, no. 7097, pp. 1068–1074, 2006.

[9] D. H. Harpole Jr., J. E. Herndon 2nd, W. G. Wolfe, J. D. Iglehart, and J. R. Marks, "A prognostic model of recurrence and death in stage I non-small cell lung cancer utilizing presentation, histopathology, and oncoprotein expression," *Cancer Research*, vol. 55, no. 1, pp. 51–56, 1995.

[10] C. Scoccianti, A. Vesin, G. Martel et al., "Prognostic value of *TP53*, *KRAS* and *EGFR* mutations in nonsmall cell lung cancer: the EUELC cohort," *European Respiratory Journal*, vol. 40, no. 1, pp. 177–184, 2012.

[11] A. Cicalese, G. Bonizzi, C. E. Pasi et al., "The Tumor Suppressor *p53* Regulates Polarity of Self-Renewing Divisions in Mammary Stem Cells," *Cell*, vol. 138, no. 6, pp. 1083–1095, 2009.

[12] Y. Tang, J. Hou, G. Li et al., "ABCG2 regulates the pattern of self-renewing divisions in cisplatin-resistant non-small cell lung cancer cell lines," *Oncology Reports*, vol. 32, no. 5, pp. 2168–2174, 2014.

[13] P. Wang, Q. Gao, Z. Suo et al., "Identification and characterization of cells with cancer stem cell properties in human primary lung cancer cell lines," *PLoS One*, vol. 8, no. 3, article e57020, 2013.

[14] X. Yan, H. Luo, X. Zhou, B. Zhu, Y. Wang, and X. Bian, "Identification of CD90 as a marker for lung cancer stem cells in A549 and H446 cell lines," *Oncology Reports*, vol. 30, no. 6, pp. 2733–2740, 2013.

[15] G. Leon, L. MacDonagh, S. P. Finn, S. Cuffe, and M. P. Barr, "Cancer stem cells in drug resistant lung cancer: targeting cell surface markers and signaling pathways," *Pharmacology & Therapeutics*, vol. 158, pp. 71–90, 2016.

[16] M. P. Barr, S. G. Gray, A. C. Hoffmann et al., "Generation and characterisation of cisplatin-resistant non-small cell lung cancer cell lines displaying a stem-like signature," *PLoS One*, vol. 8, no. 1, article e54193, 2013.

[17] F. Yu, H. Yao, P. Zhu et al., "*let-7* Regulates Self Renewal and Tumorigenicity of Breast Cancer Cells," *Cell*, vol. 131, no. 6, pp. 1109–1123, 2007.

[18] C. Gebitekin, A. S. Bayram, B. Tunca, and S. A. Balaban, "Clinical significance of p53 gene mutation in T1-2N0 non-small cell lung cancer," *Asian Cardiovascular and Thoracic Annals*, vol. 15, no. 1, pp. 35–38, 2007.

[19] M. B. Olszewski, M. Pruszko, E. Snaar-Jagalska, A. Zylicz, and M. Zylicz, "Diverse and cancer type-specific roles of the p53 R248Q gain-of-function mutation in cancer migration and invasiveness," *International Journal of Oncology*, vol. 54, no. 4, pp. 1168–1182, 2019.

[20] W. Y. Zhu, X. F. Hu, K. X. Fang et al., "Prognostic value of mutant p53, Ki-67, and TTF-1 and their correlation with EGFR mutation in patients with non-small cell lung cancer," *Histology and Histopathology*, no. article 18124, 2019.

[21] Y. Zhao, F. S. Varn, G. Cai, F. Xiao, C. I. Amos, and C. Cheng, "A P53-deficiency gene signature predicts recurrence risk of patients with early-stage lung adenocarcinoma," *Cancer Epidemiology, Biomarkers & Prevention*, vol. 27, no. 1, pp. 86–95, 2018.

[22] S. A. Ahrendt, Y. Hu, M. Buta et al., "p53 mutations and survival in stage I non-small-cell lung cancer: results of a prospective study," *Journal of the National Cancer Institute*, vol. 95, no. 13, pp. 961–970, 2003.

[23] T. Hashimoto, Y. Tokuchi, M. Hayashi et al., "*p53* null mutations undetected by immunohistochemical staining predict a poor outcome with early-stage non-small cell lung carcinomas," *Cancer Research*, vol. 59, no. 21, pp. 5572–5577, 1999.

[24] A. Mantovani, P. Allavena, A. Sica, and F. Balkwill, "Cancer-related inflammation," *Nature*, vol. 454, no. 7203, pp. 436–444, 2008.

[25] J. Li, Y. Xie, X. Wang et al., "Prognostic impact of tumor-associated macrophage infiltration in esophageal cancer: a meta-analysis," *Future Oncology*, vol. 15, no. 19, pp. 2303–2317, 2019.

[26] Y. Komohara, Y. Fujiwara, K. Ohnishi, and M. Takeya, "Tumor-associated macrophages: potential therapeutic targets for anti-cancer therapy," *Advanced Drug Delivery Reviews*, vol. 99, Part B, pp. 180–185, 2016.

[27] C. Brigati, D. M. Noonan, A. Albini, and R. Benelli, "Tumors and inflammatory infiltrates: friends or foes?," *Clinical & experimental metastasis*, vol. 19, no. 3, pp. 247–258, 2002.

[28] E. A. Komarova, V. Krivokrysenko, K. Wang et al., "p53 is a suppressor of inflammatory response in mice," *The FASEB Journal*, vol. 19, no. 8, pp. 1030–1032, 2005.

[29] R. A. Franklin, W. Liao, A. Sarkar et al., "The cellular and molecular origin of tumor-associated macrophages," *Science*, vol. 344, no. 6186, pp. 921–925, 2014.

Review Article

Effects of Anesthetics on Barrier Tissue Function

Fujing Wang [ID],[1] Yanhui Li,[1] Changlei Cui,[1] Zhaoping Xue,[2] and Haichun Ma [ID][1]

[1]*Department of Anesthesia, The First Hospital of Jilin University, No. 71 Xinmin Street, Changchun, Jilin Province 130021, China*
[2]*Postanesthesia Care Unit, The First Hospital of Jilin University, No. 71 Xinmin Street, Changchun, Jilin Province 130021, China*

Correspondence should be addressed to Haichun Ma; mahaichun2003@163.com

Anesthetics have long been proven to have additional effects other than anesthesia on different organs and tissues of the human body. Barrier tissues play critical roles in human health and diseases, yet the impacts of anesthetics on barrier tissues are still not clear. This review article is aimed at summarizing different effects of anesthetics on the skin, the respiratory, and intestinal membranes from two aspects: inflammation/immunity and ischemia-reperfusion. Among volatile, intravenous, and local anesthetics, volatile anesthetics are less influential on barrier ischemia-perfusion function. Although direct comparisons between volatile and the other two types of anesthetics are still lacking, volatile anesthetics appear to have stronger anti-inflammatory effects on different barrier tissues through various mechanisms. These results suggested that when treating patients with barrier tissue complications, volatile anesthetics can provide better therapeutic outcomes.

1. Introduction

Barrier tissues, as the first line of the protection system in living organisms, are constantly exposed to harmful components. The respiratory and intestinal mucous membranes and the skin defend the body against various biological, chemical, and physical insults. This protection function appears to be more vital with critically ill patients. Therefore, clarifying the effects of different anesthetics on barrier tissues during the induction and maintenance of anesthesia becomes critical when surgical operations are necessary. This article is aimed at summarizing and classifying the effects on barrier tissues of agents commonly used during anesthesia. It will help us to choose appropriate anesthetics depending on the complications of the patient without doing unnecessary damage to the barrier tissues.

2. Volatile Anesthetics

Volatile anesthetics refer to agents that come into effect through inhalation, including nitrous oxide and a series of fluorinated liquids (such as sevoflurane, desflurane, isoflurane), the latter needs a specific vaporizer to transform the

liquids into gases, and further lead to unconsciousness and muscle relaxant. Across all types of anesthetics, volatile anesthetics seem to be more effective at protecting both myocardial and respiratory cells [1]. According to Gargiulo et al., isoflurane has only a minor influence on the murine hemodynamic status [2], indicating that use of volatile anesthetics does not obviously reduce the blood flow in tissues. This ensures the tissues away from ischemia-reperfusion damage, which may lead to a cascade reaction including microthrombus, histohypoxia, and finally, cell damage or even cell death. Moreover, by modulating pulmonary epithelial cell secretion [3], volatile anesthetics help decrease the production and expression of inflammatory mediators including cytokine-induced neutrophil chemoattractant- (CINC-) 1 and monocyte chemoattractant protein- (MCP-) 1. Noticeably, by decreasing the expression of intercellular adhesion molecule- (ICAM-) 1 protein, which is an important mediator within the inflammatory cascade, volatile anesthetics help to avoid the adhesion of neutrophils by 71% and reduce the death rate of alveolar epithelial cells up to 26% [4]. Although the process is not clarified, it has been established that volatile anesthetics such as sevoflurane and isoflurane can reduce the neutrophil accumulation on alveolar epithelial cells and assist

the attenuation of endotoxin-induced injury mediated by multiple cytokines and chemokines. Therefore, these agents can be a supporting therapy for patients with respiratory disease as both preconditioning and postconditioning.

As widely shown, volatile anesthetics are ideal for pediatric patients, due to its painless induction and fast metabolism. When using volatile anesthetics on infants, especially those with respiratory distress syndrome, special care is required because their pulmonary surfactant is not fully developed or already damaged. Paugam-Burtz et al.'s research has found that in mechanically ventilated in vivo rat models, volatile anesthetics may reduce the synthetize of pulmonary surfactant by affecting the content of lung SP-C mRNA [5]. This indicates that when anesthetizing infants with respiratory disease, intravenous anesthesia or intravenous inhaled balanced anesthesia may have less influence on respiratory function than inhaled anesthesia alone. In short, additional consideration is necessary when dealing with pediatric patients in regard to respiratory function.

Nitrous oxide, which was widely used as an anesthetic in humans decades ago, is well accepted for its short-acting analgesic properties. Studies have shown that through the depression of receptor-dependent generation of H_2O_2, nitrous oxide also has anti-inflammatory effects on cells by attenuating the normal functions of neutrophil and interfering the leukocyte adhesion-activation cascade [6, 7]. Regardless, when combining these components together (such as sevoflurane and nitrous oxide), the anti-inflammatory effects of sevoflurane and nitrous oxide are both eliminated, and the combination even induces the inflammatory response or suppresses the normal anti-inflammatory response [8].

Few researches have investigated the protective influence of volatile anesthetic agents on intestinal membrane. According to Liu et al., clinical relevant concentrations of sevoflurane have the ability to protect the intestinal mucous by attenuating the damage derived from intestinal ischemia-reperfusion injury [9]. Although the results on concentrations of volatile anesthetics may vary slightly due to different conditioning time points, we do know that ischemia on the intestinal mucous may lead to severe damage such as inflammation, dramatic hypotension, enterobrosis, or more seriously, intestinal perforation. Therefore, the potential to reverse the damage caused by ischemia-reperfusion in the alimentary canal endorses volatile anesthetics as an important therapy for patients suffering from digestive disorders.

3. Intravenous Anesthetics

Some anesthetics can be used intravenously, entering the blood circulation system to produce unconsciousness, sedation, analgesia, and muscle relaxant. Compared to volatile anesthetics, intravenous anesthetics lead to an obvious reduction in blood pressure postinjection, especially during the induction period requiring injection of more than two kinds of agents simultaneously. This is a common phenomenon among intravenous anesthetic agents, although they differ in the degree of hypotension they may cause. This is mainly due to the vasodilation effect, which increases the peripheral vascular volume. If the decrease in blood pressure

is not managed or is excessive in duration, it can lower tissue oxygenation and culminate in ischemia. As performed by Abramovic et al., the pressure of oxygen (pO_2) in the skin is much lower when using ketamine and xylazine to provide intravenous general anesthesia in vivo in rats, compared to the group using isoflurane for inhaled general anesthesia [10]. Noticeably, when hypotension develops during intravenous general anesthesia, ischemia occurs not only in the skin but also in all body tissues. This may be avoided by monitoring or observing the patient and using vasoactive agents if necessary. In addition, caution should be used when administering intravenous general anesthesia agents to patients with skin ischemic necrosis or other dermatosis.

Burn patients, unlike other dermatosis patients, usually have multiple organ dysfunctions as well as skin damage and inflammation simultaneously. Even though this group requires repeated surgeries under general anesthesia or local anesthesia, and the agents may have diverse effects on skin function, these reactions appear to be minor compared to therapies used for other treatment purposes. Similarly, most selective surgery inpatient or day surgery patients have adequate gastrointestinal preparation before the operation, which inhibits most inflammatory and immune events and thus prevents the effects of anesthetic agents as long as the gastrointestinal tract has sufficient blood supply. In the event the patient develops intestinal complications, in most instances, the complication itself induces inflammatory or immune responses greater than those caused by anesthetics. As these anesthetics tend to have minor side effects, there are very few papers on this subject. We deduced from the inflammatory and immune protective characters of anesthetics that they may have positive impacts on intestinal mucous and skin, but this hypothesis requires additional support from further research.

The alveolar type II pneumocyte cell synthesizes and restores the pulmonary surfactant, proliferates, and differentiates into type I pneumocyte cells [11], and is thereby the most significant cell type in the recovery from respiratory diseases such as acute lung injury. Agents that might weaken the function of the alveolar type II pneumocyte cell may, in effect, obstruct the normal function of respiratory membrane. In the experiment performed by Nishina et al., they tested different anesthesia agents' impacts on keratinocyte growth factors and hepatocyte growth factors; both have been shown to be the most potent mitogen for type II epithelial cells [11]. Those medications included midazolam, ketamine, thiopental, propofol, and lidocaine. As a result, they found that none of these agents in clinical relevant concentration had any influence on the proliferation of type II epithelial cells [12]. This suggests that most commonly used intravascular anesthesia agents do not impair the normal function of lung epithelial cells.

On the contrary, intravenous anesthetics showed a striking attenuation of the inflammatory response to protect the respiratory membrane. The disturbance of invasive surgical procedures like esophagectomy may have a drastically different result compared to minor operations such as lung resection, since big trauma incurs a more powerful inflammatory response at the airway and thus makes the moderating effect
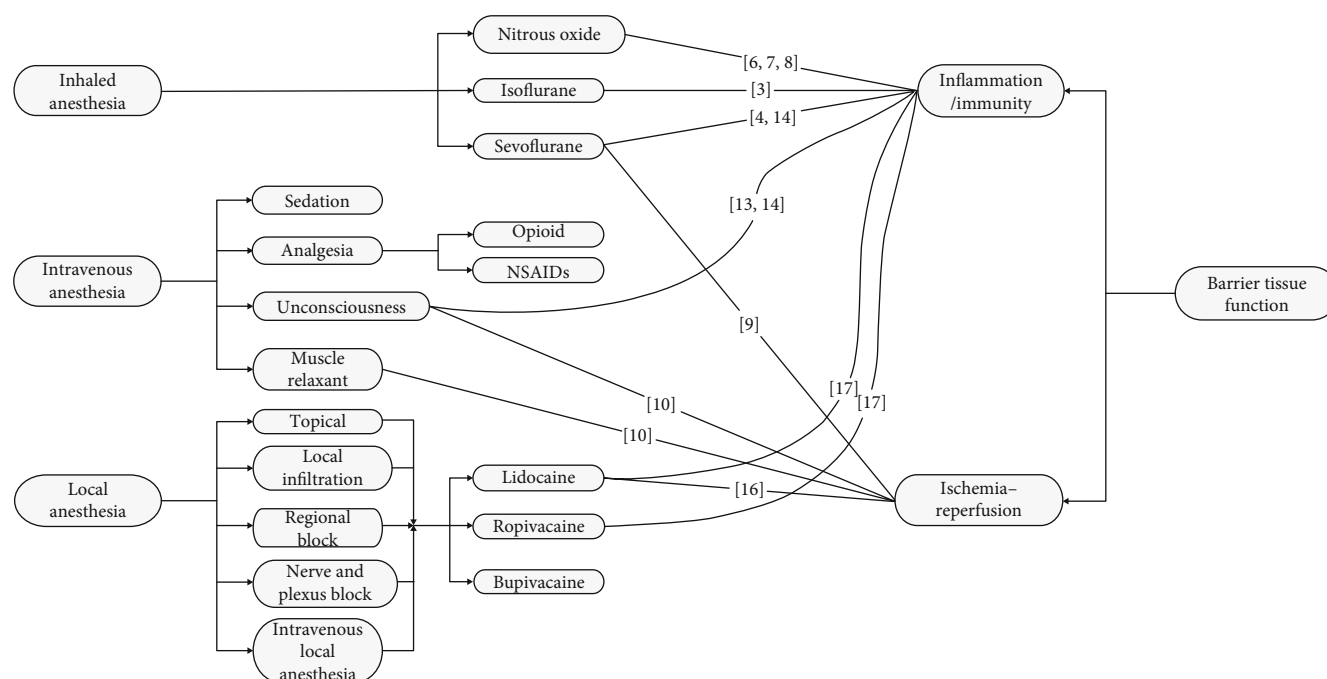
FIGURE 1: Major division and representative drug—function diagram. The main methods of anesthesia, the major classification of each, and the representative agents mentioned in the references were listed. The functions on barrier tissue of agents were classified, and the numbers refer to the references.

of anesthetic agents more apparent. According to the research of Wakabayashi et al., the inflammatory changes of the respiratory epithelial lining fluid (ELF) are more sensitive than those in the sera in esophagectomy. Within the ELF, the levels of inflammatory cytokines and chemokine including tumor necrosis factor- (TNF-) α, interleukin- (IL-) 1β, IL-6, IL-8, IL-10, and IL-12p70 were measured. TNF-α, IL-1β, and IL-6 serve as proinflammatory molecules while IL-8 serves as chemoattractant, and the IL-10 inhibits the production of proinflammatory cytokines and the normal antigen-presenting function. During the procedure, propofol showed a more potent suppression of the surgical stress-induced inflammatory perturbation in the ELF of the airway than sevoflurane, as the level of IL-6 and IL-8 in the propofol group was significantly lower than sevoflurane group, and the level of IL-10 on the contrary experienced an increase [13]. This may be the result of the esophagectomy, which is one of the most invasive operations in gastrointestinal surgeries. In another observation [14], elective lung resection was performed instead of esophagectomy when the anti-inflammatory effects of sevoflurane and propofol were observed. The result is quite different that sevoflurane showed a more pronounced anti-inflammatory effect and significantly suppressed the inflammatory response than propofol did. Thus, we can deduct that the inflammatory response caused by invasive surgeries can hardly be eliminated by anesthetics, especially when one-lung ventilation (OLV) is needed. The intrathoracic pressure changes (in both thoracoscope and open-chest procedure) and constricts the ventilated lung volume, in turn reducing the absorption and metabolism of volatile agents. Conversely, intravascular agents are not negatively

impacted by the decreased lung volume and maintain a stable concentration.

However, though propofol showed a significant protective effect on normal cells, it is widely accepted that the concentration of propofol under any clinical circumstance should be within 5 mg/kg/h. The overdose and prolonged use of propofol may also lead to the cell death of microvascular and arterial endothelial cells, due to the activation of cathepsin D and glycogen synthase kinase- (GSK-) 3 [15], thereby impairing the normal blood supply of epithelial cell, resulting in the dysfunction of respiratory epithelium.

4. Local Anesthetic

Compared to intravenous and inhaled anesthetics, local anesthetics rarely enter into the blood flow and instead affect local tissues. They block the transmission of nerve impulses without causing changes in status of consciousness. Local anesthesia includes five main types: topical anesthesia, local infiltration anesthesia, nerve and plexus block, regional block, and intravenous local anesthesia; the first two kinds may impact the barrier tissue.

In the experiment performed by Ji et al., compared to topical anesthesia, subcutaneous infiltration anesthesia showed a wider range of tissue effects when used on the skin. It stimulates the tissue to generate new, thicker collagen fiber from the necrosis during the treatment of the plasma skin regeneration system, while topical anesthesia will reduce both skin necrosis and the collage fiber regeneration [16]. One explanation for this might be that when injecting subcutaneously, the agent slightly lifts the tissue, loosens the

tissue structure, and further provokes the fibroblasts to generate more collagen fiber.

Although it has been established that the application of local anesthetics intravascularly or via surface infiltration will mitigate the airway response caused by tracheal intubation, it is unclear whether local anesthetics such as ropivacaine and lidocaine can trigger an anti-inflammatory mechanism in the pulmonary endothelial barrier. In trials run by Piegeler et al., they found that in rats, ropivacaine and lidocaine attenuate TNF-α-induced Src activation and endothelial nitric oxide synthase phosphorylation, equivalent to the blockage of the inflammatory TNF-α signal pathway [17]. This finding indicates that these two local anesthetics can prevent the pulmonary endothelial cells from an inflammatory response and further maintain the permeability of the pulmonary microvasculature. The normal function and blood supply of the pulmonary alveolar is therefore permitted. This experiment indicates that the surface infiltration of local anesthesia may improve both the recovery from acute inflammation and the stabilized stimulation caused by a tracheal tube.

5. Conclusion

Figure 1 shows the major classification of anesthesia and the representative agents; their functions were classified with the reference number marked on the lines. To sum up, direct comparison of inhaled and intravenous anesthetics is not well studied as these two types of agents are usually used in different clinical settings except for invasive surgical procedures, although they are both proved to have anti-inflammatory effect in some degrees. Furthermore, researchers tend to indicate the development of inflammatory and immune response through diverse pathways, but we can draw a conclusion that inhaled anesthetics have more extensive anti-inflammatory response than the other two types, thus should be considered as a better option when less inflammation is desired in barrier tissues.

A different surgery type requires for different methods of anesthesia, and the real complications of patients should be the basis for the selection of anesthetic agents. Patients with barrier disorder are commonly encountered during clinical treatments and require greater observation of side effects and potential risks from various anesthetic agents. Appropriate selection and utilization of anesthetics and the combination of different anesthetic methods may help address and prevent these risks and further affect patient satisfaction and safety, shorten the hospital stay, and improve patient experience.

Conflicts of Interest

The authors declare that there is no conflict of interest regarding the publication of this paper.

Funding

References

[1] K. Tanaka, L. M. Ludwig, J. R. Kersten, P. S. Pagel, and D. C. Warltier, "Mechanisms of cardioprotection by volatile anesthetics," *Anesthesiology*, vol. 100, no. 3, pp. 707–721, 2004.

[2] S. Gargiulo, M. Gramanzini, R. Liuzzi, A. Greco, A. Brunetti, and G. Vesce, "Effects of some anesthetic agents on skin microcirculation evaluated by laser Doppler perfusion imaging in mice," *BMC Veterinary Research*, vol. 9, no. 1, p. 255, 2013.

[3] O. Giraud, S. Molliex, C. Rolland et al., "Halogenated anesthetics reduce interleukin-1β-induced cytokine secretion by rat alveolar type II cells in primary culture," *Anesthesiology*, vol. 98, no. 1, pp. 74–81, 2003.

[4] T. Yue, B. Roth Z'graggen, S. Blumenthal et al., "Postconditioning with a volatile anaesthetic in alveolar epithelial cells in vitro," *The European Respiratory Journal*, vol. 31, no. 1, pp. 118–125, 2008.

[5] C. Paugam-Burtz, S. Molliex, B. Lardeux et al., "Differential effects of halothane and thiopental on surfactant protein C messenger RNA in vivo and in vitro in rats," *Anesthesiology*, vol. 93, no. 3, pp. 805–810, 2000.

[6] L. Bardosi, A. Bardosi, and H. J. Gabius, "Changes of expression of endogenous sugar receptors by polymorphonuclear leukocytes after prolonged anaesthesia and surgery," *Canadian Journal of Anesthesia*, vol. 39, no. 2, pp. 143–150, 1992.

[7] D. Frohlich, G. Rothe, G. Schmitz, and K. Taeger, "Nitrous oxide impairs the signaling of neutrophils downstream of receptors," *Toxicology Letters*, vol. 100-101, pp. 121–127, 1998.

[8] S. Kumakura, K. Yamaguchi, Y. Sugasawa et al., "Effects of nitrous oxide on the production of cytokines and chemokines by the airway epithelium during anesthesia with sevoflurane and propofol," *Molecular Medicine Reports*, vol. 8, no. 6, pp. 1643–1648, 2013.

[9] C. Liu, Z. Shen, Y. Liu et al., "Sevoflurane protects against intestinal ischemia–reperfusion injury partly by phosphatidylinositol 3 kinases/Akt pathway in rats," *Surgery*, vol. 157, no. 5, pp. 924–933, 2015.

[10] Z. Abramovic, M. Sentjurc, J. Kristl, N. Khan, H. Hou, and H. M. Swartz, "Influence of different anesthetics on skin oxygenation studied by electron paramagnetic resonance in vivo," *Skin Pharmacology and Physiology*, vol. 20, no. 2, pp. 77–84, 2007.

[11] R. J. Mason and J. M. Shannnon, "Alveolar type II cells," in *The Lung*, R. G. Crystal, J. B. West, E. R. Weibel, and P. J. Barnes, Eds., pp. 543–555, Lippincott-Raven, Philadelphia, PA, USA, 1997.

[12] K. Nishina, K. Mikawa, O. Morikawa, H. Obara, and R. J. Mason, "The effects of intravenous anesthetics and lidocaine on proliferation of cultured type II pneumocytes and lung fibroblasts," *Anesthesia & Analgesia*, vol. 94, no. 2, pp. 385–388, 2002.

[13] S. Wakabayashi, K. Yamaguchi, S. Kumakura et al., "Effects of anesthesia with sevoflurane and propofol on the cytokine/chemokine production at the airway epithelium during esophagectomy," *International Journal of Molecular Medicine*, vol. 34, no. 1, pp. 137–144, 2014.

[14] Y. Sugasawa, K. Yamaguchi, S. Kumakura et al., "Effects of sevoflurane and propofol on pulmonary inflammatory responses during lung resection," *Journal of Anesthesia*, vol. 26, no. 1, pp. 62–69, 2012.

[15] M.-C. Lin, C.-L. Chen, T.-T. Yang, P.-C. Choi, C.-H. Hsing, and C.-F. Lin, "Anesthetic propofol overdose causes

endothelial cytotoxicity in vitro and endothelial barrier dysfunction in vivo," *Toxicology and Applied Pharmacology*, vol. 265, no. 2, pp. 253–262, 2012.

[16] Y. Ji, L. Guo, Y. Zhang, and Y. Liu, "Comparison of topical anesthesia and subcutaneous infiltration anesthesia with regard to effect of plasma skin regeneration system," *Journal of Cosmetic and Laser Therapy*, vol. 17, no. 6, pp. 330–334, 2015.

[17] T. Piegeler, E. G. Votta-Velis, F. R. Bakhshi et al., "Endothelial barrier protection by local anesthetics: ropivacaine and lidocaine block tumor necrosis factor-α-induced endothelial cell Src activation," *Anesthesiology*, vol. 120, no. 6, pp. 1414–1428, 2014.

Research Article

Lipid-Rich Extract from Mexican Avocado Seed (*Persea americana* var. drymifolia) Reduces *Staphylococcus aureus* Internalization and Regulates Innate Immune Response in Bovine Mammary Epithelial Cells

Marisol Báez-Magaña,[1] **Alejandra Ochoa-Zarzosa** (ID)**,**[1] **Nayeli Alva-Murillo** (ID)**,**[2]
Rafael Salgado-Garciglia (ID)**,**[3] **and Joel Edmundo López-Meza** (ID)[1]

[1]*Centro Multidisciplinario de Estudios en Biotecnología-FMVZ, Universidad Michoacana de San Nicolás de Hidalgo, Km 9.5 Carretera Morelia-Zinapécuaro, Posta Veterinaria C.P., 58893 Morelia, Michoacán, Mexico*
[2]*Departamento de Biología, División de Ciencias Naturales y Exactas, Universidad de Guanajuato, Guanajuato, Mexico*
[3]*Instituto de Investigaciones Químico Biológicas, UMSNH. Ciudad Universitaria, Morelia, Michoacán, Mexico*

Correspondence should be addressed to Joel Edmundo López-Meza; elmeza@umich.mx

Bovine mammary epithelial cells (bMECs) are capable of initiating an innate immune response (IIR) to invading bacteria. *Staphylococcus aureus* is not classically an intracellular pathogen, although it has been shown to be internalized into bMECs. *S. aureus* internalizes into nonprofessional phagocytes, which allows the evasion of the IIR and turns antimicrobial therapy unsuccessful. An alternative treatment to control this pathogen is the modulation of the innate immune response of the host. The Mexican avocado (*Persea americana* var. drymifolia) is a source of molecules with anti-inflammatory and immunomodulatory properties. Hence, we analyze the effect of a lipid-rich extract from avocado seed (LEAS) on *S. aureus* internalization into bMECs and their innate immunity response. The effects of LEAS (1-500 ng/ml) on the *S. aureus* growth and bMEC viability were assessed by turbidimetry and MTT assays, respectively. LEAS did not show neither antimicrobial nor cytotoxic effects. *S. aureus* internalization into bMECs was analyzed by gentamicin protection assays. Interestingly, LEAS (1-200 ng/ml) decreased bacterial internalization (60-80%) into bMECs. This effect correlated with NO production and the induction of the gene expression of IL-10, while the expression of the proinflammatory cytokine TNF-α was reduced. These effects could be related to the inhibition of MAPK p38 (~60%) activation by LEAS. In conclusion, our results showed that LEAS inhibits the *S. aureus* internalization into bMECs and modulates the IIR, which indicates that avocado is a source of metabolites for control of mastitis pathogens.

1. Introduction

The innate immune response (IIR) is the first line of defense of organisms, which has a relevant role in the protection against pathogens. The participation of professional phagocytic cells (c.a. macrophages, dendritic cells, and circulating leukocytes) in the IIR is fundamental; however, nonprofessional phagocytic cells (c.a. epithelium, endothelium, osteo-

blast, and fibroblast cells) also have a relevant role [1]. In this sense, bovine mammary epithelial cells (bMECs) play an important role in the IIR of the mammary gland acting as a physical barrier and as initial sensors of danger with the capacity to mount a defense response [2]. The IIR regulation by immunomodulatory molecules such as fatty acids and vitamins has been widely demonstrated and involves epigenetics changes that can be stably maintained or adapted to

changing environments [3, 4]. For the above, the search for modulators that improve the bMEC IIR increases the opportunity to identify novel therapeutics.

S. aureus is the main pathogen responsible for subclinical bovine mastitis, a chronic and recurrent disease that affect dairy cattle worldwide [5, 6]. This bacterium has the ability to be internalized into the cells, which allows it to evade the IIR of the host; this characteristic has been associated with the recurrence of mastitis [7, 8]. In previous reports, we showed that immunomodulatory molecules (short and medium chain fatty acids, and cholecalciferol) inhibit *S. aureus* internalization into bMECs regulating the IIR, suggesting an immunomodulatory role in host-pathogen interaction [3, 8, 9].

For a long time, plants have been a rich source of antibacterial, antiviral, and immunomodulatory metabolites. In this sense, avocado (*Persea americana*) is a very nutritious fruit (rich in saturated and unsaturated fatty acids) that possesses different compounds with antioxidant, anticancer, antimicrobial, and anti-inflammatory properties [10]. Diverse reports have shown that avocado metabolites have immunomodulatory properties. For example, an avocado/soybean unsaponifiable (ASU) mixture decreased the expression of TNF-α, IL-1β, COX-2, and iNOS in bovine chondrocytes and human monocyte/macrophages [11, 12]. Likewise, seven-carbon sugars typical of avocado (mannoheptulose and perseitol) inhibited *Malassezia furfur* internalization into human keratinocytes and induced expression of the antimicrobial peptide HBD-2 [13]. Also, avocado aliphatic acetogenins (lipid derivative molecules present in mesocarp and endocarp) favored the apoptosis induction and cell cycle arrest in different human cancer cell lines [14, 15]. Furthermore, the anti-inflammatory and photoprotective effects of polyhydroxylated fatty alcohols (synonymous of acetogenins) extracted from *Persea gratissima* on human keratinocytes damaged by UV have been demonstrated [16]. However, it is unknown if lipid derivative molecules from Mexican avocado seed (*Persea americana* var. drymifolia) display immunomodulatory properties in host-pathogen interaction. Thus, in this work, we analyzed the effects of a lipid-rich extract from Mexican avocado seed (LEAS) on *S. aureus* internalization into bMECs. In addition, the effects of LEAS on the IIR of bMECs were analyzed.

2. Materials and Methods

2.1. Lipid-Rich Extract from Avocado Seed (LEAS). Mexican avocado fruits (*Persea americana* var. drymifolia) used in this study were collected when physiological maturity was achieved. The LEAS was obtained according to Rosenblat et al. [16]. Briefly, avocado seeds were separated from the fruit and frozen in liquid nitrogen, followed by trituration. The powder obtained was extracted with hexane (C_6H_{14}, J.T. Baker) for 14 h in a Soxhlet apparatus. This lipid-rich fraction was filtered and then cooled to -18°C overnight for a cold crystallization. Precipitated crystals were recovered discarding the supernatant and then drying with nitrogen gas. This extract contains abundant molecules of 16-24 carbon aliphatic chains with hydroxyl groups such as aliphatic

acetogenins and long-chain fatty acids as determined by gas chromatography-mass spectrometry (GC-MS) (Table 1). For biological assays, crystals were resuspended in dimethyl sulfoxide (DMSO 5%). In all of the experiments, the final concentration of DMSO was 0.1%.

2.2. Staphylococcus aureus Strain. The *S. aureus* subsp. *aureus* (ATCC27543) strain was used in this study. The strain was isolated from a case of bovine mastitis that has the capability to internalize into bMECs [3]. Bacteria were grown overnight in Luria-Bertani (LB) broth (Bioxon, México). For the different assays, the colony-forming units (CFU) were adjusted by measuring their optical density at 590 nm (OD $0.2 = 9.2 \times 10^7$ CFU/ml).

2.3. Primary Culture Bovine Mammary Epithelial Cells (bMECs). bMECs were isolated of alveolar tissue from the udder of a healthy lactating cow as described [17]. Cells from passages 2-8 were used in all of the experiments. The bMECs were cultured in growth medium (GM) that was composed of DMEM medium/nutrient mixture F12 Ham (DMEM/F12, Sigma) supplemented with 10% fetal bovine serum (Biowest), 10 μg/ml insulin (Sigma), 5 mg/ml hydrocortisone (Sigma), 100 U/ml penicillin, 100 μg/ml streptomycin, and 1 μg/ml amphotericin B (Sigma). The cells were grown in a 5% CO_2 atmosphere at 37°C.

2.4. Effect of Lipid-Rich Extract from Avocado Seed on S. aureus 27543 Growth and bMEC Viability. The effect of LEAS on *S. aureus* growth was determined by turbidimetry assay. For this, 9.2×10^7 CFU/ml was cultured at 37°C in LB broth supplemented with different concentrations of LEAS (1-500 ng/ml) and growth was monitored turbidimetrically (590 nm) at 2, 6, 12, and 24 h.

To analyze the effect of LEAS on bMEC viability, 1×10^4 cells were incubated with the extract (1-500 ng/ml) during 24-48 h at 37°C in 96-well flat-bottom plates in GM without supplements. Further, cells were detached with trypsin-EDTA (Sigma) and resuspended in a 1:1 dilution with 0.4% Trypan blue solution (Sigma) and incubated for 3 minutes. Finally, nonviable and viable cells were counted in a hemocytometer.

2.5. Effect of Lipid-Rich Extract from Avocado Seed on S. aureus 27543 Adhesion and Internalization into bMECs. Gentamicin protection assay was carried out using bMECs monolayers (~2×10^5 cells) cultured in 24-well dishes treated with 6-10 μg/cm^2 rat tail type I collagen (Sigma) as described [3]. bMECs were incubated with different concentrations of LEAS (1-200 ng/ml) in DMEM/F12 media (Sigma) without supplements for 24 h followed by *S. aureus* infection (MOI 30:1 bacteria per cell). For this, the bMECs were inoculated with bacterial suspensions (9.2×10^7 CFU/ml) and incubated for 2 h in 5% CO_2 at 37°C. Afterward, bMECs were washed three times with PBS (pH 7.4) and incubated with DMEM medium supplemented with 80 μg/ml gentamicin for 1 h at 37°C to eliminate extracellular bacteria. Finally, bMEC monolayers were detached with trypsin EDTA (Sigma) and lysed with 250 μl of sterile distilled water. bMEC lysates were diluted 100-fold and plated on LB agar, and Petri dishes were

TABLE 1: Composition of lipid-rich extract from Mexican avocado seed (*Persea americana* var. drymifolia).

Group	Compound	Content ($\mu g/g$)
Fatty acid derivatives (aliphatic acetogenins)	Avocatins	32.28
	Persins	10.12
	Pahuatins	4.26
	Polyhydroxy fatty acids	24.26
Long-chain fatty acids	Myristic acid	2.49
	Palmitic acid	7.1
	Linoleic acid	4.06
	Oleic acid	5.32
	Stearic acid	5.06
	Arachidic acid	2.39
	Erucic acid	2.44
	Behenic acid	3.63
	Nervonic acid	2.88
	Tetracosanoic acid	4.29

incubated overnight at 37°C. The number of CFUs was determined by the standard colony counting technique. Data are presented as the percentage of internalization in relation to control (bMECs treated with vehicle).

To determine the adhesion of *S. aureus* on bMECs, cells were cultured and treated as described above but the gentamicin treatment was omitted. Data are presented as the percentage of adhesion in relation to control (bMECs treated with vehicle).

2.6. Staphylococcus aureus Viability in bMEC-Conditioned Media. To evaluate *S. aureus* survival in conditioned media, bMECs were cultured ($\sim 2 \times 10^5$ cells) in 24-well plates with 6-10 $\mu g/cm^2$ rat tail type I collagen (Sigma). Then, bMECs were treated with LEAS (100 ng/ml) for 24 h and the culture medium was recovered. Next, conditioned media were inoculated with *S. aureus* suspension (9.2×10^7 CFU/ml) and incubated for 2 h at 37°C and 180 rpm. Finally, a dilution of this suspension (1 : 1000) was plated on LB agar and incubated overnight at 37°C. The number of CFUs was determined by the standard colony counting technique.

2.7. Effects of Lipid-Rich Extract from Avocado Seed on MAP Kinase Activation in bMECs. The evaluation of the MAP kinase activation (p38, JNK, or ERK1/2) was carried out as reported [18]. Briefly, bMEC monolayers were cultivated on 96-well flat-bottom plates that were coated (Corning-Costar) with 6-10 $\mu g/cm^2$ rat tail type I collagen (Sigma). MAP kinase activation levels were assessed by flow cytometry in bMECs pretreated with LEAS (100 ng/ml, 24 h). pp38 (T180/Y182), pJNK1/2 (T183/185), and pERK1/2 (T202/Y204) were quantitatively determined using a Flex Set Cytometric Bead Array (Becton Dickinson) according to the manufacturer's protocol using a BD Accuri™ C6 flow cytometer. Data were analyzed with FCAP software (Becton Dickinson). A total of 3000 events were acquired following the supplied protocol. The minimum detection levels for each phosphoprotein were

0.38 U/ml for pJNK and 0.64 U/ml for pp38 and pERK. The corroboration of MAPK activation was performed using different inhibitors (data not shown).

2.8. RNA Isolation and Innate Immune Response Gene Expression Analysis. To analyze the effects of LEAS and/or *S. aureus* on the expression of IIR genes of bMECs, monolayers of cells cultured in 6-well plates with 6-10 $\mu g/cm^2$ rat tail type I collagen (Sigma) were incubated with LEAS 100 ng/ml (24 h) and/or *S. aureus* for 2 h (MOI 30 : 1). bMEC total RNA (5 μg) was extracted with the TRIzol reagent (Invitrogen) according to the manufacturer's instructions. Genomic DNA contamination was removed from RNA samples with DNase I treatment (Invitrogen). Then, cDNA was synthesized as described [19]. The relative quantification of gene expression (qPCR) was performed using the comparative Ct method ($\Delta\Delta$Ct) in a StepOne Plus Real-Time PCR System (Applied Biosystems) according to the manufacturer's instructions. The reactions were carried out with VeriQuest SYBR Green qPCR Master Mix (Affymetrix). Specific primer pairs were acquired from Invitrogen and Elim Biopharm (Table 2), and their specificity was determined by endpoint PCR. The GAPDH gene was used as an internal control.

For the measurement of the TNF-α and IL-1β concentrations in the conditioned medium, bMECs were treated with LEAS (100 ng/ml) and/or *S. aureus*. The concentrations of TNF-α were measured using the DuoSet ELISA Development Kit (R&D Systems) according to the manufacturer's instructions, and the concentrations of IL-1β were assessed using the bovine IL-1β screening kit (Thermo Scientific).

2.9. Determination of Nitric Oxide (NO) and Reactive Oxygen Species (ROS). Nitric oxide was estimated by Griess reaction. For this, bMECs were cultured ($\sim 2 \times 10^5$ cells) in 24-well plates with 6-10 $\mu g/cm^2$ rat tail type I collagen (Sigma). Then, bMECs were treated with LEAS (100 ng/ml) for 24 h. After treatment, the cells were infected with *S. aureus* (2 h) and

TABLE 2: Bovine oligonucleotides used in this study.

Specificity	Primer	Sequence (5′-3′)	Fragment size (bp)	Annealing temperature (°C)	References
IL-1β	Forward	GCAGAAGGGAAGGGAAGAATGTAG	198	52	[19]
	Reverse	CAGGCTGGCTTTGAGTGAGTAGAA			
IL-6	Forward	AACCACTCCAGCCACAAACACT	179	57	[19]
	Reverse	GAATGCCCAGGAACTACCACAA			
TNF-α	Forward	CCCCTGGAGATAACCTCCCA	101	56	[19]
	Reverse	CAGACGGGAGACAGGAGAGC			
IL-10	Forward	GATGCGAGCACCCTGTCTGA	129	59	[19]
	Reverse	GCTGTGCAGTTGGTCCTTCATT			
BNBD5	Forward	GCCAGCTGAGGCTCCATC	143	55	[9]
	Reverse	TTGCCAGGGCACGAGATCG			
DEFB1	Forward	CCATCACCTGCTCCTCACA	185	54	[9]
	Reverse	ACCTCCACCTGCAGCATT			
TAP	Forward	GCGCTCCTCTTCCTGGTCCTG	216	57	[9]
	Reverse	GCACGTTCTGACTGGGCATTGA			
GAPDH	Forward	TCAACGGGAAGCTCACTGG	237	56.9	[9]
	Reverse	CCCCAGCATCGAAGGTAGA			

the conditioned medium was recovered. The NO secreted by bMECs into culture medium was evaluated by measuring the nitrite concentration (NO^{2-}) in cell-free media using the Griess reaction as described [3].

To analyze the production of ROS, the method of Tarpey and Fridovich [20] was used. For this, bMECs (1×10^5 cells) were grown in 24-well plates (Corning Costar) until 80% of confluence. Afterward, the LEAS (100 ng/ml) was added for 24 h; then, bMECs were infected with *S. aureus* (2 h). Subsequently, bMECs were detached with trypsin, recovered, and washed with PBS by centrifugation and the supernatant was removed. bMECs were incubated for 30 minutes with dihydrorhodamine-123 (DHR) 5 mM (Molecular Probes). ROS were determined by flow cytometry (BD Accuri™ C6 flow cytometer). In both evaluations, LPS was used as a positive control.

2.10. Data Analysis. The data were obtained from three independent experiments; each one was performed in triplicate and compared with one-way analysis of mean comparisons using Student's *t*-test, except for ELISA; in this case, a one-way analysis of variance (one-way ANOVA) using the Tukey-Kramer test was used. The results are reported as the means ± the standard errors (SE), and the significance level was set at $P \leq 0.05$, except for RT-qPCR analysis where fold change values greater than 2 or less than 0.5 were considered as significant differentially expressed mRNAs [18]. The data were normalized to vehicle (DMSO 0.1%).

3. Results

3.1. The Lipid-Rich Extract from Avocado Seed Does Not Affect S. aureus Growth and bMEC Viability. To evaluate the effect of LEAS on *S. aureus* growth, bacteria were cultivated in LB broth supplemented with different concentra-

tions (1-500 ng/ml). The turbidimetric results showed that the *S. aureus* growth was not affected by LEAS at the times evaluated (Figure 1(a)). In the same way, the effect of LEAS on the viability of bMECs was evaluated at 24 and 48 h using the Trypan blue exclusion assay. Data showed that LEAS did not affect bMEC viability at any concentration tested (Figure 1(b)).

3.2. The Lipid-Rich Extract from Avocado Seed Inhibits the S. aureus Internalization into bMECs. The effect of LEAS on *S. aureus* internalization into bMECs was evaluated by gentamicin protection assay. bMECs were treated with LEAS (1-200 ng/ml) 24 h before bacterial challenge. According to the CFUs recovered, the LEAS (1-200 ng/ml) significantly decreased *S. aureus* internalization into bMECs (60-80%) in all of the concentrations tested in relation to vehicle (Figure 2(a)). The more pronounced inhibitory effect was observed at 100 ng/ml (80%). Interestingly, this concentration also decreased the *S. aureus* adhesion to bMECs (~30%) (Figure 2(b)). According to these results, we used this concentration in the rest of the experiments.

3.3. The Lipid-Rich Extract from Avocado Seed Improves the Defense of bMECs. In order to evaluate if the inhibitory effect of LEAS on *S. aureus* internalization into bMECs was related to the secretion of antimicrobial products by bMECs, we evaluated bacterial viability in the presence of conditioned media (culture media of bMECs treated 24 h with LEAS). Interestingly, bacterial viability diminished by ~30% in the presence of conditioned media, which suggests that LEAS induced the production and secretion of antimicrobial molecules in bMECs (Figure 3(a)).

Then, we evaluate if reactive oxygen and nitrogen species could contribute to the antimicrobial effect showed by the conditioned media. The results showed that bMECs treated
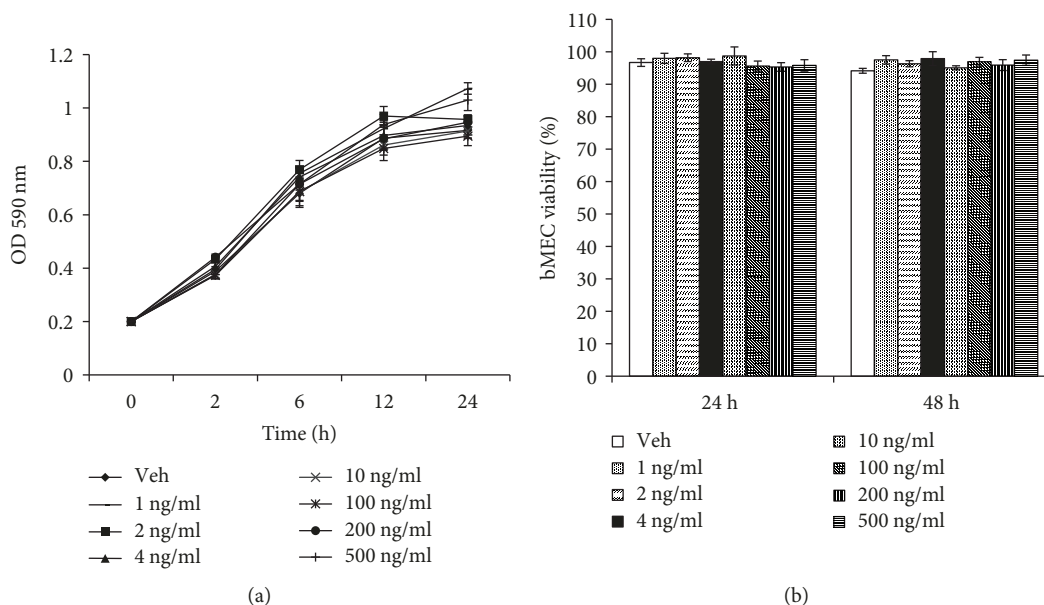
(a)

(b)

FIGURE 1: The lipid-rich avocado seed extract did not affect *S. aureus* growth and bMECs viability. (a) *S. aureus* was grown in LB at 37°C (18 h). The OD$_{590}$ was adjusted at 0.2 (9.2×10^7 CFU) and the treatments were added. The growth was monitored measuring the OD at the indicated time. (b) bMECs were grown in 96-well dishes (80% confluence) and the treatments were added. The viability was determined by Trypan blue exclusion assay at 24 and 48 h. The results correspond to three independent experiments performed by triplicate. Vehicle (DMSO 0.1%) ($P \leq 0.05$, Student's *t*-test).
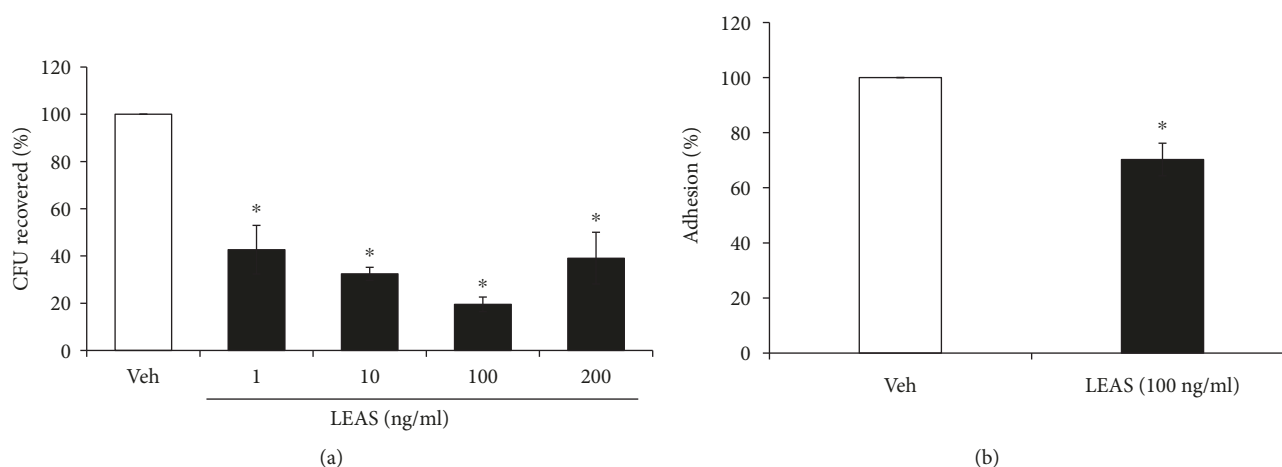

(a)

(b)

FIGURE 2: The lipid-rich avocado seed extract inhibits *S. aureus* internalization into bMECs and the adhesion. (a) The effect of LEAS on the internalization of *S. aureus* into bMECs is presented as the percentage of CFU recovered after the lysis of bMECs. The values were determined considering the vehicle (DMSO 0.1%) as 100% of internalization. The results are the average of three independent experiments performed in triplicate. Vehicle (DMSO 0.1%). * indicates significant changes ($P \leq 0.05$, Student's *t*-test). (b) To determine the adhesion of *S. aureus* on bMECs, cells were cultured and treated as described in Materials and Methods but the gentamicin treatment was omitted. Data are presented as the percentage of adhesion in relation to control (bMECs treated with vehicle). * indicates significant changes ($P \leq 0.05$, Student's *t*-test).

with LEAS (100 ng/ml) for 24 h increased the NO levels; this effect was maintained even in bMECs challenged with *S. aureus* (Figure 3(b)). However, the ROS production was not affected by LEAS treatment (Figure 3(c)). These results suggest that NO production could be involved in the antimicrobial effect detected in the conditioned media.

3.4. The Lipid-Rich Extract from Avocado Seed Inhibits p38 but Not JNK1/2 or ERK1/2 in bMECs.
MAPK activation has been involved in *S. aureus* internalization into bMECs [18]. Thus, we evaluated whether LEAS regulates MAPK activation (p38, JNK, or ERK1/2) in bMECs. Interestingly, in LEAS-pretreated bMECs the basal activation of JNK and
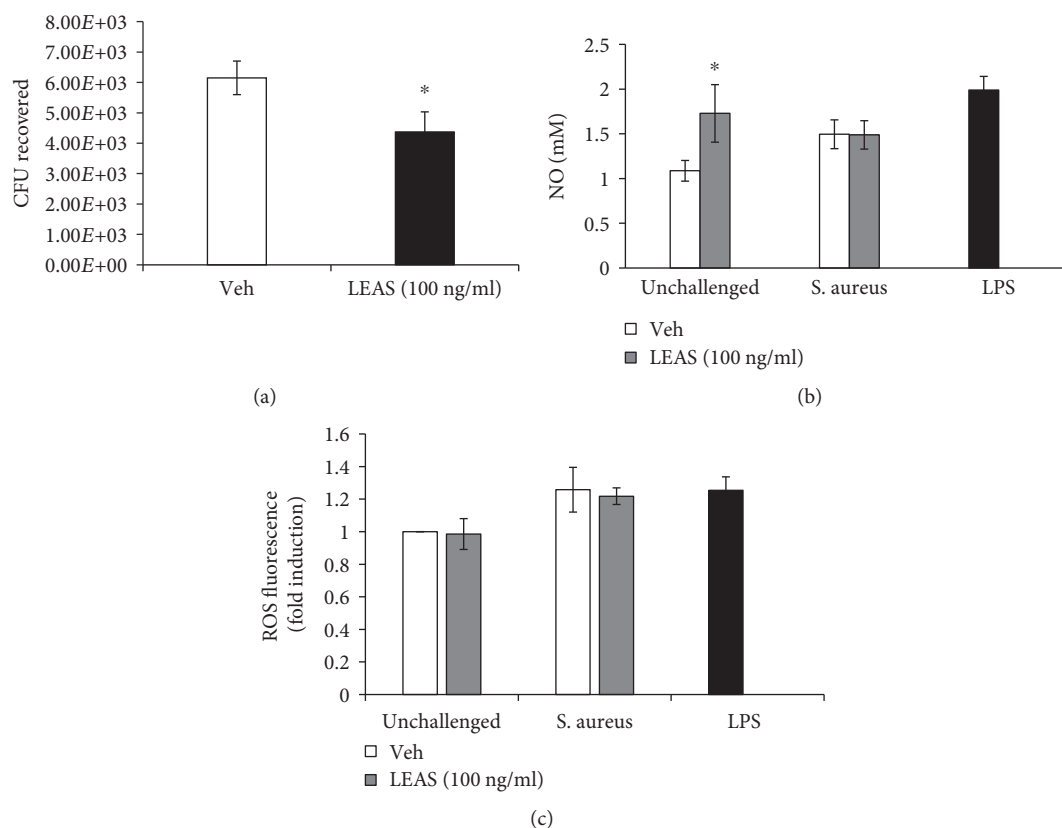
(a)

(b)

(c)

FIGURE 3: The conditioned media of LEAS-pretreated bMECs showed antimicrobial activity against *S. aureus*. (a) Effect of conditioned medium from bMECs treated with vehicle (DMSO 0.1%) or LEAS (100 ng/ml) for 24 h on *S. aureus* viability. Bacteria were incubated 2 h with conditioned media. The number of CFU recovered is shown. The results are the average of three independent experiments performed in triplicate. Vehicle (DMSO 0.1%). ∗ indicates significant changes ($P \leq 0.05$, Student's t-test). (b) Nitric oxide and (c) ROS production in bMECs treated with 100 ng/ml of LEAS for 24 h and then challenged with *S. aureus* for 2 h. NO production was measured as NO^{2-} concentration in culture medium. ROS production was evaluated by flow cytometry. In (b, c), cells stimulated with LPS (1 μg/ml, 24 h) were used as a positive control. Each bar shows the mean of triplicate ± SE of three independent experiments. ∗ indicates significant changes ($P \leq 0.05$, Student's t-test) within the treatment. Vehicle (DMSO 0.1%).

ERK1/2 was not modified; however, phosphorylated p38 was diminished by ~60% (Figure 4).

3.5. The Lipid-Rich Extract from Avocado Seed Regulates the Expression of Innate Immune Elements in bMECs. bMECs are key elements of IIR and play a significant role in the defense against pathogens. Consequently, we analyzed the mRNA levels of the proinflammatory cytokines TNF-α, IL-1β, and IL-6 and the anti-inflammatory cytokine IL-10, as well as the antimicrobial peptides TAP, DEFB1, and BNBD5 in LEAS-pretreated bMECs before and after infection. LEAS favors an anti-inflammatory response in bMECs due to the decrease in the mRNA levels of the proinflammatory cytokine TNF-α (~0.5-fold) and the increase of IL-10 mRNA levels significantly (~11-fold). Notably, the effect on IL-10 was more pronounced in bMECs challenged with *S. aureus* (~22-fold) (Table 3). Furthermore, LEAS kept the reduction of the TNF-α secretion in the infected bMECs. Only the secretion of IL-1β was increased (~1.5-fold) when the LEAS-treated cells were infected with *S. aureus* (Table 4). Also, the mRNA levels for IL-1β and IL-6 were not modified for any of the conditions evaluated. In addition, we evaluated

the mRNA levels of the antimicrobial peptides BNBD5, DEFB-1, and TAP. The treatment of bMECs with LEAS did not affect the mRNA expression of the antimicrobial peptides tested; however, the challenge with the bacteria increased the BNBD5 expression (~4-fold).

4. Discussion

IIR modulation is an alternative for therapeutic or prophylactic treatment to control and prevent diseases. Previously, we showed that short- and medium-chain fatty acids reduced *S. aureus* internalization into bMECs and improved IIR [3, 8]. In this sense, avocado (a fruit rich in fatty acids) is attractive in the search of plant compounds with immunomodulatory properties. This work demonstrates that a lipid-rich extract from Mexican avocado seed reduced *S. aureus* internalization into bMECs and regulated the IIR.

Long-chain fatty acids have antimicrobial activity against *S. aureus* [21]. Oleic acid and lauric acid (>70 μg/ml) have showed antimicrobial effects against methicillin-resistant *S. aureus* [22]. Also, eicosapentaenoic acid and docosahexaenoic acid (128-256 mg/ml) have antimicrobial effects against
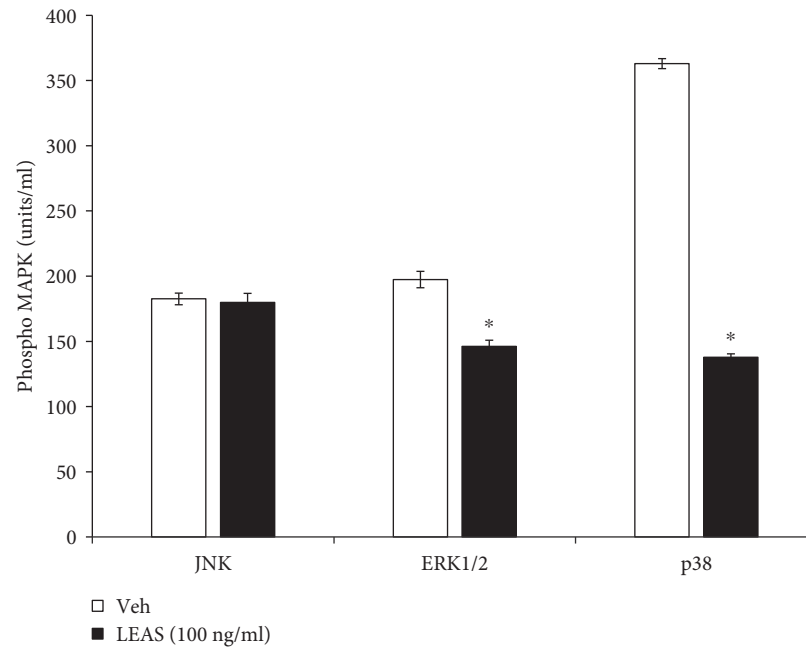
FIGURE 4: p38, JNK, and ERK1/2 activation regulated by LEAS in bMECs. MAPK phosphorylation was measured in bMECs that were treated with LEAS (100 ng/ml) by flow cytometry. Each bar shows the result of one experiment and a total of 3000 events were acquired. ∗ indicates significant changes ($P \leq 0.05$, Student's t-test) within the treatment. Vehicle (DMSO 0.1%).

TABLE 3: Effect of lipid-rich extract from avocado seed on expression of innate immune elements of bMECs.

Activity	Gene	Vehicle	LEAS (100 ng/ml)	Vehicle+S. aureus	LEAS (100 ng/ml)+S. aureus
	TNF-α	1 ± 0	0.48 ± 0.07*	1.03 ± 0.25	0.40 ± 0.09*
Pro-inflammatory	IL-1β	1 ± 0	1.03 ± 0.15	0.86 ± 0.29	1.43 ± 0.55
	IL-6	1 ± 0	0.74 ± 0.33	0.78 ± 0.18	0.59 ± 0.13
Anti-inflammatory	IL-10	1 ± 0	11.39 ± 3.57*	2.73 ± 1.46*	21.39 ± 5.9*
	BNBD5	1 ± 0	0.94 ± 0.16	0.98 ± 0.22	4.02 ± 0.32*
Antimicrobial peptide	DEFB1	1 ± 0	0.98 ± 0.29	0.51 ± 0.23*	0.35 ± 0.14*
	TAP	1 ± 0	1.38 ± 0.29	0.44 ± 0.17*	1.60 ± 0.34

Relative expression of genes was determined by RT-qPCR using GAPDH as endogenous control. The results correspond to three independent experiments and show the mean of triplicate ± SE. *Fold change values greater than 2 or less than 0.5 were considered significant differentially expressed mRNAs with respect to vehicle.

TABLE 4: Effect of lipid-rich extract from avocado seed on secretion of cytokines in bMECs.

Cytokine (pg/ml)	Vehicle	LEAS (100 ng/ml)	Vehicle+S. aureus	LEAS (100 ng/ml)+S. aureus
TNF-α	2459.83 ± 85.16[a]	2736.5 ± 72.85[a]	1614.83 ± 28.33[b]	1576.5 ± 123.92[b]
IL-1β	ND	ND	257.9 ± 24.76[b]	431.56 ± 38.02[a]

Proteins were determined by ELISA (pg/ml). The results correspond to three independent experiments and show the mean of triplicate ± SE. Different letters indicate significant differences within the row. ND: not detected.

S. aureus isolates from diverse origins, including isolates methicillin and vancomycin resistant [23]. Likewise, docosa-hexaenoic acid (30 μM) induces apoptosis in breast cancer cell lines MCF-7 and SK-BR-3 [24]. Avocado seed extract is rich in fatty acids (mainly palmitic, oleic, and linoleic), and derivatives such as acetogenins, avocatins, persins, pahuatins,

or fatty acid alcohols have antimicrobial and cytotoxic activities [14, 25]. Noteworthy, LEAS (1-500 ng/ml) did not affect the S. aureus growth and bMEC viability (Figure 1). It is important to notice that the concentrations used in this work are lower than those reported with antibacterial and cytotoxicity properties. However, preliminary results of our group

indicate that LEAS are cytotoxic to cancer cells (Caco-2) at concentrations above of 10 μg/ml (data unpublished).

Bacterial adhesion and internalization are important for the establishment of chronic bovine mastitis and thus are an attractive target in the implementation of strategies for its control. In a previous work, we demonstrated that pretreated bMECs with short- and medium-chain fatty acids showed a reduced S. aureus internalization. Sodium propionate (1-5 mM) decreased bacterial invasion by ~65%, whereas sodium butyrate (0.25 mM) inhibited it by ~50% [3]. Likewise, sodium hexanoate (0.25-5 mM) reduced S. aureus internalization by ~60% [26]. Similarly, LEAS inhibited S. aureus internalization into bMECs but its effect was more pronounced than those reported for short- and medium-chain fatty acids, reaching inhibition of 80% (Figure 2). Also, the inhibitory LEAS concentrations were lower suggesting a better effect of lipids from avocado seed. Additionally, LEAS diminished the S. aureus adhesion to bMECs (~30%), which partially explains the inhibited internalization by LEAS. Interestingly, in LEAS-pretreated bMECs, the levels of NO in conditioned media were increased and bacteria viability was reduced by ~30% when incubated with it (Figure 3(a)). This data suggests a participation of antimicrobial molecules in the reduction of bacterial internalization. This result agrees with a previous report, in which the inhibitory effect of estradiol on S. aureus internalization into bMECs was associated to the secretion of elements with antimicrobial activity in the conditioned media [27]. In the same way, de Lima et al. [28] reported that the NO production of macrophages was stimulated by fatty acids in a concentration-dependent manner; low concentrations (1-10 μM) stimulated NO production in J774 cells (murine macrophages), whereas high concentrations (50-200 μM) inhibited NO production. This data supports the fact that IIR of bMECs can be improved by immunomodulatory molecules which leads to the secretion of antimicrobial molecules that could contribute to the reduction in bacterial internalization.

On the other hand, for S. aureus internalization into bMECs, the MAPK pathway has a relevant role. When MAPK activity was blocked with pharmacological inhibitors of p38 (2.5–10 μM SB203580), JNK (5–20 μM, SP600125), or ERK1/2 (0.62–10 μM, U0126), a considerable reduction in S. aureus internalization was observed, indicating that these kinases are involved in this process [18]. Interestingly, LEAS inhibited the activation of MAPK p38 ~60% (Figure 4), suggesting that this kinase could have a relevant participation in the observed reduction of internalization. However, other approaches are necessary to determine the precise participation of p38 in this process.

Mastitis is an inflammation of the mammary gland caused principally by bacteria, which leads to the activation of the innate immune system [29]. TNF-α is a rapid-response proinflammatory cytokine expressed in bMECs and plays an important role in mastitis. Bacterial stimulation of bMECs induces the expression of TNF-α but is depending of the strain [30, 31]. bMECs challenged with S. aureus induced the expression of TNF-α up to 11-fold (data not shown), which coincides with the reported by our group

[26]. However, bMECs treated with vehicle (DMSO 0.1%) and challenged 2 h with bacteria maintained the basal expression of the TNF-α mRNA (Table 3), which was attributable to the anti-inflammatory effects of DMSO, as reported in Caco-2 cells [32]. Noteworthy, LEAS (100 ng/ml) treatment decreased the expression of this cytokine 0.5-fold in bMECs, which was maintained even when cells were infected. This result is in accordance with a downregulation of TNF-α in pretreated bMECs with cholecalciferol (a lipid molecule) [19]. Also, we detected similar levels of TNF-α secretion in bMECs infected or pretreated with LEAS before the S. aureus challenge. However, the IL-1β secretion was induced in the infected LEAS-treated cells (Table 4) but not the mRNA expression of this gene. This effect can be the consequence of the activation of other mechanisms, such as inflammasome activation, which requires further research [33]. Interestingly, pretreated bMECs with LEAS showed an upregulation in IL-10 expression, which was more pronounced in bMECs challenged with bacteria (~20-fold). These results are attractive due to the fact that this cytokine is not significantly induced by S. aureus in the udder [34]. Interestingly, these anti-inflammatory effects of LEAS on bMECs (TNF-α downregulation and IL-10 upregulation) correlated with the decrease in the internalization of S. aureus into bMECs.

With regard to antimicrobial peptides, these molecules actively contribute to IIR by direct action against microbial infection and as a component of the inflammatory response [35]. It has been reported that bMECs express diverse antimicrobial peptides: among them are the β-defensins. During IIR of the bovine mammary gland against bacterial infections, it has been reported that the expression of β-defensin and bovine neutrophil defensin 5 (BNBD5) increases significantly [3, 26]. Similarly, BNBD5 is expressed in the bovine mammary gland, especially in bMECs, and its expression levels depend on the bacterial stimulus [36]. However, in pretreated bMECs with LEAS, the expression of BNBD5 was not modified; only when these cells were challenged with S. aureus an increase was observed (Table 3). Nevertheless, it is necessary to evaluate other antimicrobial peptides in future experiments in order to determine their contribution in the S. aureus internalization reduction induced by LEAS.

According to the results of this work, we propose that LEAS could be applied as a prophylactic treatment to avoid bovine intramammary infections, because they improve bMEC innate immune response.

5. Conclusions

The results of this work shown that lipid-rich extract from avocado (LEAS) is a modulator of innate immune response in bovine mammary epithelial cells during S. aureus infection. Also, LEAS (100 ng/ml) inhibits bacterial internalization into bMECs. These data suggest that LEAS could be useful for mastitis control.

Data Availability

The data used to support the findings of this study are included within the article.

Conflicts of Interest

The authors declare no conflict of interest.

Acknowledgments

References

[1] N. Alva-Murillo, J. E. López-Meza, and A. Ochoa-Zarzosa, "Nonprofessional phagocytic cell receptors involved in *Staphylococcus aureus* internalization," *BioMed Research International*, vol. 2014, Article ID 538546, 9 pages, 2014.

[2] J. Oviedo-Boyso, J. J. Valdez-Alarcón, M. Cajero-Juárez et al., "Innate immune response of bovine mammary gland to pathogenic bacteria responsible for mastitis," *The Journal of Infection*, vol. 54, no. 4, pp. 399–409, 2007.

[3] A. Ochoa-Zarzosa, E. Villarreal-Fernández, H. Cano-Camacho, and J. E. López-Meza, "Sodium butyrate inhibits *Staphylococcus aureus* internalization in bovine mammary epithelial cells and induces the expression of antimicrobial peptide genes," *Microbial Pathogenesis*, vol. 47, no. 1, pp. 1–7, 2009.

[4] I. K. Sundar and I. Rahman, "Vitamin D and susceptibility of chronic lung diseases: role of epigenetics," *Frontiers in Pharmacology*, vol. 2, p. 50, 2011.

[5] O. K. Dego, J. E. van Dijk, and H. Nederbragt, "Factors involved in the early pathogenesis of bovine *Staphylococcus aureus* mastitis with emphasis on bacterial adhesion and invasion. A review," *The Veterinary Quarterly*, vol. 24, no. 4, pp. 181–198, 2002.

[6] S. L. Aitken, C. M. Corl, and L. M. Sordillo, "Immunopathology of mastitis: insights into disease recognition and resolution," *Journal of Mammary Gland Biology and Neoplasia*, vol. 16, no. 4, pp. 291–304, 2011.

[7] M. Fraunholz and B. Sinha, "Intracellular *Staphylococcus aureus*: live-in and let die," *Frontiers in Cellular and Infection Microbiology*, vol. 2, p. 43, 2012.

[8] N. Alva-Murillo, A. Ochoa-Zarzosa, and J. E. López-Meza, "Effects of sodium octanoate on innate immune response of mammary epithelial cells during *Staphylococcus aureus* internalization," *BioMed Research International*, vol. 2013, Article ID 927643, 8 pages, 2013.

[9] A. D. Téllez-Pérez, N. Alva-Murillo, A. Ochoa-Zarzosa, and J. E. López-Meza, "Cholecalciferol (vitamin D) differentially regulates antimicrobial peptide expression in bovine mammary epithelial cells: implications during *Staphylococcus aureus* internalization," *Veterinary Microbiology*, vol. 160, no. 1-2, pp. 91–98, 2012.

[10] D. Dabas, R. Shegog, G. Ziegler, and J. Lambert, "Avocado (*Persea americana*) seed as a source of bioactive phytochemicals," *Current Pharmaceutical Design*, vol. 19, no. 34, pp. 6133–6140, 2013.

[11] R. Y. Au, T. K. Al-Talib, A. Y. Au, P. V. Phan, and C. G. Frondoza, "Avocado soybean unsaponifiables (ASU) suppress TNF-α, IL-1β, COX-2, iNOS gene expression, and prostaglandin E_2 and nitric oxide production in articular chondrocytes and monocyte/macrophages," *Osteoarthritis and Cartilage*, vol. 15, no. 11, pp. 1249–1255, 2007.

[12] L. F. Heinecke, M. W. Grzanna, A. Y. Au, C. A. Mochal, A. Rashmir-Raven, and C. G. Frondoza, "Inhibition of cyclooxygenase-2 expression and prostaglandin E_2 production in chondrocytes by avocado soybean unsaponifiables and epigallocatechin gallate," *Osteoarthritis and Cartilage*, vol. 18, no. 2, pp. 220–227, 2010.

[13] G. Donnarumma, E. Buommino, A. Baroni et al., "Effects of AV119, a natural sugar from avocado, on *Malassezia furfur* invasiveness and on the expression of HBD-2 and cytokines in human keratinocytes," *Experimental Dermatology*, vol. 16, no. 11, pp. 912–919, 2007.

[14] S. M. D'Ambrosio, C. Han, L. Pan, A. Douglas Kinghorn, and H. Ding, "Aliphatic acetogenin constituents of avocado fruits inhibit human oral cancer cell proliferation by targeting the EGFR/RAS/RAF/MEK/ERK1/2 pathway," *Biochemical and Biophysical Research Communications*, vol. 409, no. 3, pp. 465–469, 2011.

[15] E. A. Lee, L. Angka, S. G. Rota et al., "Targeting mitochondria with Avocatin B induces selective leukemia cell death," *Cancer Research*, vol. 75, no. 12, pp. 2478–2488, 2015.

[16] G. Rosenblat, S. Meretski, J. Segal et al., "Polyhydroxylated fatty alcohols derived from avocado suppress inflammatory response and provide non-sunscreen protection against UV-induced damage in skin cells," *Archives of Dermatological Research*, vol. 303, no. 4, pp. 239–246, 2011.

[17] J. L. Anaya-López, O. E. Contreras-Guzmán, A. Cárabez-Trejo et al., "Invasive potential of bacterial isolates associated with subclinical bovine mastitis," *Research in Veterinary Science*, vol. 81, no. 3, pp. 358–361, 2006.

[18] N. Alva-Murillo, I. Medina-Estrada, M. Báez-Magaña, A. Ochoa-Zarzosa, and J. E. López-Meza, "The activation of the TLR2/p38 pathway by sodium butyrate in bovine mammary epithelial cells is involved in the reduction of *Staphylococcus aureus* internalization," *Molecular Immunology*, vol. 68, no. 2, pp. 445–455, 2015.

[19] N. Alva-Murillo, A. D. Téllez-Pérez, I. Medina-Estrada, C. Álvarez-Aguilar, A. Ochoa-Zarzosa, and J. E. López-Meza, "Modulation of the inflammatory response of bovine mammary epithelial cells by cholecalciferol (vitamin D) during *Staphylococcus aureus* internalization," *Microbial Pathogenesis*, vol. 77, pp. 24–30, 2014.

[20] M. M. Tarpey and I. Fridovich, "Methods of detection of vascular reactive species: nitric oxide, superoxide, hydrogen peroxide, and peroxynitrite," *Circulation Research*, vol. 89, no. 3, pp. 224–236, 2001.

[21] J. G. Kenny, D. Ward, E. Josefsson et al., "The *Staphylococcus aureus* response to unsaturated long chain free fatty acids: survival mechanisms and virulence implications," *PLoS One*, vol. 4, no. 2, article e4344, 2009.

[22] C. H. Chen, Y. Wang, T. Nakatsuji et al., "An innate bactericidal oleic acid effective against skin infection of methicillin-resistant *Staphylococcus aureus*: a therapy concordant with evolutionary medicine," *Journal of Microbiology and Biotechnology*, vol. 21, no. 4, pp. 391–399, 2011.

[23] A. P. Desbois and K. C. Lawlor, "Antibacterial activity of long-chain polyunsaturated fatty acids against *Propionibacterium acnes* and *Staphylococcus aureus*," *Marine Drugs*, vol. 11, no. 11, pp. 4544–4557, 2013.

[24] H. Sun, Y. Hu, Z. Gu, R. T. Owens, Y. Q. Chen, and I. J. Edwards, "Omega-3 fatty acids induce apoptosis in human breast cancer cells and mouse mammary tissue through

syndecan-1 inhibition of the MEK-Erk pathway," *Carcinogenesis*, vol. 32, no. 10, pp. 1518–1524, 2011.

[25] C. E. Rodriguez-Lopez, C. Hernandez-Brenes, and R. I. Diaz de la Garza, "A targeted metabolomics approach to characterize acetogenin profiles in avocado fruit (*Persea americana* Mill.)," *RSC Advances*, vol. 5, no. 128, pp. 106019–106029, 2015.

[26] N. Alva-Murillo, A. Ochoa-Zarzosa, and J. E. López-Meza, "Short chain fatty acids (propionic and hexanoic) decrease *Staphylococcus aureus* internalization into bovine mammary epithelial cells and modulate antimicrobial peptide expression," *Veterinary Microbiology*, vol. 155, no. 2-4, pp. 324–331, 2012.

[27] I. Medina-Estrada, J. E. López-Meza, and A. Ochoa-Zarzosa, "Anti-inflammatory and antimicrobial effects of estradiol in bovine mammary epithelial cells during *Staphylococcus aureus* internalization," *Mediators of Inflammation*, vol. 2016, Article ID 6120509, 16 pages, 2016.

[28] T. M. de Lima, L. de Sa Lima, C. Scavone, and R. Curi, "Fatty acid control of nitric oxide production by macrophages," *FEBS Letters*, vol. 580, no. 13, pp. 3287–3295, 2006.

[29] Y. H. Schukken, J. Günther, J. Fitzpatrick et al., "Host-response patterns of intramammary infections in dairy cows," *Veterinary Immunology and Immunopathology*, vol. 144, no. 3-4, pp. 270–289, 2011.

[30] Y. Strandberg, C. Gray, T. Vuocolo, L. Donaldson, M. Broadway, and R. Tellam, "Lipopolysaccharide and lipoteichoic acid induce different innate immune responses in bovine mammary epithelial cells," *Cytokine*, vol. 31, no. 1, pp. 72–86, 2005.

[31] C. Zbinden, R. Stephan, S. Johler et al., "The inflammatory response of primary bovine mammary epithelial cells to *Staphylococcus aureus* strains is linked to the bacterial phenotype," *PLoS One*, vol. 9, no. 1, article e87374, 2014.

[32] S. Hollebeeck, T. Raas, N. Piront et al., "Dimethyl sulfoxide (DMSO) attenuates the inflammatory response in the *in vitro* intestinal Caco-2 cell model," *Toxicology Letters*, vol. 206, no. 3, pp. 268–275, 2011.

[33] K. Breyne, S. K. Cool, D. Demon et al., "Non-classical proIL-1beta activation during mammary gland infection is pathogen-dependent but caspase-1 independent," *PLoS One*, vol. 9, no. 8, article e105680, 2014.

[34] D. D. Bannerman, M. J. Paape, J.-W. Lee, X. Zhao, J. C. Hope, and P. Rainard, "*Escherichia coli* and *Staphylococcus aureus* elicit differential innate immune responses following intramammary infection," *Clinical and Diagnostic Laboratory Immunology*, vol. 11, no. 3, pp. 463–472, 2004.

[35] P. Cormican, K. G. Meade, S. Cahalane et al., "Evolution, expression and effectiveness in a cluster of novel bovine β-defensins," *Immunogenetics*, vol. 60, no. 3-4, pp. 147–156, 2008.

[36] T. Goldammer, H. Zerbe, A. Molenaar et al., "Mastitis increases mammary mRNA abundance of β-defensin 5, toll-like-receptor 2 (TLR2), and TLR4 but not TLR9 in cattle," *Clinical and Vaccine Immunology*, vol. 11, no. 1, pp. 174–185, 2004.

Review Article

Immunopathology of Airway Surface Liquid Dehydration Disease

Brandon W. Lewis, Sonika Patial ⓘ, and Yogesh Saini ⓘ

Department of Comparative Biomedical Sciences, School of Veterinary Medicine, Louisiana State University, Baton Rouge, LA 70803, USA

Correspondence should be addressed to Yogesh Saini; ysaini@lsu.edu

The primary purpose of pulmonary ventilation is to supply oxygen (O_2) for sustained aerobic respiration in multicellular organisms. However, a plethora of abiotic insults and airborne pathogens present in the environment are occasionally introduced into the airspaces during inhalation, which could be detrimental to the structural integrity and functioning of the respiratory system. Multiple layers of host defense act in concert to eliminate unwanted constituents from the airspaces. In particular, the mucociliary escalator provides an effective mechanism for the continuous removal of inhaled insults including pathogens. Defects in the functioning of the mucociliary escalator compromise the mucociliary clearance (MCC) of inhaled pathogens, which favors microbial lung infection. Defective MCC is often associated with airway mucoobstruction, increased occurrence of respiratory infections, and progressive decrease in lung function in mucoobstructive lung diseases including cystic fibrosis (CF). In this disease, a mutation in the *cystic fibrosis transmembrane conductance regulator* (*CFTR*) gene results in dehydration of the airway surface liquid (ASL) layer. Several mice models of *Cftr* mutation have been developed; however, none of these models recapitulate human CF-like mucoobstructive lung disease. As an alternative, the *Scnn1b* transgenic (*Scnn1b*-Tg+) mouse model overexpressing a transgene encoding *sodium channel nonvoltage-gated 1, beta subunit* (*Scnn1b*) in airway club cells is available. The *Scnn1b*-Tg+ mouse model exhibits airway surface liquid (ASL) dehydration, impaired MCC, increased mucus production, and early spontaneous pulmonary bacterial infections. High morbidity and mortality among mucoobstructive disease patients, high economic and health burden, and lack of scientific understanding of the progression of mucoobstruction warrants in-depth investigation of the cause of mucoobstruction in mucoobstructive disease models. In this review, we will summarize published literature on the *Scnn1b*-Tg+ mouse and analyze various unanswered questions on the initiation and progression of mucoobstruction and bacterial infections.

1. Background

Aerobic processes within a cell consume oxygen (O_2) and release carbon dioxide (CO_2) during the process of respiration. Pulmonary ventilation is responsible for supplying O_2 to and eliminating CO_2 from cells undergoing aerobic respiration. In addition to oxygen, aberrant constituents of ambient air such as abiotic insults and airborne pathogens are also inhaled into the airspaces [1]. Upon entering the conducting airways, airborne insults are trapped within the airway surface liquid (ASL) layer, a thin layer of hydrated mucus that lines the airway epithelium. The airway epithelial cells are specialized to constitute a mucociliary clearance (MCC) host defense mechanism that facilitates the removal of trapped

insults [1]. Ciliated cells move the layer of mucus containing the airborne insults towards the epiglottis, thus away from airspaces [1].

Defects in the functioning of the mucociliary escalator compromise the MCC of inhaled pathogens and abiotic insults, which favors airspace infection and lung injury, respectively [2]. Impaired MCC is also often associated with airway mucoobstruction in mucoobstructive lung disease patients [2]. The cause-effect relationship between these two responses and their effect on microbial infections are unclear. High morbidity and mortality among mucoobstructive disease patients, high economic and health burden, and lack of scientific understanding of the progression of mucoobstruction warrant in-depth investigation of the

pathogenesis of mucoobstruction using mucoobstructive disease models [3–5]. In this review, we will focus our discussion on MCC defect in cystic fibrosis (CF) and its recapitulation in a widely accepted mouse model of CF, i.e., *Scnn1b*-Tg+ mouse.

2. Physiology of ASL Layer

The ASL layer, a thin layer of fluid that lines the luminal surface of the airway epithelium, is comprised of two distinct layers: the mucus layer and the periciliary layer [1]. The mucus layer is a luminal (superficial) layer of ASL that is exposed to the air and traps the airborne insults [6]. Removal of inhaled pathogens and abiotic insults involves unidirectional movement of the mucus layer towards the epiglottis [1]. Located directly underneath the mucus layer, the aqueous periciliary layer bathes the cilia projecting from the airway epithelium and facilitates ciliary beating [2]. The force generated by the ciliary beating within the periciliary layer fuels the movement of the mucus layer towards the epiglottis [1] (Figures 1(a) and 2(a)).

The two layers work on the gel-on-brush model in which the large membrane-tethered mucins and mucopolysaccharides of the periciliary layer form a brush-like network of polymers on the epithelial surface [6]. Electron microscopic examination of cultured human bronchial epithelial cells reveals the brush to be a meshwork consisting of large tethered macromolecules, i.e., MUC1, MUC4, MUC16, MUC20, and heparan sulfate, that are attached to the ciliary shaft and epithelial cell surface [6]. These large tethered macromolecules create a semipermeable gradient mesh that becomes tighter near the epithelial surface and is seemingly impenetrable to MUC5B, MUC5AC, and inhaled particles [6]. Button et al. determined that 2 nm dextran particles readily infiltrate the periciliary layer to reach the epithelial surface, while 40 nm particles are excluded from reaching the epithelial surface [6]. Thus, the brush acts as a size-exclusion barrier for infiltrating entities [6].

The periciliary brush also contributes to the regulation of ASL layer hydration by facilitating water distribution between the two layers [6]. Identical charges among the membrane-tethered macromolecules create intermolecular repulsive forces to create an osmotic pressure gradient that stabilizes the periciliary layer by opposing the osmotic pressure gradient created by the overlying mucus layer [6]. In healthy hydrated airways, osmotic pressure created by the brush keeps the mucus layer above the outstretched cilia and facilitates normal MCC [6]. During dehydration of the ASL layer in diseases such as CF, water is first drawn from the mucus layer, increasing the concentration of mucus and osmotic pressure [6]. As the pressure generated from the mucus layer increases, water is drawn from the mucus layer as well as the periciliary layer, resulting in ciliary compression and impaired MCC [6].

Contrary to a previous hypothesis that the periciliary layer is stationary, a study by Matsui et al. reveals that the periciliary layer is moved along with the mucus layer and dextran was cleared at a similar rate by both layers [7, 8]. Simple frictional interaction between the two layers does not account for the similar clearance rates [8]. Matsui et al. propose that a transfer of momentum takes place in order to facilitate the efficient movement of the two layers [8]. Ciliary beating promotes momentum transfer from the mucus layer to the periciliary layer, thus facilitating the concerted movement of both layers [8]. The transport rate and the contribution of both layers towards efficient MCC are determined by the amount and composition of the ASL.

The amount of ASL, expressed as the height of the ASL layer, is a critical factor for the normal functioning of the mucociliary escalator. While the height of the mucus layer varies depending on the airway location (7-70 μm), the optimal height of the periciliary layer in human airways is approximately 7 μm, approximately the height of outstretched cilia [1, 2, 9]. The height of the ASL layer is regulated by a concerted action of various ion channels on the apical surface of the airway epithelium [10]. Major ion channels responsible for regulating chloride (Cl^-)/sodium (Na^+) transport are the cystic fibrosis transmembrane conductance regulator (CFTR), calcium-activated chloride channels (CaCCs), and epithelial Na^+ channels (ENaC) [10]. While epithelial excretion of Cl^- is regulated by CFTR and CaCCs, epithelial Na^+ absorption is regulated by ENaC [10]. CFTR is also responsible for bicarbonate (HCO_3^-) transport that regulates the local pH of the airways [11]. The outcome of the concerted action of these ion channels regulates Cl^- and Na^+ transport across the apical surface of airway epithelial cells, thus regulating the hydration status of the airway epithelium [10].

Another factor determining the efficient functioning of the MCC system is the percent solids in the ASL layer. The constituents of the ASL layer, including secreted mucins, immune cells, ions, antimicrobial peptides, and cytokines, account for approximately 2.5% of the solids in healthy airways [1, 12].

3. ASL Dehydration in CF: A Result of Single Ion-Channel Defect

CF lung disease exemplifies how the defective functioning of a single ion channel, i.e., CFTR, results in serious disturbances in ASL physiology (Figures 1(b) and 2(b)). With the loss of CFTR function in CF epithelial cells, Cl^- is retained within the epithelial cells while Na^+ absorption by ENaC increases, leading to increased epithelial cytosolic NaCl contents [9, 13]. The increased cytosolic contents of NaCl in epithelial cells create an osmotic drive that promotes net movement of water from the ASL layer into the epithelial cells, thus leading to ASL layer dehydration.

The dehydration of the ASL layer results in the increased concentration of solutes (hyperconcentration) that leads to the compression of the periciliary layer by the overlying mucus layer, resulting in ciliary collapse and impaired MCC [6]. An increase from 2.5% to 6% solids, e.g., in CF airways, in the ASL layer compromises ciliary beat frequency and mucus layer transport [12]. Whether the increase in percent solids in mucoobstructive airways is a direct result of ASL layer dehydration or excessive accumulation or poor clearance of aberrant entities such as mucus plugs, microbes,

Normal airways

(a)

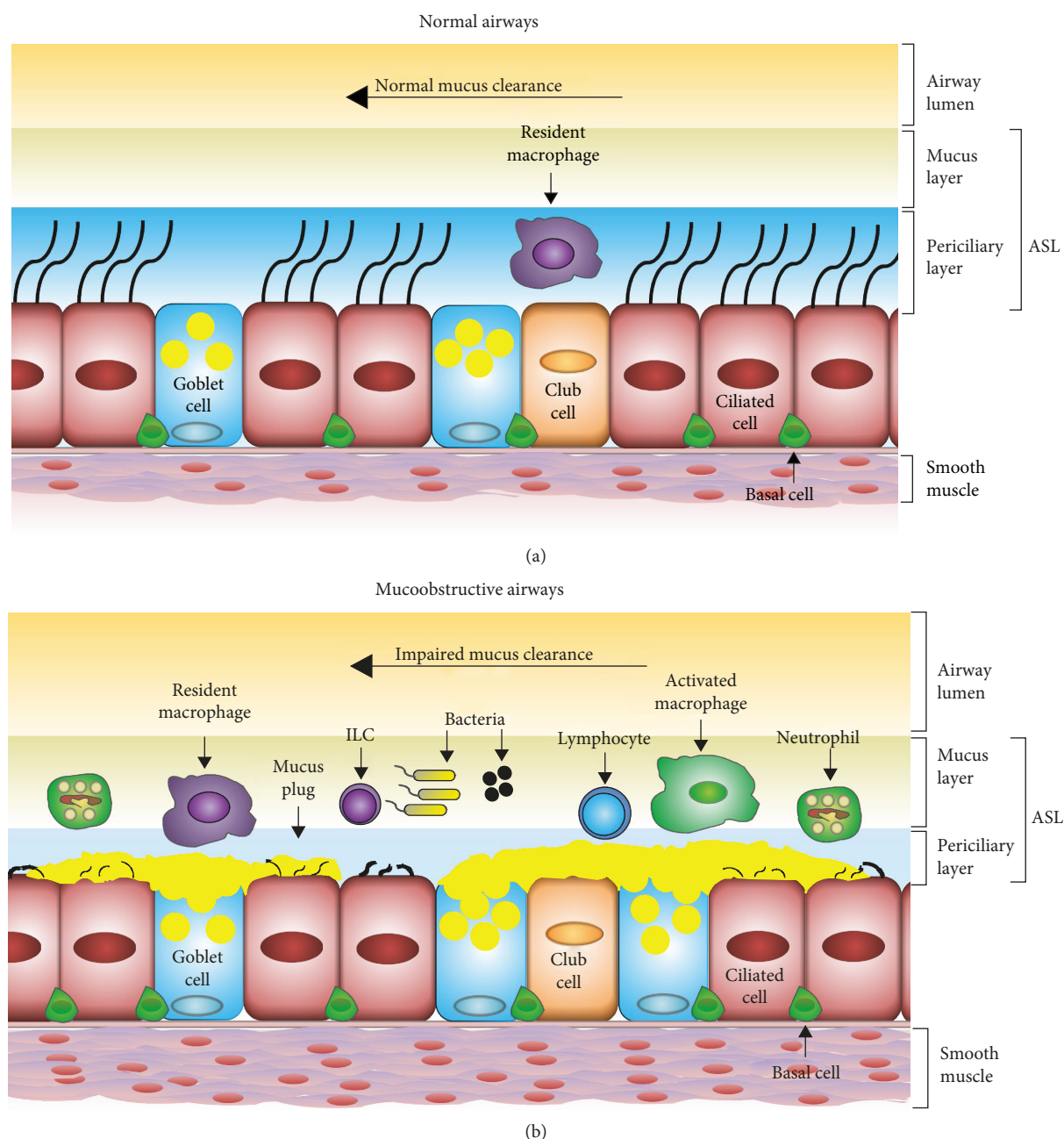Mucoobstructive airways

(b)

FIGURE 1: Diagrammatic comparisons of normal and mucoobstructive airways. (a) In normal airways, the normal functioning of epithelial ion channels maintains a healthy ASL layer. The normal functioning of the mucociliary clearance system efficiently clears aberrant ASL constituents. As a result, the epithelial layer consists of a balanced proportion of various epithelial cell types, including ciliated cells, club cells, and goblet cells. In addition, resident macrophages continue to perform their sentinel roles. (b) In mucoobstructive airways, an ion-channel defect causes ASL dehydration, which leads to mucus hyperconcentration, mucoobstruction, mucous cell metaplasia, bacterial infection, and airway inflammation.

inflammatory cells, and cellular debris, or a combination of all three outcomes, remains unclear.

4. Animal Models of ASL Dehydration

Although CF affects multiple organs, mucoobstructive lung disease is the major contributor to the morbidity and mortality associated with CF [14]. Various *Cftr*-knockout animal models including mice, pigs, ferrets, and rats have been

generated with the intent of recapitulating mucociliary clearance impairment of human CF airways. In Sections 4.1, 4.2, 4.3, 4.4, and 4.5, the advantages and limitations of various animal models of impaired *Cftr* functioning and ASL dehydration will be discussed.

4.1. Mice. The availability of strains with genetic alterations of genes related to various inflammatory or pathological outcomes is an unmatched advantage of employing mouse as

(a) Normal airways

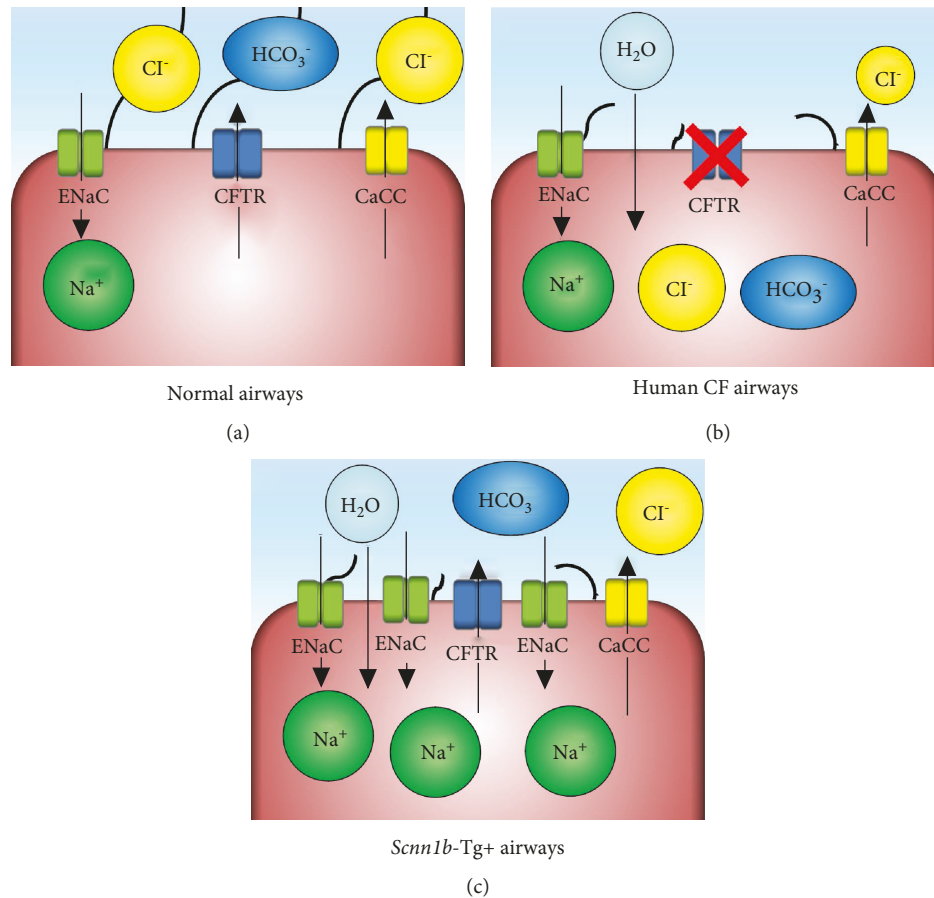(b) Human CF airways

(c) *Scnn1b*-Tg+ airways

FIGURE 2: Ion-channel physiology in airways. (a) The hydration state of normal airways in airway surface liquid (ASL) is regulated by the concerted action of ion channels. Major ion channels responsible for regulating chloride (Cl^-)/sodium (Na^+) transport are the cystic fibrosis transmembrane conductance regulator (CFTR), calcium-activated chloride channels (CaCCs), and epithelial Na^+ channels (ENaC). CFTR and CaCCs are responsible for regulating Cl^- transport, while ENaC facilitates epithelial Na^+ absorption. CFTR is also responsible for bicarbonate (HCO_3^-) transport that regulates the local pH of the airways. Balanced ionic transport maintains water contents of ASL in the physiological range. (b) In cystic fibrosis, a dysfunctional CFTR channel results in the net movement of sodium ions into the cytoplasm of airway epithelial cells. The osmotic drive due to sodium hyperabsorption dictates the net movement of ASL water into the cytoplasm of airway epithelial cells. These alterations result in the pathology of CF lung disease. (c) In mice, the chloride ion transport inhibition due to the genetic inactivation of a CFTR channel defect is compensated by relatively more prominent CaCCs. In *Scnn1b*-Tg+ airways, the overexpression of ENaC results in the hyperabsorption of sodium ion into the cytoplasm of airway epithelial cells, an ionic imbalance defect similar to human CF airways.

a disease model. Therefore, to recapitulate human CF-like lung disease, a number of mouse models have been developed over the past two decades (summarized in Table 1).

To begin with, in 1992, Snouwaert et al. generated the *Cftr*[tm1UNC] mouse via targeted disruption of the *Cftr* gene (Table 1) [15]. When compared with wild-type (WT) mice, *Cftr*[tm1UNC] mice exhibited mortality due to intestinal mucoobstruction; however, contrary to many pathological changes observed in human CF patients, these mice did not exhibit significant pathological changes in the pancreas, male reproductive system, liver, and gallbladder [15]. Although mucoobstruction and bacterial infection were not observed in the airways in *Cftr*[tm1UNC] mice, an increase in goblet cells in the proximal airways and impaired MCC were observed [15, 16]. Although the *Cftr*[tm1UNC] mouse model exhibited impaired MCC upon bacterial challenge, it did not recapitulate the spontaneously arising airway mucoobstruction and bacterial infection observed in CF patients.

In 1992, Dorin et al. generated the *Cftr*[tm1HGU] mouse model also via targeted disruption of exon 10 [17]. Similar to *Cftr*[tm1UNC] mice, the *Cftr*[tm1HGU] mice exhibited no pathological abnormalities in the pancreas and reproductive system, although one male exhibited increased mucus accumulation in the vas deferens [17]. Unlike the *Cftr*[tm1UNC] mouse model, however, the *Cftr*[tm1HGU] mouse model exhibited only mild intestinal mucoobstruction and all pups were able to survive past weaning [17]. Although the airway mucoobstructive phenotype associated with CF was not observed, upon challenge with two types of bacteria commonly associated with CF, i.e., *Staphylococcus aureus* and *Burkholderia cepacia*, *Cftr*[tm1HGU] mice exhibited pathological features of CF lung disease [18]. *Cftr*[tm1HGU] mice exhibited difficulty in clearing the bacteria from the airspaces as effectively as WT littermates [18]. The airways of *Cftr*[tm1HGU] mice also exhibited a marked increase in the abundance of goblet cells and mucoobstruction in response to bacterial

Table 1: Mouse models of single ion-channel defect.

S. No.	Model name	Strain background	Transgene/mutation	Spontaneous onset of lung disease	Airway mucus obstruction	Airway mucous cell metaplasia	Spontaneous airway bacterial infection	Chronic airway inflammation	Mortality	Reference
1	$Cftr^{tm}$ 1UNC	C57BL/6	Mutation (exon 10)	No	Absent	Present only upon bacterial challenge	Absent	Neutrophilic infiltration at day 30	Yes	(Snouwaert et al., [15])
2	$Cftr^{tm}$ 1HGU	MF1	Mutation (exon 10)	No	Absent	Present only upon bacterial challenge	Absent	Absent	No	(Dorin et al., [17])
3	$Cftr^{tm}$ 1CAM	C57BL/6	Mutation (exon 10)	No	Absent	Absent	Absent	Absent	Yes	(Ratcliff et al., [19])
4	$Cftr^{tm}$ 1BAY	C57BL/6 × 129	Mutation (exon 3)	No	Absent	Absent	Absent	Absent	Yes	(O'Neal et al., [20])
5	$Cftr^{tm}$ 3BAY	129/Sv	Mutation (exon 2)	No	Absent	Absent	Absent	Absent	Yes	(Hasty et al., [21])
6	$Cftr^{tm}$ 2CAM	C57BL/6	Mutation ($\Delta F508$)	No	Absent	Absent	Absent	Absent	Yes	(Colledge et al., [23])
7	$Cftr^{tm}$ 1EUR	FVB	Mutation ($\Delta F508$)	No	Absent	Absent	Absent	Absent	No	(van Doorninck et al., [25])
8	$Cftr^{tm}$ 1KTH	C57BL/6 × 129	Mutation ($\Delta F508$)	No	Absent	Absent	Absent	Absent	Yes	(Zeiher et al., [24])
9	$Cftr^{tm}$ 1HSC	129/SV	Mutation (exon 1)	No	Absent	Absent	Absent	Absent	Yes	(Rozmahel et al., [22])
10	$Cftr^{G5}$ 51D	CD1/129	Mutation (G551D)	No	Absent	Absent	Absent	Absent	Yes	(Delaney et al., [26])
11	$Cftr^{tm}$ 2HGU	C57BL/6 × 129	Mutation (G480C)	No	Absent	Absent	Absent	Absent	No	(Dickinson et al., [27])
12	Scnn1b-Tg+	C3H : C57	Transgene (Scnn1b)	Yes	Yes	Yes	Postnatal	Yes	Yes	(Mall et al., [36])
13	$Cftr^{tm}$ 2UTH	C57BL/6	Mutation (R117H)	No	Absent	Absent	Absent	Absent	No	(van Heeckeren et al., [28])
14	$Cftr^{tm}$ 3UTH	C57BL/6	Mutation (Y122X)	No	Absent	Absent	Absent	Absent	Yes	(van Heeckeren et al., [28])

challenge [18]. Although the $Cftr^{tm1HGU}$ mouse model, similar to $Cftr^{tm1UNC}$, exhibited impaired MCC in response to challenge, it also did not exhibit the spontaneously occurring mucoobstructive phenotype seen in CF airways.

Similar to the previously mentioned models, Ratcliff et al. targeted exon 10 of $Cftr$ to generate the $Cftr^{tm1CAM}$ mouse model [19]. Similar to $Cftr^{tm1UNC}$, $Cftr^{tm1CAM}$ pups exhibited increased mortality attributed to intestinal mucoobstruction [19]. Similar to human CF patients, $Cftr^{tm1CAM}$ mice exhibited obstruction of the pancreatic ducts, a phenotype not observed in $Cftr^{tm1UNC}$ and $Cftr^{tm1HGU}$ mice [19]. An interesting phenotype observed in the $Cftr^{tm1CAM}$ model that was previously not reported in $Cftr^{-/-}$ mice was the susceptibility to ocular infections and lacrimal gland abnormalities [19]. Although the $Cftr^{tm1CAM}$ mouse exhibited increased mortality, intestinal mucus obstruction, and pancreatic abnormalities, this model still did not exhibit mucus accumulation in the airways as seen in CF [19].

In 1993, O'Neal et al. generated the $Cftr^{tm1BAY}$ mouse model by targeted disruption of exon 3 in the $Cftr$ locus [20]. No pathological abnormalities, i.e., mucus obstruction, were observed in the lungs of $Cftr^{tm1BAY}$ [20]. This mouse model also exhibited increased mortality-associated mucoobstruction of the intestines [20]. In 1995, Hasty et al. targeted exon 2 of the $Cftr$ in order to generate the $Cftr^{tm3BAY}$ mouse model [21]. In accordance to the previous mouse models, $Cftr^{tm3BAY}$ mice exhibited high mortality as a result of severe intestinal mucoobstruction [21]. $Cftr^{tm3BAY}$ mice also did not exhibit an onset of lung disease, liver disease, or obstruction of the pancreatic ducts when examined at birth, one week of age, or three to four weeks of age [21]. A clinical phenotype that is commonly associated with male CF patients is sterility [15]. Contrary to the phenotype observed in male CF patients, $Cftr^{tm3BAY}$ males exhibited no reproductive abnormalities, whereas most females were sterile [21]. In 1996, Rozmahel et al. generated the $Cftr^{tm1HSC}$ mouse model on a 129/SV background by targeted disruption of exon 1 [22]. As seen in previously discussed models, the $Cftr^{tm1HSC}$ mouse model exhibited severe intestinal mucoobstruction that led to high mortality rates [22].

In 1995, two mouse models, i.e., $Cftr^{tm2CAM}$ and $Cftr^{tm1KTH}$, incorporating a deletion of phenylalanine at position 508 (ΔF508) of the $Cftr$ gene locus, the most common genetic mutation associated with human CF, were generated by two separate groups [23, 24]. Although significant mortality due to intestinal mucoobstruction was observed in both strains, no abnormalities in the pancreas, male reproductive system, or lungs were evident [23, 24]. In 1995, a third mouse, $Cftr^{tm1EUR}$, with the ΔF508 mutation was generated on an FVB background [25]. As seen in $Cftr^{tm2CAM}$ and $Cftr^{tm1KTH}$, pathological abnormalities, i.e., mucus retention, were not observed in the lungs, pancreas, liver, or vas deferens in these mice. However, these mice did not exhibit mortality due to intestinal mucus obstruction, but they did exhibit hypertrophy of goblet cells in the intestines [25]. The observed differences in the rate of mortality may be attributed to the strain background.

Also in 1996, Delaney et al. generated a mouse model possessing another mutation associated with human CF,

the G551D mutation ($Cftr^{G551D}$) that occurs in approximately 3% of CF patients [26]. The $Cftr^{G551D}$ also exhibited increased mortality due to intestinal mucoobstruction [26]. No pathological differences in the lungs, pancreas, and reproductive system were observed in $Cftr^{G551D}$ mice [26]. In 2002, Dickinson et al. generated the $Cftr^{tm2HGU}$ targeted integration of the G480C mutation, a mutation associated with human CF [27]. The $Cftr^{tm2HGU}$ exhibited comparable survival to WT littermates, and no intestinal mucoobstruction was observed [27]. Mild goblet cell hypertrophy was observed in the intestines of the $Cftr^{tm2HGU}$ mice [27]. There were no abnormalities reported in the lungs and the reproductive systems [27]. The $Cftr^{tm2UTH}$ model was generated by the integration of the R117H mutation, a mutation characterized by CFTR reaching the apical surface of the epithelium but not properly functioning [28]. Upon challenge with $Pseudomonas\ aeruginosa$, the $Cftr^{tm2UTH}$ mouse model exhibited significantly lower neutrophil counts as compared to similar inflammatory responses to a previous $Cftr^{-/-}$ mouse model, i.e., $Cftr^{tm1UNC}$, but presented no significant differences in inflammatory cytokine levels [28]. The $Cftr^{tm3UTH}$ mouse model was generated by integrating the Y122X mutation [28]. The $Cftr^{tm3UTH}$ mouse model exhibited lower levels of tumor necrosis factor alpha (TNF-α) and - interleukin 1 beta (IL-1β) when compared to the $Cftr^{tm1UNC}$ mouse model in response to $Pseudomonas\ aeruginosa$ [28]. Taken together, there were no substantial differences between the tested $Cftr^{-/-}$ mouse models in response to $Pseudomonas\ aeruginosa$ challenge [28]. Although mouse models of $Cftr$ knockdown or various functional mutations recapitulated the intestinal mucoobstruction, none of these models produced the spontaneous onset of airway mucoobstruction and airway bacterial infection exhibited in CF, warranting a need for an animal model that recapitulates human CF.

4.2. Pig. In order to address the limitations observed in CF mouse models, Rogers et al. generated $Cftr^{-/-}$ pigs that exhibited gastrointestinal, pancreatic, and reproductive abnormalities commonly associated with CF [29]. All $Cftr^{-/-}$ piglets exhibited meconium ileus, a phenotype seen in ~15% of human CF patients [29]. The pancreas of $Cftr^{-/-}$ piglets was morphologically smaller when compared with WT littermates and exhibited ductal obstruction [29]. Male $Cftr^{-/-}$ pigs were also infertile, a phenotype commonly associated with human male CF patients [29]. Pertaining to lung disease manifestation, no lung inflammation, mucus obstruction, or infection was observed at 6-12 hours after birth [29, 30]. However, $Cftr^{-/-}$ newborn pigs exhibited difficulty in clearing bacteria upon challenge, i.e., $Staphylococcus\ aureus$ [30]. $Cftr^{-/-}$ pigs that survived more than two months exhibited delayed onset of lung disease characterized by airway inflammation and mucoobstruction [30]. Although the $Cftr^{-/-}$ pig phenotypically expressed common hallmarks of CF, the mucoobstructive airway phenotypes in this model have been described as variable, ranging from no to severe manifestation [30].

4.3. Ferret. In 2010, Sun et al. generated the $Cftr^{-/-}$ ferret by targeted disruption that exhibited meconium ileus,

pancreatic lesions, degenerate or absent vas deferens, dehydration of the ASL layer, severe airway inflammation, and a predisposition to lung infections [31]. Due to the susceptibility to lung infections, antibiotic treatment was necessary for the survival of the $Cftr^{-/-}$ ferret [32]. The $Cftr^{-/-}$ ferret exhibited mortality by the age of six months with antibiotic treatment, with 3 of 11 $Cftr^{-/-}$ ferrets surviving [32]. In order to investigate the progression of lung disease, Sun et al. removed the $Cftr^{-/-}$ ferret from antibiotics at three months of age [32]. Upon cessation of antibiotic treatment, progressive lung disease that resembled human CF, i.e., mucoobstruction and bacterial colonization, was observed in the major and small airways [32]. Thus, antibiotic intervention was needed to enhance survival to induce a more applicable CF lung phenotype in the $Cftr^{-/-}$ ferret.

4.4. Rat.

In 2014, Tuggle et al. generated the $Cftr^{-/-}$ rat model by targeted disruption [33]. There was no significant difference in survival between $Cftr^{-/-}$ and WT littermates until weaning but survival was drastically decreased in the $Cftr^{-/-}$ rat by the age of six weeks [33]. Decreased survival was a result of intestinal mucoobstruction and complications [33]. There were no pancreatic abnormalities observed in the $Cftr^{-/-}$ rat [33]. Although the ASL layer in the $Cftr^{-/-}$ rat model was dehydrated, no pathological abnormalities were observed in the lungs at the age of 22 to 42 days [33]. Abnormal lung pathology developed as the $Cftr^{-/-}$ rats aged due to the development of submucosal gland hypertrophy [34]. At six months of age, the small airways of the $Cftr^{-/-}$ rat exhibited increased mucus secretion and accumulation leading to delayed mucus transport [34]. The $Cftr^{-/-}$ rat model did not exhibit airway obstruction or spontaneously arising bacterial infection [34].

While nonmurine $Cftr^{-/-}$ models have been somewhat successful in recapitulating the human CF-like spontaneous mucoobstruction and bacterial infection, unlike mice models, it remains challenging to introduce genetic changes into their genomes. The $Scnn1b$-Tg+ mouse model, although with an intact $Cftr$ gene, exhibits CF-like lung pathology. In Section 4.5, we will review the characteristics of this strain and modulation of $Scnn1b$-Tg+ lung disease upon various other genetic alterations.

4.5. Scnn1b-Tg+ Mouse Model.

None of the $Cftr^{-/-}$ mice models spontaneously recapitulate human CF-like disease, most likely due to the functional compensation by CaCCs [35]. To circumvent this issue, the $Scnn1b$-Tg+ mouse was generated to accomplish increased Na^+ absorption into the airway epithelial cells [36]. The increased Na^+ absorption in $Scnn1b$-Tg+ mice was achieved via overexpressing a transgene encoding sodium channel nonvoltage-gated 1, beta subunit ($Scnn1b$) in club cells (Figure 2(c)) [36]. Na^+ absorption is enhanced in tracheal tissues of adult and neonatal $Scnn1b$-Tg+ mice; the Cl^- secretion remained unaffected (Figure 2(c)) [36].

These mice exhibit various features of mucoobstructive airway diseases. The increased Na^+ absorption into the airway epithelium of $Scnn1b$-Tg+ mice is evident as early as postnatal day (PND) 3 that results in the dehydration of the ASL layer leading to mucoobstruction and impaired MCC [36, 37]. A longitudinal study revealed that high mortality (~50% in the first two weeks of life) is a result of asphyxiation related to airway mucoobstruction [37]. The $Scnn1b$-Tg+ mice exhibited difficulty in clearing bacteria upon challenge with Haemophilus influenzae and Pseudomonas aeruginosa [36].

The initial microbiological studies on bronchoalveolar lavage fluid (BALF) from $Scnn1b$-Tg+ adult mice failed to detect spontaneous bacterial infection [36]. Since the initial microbiological studies were conducted only in adult mice and speculating that mucoobstruction creates a microaerophilic environment, Livraghi-Butrico et al. hypothesized that $Scnn1b$-Tg+ mice would be more susceptible to pulmonary infections by microaerophilic bacteria in neonatal age when the immune system is underdeveloped as compared to adult $Scnn1b$-Tg+ mice [38]. Under microaerophilic conditions, BALF from $Scnn1b$-Tg+ neonates showed the presence of polymicrobial bacterial species of oropharyngeal origin [38].

The $Scnn1b$-Tg+ mouse model also exhibited necrosis of epithelial cells in the airways at newborn (PND 0.5) and neonatal (PND 3.5) stages [37]. Interestingly, epithelial cell hypoxia was observed in the mucoobstructive airways of $Scnn1b$-Tg+ mice [37]. It is likely that the hypoxic stress to the airway epithelial cells caused by mucoobstruction leads to epithelial necrosis [37]. The blood gas analyses on neonatal (PND 3.5-5.5) $Scnn1b$-Tg+ mice revealed a significant reduction in the partial pressure of oxygen (P_{O2}) and oxygen saturation, indicative of a systemic hypoxic environment [37]. This is most likely a result of bronchopulmonary dysplasia or emphysematous changes that are evident in $Scnn1b$-Tg+ mice. The $Scnn1b$-Tg+ mice manifest airway inflammation accompanied by granulocyte (neutrophil and eosinophil) infiltration and macrophage activation [37].

In the remaining parts of this review, we will discuss various immune cells in the context of muco-obstructive disease evolution in $Scnn1b$-Tg+ mice.

5. Macrophages

Macrophages are key sentinel cells that express pro- or anti-inflammatory functions based on the external cytokine milieu, broadly classified as M1 and M2 activation, respectively. M1 macrophages are associated with the elimination of pathogens and the secretion of proinflammatory cytokines, e.g., IL-1, IL-6, and IL-23 [39]. M1 macrophages also facilitate the expansion of TH17 lymphocytes that recruit neutrophils through the secretion of IL-17 [39]. Stimulation of M1 macrophages is facilitated by interferon gamma (IFN-γ), lipopolysaccharide (LPS), and other activators of Toll-like receptors (TLRs) [40–42]. Most of the TLRs require an adaptor molecule, myeloid differentiation factor 88 (MyD88), to initiate a downstream intracellular signaling cascade [43]. The MyD88 pathway leads to the activation of nuclear factor-kappa B (NF-κB), a key transcription factor in M1 activation that regulates the expression of a variety of inflammatory genes, e.g., TNF-α, IL1β, and interleukin 6 (IL-6) [44].

M2 macrophages are associated with parasitic infection, tissue remodeling, and promotion of Th2 responses [44]. Stimulation of M2 macrophages is facilitated through IL-4, IL-13, and IL-10 [45–47]. IL-4 and IL-13 facilitate the polarization of M2 macrophages through signal transducer and activator of transcription (STAT) 6, whereas IL-10 acts through STAT3 [48, 49].

Mall et al. initially observed morphological activation of pulmonary macrophages at two weeks, a phenotype that was found to persist into adulthood [37]. To profile molecular signatures of macrophages as they relate to the development of mucoobstructive lung disease, we performed gene expression analyses on purified *Scnn1b*-Tg+ macrophages at four disease-relevant time-points, i.e., PND 0 (less than 24 hours of age), 3, 10, and 42 [50]. There was evidence of both M1 and M2 macrophages in the BALF of *Scnn1b*-Tg+ mice at PND 3, with M1 as the more robust polarization state [50]. The predominance of M1 macrophages at PND 3 was found to be consistent with the presence of pulmonary bacterial infection typical of *Scnn1b*-Tg+ neonates [50]. The macrophage activation status experienced a shift to the M2 state at PND 10, and M2 was found to be more robust at PND 42 [50]. The robust molecular signatures exhibited by pulmonary macrophages during the progression of mucoobstructive lung disease in *Scnn1b*-Tg+ mice indicated their critical role in disease pathogenesis [50].

To elucidate the role of pulmonary macrophages in neonatal (PND 5-7) *Scnn1b*-Tg+ mice, we generated *Scnn1b*-Tg+ mice with macrophage deficiency [51]. In this strain, the expression of apoptosis-inducing diphtheria toxin A (DTA) was targeted to pulmonary macrophages via the myeloid cell-specific Lysozyme M (LysM) promoter [51, 52]. The superimposition of impaired MCC on macrophage depletion (DTA$^+$-*Scnn1b*-Tg+) resulted in ~51% mortality due to an emaciated phenotype characterized by reduced weight gain, "flaky discoloration," lethargy, and mortality [51]. Interestingly, macrophage depletion affected various inflammatory characteristics, i.e., alveolar space consolidation, airway inflammation, mucoobstruction, immune cell infiltration, and bacterial infection in *Scnn1b*-Tg+ [51]. The macrophage-depleted *Scnn1b*-Tg+ mice exhibited a significantly higher bacterial burden [51]. Although there was a presence of additional bacterial species, *Pasteurella pneumotropica* remained the predominant microbial inhabitant in the airways of macrophage-depleted mice.

To elucidate the contribution of pulmonary macrophages in mucoobstructive lung disease in adulthood, we compared the lung pathology of surviving macrophage-depleted adult mice [53]. Adult mice with macrophage deficiency exhibited a significantly higher degree of alveolar space consolidation [53]. Interestingly, DTA$^+$-*Scnn1b*-Tg+ adult mice exhibited a significantly higher degree of mucoobstruction in airways and an increased number of mucus-producing cells compared to DTA$^-$-*Scnn1b*-Tg+ littermates [53]. Taken together, these mechanistic reports that focused on the numerical depletion of macrophages highlighted the critical roles of these cells in the pathogenesis of lung disease in *Scnn1b*-Tg+ mice.

Matrix metalloproteinase- (*MMP-*) *12*, a candidate genetic contributor to the development of emphysema, was found to be upregulated in the lungs of *Scnn1b*-Tg+ mice [54]. MMP12 was also found to be significantly upregulated in BALF macrophages of CF patients [54]. Trojanek et al. determined that MMP12 proteolytic activity was significantly higher on the surface of activated BALF macrophages of *Scnn1b*-Tg+ mice [54]. The administration of pharmacological inhibitors as well as the genetic deletion of *Mmp12* in *Scnn1b*-Tg+ mice significantly reduced mean linear intercepts and destructive index [54]. Since MMP12 is expressed in non-macrophage cells as well, it remains to be determined whether inactivation or deletion of macrophage-originated *Mmp12* accounts for the amelioration of alveolar space pathology in *Scnn1b*-Tg+ mice. Further investigation employing macrophage-specific deletion of various functionally relevant genes is necessary to determine the effect of functionally compromised macrophages on various pathological features of *Scnn1b-Tg+* mice.

6. Neutrophils

Neutrophils are cells of the innate immune system that are typically the first cells to be recruited during inflammation and serve to eliminate invading pathogens [55]. Neutrophils employ a variety of mechanisms for bacterial killing, e.g., phagocytosis, degranulation, or release of neutrophil extracellular traps (NETs) [56]. In the process of phagocytosis, neutrophils engulf pathogens that are subsequently encapsulated in phagosomes [55]. Encapsulated pathogens are killed by the use of NADPH oxygenase-dependent mechanisms (reactive oxygen species) or antibacterial proteins contained within the neutrophilic granules [55]. These neutrophilic granules can also be released extracellularly through the process of degranulation in order to act upon extracellular pathogens [55]. Highly activated neutrophils produce NETs that can immobilize the pathogens for subsequent phagocytosis or directly kill the entrapped pathogens [56]. NETs are also composed of antimicrobial proteins and enzymes, e.g., lactoferrin, cathepsin, and neutrophil elastase (NE), responsible for the elimination of invading pathogens [56]. Interestingly, NE has been linked to both beneficial and detrimental roles in the pathogenesis of CF [57].

The S*cnn1b*-Tg+ mice exhibited neutrophilic airspace infiltration accompanied by increased expression of neutrophil chemoattractants, i.e., keratinocyte chemoattractant (KC), lipopolysaccharide-induced CXC chemokine (LIX), macrophage inflammatory protein 2 (MIP-2), and granulocyte-colony-stimulating factor (G-CSF), beginning in the neonatal stages and persisting into adulthood [37, 38]. NE has been implicated in the induction of emphysema [58], mucous cell metaplasia (MCM), and mucus hypersecretion [59, 60]. The ablation of *Ne* in *Scnn1b*-Tg+ mice resulted in a significant decrease in lung volume, mean linear intercepts, and destructive index as compared to *Scnn1b*-Tg+ littermates [57]. The *Ne*$^{-/-}$-*Scnn1b*-Tg+ mice also had reduced MCM and expression levels of genes associated with goblet cells and mucus secretion, i.e., *Gob5*, *Muc5ac*, and *Muc5b*, involved in this response [57]. These

results suggested that compromised neutrophil function via NE deletion ameliorates lung pathology in *Scnn1b*-Tg+ mice [57].

Myeloid differentiation primary response 88 (MyD88) is a cytosolic adaptor molecule that is required for the downstream signaling upon TLR ligation. The ablation of the *Myd88* gene in *Scnn1b*-Tg+ mice resulted in significantly increased mortality when compared to $Myd88^{+/-}$-*Scnn1b*-Tg+ littermates [38]. $Myd88^{-/-}$-*Scnn1b*-Tg+ mice also exhibited significantly increased bacterial burden by a greater diversity of bacterial species [61]. As compared to $Myd88^{+/-}$-*Scnn1b*-Tg+ mice, the $Myd88^{-/-}$-*Scnn1b*-Tg+ mice exhibited a significant reduction in neutrophils and BALF levels of neutrophil chemokines, i.e., KC, LIX, MIP-2, and G-CSF [38]. These data suggested that the ablation of TLR signaling in *Scnn1b*-Tg+ mice leads to the reduced production of neutrophil chemoattractants and poor neutrophil recruitment; thus, there is poor bacterial clearance.

7. Eosinophils

Eosinophils are granulated cells of the innate immune system that respond to helminths and allergies [62]. The eosinophilic granules have been found to contain IL-4, IL-6, IL-10, and TNF-α [63]. As compared to WT mice, the *Scnn1b*-Tg+ mice exhibited significantly increased eosinophilia that, unlike neutrophilia that persisted into adulthood, peaked during the juvenile (2-3 weeks) stages and subsided during the adult stages [37]. The eosinophil chemoattractant, Eotaxin 1, was found to be overexpressed in the *Scnn1b*-Tg+ mouse as compared to WT littermates [37]. The ablation of *interleukin- (IL-) 4 receptor alpha* (*Il4rα*), the receptor for IL-4 and IL-13, significantly reduced eosinophilic infiltration in 10-day old *Scnn1b*-Tg+ mice, suggesting the involvement of IL4Rα ligands in eosinophilic recruitment [64, 65]. However, the exact role of eosinophils in *Scnn1b*-Tg+ lung disease is not yet clear.

8. Natural Killer Cells

Natural killer (NK) cells are cells of the innate immune system that are responsible for eliminating tumor cells and virally infected cells [66, 67]. Johannson et al. found that NK cells determine "self" from "nonself" through the recognition of major histocompatibility complex class I (MHC-I) [68]. NK cells not only possess the ability to kill target cells but also possess the ability to produce IFN-γ and TNF-α [69]. Through the production of IFN-γ, NK cells have also been shown to be involved in the differentiation of Th1 lymphocytes [70]. While the levels of IFN-γ and TNF-α are found to be elevated in the BALF from *Scnn1b*-Tg+ mice, whether NK cells are involved in the pathogenesis of *Scnn1b*-Tg+ mice remains unexplored.

9. T-Lymphocytes

The cells of the adaptive immune system, i.e., T- and B-lymphocytes, possess antigen-specific surface receptors that undergo recombination in order to mature [71]. The recombination is facilitated through *recombinase activating gene- (RAG-) 1* and *RAG-2* [72]. T-lymphocytes are cells of the adaptive immune system and can functionally be divided into subsets, e.g., Th1, Th2, Th17, and T regulatory lymphocytes (Tregs) [73].

Th1 lymphocytes are responsible for controlling intracellular pathogens and are associated with the production of TNF-α and interferon-gamma (IFN-γ) [73]. Th2 lymphocytes are associated with the production with IL-4, IL-5, and IL-13 [73, 74]. As discussed previously, IL-4 and IL-13 have been linked to MCM and increased mucus production [75, 76]. Th17 lymphocytes secrete IL-17, a key proinflammatory cytokine associated with neutrophil recruitment [77]. Th17 lymphocytes are present during the early stages of CF, and a significant correlation exists between IL-17 and the total number of neutrophils [78]. *Pseudomonas aeruginosa* infection in BALF from CF patients is associated with significantly higher Th17-associated cytokines (IL-17, IL-6, IL-1β, and IL-8) [79]. Tregs are associated with the suppression of exacerbated Th2/Th17 inflammation [80]. CF patients with chronic *Pseudomonas aeruginosa* infection exhibited lower Treg counts when compared to CF patients without *Pseudomonas aeruginosa* infection [81].

Lymphocyte counts tend to be higher in BALF from *Scnn1b*-Tg+ mice as compared to their WT littermates, but a significant increase is evident only in adult *Scnn1b*-Tg+ mice [37]. While IFN-γ remains comparable between *Scnn1b*-Tg+ and their WT littermates, BALF levels of TNF-α, a Th1-associated cytokine, are elevated in the BALF of *Scnn1b*-Tg+ neonates [37]. Mall et al. found significantly higher levels of IL-13 starting at one week of age and waning after three weeks of age [37]. During this time, the *Scnn1b*-Tg+ mouse model exhibited significantly increased MCM and mucoobstruction [37]. A detailed analysis of the lungs for the presence of various subtypes of Th cells is warranted to completely understand the Th-associated responses in the *Scnn1b*-Tg+ mice.

10. B-Lymphocytes

B-lymphocytes (B-cells) secrete antigen-specific immunoglobulins (Ig) that constitute antigen-specific humoral immunity. In addition to bone marrow, spleen, and lymph nodes, B-cells localize in the tertiary lymphoid structures such as bronchus-associated lymphoid tissue (BALT) that surrounds bronchi in the lungs. BALTs are frequently found in CF patients and *Scnn1b*-Tg+ adult mice [38, 53, 82].

CF patients exhibit significantly higher levels of *Pseudomonas*-specific IgG antibodies [83]. Secretory IgA levels are also significantly upregulated in the nasal secretions of CF patients infected with *Pseudomonas aeruginosa* [84]. Livraghi-Butrico et al. found that $Myd88^{-/-}$-*Scnn1b*-Tg+ mice exhibited significantly more lymphoid aggregates at eight weeks of age than $Myd88^{+/-}$-*Scnn1b*-Tg+ littermates [38]. In our recent report, a significant increase in the presence of BALTs in the lung parenchyma of macrophage-deficient *Scnn1b*-Tg+ adults was observed [53]. The presence of these lymphoid aggregates was associated with higher levels of immunoglobulin (Ig) subtypes, i.e., IgA, IgM, IgG1, IgG2b,

and IgG3, in BALF from macrophage-deficient *Scnn1b*-Tg+ adults [53]. While the antigen specificity of these immuno-globulins remains to be investigated, their increased levels in mice with BALTs likely reflect local adaptive response to bacterial infections.

11. Innate Lymphoid Cells (ILCs)

Innate lymphoid cells (ILCs) are innate immune cells that secrete Th effector cytokines but lack antigen-specific receptors that require recombination [85]. In simpler description, the ILCs (ILC1, 2, and 3) are the amnestic equivalent of Th subtypes (Th1, Th2, and Th17) [85]. ILCs delineate separately from T lymphocytes based on the expression of the transcription factor inhibitor of DNA binding 2 (Id2) [86]. ILCs also require the common cytokine receptor γ-chain (also known as Il2rg) [87]. ILCs have been classified based on their expression of transcription factors and cytokines [87].

ILC1s differentiate independently from NK cells from Id2 expressing common helper ILC precursors (ChILPs) [86]. Moro et al. identified ILC2s in mouse mesentery that produce high levels of Th2-associated cytokines, i.e., IL-5 and IL-13, in response to IL-33 [88]. Subsequent studies revealed that ILC2s could also produce the Th2-associated cytokine IL-4 and rely on GATA-3 for differentiation and maintenance [89, 90]. Takatori et al. identified ILC3s that produce Th17-associated cytokines, i.e., IL-17 and IL-22, in response to IL-1β as well as IL-23 and produce IL-17 and IL-22 [91]. ILC3s rely on the expression of rare orphan receptor-(ROR-) γt for differentiation [87]. The role of ILCs in the pathogenesis and progression of lung disease in the *Scnn1b*-Tg+ mouse model remains unclear and warrants extensive investigation.

Given the predominance of Th-mediated responses in *Scnn1b*-Tg+ mice of different ages, it is critical to characterize ILC as well as Th populations in the *Scnn1b*-Tg+ mice. These studies when followed by ILCs and Th subtype depletion studies will dissect cell-specific roles in mucoobstructive lung disease in *Scnn1b*-Tg+ mice.

12. Spontaneous Bacterial Infection in CF

CF is characterized by early bacterial colonization by microbes originating from the oral cavity and progressively shifts to a pathogen-dominated environment [92]. Muhlebach et al. conducted a longitudinal study to characterize the microbiome in young CF patients [92]. The lower airways of CF infants were determined to be relatively sterile, but microbes commonly associated with the oral cavity, e.g., *Streptococcus* and *Prevotella*, were predominant in the airways by the age of two years [92]. Of note, the origin of spontaneous bacterial colonization in *Scnn1b*-Tg+ neonates was also determined to be oropharyngeal [38]. At four years of age, the microbiome analyses from CF patients revealed the presence of pathogenic bacterial species, e.g., *Staphylococcus aureus*, *Haemophilus influenzae*, and *Pseudomonas aeruginosa* [92]. The presence of a pathogenic species in CF patients was associated with significantly increased inflam-

mation and structural damage in the lungs [92]. Coburn et al. found that CF patients over the age of 25 exhibited a prevalence of *Pseudomonas aeruginosa* that was associated with declining lung function [93]. The progressive decline in lung function associated with *Pseudomonas aeruginosa* infection leads to respiratory failure and death in CF patients [94].

13. Does Infection Lead to the Airway Inflammation?

Whether inflammatory responses in mucoobstructive airways originate from infectious agents remained unclear until recently. To determine if the bacterial infection is essential for airway inflammation in *Scnn1b*-Tg+ mice, Livraghi-Butrico et al. rederived *Scnn1b*-Tg+ mice in a germ-free environment [38]. While, as expected, the germ-free *Scnn1b*-Tg+ mice did not exhibit airway bacterial colonization, other phenotypes including airway inflammation, macrophage activation, MCM, and airway mucoobstruction were still present [38]. Indeed, the macrophage activation was found to be more exaggerated in germ-free *Scnn1b*-Tg+ mice as compared to specific pathogen-free *Scnn1b*-Tg+ mice [50]. These results suggested that the inflammatory responses observed in germ-free *Scnn1b*-Tg+ mice were not dependent on the presence of microbes or pathogen-associated molecular patterns (PAMPs). Along the same lines, antibiotic treatment of spontaneously-infected *Cftr*$^{-/-}$ ferrets failed to mitigate airway inflammation [95]. Therefore, it is likely that the ASL dehydration-induced stress to the airway cells, i.e., epithelium and immune cells, induces the release of proinflammatory damage-associated molecular patterns (DAMPs) that, in turn, mediates inflammatory responses in the airways.

Various DAMPs have been implicated in the pathogenesis of mucoinflammatory outcomes including airway inflammation, mucin hypersecretion, and MCM. IL-1α, a potent inducer of neutrophilic recruitment, is present at significantly higher levels in BALF from 5-day-old *Scnn1b*-Tg+ pups [96, 97]. The genetic deletion of *Il1r1*, a gene encoding the receptor for IL-1α and IL-1β, abolishes airway neutrophilia and significantly reduces mortality, mucoobstruction, and emphysema in *Scnn1b*-Tg+ pups [97]. Another DAMP, high-mobility group box 1 (HMGB1), is elevated in the sputum from CF patients [98]. Interestingly, HMGB1 levels are also elevated in the BALF from *Scnn1b*-Tg+ mice [98]. Since HMGB1 acts as a ligand for TLR2 and TLR4, its effect is expected to produce responses similar to PAMPs (LPS and lipoteichoic acid) [99, 100].

IL-33, a potent stimulator of Th2-associated responses, acts as a potent DAMP upon release by airway epithelial cells into the airspaces [101]. IL-33 binds to the ST2 receptor that is present on mast cells, macrophages, Th2 cells, and type 2 innate lymphoid cells (ILC2s) [102]. Administration of IL-33 induces the production of cytokines by Th2 lymphocytes *in vivo* [103]. IL-33 has also been linked to the activation of ILC2s that also release Th2-associated cytokines [104]. IL-33 levels are elevated in the juvenile *Scnn1b*-Tg+ mice [105]. Secondhand-smoke exposure to

TABLE 2: Various genetic modifications in the *Scnn1b*-Tg+ mouse model.

Genotype	Description	Macrophage infiltration	Neutrophil infiltration	Eosinophil infiltration	Lymphocyte infiltration	Mucous cell metaplasia	Airway mucus obstruction	Distal airspace enlargement	Reference
Tnfα−/−-*Scnn1b*-Tg+	Global deletion of *Tnfα*	No significant difference	No significant difference	No significant difference	No significant difference	No significant difference	No significant difference	No significant difference	(Livraghi et al., [65])
Tnfr1−/−-*Scnn1b*-Tg+	Global deletion of *Tnfr1*	No significant difference	No significant difference	No significant difference	No significant difference	No significant difference	No significant difference	No significant difference	(Livraghi et al., [65])
Il4rα−/−-*Scnn1b*-Tg+	Global deletion of *Il4rα*	No significant difference	No significant difference	Significantly reduced at PND 10 and 5 weeks of age	No significant difference	Significantly reduced at PND 10	No significant difference	No significant difference	(Livraghi et al., [65])
Myd88−/− *Scnn1b*-Tg+	Global deletion of *Myd88*	Significantly higher at PND 10; no significant difference at other observed time-points	Significantly reduced	No significant difference	Lymphoid hyperplasia significantly increased at 8 weeks of age	Significantly reduced at PND 5-7, but not at other time-points	Significantly reduced at PND 5-7, but not at any other observed time-point	Not reported	(Livraghi-Butrico et al., [38])
Ne−/−-*Scnn1b*-Tg+	Global deletion of *neutrophil elastase*	No significant difference	Significantly reduced	No significant difference	No significant difference	Significantly reduced	No significant difference	Significantly reduced	(Gehrig et al., [57])
Il1r−/−-*Scnn1b*-Tg+	Global deletion of *Il1r*	No significant difference	Significantly reduced	No significant difference	No significant difference	Not reported	Significantly reduced	Significantly reduced	(Fritzsching et al., [97])
DTA+-*Scnn1b*-Tg+	Partial deficiency of macrophages	No significant difference in total number of macrophage infiltration, significantly reduced in total percentage	Significantly increased	No significant difference	Increased occurrence of lymphoid aggregates in adult mice; significant infiltration in nonemaciated phenotype	Significantly reduced in emaciated phenotype	Significantly reduced in emaciated phenotype	No significant difference	(Saini et al., [51, 53])
Muc5b−/−-*Scnn1b*-Tg+	Global deletion of *Muc5b*	No significant difference	No significant difference	Not reported	Increased lymphoid aggregates, but no significant difference in BALF lymphocytes	Not reported	Significantly reduced	No significant difference	(Livraghi-Butrico et al., [108])
Muc5ac−/−-*Scnn1b*-Tg+	Global deletion of *Muc5ac*	No significant difference	No significant difference	Not reported	No significant difference in incidence of lymphoid aggregates	Not reported	Significantly reduced	Not reported	(Livraghi-Butrico et al., [108])
Spdef−/−-*Scnn1b*-Tg+	Global deletion of *Spdef*	No significant difference	Significantly increased in neonates	No significant difference	No significant difference	Not reported	No significant difference	Not reported	(Chen et al., [109])

Scnn1b-Tg+ mice results in diminished IL-33 expression and BALF levels, which is strongly associated with diminished MCM and reduced expression of MCM-associated genes [105]. Further investigation on the mice with a genetic deletion of IL-33 on an *Scnn1b*-Tg+ background will confirm the role of IL-33 in the manifestation of mucoobstructive responses.

14. Does Mucous Cell Metaplasia (MCM) Lead to Mucoobstruction?

MCM refers to an epithelial remodeling response that increases the number of mucous cells in the airway epithelium and upregulates the expression of genes involved in mucin expression and secretion. *Scnn1b*-Tg+ mice exhibit a significantly higher number of mucous cells in proximal and distal airways as compared to their WT littermates [37]. Interestingly, the neonatal (PND 3.5) *Scnn1b*-Tg+ pups exhibit mucoobstruction in the trachea but in the absence of MCM, suggesting that mucus accumulation, rather than mucus overproduction, contributes to mucus plugging at this early age [37]. However, in 2–3-week-old *Scnn1b*-Tg+ mice, mucoobstruction along with MCM is found to be most prominent in the large and distal conducting airways, a feature that persisted into the adult *Scnn1b*-Tg+ mice [37, 105].

MCM is commonly associated with Th2-associated cytokines, i.e., IL-4 and IL-13 [75, 76]. As discussed before, the ablation of *Il4rα*, a common receptor for IL-4 and IL-13, significantly decreases neonatal mortality, MCM, and eosinophilic inflammation in the 10-day-old *Scnn1b*-Tg+ mice [65]. Interestingly, the ablation of *Il4rα* does not alter the severity of mucus plugging [65]. It appears that the normal production rate of mucus in the ASL-dehydrated state is capable of producing mucoobstruction; however, further experiments are required to ascertain this possibility.

15. Conclusions

Due to the high morbidity and mortality associated with CF-like mucoobstructive lung disease, an in-depth investigation of the immunological responses initiated as a result of ASL dehydration and mucoobstruction is warranted. Although several mice models incorporating different *Cftr* mutations are available, none of the mouse models effectively recapitulate CF-like mucoobstructive lung disease. Although not modulating the functioning of CFTR channels, the *Scnn1b*-Tg+ mouse model effectively demonstrates how a single ion-channel defect results in an imbalance in ion transport, which ultimately leads to ASL dehydration and associated lung disease.

The earliest manifestation of lung disease, i.e., ASL layer dehydration, mucoobstruction, immune cell infiltration, and spontaneous bacterial infections, exhibited in the *Scnn1b*-Tg+ mouse model provides a most representative model for the investigation of the pathogenesis and progression of human CF-like lung disease. The *Scnn1b*-Tg+ mouse also presents an outstanding tool to investigate the impact of various environmental insults, e.g., cigarette smoke, nanoparticles, and fungal spores, on the development and progression of mucoobstructive lung disease [105–107].

A complete understanding of the evolution of various pathological manifestations in this strain is still unclear. The availability of numerous genetic strains on a congenic C57BL/6 background presents an opportunity to investigate the development of complex mucoobstructive lung disease which otherwise is challenging to pursue. A list of studies employing various genetic alterations has been summarized in Table 2. Selective introduction of additional genetic alterations into the *Scnn1b*-Tg+ strain have already begun to dissect the pathway-specific roles of various genes in the pathogenesis of mucoobstructive lung disease.

Conflicts of Interest

The authors declare that they have no competing interests.

Authors' Contributions

BWL, SP, and YS wrote the review.

Acknowledgments

References

[1] M. R. Knowles and R. C. Boucher, "Mucus clearance as a primary innate defense mechanism for mammalian airways," *The Journal of Clinical Investigation*, vol. 109, no. 5, pp. 571–577, 2002.

[2] J. V. Fahy and B. F. Dickey, "Airway mucus function and dysfunction," *The New England Journal of Medicine*, vol. 363, no. 23, pp. 2233–2247, 2010.

[3] Z. Zhou, J. Duerr, B. Johannesson et al., "The ENaC-overexpressing mouse as a model of cystic fibrosis lung disease," *Journal of Cystic Fibrosis*, vol. 10, pp. S172–S182, 2011.

[4] C. Krauth, N. Jalilvand, T. Welte, and R. Busse, "Cystic fibrosis: cost of illness and considerations for the economic evaluation of potential therapies," *PharmacoEconomics*, vol. 21, no. 14, pp. 1001–1024, 2003.

[5] A. Schibler, I. Bolt, S. Gallati, M. H. Schoni, and R. Kraemer, "High morbidity and mortality in cystic fibrosis patients compound heterozygous for 3905insT and ΔF508," *The European Respiratory Journal*, vol. 17, no. 6, pp. 1181–1186, 2001.

[6] B. Button, L. H. Cai, C. Ehre et al., "A periciliary brush promotes the lung health by separating the mucus layer from airway epithelia," *Science*, vol. 337, no. 6097, pp. 937–941, 2012.

[7] P. Satir and M. A. Sleigh, "The physiology of cilia and mucociliary interactions," *Annual Review of Physiology*, vol. 52, no. 1, pp. 137–155, 1990.

[8] H. Matsui, S. H. Randell, S. W. Peretti, C. W. Davis, and R. C. Boucher, "Coordinated clearance of periciliary liquid and

mucus from airway surfaces," *The Journal of Clinical Investigation*, vol. 102, no. 6, pp. 1125–1131, 1998.

[9] R. Tarran, "Regulation of airway surface liquid volume and mucus transport by active ion transport," *Proceedings of the American Thoracic Society*, vol. 1, no. 1, pp. 42–46, 2004.

[10] S. H. Randell, R. C. Boucher, and University of North Carolina Virtual Lung Group, "Effective mucus clearance is essential for respiratory health," *American Journal of Respiratory Cell and Molecular Biology*, vol. 35, no. 1, pp. 20–28, 2006.

[11] D. Borowitz, "CFTR, bicarbonate, and the pathophysiology of cystic fibrosis," *Pediatric Pulmonology*, vol. 50, pp. 2S4–S30, 2015.

[12] R. C. Boucher, "Evidence for airway surface dehydration as the initiating event in CF airway disease," *Journal of Internal Medicine*, vol. 261, no. 1, pp. 5–16, 2007.

[13] M. Knowles, M. Stutts, A. Spock, N. Fischer, J. Gatzy, and R. Boucher, "Abnormal ion permeation through cystic fibrosis respiratory epithelium," *Science*, vol. 221, no. 4615, pp. 1067–1070, 1983.

[14] S. M. Rowe, S. Miller, and E. J. Sorscher, "Cystic fibrosis," *The New England Journal of Medicine*, vol. 352, no. 19, pp. 1992–2001, 2005.

[15] J. N. Snouwaert, K. K. Brigman, A. M. Latour et al., "An animal model for cystic fibrosis made by gene targeting," *Science*, vol. 257, no. 5073, pp. 1083–1088, 1992.

[16] E. A. Cowley, C. G. Wang, D. Gosselin, D. Radzioch, and D. H. Eidelman, "Mucociliary clearance in cystic fibrosis knockout mice infected with *Pseudomonas aeruginosa*," *The European Respiratory Journal*, vol. 10, no. 10, pp. 2312–2318, 1997.

[17] J. R. Dorin, P. Dickinson, E. W. Alton et al., "Cystic fibrosis in the mouse by targeted insertional mutagenesis," *Nature*, vol. 359, no. 6392, pp. 211–215, 1992.

[18] D. J. Davidson, J. R. Dorin, G. McLachlan et al., "Lung disease in the cystic fibrosis mouse exposed to bacterial pathogens," *Nature Genetics*, vol. 9, no. 4, pp. 351–357, 1995.

[19] R. Ratcliff, M. J. Evans, A. W. Cuthbert et al., "Production of a severe cystic fibrosis mutation in mice by gene targeting," *Nature Genetics*, vol. 4, no. 1, pp. 35–41, 1993.

[20] W. K. O'Neal, P. Hasty, P. B. McCray Jr. et al., "A severe phenotype in mice with a duplication of exon 3 in the cystic fibrosis locus," *Human Molecular Genetics*, vol. 2, no. 10, pp. 1561–1569, 1993.

[21] P. Hasty, W. K. O'Neal, K. Q. Liu et al., "Severe phenotype in mice with termination mutation in exon 2 of cystic fibrosis gene," *Somatic Cell and Molecular Genetics*, vol. 21, no. 3, pp. 177–187, 1995.

[22] R. Rozmahel, M. Wilschanski, A. Matin et al., "Modulation of disease severity in cystic fibrosis transmembrane conductance regulator deficient mice by a secondary genetic factor," *Nature Genetics*, vol. 12, no. 3, pp. 280–287, 1996.

[23] W. H. Colledge, B. S. Abella, K. W. Southern et al., "Generation and characterization of a ΔF508 cystic fibrosis mouse model," *Nature Genetics*, vol. 10, no. 4, pp. 445–452, 1995.

[24] B. G. Zeiher, E. Eichwald, J. Zabner et al., "A mouse model for the delta F508 allele of cystic fibrosis," *The Journal of Clinical Investigation*, vol. 96, no. 4, pp. 2051–2064, 1995.

[25] J. H. van Doorninck, P. J. French, E. Verbeek et al., "A mouse model for the cystic fibrosis delta F508 mutation," *The EMBO Journal*, vol. 14, no. 18, pp. 4403–4411, 1995.

[26] S. J. Delaney, E. W. Alton, S. N. Smith et al., "Cystic fibrosis mice carrying the missense mutation G551D replicate human genotype-phenotype correlations," *The EMBO Journal*, vol. 15, no. 5, pp. 955–963, 1996.

[27] P. Dickinson, S. N. Smith, S. Webb et al., "The severe G480C cystic fibrosis mutation, when replicated in the mouse, demonstrates mistrafficking, normal survival and organ-specific bioelectrics," *Human Molecular Genetics*, vol. 11, no. 3, pp. 243–251, 2002.

[28] A. M. van Heeckeren, M. D. Schluchter, M. L. Drumm, and P. B. Davis, "Role of Cftr genotype in the response to chronic *Pseudomonas aeruginosa* lung infection in mice," *American Journal of Physiology. Lung Cellular and Molecular Physiology*, vol. 287, no. 5, pp. L944–L952, 2004.

[29] C. S. Rogers, D. A. Stoltz, D. K. Meyerholz et al., "Disruption of the *CFTR* gene produces a model of cystic fibrosis in newborn pigs," *Science*, vol. 321, no. 5897, pp. 1837–1841, 2008.

[30] D. A. Stoltz, D. K. Meyerholz, A. A. Pezzulo et al., "Cystic fibrosis pigs develop lung disease and exhibit defective bacterial eradication at birth," *Science Translational Medicine*, vol. 2, no. 29, article 29ra31, 2010.

[31] X. Sun, H. Sui, J. T. Fisher et al., "Disease phenotype of a ferret *CFTR*-knockout model of cystic fibrosis," *The Journal of Clinical Investigation*, vol. 120, no. 9, pp. 3149–3160, 2010.

[32] X. Sun, A. K. Olivier, B. Liang et al., "Lung phenotype of juvenile and adult cystic fibrosis transmembrane conductance regulator–knockout ferrets," *American Journal of Respiratory Cell and Molecular Biology*, vol. 50, no. 3, pp. 502–512, 2014.

[33] K. L. Tuggle, S. E. Birket, X. Cui et al., "Characterization of defects in ion transport and tissue development in cystic fibrosis transmembrane conductance regulator (CFTR)-knockout rats," *PLoS One*, vol. 9, no. 3, article e91253, 2014.

[34] S. E. Birket, J. M. Davis, C. M. Fernandez et al., "Development of an airway mucus defect in the cystic fibrosis rat," *JCI Insight*, vol. 3, no. 1, 2018.

[35] B. R. Grubb, A. M. Paradiso, and R. C. Boucher, "Anomalies in ion transport in CF mouse tracheal epithelium," *American Journal of Physiology-Cell Physiology*, vol. 267, no. 1, pp. C293–C300, 1994.

[36] M. Mall, B. R. Grubb, J. R. Harkema, W. K. O'Neal, and R. C. Boucher, "Increased airway epithelial Na$^+$ absorption produces cystic fibrosis-like lung disease in mice," *Nature Medicine*, vol. 10, no. 5, pp. 487–493, 2004.

[37] M. A. Mall, J. R. Harkema, J. B. Trojanek et al., "Development of chronic bronchitis and emphysema in beta-epithelial Na^{+-} channel-overexpressing mice," *American Journal of Respiratory and Critical Care Medicine*, vol. 177, no. 7, pp. 730–742, 2008.

[38] A. Livraghi-Butrico, E. J. Kelly, E. R. Klem et al., "Mucus clearance, MyD88-dependent and MyD88-independent immunity modulate lung susceptibility to spontaneous bacterial infection and inflammation," *Mucosal Immunology*, vol. 5, no. 4, pp. 397–408, 2012.

[39] D. M. Mosser and J. P. Edwards, "Exploring the full spectrum of macrophage activation," *Nature Reviews. Immunology*, vol. 8, no. 12, pp. 958–969, 2008.

[40] C. F. Nathan, H. W. Murray, M. E. Wiebe, and B. Y. Rubin, "Identification of interferon-gamma as the lymphokine that activates human macrophage oxidative metabolism and antimicrobial activity," *The Journal of Experimental Medicine*, vol. 158, no. 3, pp. 670–689, 1983.

[41] T. K. Means, B. W. Jones, A. B. Schromm et al., "Differential effects of a Toll-like receptor antagonist on *Mycobacterium tuberculosis*-induced macrophage responses," *Journal of Immunology*, vol. 166, no. 6, pp. 4074–4082, 2001.

[42] B. W. Jones, T. K. Means, K. A. Heldwein et al., "Different Toll-like receptor agonists induce distinct macrophage responses," *Journal of Leukocyte Biology*, vol. 69, pp. 1036–1044, 2001.

[43] R. Medzhitov, P. Preston-Hurlburt, E. Kopp et al., "MyD88 is an adaptor protein in the hToll/IL-1 receptor family signaling pathways," *Molecular Cell*, vol. 2, no. 2, pp. 253–258, 1998.

[44] N. Wang, H. Liang, and K. Zen, "Molecular mechanisms that influence the macrophage m1–m2 polarization balance," *Frontiers in Immunology*, vol. 5, p. 614, 2014.

[45] M. Stein, S. Keshav, N. Harris, and S. Gordon, "Interleukin 4 potently enhances murine macrophage mannose receptor activity: a marker of alternative immunologic macrophage activation," *The Journal of Experimental Medicine*, vol. 176, no. 1, pp. 287–292, 1992.

[46] T. M. Doherty, R. Kastelein, S. Menon, S. Andrade, and R. L. Coffman, "Modulation of murine macrophage function by IL-13," *The Journal of Immunology*, vol. 151, no. 12, pp. 7151–7160, 1993.

[47] R. Lang, D. Patel, J. J. Morris, R. L. Rutschman, and P. J. Murray, "Shaping gene expression in activated and resting primary macrophages by IL-10," *Journal of Immunology*, vol. 169, no. 5, pp. 2253–2263, 2002.

[48] M. Terabe, S. Matsui, N. Noben-Trauth et al., "NKT cell-mediated repression of tumor immunosurveillance by IL-13 and the IL-4R-STAT6 pathway," *Nature Immunology*, vol. 1, no. 6, pp. 515–520, 2000.

[49] A. M. O'Farrell, Y. Liu, K. W. Moore, and A. L. Mui, "IL-10 inhibits macrophage activation and proliferation by distinct signaling mechanisms: evidence for Stat3-dependent and -independent pathways," *The EMBO Journal*, vol. 17, no. 4, pp. 1006–1018, 1998.

[50] Y. Saini, H. Dang, A. Livraghi-Butrico et al., "Gene expression in whole lung and pulmonary macrophages reflects the dynamic pathology associated with airway surface dehydration," *BMC Genomics*, vol. 15, no. 1, p. 726, 2014.

[51] Y. Saini, K. J. Wilkinson, K. A. Terrell et al., "Neonatal pulmonary macrophage depletion coupled to defective mucus clearance increases susceptibility to pneumonia and alters pulmonary immune responses," *American Journal of Respiratory Cell and Molecular Biology*, vol. 54, no. 2, pp. 210–221, 2016.

[52] D. Kreisel, R. G. Nava, W. Li et al., "In vivo two-photon imaging reveals monocyte-dependent neutrophil extravasation during pulmonary inflammation," *Proceedings of the National Academy of Sciences of the United States of America*, vol. 107, no. 42, pp. 18073–18078, 2010.

[53] Y. Saini, B. W. Lewis, D. Yu et al., "Effect of LysM+ macrophage depletion on lung pathology in mice with chronic bronchitis," *Physiological Reports*, vol. 6, no. 8, article e13677, 2018.

[54] J. B. Trojanek, A. Cobos-Correa, S. Diemer et al., "Airway mucus obstruction triggers macrophage activation and matrix metalloproteinase 12-dependent emphysema," *American Journal of Respiratory Cell and Molecular Biology*, vol. 51, no. 5, pp. 709–720, 2014.

[55] E. Kolaczkowska and P. Kubes, "Neutrophil recruitment and function in health and inflammation," *Nature Reviews. Immunology*, vol. 13, no. 3, pp. 159–175, 2013.

[56] V. Brinkmann, U. Reichard, C. Goosmann et al., "Neutrophil extracellular traps kill bacteria," *Science*, vol. 303, no. 5663, pp. 1532–1535, 2004.

[57] S. Gehrig, J. Duerr, M. Weitnauer et al., "Lack of neutrophil elastase reduces inflammation, mucus hypersecretion, and emphysema, but not mucus obstruction, in mice with cystic fibrosis-like lung disease," *American Journal of Respiratory and Critical Care Medicine*, vol. 189, no. 9, pp. 1082–1092, 2014.

[58] S. D. Shapiro, N. M. Goldstein, A. M. Houghton, D. K. Kobayashi, D. Kelley, and A. Belaaouaj, "Neutrophil elastase contributes to cigarette smoke-induced emphysema in mice," *The American Journal of Pathology*, vol. 163, no. 6, pp. 2329–2335, 2003.

[59] J. A. Voynow, B. M. Fischer, D. E. Malarkey et al., "Neutrophil elastase induces mucus cell metaplasia in mouse lung," *American Journal of Physiology. Lung Cellular and Molecular Physiology*, vol. 287, no. 6, pp. L1293–L1302, 2004.

[60] J. A. Voynow, L. R. Young, Y. Wang, T. Horger, M. C. Rose, and B. M. Fischer, "Neutrophil elastase increases *MUC5AC* mRNA and protein expression in respiratory epithelial cells," *American Journal of Physiology-Lung Cellular and Molecular Physiology*, vol. 276, no. 5, pp. L835–L843, 1999.

[61] A. Livraghi-Butrico, B. R. Grubb, E. J. Kelly et al., "Genetically determined heterogeneity of lung disease in a mouse model of airway mucus obstruction," *Physiological Genomics*, vol. 44, no. 8, pp. 470–484, 2012.

[62] P. F. Weller and L. A. Spencer, "Functions of tissue-resident eosinophils," *Nature Reviews. Immunology*, vol. 17, no. 12, pp. 746–760, 2017.

[63] V. T. Chu and C. Berek, "Immunization induces activation of bone marrow eosinophils required for plasma cell survival," *European Journal of Immunology*, vol. 42, no. 1, pp. 130–137, 2012.

[64] K. Nelms, A. D. Keegan, J. Zamorano, J. J. Ryan, and W. E. Paul, "The IL-4 receptor: signaling mechanisms and biologic functions," *Annual Review of Immunology*, vol. 17, no. 1, pp. 701–738, 1999.

[65] A. Livraghi, B. R. Grubb, E. J. Hudson et al., "Airway and lung pathology due to mucosal surface dehydration in (beta)-epithelial Na$^+$ channel-overexpressing mice: role of TNF-(alpha) and IL-4R(alpha) signaling, influence of neonatal development, and limited efficacy of glucocorticoid treatment," *Journal of Immunology*, vol. 182, no. 7, pp. 4357–4367, 2009.

[66] R. Kiessling, E. Klein, and H. Wigzell, ""Natural" killer cells in the mouse. I. Cytotoxic cells with specificity for mouse Moloney leukemia cells. Specificity and distribution according to genotype," *European Journal of Immunology*, vol. 5, no. 2, pp. 112–117, 1975.

[67] R. M. Welsh, J. O. Brubaker, M. Vargas-Cortes, and C. L. O'Donnell, "Natural killer (NK) cell response to virus infections in mice with severe combined immunodeficiency. The stimulation of NK cells and the NK cell-dependent control of virus infections occur independently of T and B cell function," *Journal of Experimental Medicine*, vol. 173, no. 5, pp. 1053–1063, 1991.

[68] M. H. Johansson, C. Bieberich, G. Jay, K. Karre, and P. Hoglund, "Natural killer cell tolerance in mice with mosaic

expression of major histocompatibility complex class I transgene," *The Journal of Experimental Medicine*, vol. 186, no. 3, pp. 353–364, 1997.

[69] S. A. Wolfe, D. E. Tracey, and C. S. Henney, "Induction of "natural killer" cells by BCG," *Nature*, vol. 262, no. 5569, pp. 584–586, 1976.

[70] A. Martin-Fontecha, L. L. Thomsen, S. Brett et al., "Induced recruitment of NK cells to lymph nodes provides IFN-gamma for T(H)1 priming," *Nature Immunology*, vol. 5, no. 12, pp. 1260–1265, 2004.

[71] F. W. Alt, G. D. Yancopoulos, T. K. Blackwell et al., "Ordered rearrangement of immunoglobulin heavy chain variable region segments," *The EMBO Journal*, vol. 3, no. 6, pp. 1209–1219, 1984.

[72] M. A. Oettinger, D. G. Schatz, C. Gorka, and D. Baltimore, "RAG-1 and RAG-2, adjacent genes that synergistically activate V(D)J recombination," *Science*, vol. 248, no. 4962, pp. 1517–1523, 1990.

[73] S. L. Constant and K. Bottomly, "Induction of Th1 and Th2 CD4+ T cell responses: the alternative approaches," *Annual Review of Immunology*, vol. 15, no. 1, pp. 297–322, 1997.

[74] A. N. McKenzie, J. A. Culpepper, R. de Waal Malefyt et al., "Interleukin 13, a T-cell-derived cytokine that regulates human monocyte and B-cell function," *Proceedings of the National Academy of Sciences of the United States of America*, vol. 90, no. 8, pp. 3735–3739, 1993.

[75] K. Dabbagh, K. Takeyama, H. M. Lee, I. F. Ueki, J. A. Lausier, and J. A. Nadel, "IL-4 induces mucin gene expression and goblet cell metaplasia in vitro and in vivo," *The Journal of Immunology*, vol. 162, no. 10, pp. 6233–6237, 1999.

[76] Z. Zhu, R. J. Homer, Z. Wang et al., "Pulmonary expression of interleukin-13 causes inflammation, mucus hypersecretion, subepithelial fibrosis, physiologic abnormalities, and eotaxin production," *The Journal of Clinical Investigation*, vol. 103, no. 6, pp. 779–788, 1999.

[77] S. J. Aujla, P. J. Dubin, and J. K. Kolls, "Th17 cells and mucosal host defense," *Seminars in Immunology*, vol. 19, no. 6, pp. 377–382, 2007.

[78] H. L. Tan, N. Regamey, S. Brown, A. Bush, C. M. Lloyd, and J. C. Davies, "The Th17 pathway in cystic fibrosis lung disease," *American Journal of Respiratory and Critical Care Medicine*, vol. 184, no. 2, pp. 252–258, 2011.

[79] K. Tiringer, A. Treis, P. Fucik et al., "A Th17- and Th2-skewed cytokine profile in cystic fibrosis lungs represents a potential risk factor for *Pseudomonas aeruginosa* infection," *American Journal of Respiratory and Critical Care Medicine*, vol. 187, no. 6, pp. 621–629, 2013.

[80] S. Z. Josefowicz, L. F. Lu, and A. Y. Rudensky, "Regulatory T cells: mechanisms of differentiation and function," *Annual Review of Immunology*, vol. 30, no. 1, pp. 531–564, 2012.

[81] A. Hector, H. Schafer, S. Poschel et al., "Regulatory T-cell impairment in cystic fibrosis patients with chronic *Pseudomonas* infection," *American Journal of Respiratory and Critical Care Medicine*, vol. 191, no. 8, pp. 914–923, 2015.

[82] E. J. Lammertyn, E. Vandermeulen, H. Bellon et al., "End-stage cystic fibrosis lung disease is characterised by a diverse inflammatory pattern: an immunohistochemical analysis," *Respiratory Research*, vol. 18, no. 1, p. 10, 2017.

[83] T. Pressler, B. Frederiksen, M. Skov, P. Garred, C. Koch, and N. Hoiby, "Early rise of anti-pseudomonas antibodies and a mucoid phenotype of *Pseudomonas aeruginosa* are risk

factors for development of chronic lung infection—a case control study," *Journal of Cystic Fibrosis*, vol. 5, no. 1, pp. 9–15, 2006.

[84] K. Aanaes, H. K. Johansen, S. S. Poulsen, T. Pressler, C. Buchwald, and N. Hoiby, "Secretory IgA as a diagnostic tool for *Pseudomonas aeruginosa* respiratory colonization," *Journal of Cystic Fibrosis*, vol. 12, no. 1, pp. 81–87, 2013.

[85] G. Eberl, M. Colonna, J. P. Di Santo, and A. N. McKenzie, "Innate lymphoid cells: a new paradigm in immunology," *Science*, vol. 348, no. 6237, article aaa6566, 2015.

[86] C. S. N. Klose, M. Flach, L. Mohle et al., "Differentiation of type 1 ILCs from a common progenitor to all helper-like innate lymphoid cell lineages," *Cell*, vol. 157, no. 2, pp. 340–356, 2014.

[87] H. Spits, D. Artis, M. Colonna et al., "Innate lymphoid cells — a proposal for uniform nomenclature," *Nature Reviews Immunology*, vol. 13, no. 2, pp. 145–149, 2013.

[88] K. Moro, T. Yamada, M. Tanabe et al., "Innate production of T(H)2 cytokines by adipose tissue-associated c-Kit(+)Sca-1(+) lymphoid cells," *Nature*, vol. 463, no. 7280, pp. 540–544, 2010.

[89] J. Mjosberg, J. Bernink, K. Golebski et al., "The transcription factor GATA3 is essential for the function of human type 2 innate lymphoid cells," *Immunity*, vol. 37, no. 4, pp. 649–659, 2012.

[90] T. Hoyler, C. S. Klose, A. Souabni et al., "The transcription factor GATA-3 controls cell fate and maintenance of type 2 innate lymphoid cells," *Immunity*, vol. 37, no. 4, pp. 634–648, 2012.

[91] H. Takatori, Y. Kanno, W. T. Watford et al., "Lymphoid tissue inducer-like cells are an innate source of IL-17 and IL-22," *The Journal of Experimental Medicine*, vol. 206, no. 1, pp. 35–41, 2009.

[92] M. S. Muhlebach, B. T. Zorn, C. R. Esther et al., "Initial acquisition and succession of the cystic fibrosis lung microbiome is associated with disease progression in infants and preschool children," *PLoS Pathogens*, vol. 14, no. 1, article e1006798, 2018.

[93] B. Coburn, P. W. Wang, J. Diaz Caballero et al., "Lung microbiota across age and disease stage in cystic fibrosis," *Scientific Reports*, vol. 5, no. 1, article 10241, 2015.

[94] N. Hoiby, "Recent advances in the treatment of *Pseudomonas aeruginosa* infections in cystic fibrosis," *BMC Medicine*, vol. 9, no. 1, p. 32, 2011.

[95] B. H. Rosen, T. I. A. Evans, S. R. Moll et al., "Infection is not required for mucoinflammatory lung disease in CFTR-knockout ferrets," *American Journal of Respiratory and Critical Care Medicine*, vol. 197, no. 10, pp. 1308–1318, 2018.

[96] P. Rider, Y. Carmi, O. Guttman et al., "IL-1α and IL-1β recruit different myeloid cells and promote different stages of sterile inflammation," *The Journal of Immunology*, vol. 187, no. 9, pp. 4835–4843, 2011.

[97] B. Fritzsching, Z. Zhou-Suckow, J. B. Trojanek et al., "Hypoxic epithelial necrosis triggers neutrophilic inflammation via IL-1 receptor signaling in cystic fibrosis lung disease," *American Journal of Respiratory and Critical Care Medicine*, vol. 191, no. 8, pp. 902–913, 2015.

[98] S. M. Rowe, P. L. Jackson, G. Liu et al., "Potential role of high-mobility group box 1 in cystic fibrosis airway disease," *American Journal of Respiratory and Critical Care Medicine*, vol. 178, no. 8, pp. 822–831, 2008.

[99] J. S. Park, D. Svetkauskaite, Q. He et al., "Involvement of toll-like receptors 2 and 4 in cellular activation by high mobility group box 1 protein," *The Journal of Biological Chemistry*, vol. 279, no. 9, pp. 7370–7377, 2004.

[100] J. S. Park, F. Gamboni-Robertson, Q. He et al., "High mobility group box 1 protein interacts with multiple Toll-like receptors," *American Journal of Physiology. Cell Physiology*, vol. 290, no. 3, pp. C917–C924, 2006.

[101] C. Cayrol and J. P. Girard, "IL-33: an alarmin cytokine with crucial roles in innate immunity, inflammation and allergy," *Current Opinion in Immunology*, vol. 31, pp. 31–37, 2014.

[102] S. Chen, B. Chen, Z. Wen, Z. Huang, and L. Ye, "IL-33/ST2-mediated inflammation in macrophages is directly abrogated by IL-10 during rheumatoid arthritis," *Oncotarget*, vol. 8, no. 20, pp. 32407–32418, 2017.

[103] J. Schmitz, A. Owyang, E. Oldham et al., "IL-33, an interleukin-1-like cytokine that signals via the IL-1 receptor-related protein ST2 and induces T helper type 2-associated cytokines," *Immunity*, vol. 23, no. 5, pp. 479–490, 2005.

[104] K. R. Bartemes, K. Iijima, T. Kobayashi, G. M. Kephart, A. N. McKenzie, and H. Kita, "IL-33-responsive lineage—CD25+ CD44(hi) lymphoid cells mediate innate type 2 immunity and allergic inflammation in the lungs," *Journal of Immunology*, vol. 188, no. 3, pp. 1503–1513, 2012.

[105] B. W. Lewis, R. Sultana, R. Sharma et al., "Early postnatal secondhand smoke exposure disrupts bacterial clearance and abolishes immune responses in muco-obstructive lung disease," *Journal of Immunology*, vol. 199, no. 3, pp. 1170–1183, 2017.

[106] M. Geiser, O. Quaile, A. Wenk et al., "Cellular uptake and localization of inhaled gold nanoparticles in lungs of mice with chronic obstructive pulmonary disease," *Particle and Fibre Toxicology*, vol. 10, no. 1, p. 19, 2013.

[107] M. Geiser, C. Wigge, M. L. Conrad et al., "Nanoparticle uptake by airway phagocytes after fungal spore challenge in murine allergic asthma and chronic bronchitis," *BMC Pulmonary Medicine*, vol. 14, no. 1, p. 116, 2014.

[108] A. Livraghi-Butrico, B. R. Grubb, K. J. Wilkinson et al., "Contribution of mucus concentration and secreted mucins Muc5ac and Muc5b to the pathogenesis of muco-obstructive lung disease," *Mucosal Immunology*, vol. 10, no. 2, pp. 395–407, 2017.

[109] G. Chen, A. S. Volmer, K. J. Wilkinson et al., "Role of Spdef in the regulation of Muc5b expression in the airways of naive and mucoobstructed mice," *American Journal of Respiratory Cell and Molecular Biology*, vol. 59, no. 3, pp. 383–396, 2018.